The Dissertation Committee for Rachel Zepeda Wolf Certifies that this is the approved version of the following dissertation:

Nuclear-Encoded Splicing Factors for Yeast Mitochondrial Introns

Committee:

Alan M. Lambowitz, Supervisor

Dean R. Appling

Karen S. Browning

Rick Russell

Scott W. Stevens

Nuclear-Encoded Splicing Factors for Yeast Mitochondrial Introns

by

Rachel Zepeda Wolf, B.A.; M.S.; M.S.

Dissertation

Presented to the Faculty of the Graduate School of

The University of Texas at Austin

in Partial Fulfillment

of the Requirements

for the Degree of

Doctor of Philosophy

The University of Texas at Austin

August 2015

Acknowledgements

I would like to express my heartfelt gratitude to my advisor, Dr. Alan M. Lambowitz, for his kindness and the faith he showed in me by accepting me into his lab when I was an "orphaned" graduate student. His patience and depth of knowledge provided the guidance I needed to grow as a research scientist. I would also like to thank Dr. Dean Appling, Dr. Karen Browning, Dr. Rick Russell, and Dr. Scott Stevens for serving as my committee members and providing knowledgeable advice and direction. I also acknowledge my deep appreciation for the help and support I received from all my colleagues in the Lambowitz lab, past and present, in particular Dr. Georg Mohr whose experience guided me through this project; and the help and friendship of Marta Mastroianni, whose smile and laughter always brightened the day. I owe a debt of gratitude to Dr. Stephen J. Mattingly and Dr. William Haldenwang, both formerly of the University of Texas Health Science Center at San Antonio: To Dr. Mattingly for his vision to educate teachers and for setting me on this new career path; and to Dr. Haldenwang for the excellent laboratory experience I gained under his supervision and for his support and encouragement in my decision to pursue this degree. Lastly, I wish to acknowledge all my friends who supported me throughout this time (including those who suggested I was too old!), in particular my childhood friend, Humberto Arriaga, Jr. (who had been urging me to pursue a Ph.D. for many years!) and Toast and Whisper, who patiently tolerated life in a tiny condo. Thank you.

Nuclear-Encoded Splicing Factors for Yeast Mitochondrial Introns

Rachel Zepeda Wolf, Ph.D.

The University of Texas at Austin, 2015

Supervisor: Alan M. Lambowitz

Hypothesized to be ancestors of eukaryotic spliceosomal introns, extant group II introns are found in bacteria, archaea, and in the mitochondria and chloroplast genomes of some eukaryotes. While some of these catalytic intron RNAs encode an intron-encoded maturase to assist in their splicing, not all do, eliciting the question of how these introns are spliced out. Two such introns are the mitochondrial introns aI5γ and bI1 of *Saccharomyces cerevisiae*. Previous *in vitro* studies on the self-splicing activity of these introns revealed requirements for non-physiologically high salt concentration and temperature for catalytic activity, suggesting a dependence upon proteins *in vivo*. With most mitochondrial proteins known to be encoded by the nucleus, it seems likely that some exist to assist, either directly or indirectly, in the correct splicing of these introns. Previous searches for such proteins relied on a combination of two genetic screens: looking for a mutant's inability to grow on the non-fermentable carbon source glycerol- (Gly^- phenotype)- in the presence of a given intron, and a Gly^+ phenotype in the intron's absence. In contrast, this study employs Northern hybridization to identify splicing defects in a series of mutants constructed by targeted gene deletion, allowing for

identification of proteins required for splicing that would not have been otherwise detectable. In order to identify associated proteins, this method is complemented by Tandem Affinity Purification of Mss116, the DEAD-box RNA chaperone required for splicing of all the yeast mitochondrial introns. In addition to Mss116, special attention was given to the insertase Oxa1, found to be required for aI5γ and bI1splicing specifically; and to Mne1, found to be required for splicing group I intron aI5β. The results point to distinctly different auxiliary protein requirements for group I introns, group II introns that encode their own maturases, and group II introns that do not encode maturases. My findings are consistent with the possibility that the splicing of aI5γ and bI1, group II introns that do not encode maturases, is coordinated by multiple proteins comprising a splicing complex situated at the surface of the mitochondrial inner membrane in close association with the mitoribosomes.

Table of Contents

List of Tables

List of Figures

Chapter 1: Introduction

1.1 INTRONS

1.1.1 Four classes of introns

Introns are nucleotide sequences found within a gene that must be removed from the precursor RNA to allow the proper expression of the gene product. Four distinct classes of introns have been identified to date: introns in nuclear protein-coding genes that are excised by spliceosomes; introns in nuclear and archaeal transfer RNA genes that are spliced by proteins (tRNA splicing enzymes); and two classes of self-splicing introns that are removed by RNA catalysis, group I and group II introns.

Those of the last two classes, the group I and group II introns, are catalytic RNAs thought to be vestiges of the RNA World (Gilbert 1986; Lambowitz et al. 1999). Introns capable of self-splicing have been identified in organisms from all three domains of life: bacteria, archaea and eukaryotes (Lambowitz and Caprara 1999; Simon et al. 2008; Tocchini-Valentini et al. 2011). Group I and group II introns can be distinguished based on their splicing mechanisms and secondary and tertiary structures, with each group displaying distinctively characteristic mechanisms and structures despite having few conserved nucleotides.

1.1.2 Structure of group I and group II introns

The core secondary structure of group I introns generally consists of nine paired segments (P1-P9) that fold into two principal domains: the P4-P6 domain (formed from

the stacking of P5, P4, P6 and P6a helices) and the P3-P9 domain (formed from the P8, P3, P7 and P9 helices) with additional peripheral segments that differ between intron subclasses (Figure 1.1 A) (Saldanha et al. 1993; Cate et al. 1996; Woodson 2005). Examples of these introns can be found in bacteria, in the plastids and mitochondria of lower eukaryotes and in the rRNA genes of the nucleus of protozoa and certain other lower eukaryotes.

The group II secondary structure consists of six conserved stem-loop domains, (termed DI-DVI) that radiate from a central core to bring the 5' and 3' splice junctions into close proximity of one another (Fig. 1.1 B) (Marcia et al. 2013). DI is the scaffold for the assembly of the catalytic core and is further divided into subdomains. Though not essential, domains II and III enhance the catalytic rate. Domain IV is not conserved in sequence but may harbor an ORF for a multifunctional intron-encoded-protein (IEP) that assists in the intron's excision and mobility. DV is a central component of the ribozyme active site (Lehmann and Schmidt 2003; Pyle and Lambowitz 2006) and together with domain I, forms the minimal catalytic core of the intron. Domain VI contains a bulged adenosine residue, whose 2′-OH is the nucleophile that initiates the splicing reaction. Group II introns are further divided into subgroups IIA, IIB and IIC, which have distinctive structural features. Noteworthy distinctions are the interactions of the exon/intron binding sites that differ among the three main subgroups. The subgroups also differ in DV and several tertiary interaction motifs (Lambowitz and Zimmerly 2011). Like group I introns, group II introns have been found in bacteria, as well as in the plastid and mitochondrial genomes of lower eukaryotes (Lambowitz and Zimmerly 2011).

1.1.3 Splicing mechanisms of group I and group II introns

The splicing of group I introns proceeds via two sequential transesterification reactions (Cech 1986). The first of these is initiated by an exogenous guanosine (exoG) docking into the G-binding site located in P7 (Figure 1.2 A). The 3'-OH of this exoG is positioned to attack the phosphodiester bond at the 5' splice site in P1, leaving a free 3'-OH at the upstream exon and the exoG covalently attached to the 5' end of the intron. In the second transesterification reaction, the 5′ exon attacks the 3′ splice site so that the terminal G of the intron replaces the exoG and occupies the G-binding site. This results in ligation of the two adjacent exons and the excised linear intron (Cech 1990).

Like group I splicing, group II splicing also occurs via two sequential transesterification steps; however, the reactions are distinctively different from those of group I introns (Figure 1.2 B) (Cech 1993). Group II excision occurs in the absence of GTP and instead is initiated when the 2'-OH of a bulged adenosine in domain VI attacks the 5' splice site, generating a lariat with an unusual 3-phosphodiester-bond structure. This is followed by the second nucleophilic attack: that of the 3'-OH of the upstream exon on the 3' splice site, ligating both exons, and releasing the looped intron. This mechanism is identical to that used by the spliceosome in the splicing of nuclear pre-mRNA (Lambowitz and Zimmerly 2011; Lambowitz and Belfort 2015).

1.2 GROUP II INTRONS AS PROGENITORS OF THE SPLICEOSOME

There is general consensus today that group II introns are the ancestors of spliceosomal introns (Sharp 1985; Cech 1986; Rogers 1989; Cavalier-Smith 1991;

Lambowitz and Belfort 2015). With their similarities in splicing mechanisms, the use of a 2′-OH group on a branchpoint adenosine, lariat intermediates, and RNA helicases as co-factors (Lambowitz and Zimmerly 2004; Huang et al. 2005; Cordin et al. 2012), the evidence appears strong.

The parallels extend further: To fold into catalytically-active structures *in vivo*, group II introns often use intron-encoded proteins, termed maturases (Matsuura et al. 2001). Spliceosomal introns do not encode maturases nor fold as group II introns do, but rely instead on snRNAs provided in *trans* for their excision (Matera and Wang 2014). Similarities between snRNAs and group II intron domains have long been noted, with the former being famously described as introns in "five easy pieces" (Sharp 1991). For example, group II intron domain V has strong structural similarities to the U6 snRNA (Sashital et al. 2004; Seetharaman et al. 2006); and snRNA U5 was found to functionally complement the stem loop from a subdomain of group II intron domain I (Hetzer et al. 1997). The snRNAs do not act alone, however, but instead coordinate with a large number of proteins to form RNA-protein complexes that constitute the spliceosome (Matera and Wang 2014). Some group II introns do not have intron-encoded maturases and in that respect, more closely resemble spliceosomal introns than introns that do encode maturases. Do they, like their spliceosomal descendants, have auxiliary proteins that work in *trans* to assist in their folding? If so, what are they? Could those proteins give us clues to the ancestry of the spliceosome?

1.3 INTRON INVASION FROM AN ENDOSYMBIONT

Though the specifics as to *how* are still being debated, it is now widely accepted that mitochondria originated from an endosymbiotic event between an ancestral α-proteobacterium and a proto-eukaryotic host (Wallin 1927; Sagan 1967). The ancestral proteobacterium is thought to have contained group II introns, since these have now been identified in many extant bacterial genomes (Martinez-Abarca and Toro 2000). Over time, it is believed that a large number of the endosymbiont's genes were transferred to the host, so that today, mitochondrial proteins are mostly encoded by the nucleus. Importantly, introns are presumed to have been among the genetic material transferred to the host (Rogozin et al. 2012) perhaps triggering eukaryogenesis as hypothesized by some (Martin and Koonin 2006). Though mitochondria of many higher eukaryotes do not contain introns, those of some extant organisms such as yeast still do, and thus make good models to study the putative evolutionary relationship between group II introns and the spliceosome.

1.4 THE YEAST MITOCHONDRIAL SYSTEM

1.4.1 The yeast mitochondrial genome (mtDNA)

Having once been free-living α-proteobacteria, mitochondria have retained much of their prokaryotic physiology (Martin and Muller 1998; Gray et al. 1999). Two of the ways that mitochondria are thought to have done so is through the persistence of a circular genome and their own translational machinery.

The *Saccharomyces cerevisiae* genome, also known as the *rho* factor (ρ) (Williamson 2002), is often up to 8.6 kb in size, though it may be smaller, largely depending on the number of introns present (Fig. 1.3) (Turk et al. 2013). Wild-type yeast cells which respire normally and form large or *grande* colonies, are termed ρ^+. *Petites* (ρ^-), which have deletions of 20-99.9% of the genome, form small colonies and are unable to respire (Borst and Grivell 1978). In the event of total loss of the mt genome, the cells are referred to as ρ^0. As a consequence of losing portions of its genome, the mitochondrion almost invariably loses genes, such as tRNA and rRNA genes, needed for its translation machinery as well as those required for respiration, making them unable to grow on non-fermentable carbon sources such as glycerol (Gly^- phenotype).

1.4.2 Few proteins are encoded in the mt genome

In addition to several intron-encoded ORFs, there are eight major proteins encoded by the extant mtDNA of *S. cerevisiae* (Williamson 2002; Sickmann et al. 2003). These proteins and their associated genes are cytochrome *c* oxidase subunits I, II and III (*COX1*, *COX2* and *COX3*), cytochrome *b* (*COB*), ATP synthase subunits 6, 8 and 9 (*ATP6*, *ATP8* and *ATP9*), and small subunit ribosomal protein Var1 (*VAR1*). Except for Var1, these are hydrophobic proteins and key components of the electron transport chain located within the inner mt membrane (Sickmann et al. 2003).

With so few proteins encoded in the mitochondria, most of the estimated 590 to over 800 mitochondrial proteins are nuclear-encoded, many being essential (Perocchi et al. 2006; Elstner et al. 2009). Thus, despite having its own genome and translational

machinery, the mitochondrion is highly dependent on extra-mitochondrial processes for its function and biogenesis.

1.4.3 Group I and group II introns are found in three yeast mitochondrial genes

It is within the *COX1*, *COB* and *21S rRNA* genes that the yeast mitochondrial introns are found (Figure 1.4). *COX1* harbors up to four group I introns (aI3, aI4, aI5α and aI5β) and 3 group II introns (aI1, aI2, aI5γ). *COB* may have up to four group I introns (bI2, bI3, bI4, bI5) and one group II intron, bI1 (Pel and Grivell 1993). In most strains, the group II intron aI5γ is the last intron found in the *COX I* gene; while the group II intron bI1 is the first of 5 introns in the *COB* gene (Pel and Grivell 1993). An additional group I intron (ω) may be present within the gene encoding the *21S rRNA*, so that a yeast strain may have up to 13 introns or none at all, (I^0).

1.4.4 Maturases, intron-encoded proteins that assist in splicing

In vitro, some introns are self-splicing (Peebles et al. 1986), but *in vivo*, many introns are assisted by intron-encoded maturases in order to fold into their catalytically-active tertiary structures (Lambowitz and Caprara 1999)Many introns are assisted by intron-encoded maturases, most of which are specific to the intron from which they are encoded (Saldanha et al. 1993). Group II intron maturases are encoded by ORFs within intron domain IV, and are thought to act by stabilizing the catalytic RNA structure via long-range intron-intron and intron-exon interactions (Matsuura et al. 2001).

The known maturases of the yeast mitochondria are diagrammed in Fig. 1.4. Within *COX1*, introns aI1 and aI2 encode their own maturases; while aI4 encodes an inactive

one. Within *COB,* introns bI2, bI3 and bI4 encode their own maturases, the latter of which, in addition to assisting in its own splicing, also assists with the splicing of aI4 (Goguel et al. 1989). Two group II introns, aI5γ and bI1, do not have ORFs and consequently, do not encode maturases.

1.5 NUCLEAR-ENCODED INTRON-SPECIFIC SPLICING FACTORS

In addition to the intron-encoded maturases, several nuclear-encoded proteins have been identified that act specifically as splicing factors for one or more yeast mt introns (Fig. 1.4) (McGraw and Tzagoloff 1983; Seraphin et al. 1988; Costanzo et al. 1989; Valencik et al. 1989; Bousquet et al. 1990; Gampel and Cech 1991; Naithani et al. 2003; Kaspar et al. 2008; Watts et al. 2011). Many of these were identified in screens for nuclear mutations that cause respiratory deficiency only in strains whose mtDNA contains introns. To date, other than the general RNA chaperone Mss116 (which is required for the splicing of all yeast mt introns), no splicing factors other than the IEPs of aI1 and aI2 have been identified for yeast mt group II introns (Seraphin et al. 1989; Huang et al. 2005; Mohr et al. 2006) possibly reflecting the differences between group I and group II splicing mechanisms. Thus, introns aI5γ and bI1 have neither intron-encoded maturases nor nuclear-encoded splicing factors that have yet been identified.

1.6 MSS116, A DEAD-BOX PROTEIN THAT FUNCTIONS AS A GENERAL RNA CHAPERONE

DEAD-box proteins are ubiquitous RNA helicases which function in various RNA-mediated processes: transcription, translation, ribosome biogenesis, RNA export, and both nuclear and mitochondrial pre-mRNA splicing (de la Cruz et al. 1999; Linder

2003; Pan and Russell 2010; Jarmoskaite and Russell 2011; Jarmoskaite and Russell 2014)

Named for an eponymous four amino acid residue motif, DEAD-box helicases play key roles in remodeling many cellular RNAs from inactive but stable states to their active three-dimensional conformations (Jarmoskaite and Russell 2014). They function by coupling cycles of ATP binding and hydrolysis to alter their affinity for single-stranded RNA, effectively separating the strands of short RNA duplexes in a non-processive manner (Fairman-Williams et al. 2010).

Spliceosomal introns require several DEAD-box proteins for proper splicing (Cordin et al. 2012). Within the yeast mitochondrion, the DEAD-box protein Mss116 (Fig. 1.5) is required for the splicing of all thirteen mt group I and group II introns (Huang et al. 2005).

The domain structure of Mss116 is shown in Fig. 1.5 (Mohr et al. 2011; Russell et al. 2013). Mss116 is expressed in the cytoplasm and targeted to the mitochondrion with the N-terminal mitochondrial localization signal (Fig. 1.5, Mt, diagonal lines) which is cleaved off to form the mature protein upon mitochondrial import. The N-terminal extension (NTE) precedes the helicase core of the protein, which is itself comprised of two RecA-like helicase domains, D1 and D2. Distributed within D1 and D2 are thirteen conserved motifs, common to all DEAD-box proteins: Q, I, Ia, Ib, Ic, II, III, IV, IVa, V,Va,Vb, and VI (Fairman-Williams et al. 2010), some of which function primarily for ATP binding (orange bands); others for ssRNA binding (green bands). D1 and D2 are joined by a linker that allows the protein to adopt either an open or closed conformation

(Cao et al. 2011). Following D2 are the C-terminal extension (CTE) and the C-tail. While much is known about Mss116, details of how its different domains and motifs contribute to splicing have remained unclear.

1.7 Overview and significance of research project

1.7.1 Overview

This study was principally designed to identify nuclear-encoded proteins involved in the splicing of mitochondrial group II introns aI5γ and bI1 in *Saccharomyces cerevisiae*. Not having intron-encoded maturases, these introns are presumed to have as-yet-unidentified nuclear-encoded proteins that assist in their splicing. This notion is supported by the finding that self-splicing of these introns *in vitro* is possible only at non-physiologically high salt concentration and temperature, suggesting a dependence upon proteins for splicing *in vivo* (Peebles et al. 1986; Schmelzer and Schweyen 1986; Jarrell et al. 1988). Previous searches unsuccessfully relied on a combination of two screening steps: looking for a Gly^- phenotype in the presence of a given intron and a Gly^+ phenotype in the intron's absence (Séraphin et al. 1987; Luban 2005).

Here, I employed Northern hybridization to identify splicing defects in knock-out strains, allowing for recognition of proteins that would not have been detectable by previously used methods. One important limitation to the screen is its inability to test essential proteins or proteins not yet identified as being mitochondrial. To circumvent this problem, the screen was complemented by pull-down assays in which RNA

chaperone Mss116, known to be required for the splicing of all the yeast mt introns, was tagged and its associated proteins were identified.

It has been long recognized that yeast mitochondrial intron splicing and functionality of the mitoribosomes are linked (Rodeheffer and Shadel 2003). The most common view is that without functional mitoribosomes, intron-encoded maturases cannot be translated, thereby blocking splicing (Pel and Grivell 1993). Here, I provide evidence that the splicing of introns lacking intron-encoded maturases is also impacted by mitoribosomes *in vivo* (Chapter 3). Interestingly, this splicing block due to lack of functional mitoribosomes could sometimes be circumvented by putative second-site suppressor mutations. To eliminate secondary effects due to inhibition of translation, deletions were made in ρ^- strains using a list of candidate proteins determined by mass spectroscopy analysis (Chapter 4). Chapters 5 and 6 each focus on two different proteins, Oxa1 and Mne1, respectively, which were found to be of interest during the preliminary screens. Oxa1 is an insertase closely associated with the mitoribosome. Its deletion caused severe splicing defects in introns aI5γ and bI1, though not in introns aI1, aI2, aI4, bI4 or bI5. Splicing defects in aI5γ and bI1 were also found to be growth medium-dependent. Together, the data suggest that the splicing of aI5γ and bI1 is indirectly affected by Oxa1's insertase function in rapidly dividing cells. Mne1 was found to be a splicing factor for the group I intron aI5β, adding to the array of proteins required for the splicing of that intron. In Chapter 7, the splicing capabilities of Mss116 mutants were investigated and measurements were made of wild-type Mss116 levels and the minimal amount of the protein needed for splicing. Through the use of TAP-tag pull-down

analysis, other proteins associated with Mss116 were identified which included primarily mitoribosomal proteins and several known splicing factors. Treatment with RNase suggests that Mss116's association with the mitoribosomes is via the rRNAs.

1.7.2 Significance

The impact introns have had on evolution cannot be underestimated. One hypothesis purports that group II intron invasion from an endosymbiont to the host was the key factor for the emergence of the nucleus, and consequently, for eukaryogenesis (Koonin 2006; Martin and Koonin 2006). Their catalytic properties and genetic information storage capabilities have engendered the notion that life on primordial Earth was originally RNA-based, an idea known as the RNA World Hypothesis (Gilbert 1986). How these RNAs fold into their catalytic conformations is not yet fully understood. Of key interest is the possible evolutionary relatedness based on the similarity in splicing mechanisms shared by group II introns and the spliceosome.

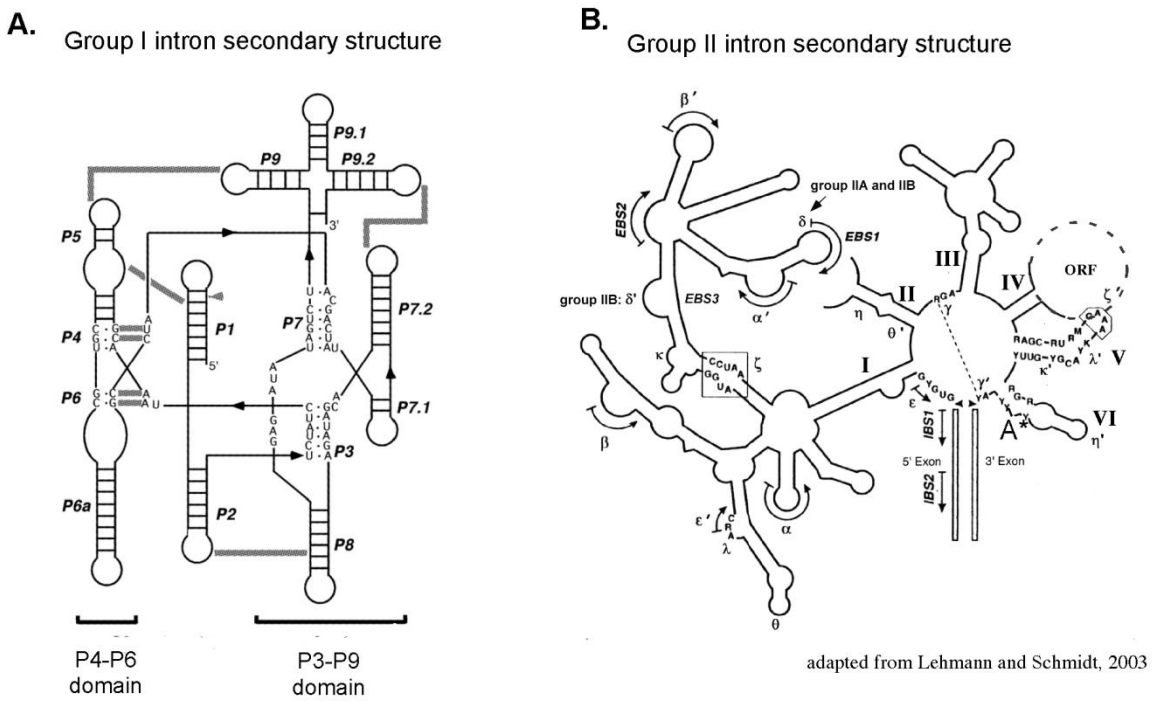

Figure 1.1: Secondary structures of group I and group II introns.

(A) The group I intron secondary structure consists of two main domains P4-P6 and P3-P9, made up of nine base-paired helices (P1- P9). (B) Group II intron structure consists of six domains (Roman numerals I- VI). Domain IV sometimes contains an ORF (dotted circle) which is lacking in introns aI5γ and bI1. The branchpoint adenosine in domain VI is indicated by A*. Greek letters indicate the location of sequence motifs involved in long-range tertiary interactions. The exon-binding sites, EBS1 and EBS2 base pair to the intron binding sites, IBS1 and IBS2 in the 5′ exon; sequences within the 3′ exon base pair to δ sequences.

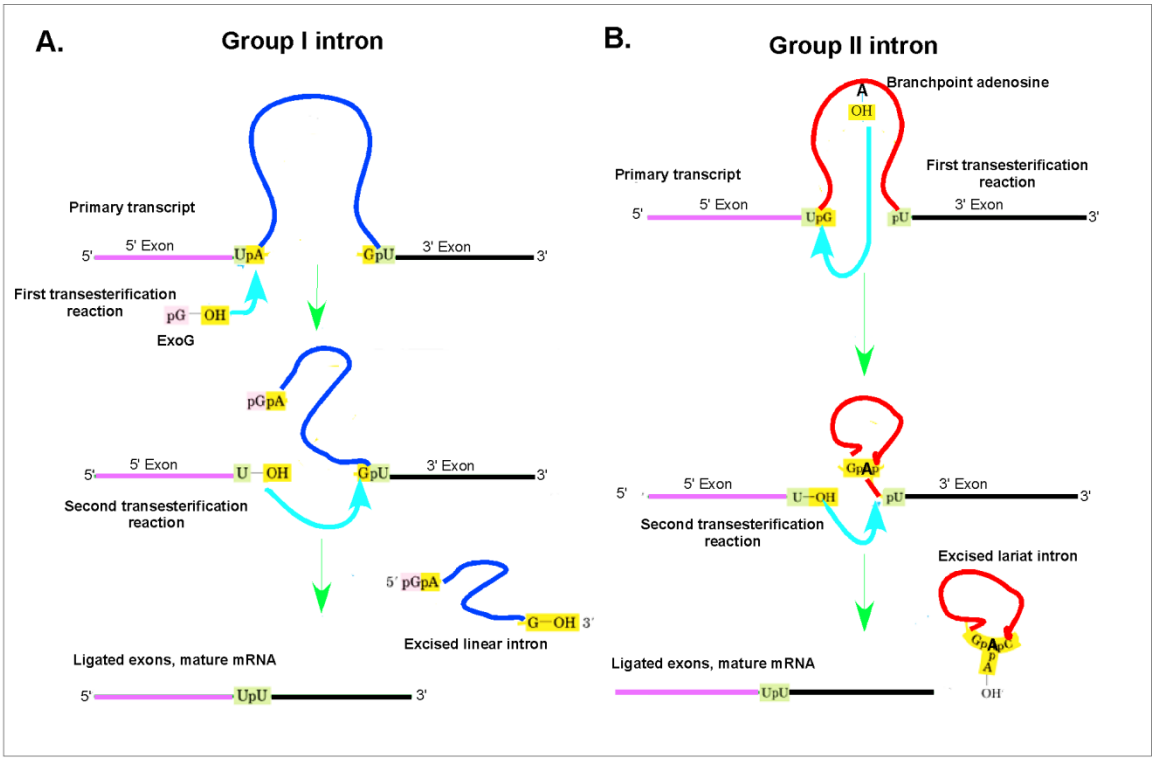

Figure 1.2: The splicing mechanisms of group I and group II introns.

(A) A group I intron (blue loop) lies between the 5′ and 3′ exons (fuchsia and black lines, respectively). An exogenous guanosine (exoG) initiates the first transesterification reaction (teal arrow), leaving exoG covalently attached to the 5′ end of the intron as well as a free 5′ exon with an available 3′OH group. The second transesterification reaction is initiated by the 3′ OH of the 5′ exon (teal arrow, middle) resulting in the release of the excised linear intron and ligation of both exons (bottom). (B) A group II intron (red loop) lies between the 5′ and 3′ exons (fuchsia and black lines, respectively) and contains a bulged branchpoint adenosine, **A,** that initiates the first transesterification reaction (teal arrow, top), resulting in a lariat with a 2′5′-phosphodiester bonds (red lariat, center). The 3′OH of the 5′ exon initiates the second transesterification reaction (teal arrow, middle) resulting in the release of the excised lariat intron and ligation of both exons (bottom).

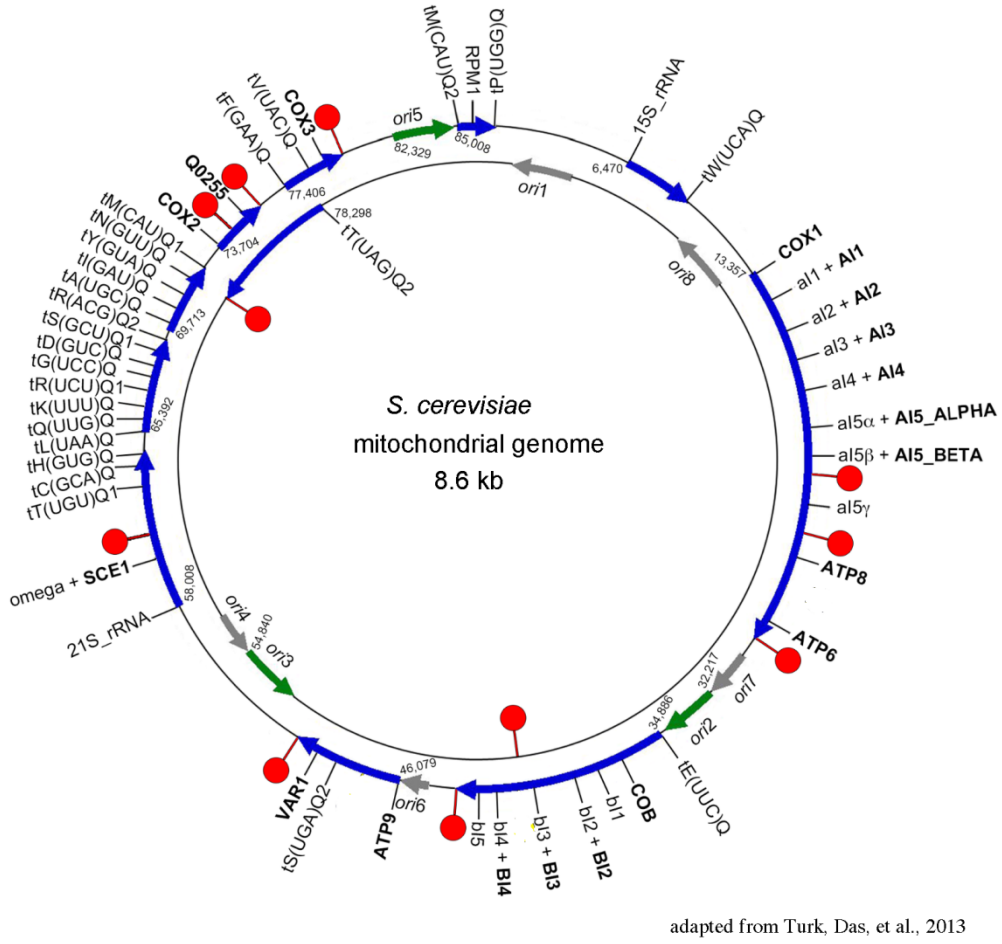

Figure 1.3: The *S. cerevisiae* mitochondrial genome

The 8.6-kb genome with 13 introns. The relative positions of the primary transcripts (blue arrows), with protein-coding names (upper case, bold), dodecamer termination sequences (red lollipops), introns (lower case), and intron-encoded proteins (+ upper case, bold) are shown on the map. Adapted from (Turk et al. 2013).

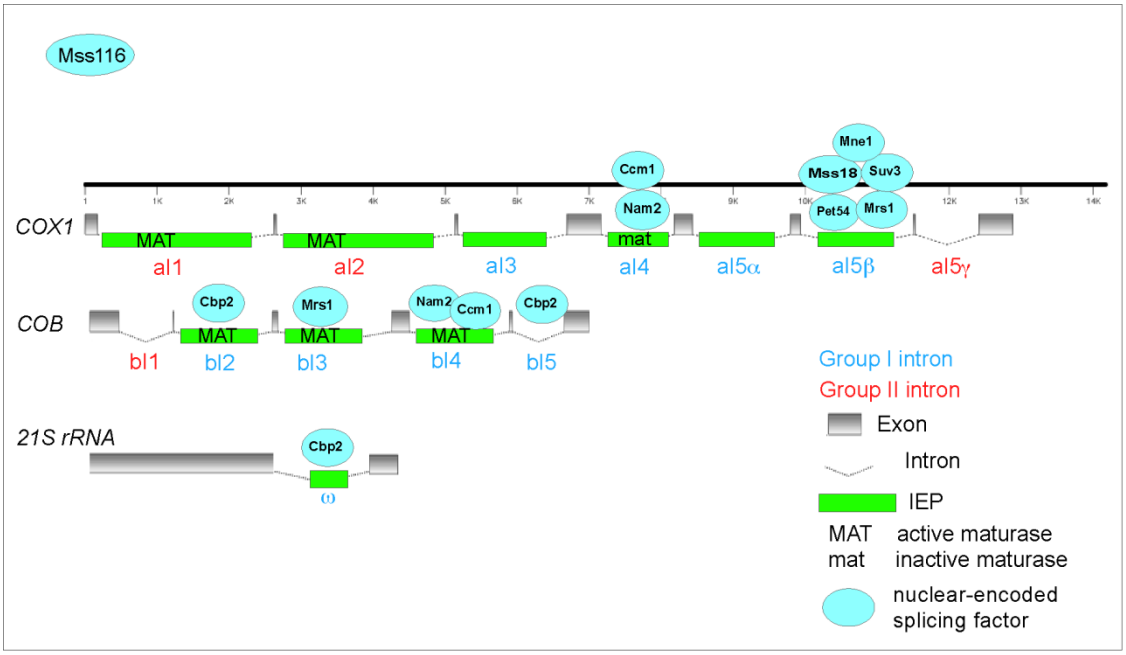

Figure 1.4: Yeast mt introns, their intron-encoded maturases, and known nuclear-encoded splicing factors.

Gene names are indicated to the left of the figure. Exons and introns are indicated by gray rectangles and dotted lines, respectively. Group I introns are indicated in blue and group II introns are indicated in red. Intron-encoded proteins (IEPs) are indicated by green rectangles with active (MAT) and inactive (mat) intron-encoded maturases indicated within. Blue ovals represent known splicing factors for the associated introns, with the exception of Mss116, which is a general RNA chaperone required for the splicing of all 13 introns.

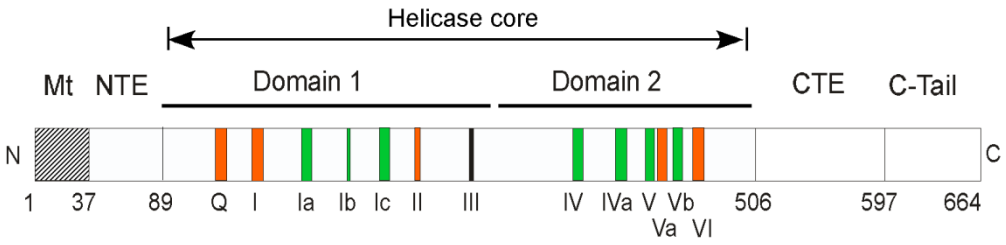

Figure 1.5: Schematic of wild-type Mss116.

Diagram of Mss116 showing domain architecture and the location of conserved sequence motifs. The pre-protein begins with an N-terminal mitochondrial target sequence (Mt), which is cleaved during transport into the mitochondrion, followed by an N-terminal extension (NTE), and Domain 1 which contains motifs Q, I, Ia, Ib, Ic, II, and III. Following Domain 1 is Domain 2 which contains motifs IV, Iva, V, Va, Vb, and VI. Domain 2 is followed by a C-terminal extension (CTE) and the C-tail. Motifs colored orange interact with ATP and those colored green interact with ssRNA. Motif III (black) does not contact either ATP or RNA, but is instead involved in bridging domains 1 and 2. Amino acid residues at the boundaries between different regions are numbered below. Adapted from (Mohr et al. 2011; Russell et al. 2013).

Chapter 2: Methods and Materials

2.1 *S. CEREVISIAE* STRAINS USED

S. cerevisiae strains used in this study are derivatives of wild-type strain 161-U7 which has the nuclear background *MATa ade1 lys1 ura3* and can have up to 12 group I and group II mitochondrial introns (Foury et al. 1998; Huang et al. 2005). The isogenic $1^{+}2^{+}$ strain harbored all 12 of the group I and group II introns found in the *COX1* and *COB* genes and the I^{0} strain had none. The single-intron strains contained either intron aI1, aI2, aI5γ, bI1, or LSU. Strain HRH422 contained only introns aI4, bI4 and bI5. The petite strains aI5γ ρ^{-} and bI1ρ^{-} were isogenic derivatives of the aI5γ and bI1 strains. All strains were obtained from Dr. Philip Perlman (Howard Hughes Medical Institute).

To engineer null mutants for each protein of interest, the kanamycin KanMX module was amplified by colony PCR (described below) from the commercially available BY4741 knock-out strains (Open Biosystems' *Saccharomcyces cerevisiae* Genome Deletion collection) using pairs of oligonucleotide primers specific for each gene of interest (Appendix B). The resulting PCR products were then used to replace the corresponding target gene in the experimental strains by a standard yeast transformation protocol (Gietz and Schiestl 2007), as described in more detail below. Confirmation of the correct gene replacement was performed using two pairs of primers: One pair at the 5′ end of the kanamycin cassette with the forward primer upstream of the transforming PCR product and the reverse primer within the kanamycin cassette. The second pair tested the 3′ region using a forward primer within the kanamycin cassette and the reverse

primer downstream of the transforming cassette. All the null mutants in the screen are then formally *orf*Δ0::KANMX, but will be designated in this thesis by the shortened *orf*Δ.

S. cerevisiae strains used for the Mne1study (chapter 6) were W303 (MATα *ade2-1 his3-1, 15 leu2-3, 112 trp1-1 ura3-1),* containing all twelve *COX1* and *COB* introns, and the corresponding *mne1*Δ mutant (Kispal et al. 1999; Watts et al. 2011).

2.2 YEAST COLONY PCR

Amplification of the kanamycin cassette and confirmation of correct gene replacement were both performed by colony PCR, a method adapted from the Eckdahl lab website at Davidson-Missouri Western State University (Eckdahl 2014). Oligonucleotides were designed to PCR-amplify the appropriate region from the appropriate BY4741 knock-out strain including the kanamycin cassette plus upstream and downstream flanking regions of at least 50 nt for each gene of interest. A second set of oligonucleotides lying outside of the transformation cassette was designed to confirm proper gene replacement. Primers used are listed in the Appendix.

For colony PCR, a small amount of cells was transferred with a sterile pipette tipfrom a plate to the bottom of a PCR tube and placed in -80°C for 15 min before microwaving at full power for 1 min. Cells were then placed on ice. The PCR reaction was prepared as follows: 25 µl of Phusion Master mix (NEB), 0.3 µl of mixed 100 µM oligonucleotides, and 24.7 µl ddH_2O. The starting thermocycler program used was: 98°C for 10s for initialization, followed by 30 cycles of 10 s at 98°C, 30 s at 55°C and 45 s at 72°. The

final elongation step was 5 min at 72°. Denaturing and annealing times and temperatures were adjusted as required by the primers used and length of the expected product.

2.3 YEAST TRANSFORMATION

Yeast strains were transformed by adapting a method previously described (Agatep et al. 1998). Each yeast strain to be transformed was streaked out onto 2% agar YPG plates (Yeast Peptone with 2% glycerol as carbon source) and grown at 30° C for 2-3 days. Isolated colonies were used to inoculate 50 ml of YPD (Yeast Peptone with 2% glucose) and grown at 30° C overnight with shaking. The following morning, the $O.D._{600}$ of the culture was measured and the volume equivalent to 2.5×10^8 cells was diluted in 50 ml total volume of pre-warmed YPD, giving a starting titer of about 5×10^6 cells/ml ($O.D._{600} = 0.5$). A culture was grown 3-5 h to $O.D._{600} = 2$, yielding approximately 2×10^7 cells/ml. (For most strains, an $O.D._{600} = 0.1$ corresponds to approximately 1×10^6 cells/ml.) The culture was centrifuged in a 50 ml conical tube in a Sorvall JA14 at 3,000 rpm for 5 min at 25°C. The resulting pellet was resuspended in 25 ml of ddH_2O and centrifuged a second time at 1,000 rpm for 4 min. The washed pellet was resuspended in 900 µl of ddH_2O and transferred to a 1.5 ml microcentrifuge tube. The cells were then pelleted at 13,000 rpm for 1 min in an Eppendorf microcentrifuge 5424 and the resulting supernatant removed by pipetting. The cells were resuspended in approximately 700 µl 0.1 M LiAc to a final volume of 1 ml and incubated at 30°C for 10 min. For each 1X transformation reaction, 100 µl of the LiAc cell suspension were aliquotted into a fresh microcentrifuge tube. The cells were then pelleted at 13,000 rpm for 1 min in a microcentrifuge and the supernatant was discarded. The following reagents were added to the pellet in the following order: 240 µl of 50% polyethelene glycol (3350 PEG); 36 µl of 1M LiAc; 10 µl of 10 mg/ml single-stranded carrier DNA (Sigma-Aldrich); 100 ng of the

DNA being transformed; and sufficient ddH_2O to bring the total volume to 360 µl. The tubes were vortexed vigorously until cells had been resuspended, then incubated at 30°C for 30 min. Cells were heat-shocked in a 42°C water bath for 30 min. Cells were pelleted at 13,000 rpm in a microcentrifuge for 1 min then resuspended in 1 ml YPD and incubated on a rocker overnight at 30°C. Transformants were selected by plating the cells onto selective media as required, either YPD/G418 or HC/Ura$^-$/Glu (Hartwell Complete media lacking uracil with 2% glucose) (Amberg et al. 2005) and grown for 2-3 days.

2.4 TOTAL RNA ISOLATION

Cultures were grown in 30 ml YPR (Yeast Peptone with 2% raffinose) or HCR/Ura-(Hartwell's Complete defined medium lacking uracil with 2% raffinose) in 250 ml Erlenmeyer flasks in a 30°C shaker for 20 h or to $O.D._{600}$ = 0.5 – 0.8. Cells were centrifuged in a Sorvall JA14 rotor at 5,000 rpm in 50 ml conical tubes for 4 min at room temperature, and the resulting pellets resuspended in 400 µl of AE buffer (50 mM NaOAc pH 5.3, 10 mM EDTA), then transferred to a 1.5 ml microcentrifuge tube. Pellets that were not used immediately were stored at -80° in 25% glycerol for later use. (Frozen pellets that had been stored in glycerol were centrifuged at 13,000 rpm for 2 min to remove glycerol. The pellets were then resuspended in room temperature AE buffer and brought to 30° for 15 min prior to continuing with the preparation as described here.) Cells were centrifuged at 5,000 rpm for 6 min and the resulting pellet resuspended in 400 µl AE buffer plus 40 µl of 10% SDS. This and subsequent centrifugations were performed in an Eppendorf microcentrifuge. Tubes were vortexed vigorously for 1 min. To remove DNA, 550 µl of acid phenol (pre-equilibrated with AE buffer; Ambion/Life

Technologies) were added to the tube, which was then vortexed for an additional 3-4 min and incubated in a 65°C water bath for 4 min. The tube was chilled in a dry ice/ethanol bath until phenol crystals appeared (about 5 min) then centrifuged at 12,000 rpm for 6 min at room temperature to separate the phenol and aqueous phases. The upper aqueous phase (400-500 μl) was transferred to a fresh microcentrifuge tube leaving some aqueous layer behind to minimize the likelihood the sample contained contaminating protein. The sample was extracted with equal volume (~500 μl) phenol/chloroform/isoamyl alcohol (25:24:1) (Ambion/Life Technologies) at room temperature for 5 min, then centrifuged in a microcentrifuge at 12,000 rpm for 6 min to separate the phases. The upper aqueous phase was again transferred to a fresh microcentrifuge tube, taking the same precautions as before. 40 μl of 3 M NaOAc, pH 5.3 and 2.5 volumes (1 ml) ice cold 100% ethanol were added to the sample to precipitate the RNA. The tubes were left at -80° for at least 1 h prior to pelleting in an Eppendorf 5415 microcentrifuge at 13,000 rpm at 4°C for 20 min. The supernatant was discarded and the resulting pellet was washed with 1 ml ice cold 70% ethanol, then repelleted at 12,000 rpm at 4°C for 5-10 min. As much of the ethanol as possible was removed by pipetting without disturbing the pellet. The pellet was resuspended in a volume of Rnase-free Millipore ddH_2O to give RNA concentrations between 2.0-2.9 μg/μl at 260 nm as determined by Nanodrop 1000 (Thermo Scientific).

2.5 NORTHERN HYBRIDIZATIONS

For Northern hybridization, cells were grown and RNA isolated as described above. Samples containing 1.2 μg of RNA were denatured by incubation with 20%

(vol/vol) glyoxal at 65 °C for 15 min and electrophoresed in an RNA-grade 1.5% agarose gel with 1× TAE buffer (40 mM Tris–acetate, pH 8 and 1 mM EDTA) at 25 °C. The gels were blotted onto a nylon membrane (Hybond-XL; GE Healthcare) overnight, UV crosslinked (Stratogene Stratolinker 2400), and hybridized with a 5′-^{32}P-end-labeled DNA oligonucleotide probe as detailed in Table 2.1. Following overnight hybridization, the membrane was scanned with a PhosphorImager (Amersham), visualized with Canvas 9 software (ACD Systems of America), and measured with GelQuant.NET software provided by biochemlabsolutions.com.

2.6 PREPARATION OF INTERNALLY-LABELED PCR PROBES

The PCR reaction was prepared as follows: 9.25 µl ddH_2O, 2.0 µl ThermoPol buffer (Invitrogen), 0.2 µl PCR template (prepared from the wild-type strain), 0.5 µl each of 10 mM dATP, dCTP, and dGTP, 0.25 µl 1 mM dTTP, 6.0 µl α–^{32}P dTTP (Perkin-Elmer),0.5 µl Taq DNA polymerase (Invitrogen), 0.3 µl 100 µM mixed oligonucleotides (seeTable 2.1) for a total reaction volume of 20 µl. The thermocycler program used was: 94°C for 60s for initialization, followed by 25 cycles of 45 s at 98°C, 45 s at 55°C and 60 s at 72°. The final elongation step was 7 min at 72°. Denaturing and annealing times and temperatures were adjusted as required by the primers used and length of the expected product. The PCR product was cleaned with a Qiagen PCR Clean-up kit, eluting in 30 µl ddH_2O, and then incubating the eluate at 95°C for 10 min prior to use.

2.7 ISOLATION OF MITOCHONDRIA

Overnight starter cultures were grown with shaking (200 rpm) at 30° in 50 ml HC /Ura$^-$ media using 2% glucose as the carbon source. 1 ml of starter culture was inoculated into 1 l of HC/Ura$^-$ media with 2% raffinose and grown to an $O.D._{600}$ of ~3.0 The cells were pelleted in a Beckman Avanti J-20I JLA 8.1 rotor at 3,500 rpm at 6° for 5 min and kept on ice until cultures for that day's experiments reached the appropriate $O.D._{600.}$ Pellets were then resuspended in 100 ml of room temperature TE resuspension buffer (10 mM Tris, pH 9.5; 1 mM EDTA, pH 7.5) plus 0.5 ml β-mercaptoethanol, transferred to 250 ml centrifuge bottles and centrifuged again at 3,500 rpm in a Beckman Avanti JA14 rotor for 5 min at 25°. Pellets were then resuspended in 25 ml of citrate buffer (1.2 M sorbitol, 26 mM K_2HPO_4, 20 mM citrate monohydrate, 1.26 mM EDTA, adjusted to pH 5.8 with NaOH) and centrifuged once more under the same conditions. Each pellet was then resuspended in 50 ml of citrate buffer plus 1 ml (5,000 units) lyticase (Sigma) in H_2O and incubated for 30 min in a 30° water bath. A 50 μl aliquot of cells mixed with 10 μl of 10% SDS was tested for cell lysis, indicative of protoplast formation. Protoplasts were centrifuged at 3,500 rpm for 5 min at 4°, then carefully resuspended in 25 ml 15% sucrose plus 20 ml acid-washed glass beads (425-600 μm, Sigma) and mixed by hand for 3 min. The supernatant was transferred to a fresh 250 ml Beckman bottle. The beads were washed 2X with 50 ml 15% sucrose with both washes combined with the supernatant in the fresh bottle. This was centrifuged in Beckman rotor JA14 at 3,500 rpm for 5 min at 4° with the resulting supernatant once again being transferred to a fresh 250 ml Beckman

bottle. This was then centrifuged in Beckman rotor JA14 at 13,000 rpm for 15 min at 4° retaining the resulting pellet and discarding the supernatant. The pellet was carefully resuspended in the residual 15% sucrose and transferred to a 25 X 89 mm Ultra-Clear™ ultracentrifuge tube (Beckman). 12 ml of 65% sucrose (65% sucrose, 10 mM tricine, 0.05 mM EDTA, pH 7.5) were added a bit at a time with stirring. This was overlaid with 12 ml 53% sucrose (53% sucrose, 10 mM tricine, 0.05 mM EDTA, pH 7.5), followed by a 13 ml layer of 44% sucrose (44% sucrose, 10 mM tricine, 0.05 mM EDTA, pH 7.5). The tubes were centrifuged in a Beckman Optima LE-80K ultracentrifuge SW28 rotor at 27,000 rpm for 2 h 10 min at 4°. Intact mitochondria migrated to the interface between the 44% and 53% sucrose phases and were moved to a 15 ml conical tube. The mitochondria were gently mixed with an equal volume (about 5 ml) of HKCTD (0.5 M KCl, 0.05 M $CaCl_2$, 0.025 M Tris-HCl pH 7.5). Following a 15 min centrifugation at 13,000 rpm at 4°, the supernatant was discarded and the mitochondrial pellets were stored at -80° until use.

2.8 RIBONUCLEOPROTEIN (RNP) PREPARATION

RNP preparations and analyses were performed by Dr. Georg Mohr following a method previously described (Kennell et al. 1993). Yeast strains were grown to early log phase in YPR and mitochondria were isolated as described above. Mitochondria were resuspended in HKCTD and lysed with 0.2% Nonidet P40. The lysates were layered over 1.85 M sucrose cushions containing HKCTD and centrifuged in a Beckman Optima LE 80K ultracentrifuge using rotor SW28. Following a 17 h spin at 50, 000 rpm at 4°, the

clear, gelatinous pellet was washed three times with Rnase-free ddH_2O, then resuspended in 10 mM Tris-HCl pH 7.5 and 1 mM DTT and transferred to a microcentrifuge tube and placed on ice. Resuspended RNP particles were stored at -80° until use.

2.9 CONSTRUCTION OF *OXA1* MUTANTS

The *OXA1* gene was amplified from the wild-type 1^+2^+ strain by colony PCR using oligonucleotides (Table 2.1) that were designed to allow directional cloning into the BamHI and SacI sites of the multi-cloning site (MCS) in yeast CEN plasmid pRS416 (Agilent Technologies). This vector contains an ampicillin cassette for selection of *E. coli*, and a *URA3* marker for auxotrophic selection of yeast in Ura^- media. Deletions of the Loop 1 and the C-terminal domains in Oxa1 were engineered by PCR stitching (Table 2.1) and cloned into pRS416 at the same restriction sites. Following sequence confirmation, plasmids were transformed by standard protocol as described above into *oxa1*Δ mutants of the single-intron strains 161-U7/aI5γ and 161-U7/bI1 and the *oxa1*Δ isogenic intronless strain (I^0) used as control.

2.10 TOTAL PROTEIN ISOLATION

For Western blots, whole-cell proteins were isolated by trichloroacetic acid (TCA) precipitation (Yaffe and Schatz 1984). Briefly, 3 $O.D._{600}$ units of culture were collected and pelleted at 1,000 x *g* in an Eppendorf 5424 tabletop microcentrifuge for 5 min. The pellet was resuspended in 1 ml of H_2O and 160 µl of freshly-prepared SB buffer (1.85 M NaOH, 7.4% β-mercaptoethanol) and moved to a 1.7 ml microcentrifuge tube.

After 10 min on ice, 160 µl of 50% trichloroacetic acid was added to the slurry and the tube was returned to sit on ice for another 10 min. Following a 2 min microcentrifugation, the supernatant was discarded. The pellet was washed (not resuspended) with 0.5 ml 1 M Tris-base (pH not adjusted), then centrifuged at top speed for 15 s and the supernatant discarded. The protein pellets were dissolved in 150 µl of SDS-PAGE sample buffer (50 mM Tris-HCl, pH 6.8; 2% SDS; 10% glycerol; 1% β–mercaptoethanol; 12.5 mM EDTA).

2.11 WESTERN BLOT ANALYSIS

Samples (~60 µg of protein measured as $O.D._{280}$ by Nanodrop) were run in a pre-cast 4–20% polyacrylamide gradient gel (NuPAGE BioRad) with 0.1% SDS in the running buffer and transferred to a Sequi-Blot™ polyvinylidene fluoride membrane (PVDF) membrane (BioRad) using a BioRad Criterion blotter apparatus. The membrane was cut and the top portion probed with a guinea pig anti-Mss116 antibody (1:5,000 dilution) (gift of the Perlman lab; (Huang 2004)) while the lower portion was probed with mouse anti-porin antibody (Abcam) to confirm equal loading when needed. Each membrane was developed using an ECL Plus Western Blotting kit (GE Healthcare), and imaged using a Cell Biosciences (Santa Clara, CA) HD2 imager or Kodak Biomax XAR film. Afterward, the membranes were stripped of antibodies with Restore™ Plus Western Blot Stripping Buffer (ThermoScientific, Waltham, MA) and stained with AuroDye Forte (GE Healthcare) or Colloidal Gold Total Protein Stain (Bio-Rad), following the manufacturers' directions, to additionally confirm equal loading of protein samples.

2.12 FRACTIONATION OF MITOCHONDRIAL INNER MEMBRANE

This method was adapted from one described by the Martinou lab (Da Cruz et al. 2003). Mitochondria were isolated as described above from 5 l cultures of isogenic aI5γ strains with wild-type and *oxa1*Δ nuclear backgrounds grown in YPR at 30° C with shaking to $O.D._{600}$ = 3.0. Mitochondrial pellets were resuspended in 0.2 mM phenylmethanesulfonylfluoride (PMSF) and ddH_2O to a concentration of 5 mg/ml and stirred on ice for 20 min. The suspension was homogenized 20 times with a Dounce homogenizer and centrifuged at 15,000 rpm for 10 min at 4°. The resulting mitoplasts were treated with 0.1 M Na_2CO_3, pH 11.5 at a final concentration of 0.5 mg/ml for 20 min on ice. Each mixture was transferred to a thick walled 25 X 89 mm Beckman Ultra-Clear™ polycarbonate tube. The mitochondrial inner membrane proteins were pelleted at 24,000 rpm at 4° for 30 min in a Beckman Optima LE 80K ultracentrifuge using rotor SW28. The pelleted proteins were resuspended in 2X sample buffer (0.1% digitonin, 20% glycerol, 120 mM Tris-HCl, pH 6.8) and run approximately 1 cm on a 4-12% Bis-Tris NuPAGE gel. Following staining with fresh Coomassie blue, the large protein band was cut from the gel and submitted to the University of Texas at Austin Protein Facility for in-gel digest, then run on the Dionex LC and Orbitrap Elite for LC-MS/MS with a 30 min run time. The SEQUEST HT analysis references both the SwissProt protein database and the yeast database for protein identification.

2.13 MODULATING *MSS116* EXPRESSION

For experiments to determine Mss116 abundance, *MSS116* was digested from plasmid pHRH197 (Huang et al. 2005) using restriction enzymes HindIII and SacI and cloned behind a calibrated set of Translation Elongation Factor (TEF) promoters in plasmid p416-TEF-yECitrine that had been engineered to vary in strength (Alper, et al. PNAS, 2005) by replacing the original citrine reporter gene with *MSS116*.

Mutations in the *MSS116* promoter were constructed in plasmid pHRH197 (Huang et al. 2005). For the deletion of the region flanked by the two ClaI sites (-704/356), pHRH197 was digested with ClaI and 29runk29ted by standard methods. This plasmid, pRZW212, was then used as the template for the remaining deletion constructs. To delete various portions of the *MSS116* promoter, stitch PCR was used with oligonucleotides listed in Table 2.1 and cloned into plasmid pRZW212. Sequence-verified plasmids amplified in *E. coli* (DH5α) with selection on LB/Amp^R plates. Plasmids were transformed into the 1^+2^+ *mss116*Δ strain using the yeast transformation protocol described above. For subsequent Western blots, cultures were grown at 30°C in 30 ml HC/Ura^- media, with 2% raffinose as carbon source to $O.D._{600}$ = 1.5.

2.14 CONSTRUCTION AND EXPRESSION OF TAP-TAGGED WILD-TYPE MSS116

Tandem Affinity Purification (TAP)-tagged Mss116 proteins were expressed from plasmid HRH197, a derivative of the centromeric shuttle vector pRS416 (Agilent Technologies) that contains an amp^R marker for *E. coli* (DH5α) selection and a *URA3* marker for yeast selection on media lacking uracil. The TAP tag was PCR-amplified from

a commercially available strain (GE Healthcare) using oligonucleotides that allow for in-frame, directional cloning into plasmid HRH197, harboring the full length *MSS116* gene and upstream promoter region. The plasmids were transformed into the $1^{+}2^{+}$, I^{0}, and single-intron aI5γ ρ^{-} and bI1 ρ^{-} strains, all of which had nuclear background *mss116*Δ , then selected on HC/Ura^{-} agar plates with 2% glucose.

2.15 TANDEM AFFINITY PURIFICATION

TAP-tagged Mss116 proteins were isolated from mitochondria prepared as described above. All the TAP purification steps were carried out at 4° unless otherwise indicated. All rotations were performed on a Labquake rotisserie (Thermo Scientific). The 200 µl mt pellet was defrosted at 30°C or room temperature, moved to a microcentrifuge tube and centrifuged at 12,000 rpm for 5 min. The pellet was immediately resuspended in 3 ml ice-cold solubilization buffer (SB) (20 mM Hepes-KOH, pH 7.4; 250 mM sucrose; 200 mM KCl; 1 mM EDTA; 1 mM spermidine; 7 mM β–mercaptoethanol; 0.2 mM PMSF). 75 µl of 20% NP40 (Sigma) was added slowly, drop by drop to 0.5%, followed by incubation on ice for 15 min. The lysate was split in half, with approximately 1.5 ml in each microcentrifuge tube. These were centrifuged at 20,000 rpm for 10 min, and the clear supernatant moved to a non-stick 1.5 ml Phenix tube (Phenix Research) containing 50 µl pre-washed Protein A Sepharose 4B FF beads. Following a1 h incubation at slow rotation, the supernatant was separated from the beads on a touch spin microfuge and transferred to a fresh non-stick Phenix tube with 25 µl pre-washed IgG Sepharose 6FF beads. (IgG/Sepharose beads were prepared by washing with

NP40 buffer (no inhibitors) to remove ethanol and resuspended in 1:1 slurry with NP40 buffer.) Following a 3 h rotation, the supernatant was discarded. Beads were washed 5 times with 1.5 ml SB + 0.1% NP40, lacking EDTA (wash buffer). The beads from both tubes were combined into a 0.6 ml non-stick Phenix microcentrifuge tube, and resuspended in 500 µl wash buffer containing 10 µl AcTEV protease (expressed in *E. coli* and purified by Lilian Lamech). Following a 6 h incubation with rotation, the eluate was separated from the beads using a touch spin microfuge. The eluate was transferred to a fresh 0.5 ml tube containing 25 µl Calmodulin Sepharose 4B beads pre-washed with wash buffer containing 2 mM $CaCl_2$ and allowed to incubate for 3 h with rotation. The beads were washed 5 times with wash buffer and 2 mM $CaCl_2$, followed by 2 washes with $CaCl_2$-free buffer. The protein was eluted from the beads by boiling in 30 µl of NuPAGE LDS loading buffer (Life Technologies). 15 µl were used for visualizing the polypeptides separated by electrophoresis in a 4-12% Bis-Tris NuPAGE gel (Life Technologies) and stained with fresh Coomassie blue. The remaining 15 µl were loaded onto a separate gel and run approximately 1 cm, and stained with fresh Coomassie blue. The large protein band was sliced from the gel and submitted to the University of Texas, Austin, Protein Facility for LC-MS/MS analysis as described above.

2.16 PROTEIN ANALYSIS

The software used to validate MS/MS peptide and protein identifications was Scaffold (version 4.4.1.1, Proteome Software, Inc, Portland OR). Protein identifications were considered valid if they were comprised of at least two identified peptides at a

greater than 97% probability. Proteins were annotated with terms from gene_association.goa_uniprot (downloaded Jul 14, 2014) (Ashburner et al. 2000).

2.17 OLIGONUCLEOTIDES USED IN THIS STUDY

The oligonucleotides used to PCR amplify the kanamycin cassette from the commercial strains as described in section 2.2 are listed in Appendix B. In the table below are the oligonucleotides used for Northern hybridizations and cloning in this study.

***COX1* exons**	
E1(s)	AGTGGTATGGCAGGAACAGC
E2 (as)	CATTAATACAGCATGACCAACTAC
E3 (s)	GTAATGCCTGCTTTAATTGGAGG
E3 (as)	CCTCCAATTAAAGCAGGCATTAC
E4 (as1)	CTACACTAGGTCCTGAATGTGC
E4 (as2)	GCTCGTATAAGATTGGGTCACC
E5a 8377 (as)	GGAATTGCAATAATCATTAGTGCAG
E5b (as)	GTGGAATGCTACATCTAATGAG
E5g 11505 (as)	ATGTCCCACCACGTAGT
E6 (as) terminal exon probe	GAATAATGATAATAGTGCAATGAATGAACC
***COX1* introns**	
aI1 851 (as)	GTTTCTAATGTTGTACCTGGAG
aI2 270 (as)	GAATAAACAGAGATATGTTTATC
aI3 (as)	GCTAAATAAGGTCCCAACTTATC
aI3 (s1)	GGGTTGAAGATATAGTC
aI3 (s2)	AGAGACTACACGTGTTGCACC
aI4 7432 (as)	CCATCACCATCAATTAATCCAGC
aI5a (as)	TCTATTTGATCTTGGATAAATATC
aI5b TTT (as1)	TAATTATAAGAGTTTCCCCGT
aI5b (as2)	CATTCACGTTTAGTCTCTAC
Snab aI5g (as)	GGTTTATTCTGTTTTATC

***COB* exons**	
E1(s)	GATTCACCACAACCATCATCAATTAATT
E3 (as)	CCCACCTCATAATCAAGATACAATATC
E4 (as)	GCAAAGAATCTCTGGATTAGAGGGTT
E5 (as)	GGATTACCAGGAATATAGTTATCAGG
E6 (s)	GTACCTGAATGATACTTATTACCATTCTATGC
E6 (as) terminal exon probe	AATGTAGCGATTTGTCCCATTAAGAC
***COB* introns**	
bI1 (s)	GTGAGACAAGTATAAGTATATTATT
bI1 170 (as1)	TACGCTATCCATATGAATCTTACC
bI1 714 (as2)	CCACTCAGAACTGTACGTACTACTTTCA
bI2 (as)	CCTTTTCTTTTTTCAGCATGACCATCTCC
bI3 (as)	GAGTATTAAATGGTTTAATAGGACG
bI4 (as)	ATAGTACCATCAGCATCAAAGAACC
bI5 (as)	CCTTATGGGAGTTCCCACAAAGCGG
***21srRNA* non-coding exon**	
21s rRNA 3-640 (as)	GCAACATCAACCTGTTCGATCG
***21s rRNA* intron (omega)**	
21s rRNA 746 (as)	TCTCATTTACCTCCATCATCT
***COX2* (as)**	AGGTAATGATACTGCTTCGATC
RF1 (s)	CTGAAGGTTCATTTGATCTATCTCC
RF1 (as)	AGAGCTGCTGGTCTATAACCAG

Table 2.1: Oligonucleotides used for Northern hybridizations and cloning in this study

OXA1 deletion mutants	
BamHI wtOxa1 (s-1)	ATTGGATCCTCAGTCAGTCAGACGTGTTCCGTTCTTATGTTCG
DeltaLoop1 (as-2)	GCCATCTGTTAACAGTATCAGAGGACTTGACATAGAGGGGAA
DeltaLoop1 (s-3)	TCTGATACTGTTAACAGATGGCTGGCCGCACC
Myc (s-5)	TTCTGAAGAAGATCTGTGAATAAAGGCTCTATATCTCTCTGT
Myc (as-6)	TTCACAGATCTTCTTCAGAAATAAGTTTTTGTTCTTTTTTGTTATTAATGAAGT
Myc 34runk (s)	AAACAAATGGGAACAAAAACTTATTTCTGAAGAAGATCTGTGAATAAAGGCTCTA
Myc 34runk (as-8)	AATAAGTTTTTGTTCCCATTTGTTTCTCAAAATCATTGTCTGTAGGACGGA

Mss116 promoter mutants	
ClaI KasI	CGG TAT CGA TTT TGC TGG CGC CGG AG
KasI MscI	CGC TGG CGC CGG ATG ATG GCC ACT A
ClaI MscI	CGG TAT CGA TTT TTG ATG GCC ACT AT
Mss116 promoter deletion stitch PCR primers	
BsrGI del 5' R-10	TGC TGT ACA GGA GTT AAA CCG GGA AAT TCC ATC CTG
ClaI del 5 F-9	GGT ATC GAT ATG TTG ACC TCT ATA TTG ATA AAA GGT CGC ACA

TAP tagged Mss116	
Mss116 1536 Xba1F	ATAAAATCTGAGGTTCTAGAGGC
Mss116 3'TAPstopR2	CCGCGGCTAATTCGCGTCTA
Mss116 3'TAPstopF	TAGACGCGAATTAGCCGCGG
Mss116 R4	GAGCTCCTTCCATCCGTTTAAA

Table 2.1: Oligonucleotides used for Northern hybridizations and cloning in this study

Chapter 3: Screen for nuclear-encoded splicing factors for yeast mitochondrial introns aI5γ and bI1

3.1 BACKGROUND

3.1.1 Screen, Phase I and Phase II

As discussed in the Introduction, earlier work had identified some auxiliary, nuclear-encoded splicing factors specific for several yeast mt introns, though none have yet been found for any group II intron (Fig.1.3). Many of these nuclear-encoded splicing factors were identified by comparing a knock-out strain harboring introns that was unable to grow on glycerol to an isogenic strain without introns that maintained that ability (Seraphin et al. 1989; Barros et al. 2006; Turk and Caprara 2010). This type of screen was based on the fact that yeast with dysfunctional mitochondria cannot carry out oxidative phosphorylation, but get energy from fermentation instead. Consequently, dysfunctional strains cannot grow on non-fermentable carbon sources like glycerol, lactate, or ethanol. This method, however, fails to uncover dual-functioning proteins whose primary role may be required for respiration.

To better detect other candidate splicing factors, a more sensitive screen was devised and used here: Using the commercially-available knock-out collection of strain BY4741 (GE Healthcare Healthcare Open Biosystems), known mitochondria-localized proteins were tested for a glycerol growth defect. This haploid strain harbors all known introns within the *COX1* and *COB* genes. Those 466 strains that had a mild-to-severe glycerol growth defect, but maintained wild type mtDNA ($gly^{-/+}/\rho^{+}$) comprised Phase I of the study and was conducted by Tarah Nyberg in lab of Dr. Philip Perlman. The

remaining 163 strains that failed to grow on glycerol and had defective mtDNA (gly^-/ρ^-) (see Appendix) comprised the candidate pool of this, Phase II of the screen for my dissertation research. During Phase I of the screen, the nuclear deletions in BY4741 were tested by Northern hybridization for the effect each deletion had on the various *COX1* and *COB* introns. Ten splicing factors were identified, of which five had been previously unknown (Nyberg 2006). One candidate, Mne1, was observed to be defective for splicing of the group I intron, aI5β. This protein was further examined in this study and the results will be discussed in Chapter 6. Among the ten identified candidate factors, only Mss116, a previously identified general RNA chaperone, was found to be required for splicing aI5γ and bI1, the two yeast mt group II introns that do not encode maturases (Nyberg 2006).

In Phase II of the screen, I focused on these two introns whose lack of intron-encoded maturases makes their study of particular interest. To do this, I used single-intron strains that contained only the introns aI5γ or bI1. Using Northern hybridization analysis, I tested the effect of the deletion of nuclear-encoded mitochondrial proteins on the splicing of these group II introns.

3.1.2 The processing of the *COX1*, *COB* and *COX2* transcripts

The 6.6-kb primary transcript for the *COX1* gene is a polycistronic message that includes *ATP8* and *ATP6* (Osinga et al. 1984) (Fig.3.1A). The 161-U7 strain used here does not have the *ENS* gene sometimes found downstream of *ATP6* in some yeast strains. In the single intron aI5γ strain, the *COX1* precursor is 3.1 kb which, after endonucleolytic

cleavage between *COX1* and *ATP8*, releases the individual mRNAs (Simon and Faye 1984). Following the excision of the 886-nt intron, the 2.2-kb mature mRNA results. In the Northern hybridizations that follow, these various RNA species were visualized by using a ^{32}P-labeled DNA oligonucleotide complementary to the terminal exon of *COX1* (small arrow below *COX1* in the figure).

The *COB* 8.4-kb primary transcript is bicistronic, also containing the upstream *tRNA(Glu)* gene (Fig. 3.1B). The primary *tRNA(Glu)/COB* transcript undergoes several processing events, including removal of the 71-nt *tRNA(Glu)* transcript and production of the mature 5' end of the *COB* mRNA (Mittelmeier 1993; Chen and Dieckmann 1994), generating the 3.0- and 2.9-kb precursors (Pre-1 and Pre-2). The mature 2.2-kb mRNA is generated with the excision of the 0.8-kb bI1 intron. In the Northern hybridization analyses that follow, these various *COB* RNA species were visualized by using a ^{32}P-labeled DNA oligonucleotide complementary to the terminal exon of *COB* (small arrow below *COB* in the figure).

The 0.9-kb mature *COX2* mRNA originates from the processing of a biscistronic 2.5-kb primary transcript also containing an uncharacterized, maturase-like ORF, *RF1*, (Fig. 3.1C). The 5´ end of *RF1* overlaps the 3´end of *COX2* and is indicated in the figure by a stippled rectangle. *COX2* is processed 75 nt downstream of its stop codon (first dodecamer lollipop), well into *RF1*, truncating that putative protein (Bordonne et al. 1988). In the Northern hybridization analyses that follow, the two *COX2* RNA species were visualized by using a ^{32}P-labeled DNA oligonucleotide complementary to the 3´ region of *COX2* just upstream of the *RF1* overlap (small arrow below *COX2* in the

figure). The *RF1* RNAs were probed using a ^{32}P-labeled DNA oligonucleotide complementary to its 3′ end (small arrow below *RF1* in the figure).

3.2. RESULTS

3.2.1. Deletion of many ribosomal proteins causes processing and splicing defects

Among the first genes in the screen to be deleted were those encoding mitoribosomal proteins. I deleted these genes in both the 161-U7/aI5γ and 161-U7/bI1 strains. Mitoribosomal proteins are nuclear-encoded, translated in the cytosol and subsequently imported into the mitochondrion for assembly into the mature mitoribosome. During the course of evolution, there has been a considerable amount of change to the mitoribosome when compared to its bacterial predecessor, presumably in adapting to expressing the largely hydrophobic proteins of the electron transport chain in the mt inner membrane (Smits et al. 2007; Amunts et al. 2014).

Loss of mitoribosomal proteins from both the large and small subunits were found to cause splicing defects of varying degrees. Of the 18 mitoribosomal proteins tested, 14 (77%) caused splicing defects, in the splicing of both aI5γ and bI1, as observed in the Northern hybridization analyses in Figs. 3.2 and 3.3, respectively. The degree of the defect was measured using GelQuant.net software (BioChem Lab Solutions) with two values were calculated for each: The percentage of splicing as a ratio of the signal of the mRNA band to that of the mRNA and precursor signals combined (upper value); and the ratio of the mRNA to the combined signals of mRNA, precursor and primary transcripts

(lower value). Unless otherwise stated, the values referred to below are those of the first category.

3.2.1.1 Effect of the deletion of mitoribosomal proteins on COX1 processing and aI5γ splicing

In the Northern blot in Fig. 3.2 (and others to follow), the 6.6-kb unprocessed *COX1* primary transcript is visible as the uppermost band in many of the deletion strains, though the band is not evident in wild type. Immediately beneath this band, the faint band of the polycistronic transcript following excision of the aI5γ intron is visible in most of the deletion mutants. The next main band down is the *COX1* precursor at about 3.1 kb, which, with the excision of the 0.89-kb aI5γ intron, generates the lowest band on the membranes, the 2.2-kb mature mRNA. Note that in the wild-type aI5γ strain, a small fraction of precursor remains visible, yet the ratio of mature mRNA to precursor is high.

In contrast to the typical aI5γ splicing observed in the wild-type strain, deletion of most of the mitoribosomal proteins tested caused splicing defects resulting in reduced levels of mature mRNA. In the wild-type, single-intron aI5γ strain, there often remains a small amount of precursor RNA containing unspliced intron; however, the ratio of mature to unspliced precursor RNA is high at 88% (Fig.3.2, lane 1). In contrast, deletion of most of the tested mitoribosomal proteins resulted in lower ratios (mean value = 60%) of mature to precursor RNA (Fig. 3.2, lanes 2-15.)

The unprocessed *COX1* primary transcript is not evident in the wild-type strain (Fig. 3.2, lane 1), but is clearly apparent to varying degrees in all of the mitoribosomal

protein deletion strains exhibiting a splicing defect. This suggests a direct or indirect role for either the individual ribosomal proteins or the ribosome as a whole for primary *COX1* transcript processing. The presence of the faint secondary band beneath the primary transcript and the significant amount of visible precursor, indicate that splicing of aI5γ can occur prior to the complete endonucleolytic processing of the primary transcript.

The strongest splicing defect among this set of proteins were observed with the deletion of mitoribosomal protein Mrp10 which exhibited 36% splicing (Fig. 3.2, lane 5). Mrp10 is a small subunit protein with a conserved CHCH domain [coiled coil 1]-[helix 1]-[coiled coil 2]-[helix 2] that, unlike other CHCH proteins, is not confined to the inner membrane space (Jin et al. 1997). Though the Mrp10 protein is well-conserved among eukaryotes and is found to be essential for yeast mt translation, a BLAST search revealed no known bacterial homologs (Smits et al. 2007), suggesting this protein may have evolved to be mitochondria-specific.

Though the deletion of Mrpl13 did not cause as severe a splicing defect as did Mrp10, it nonetheless produced a significant defect at 40% splicing (lane 8). Mrpl13 is an organelle-specific protein found within the mitoribosomal tunnel exit (Gruschke et al. 2010). Interestingly, this protein is not strictly essential for mitochondrial translation (Grohmann et al. 1994), suggesting that this protein may have a secondary role, one that may be associated with splicing.

The mitoribosomal proteins whose deletion caused the weakest splicing defects were Img2 (80%), Mrp1 (72%), and Mrp17 (68%) (lanes 3,4, and 6, respectively). However, these strains also had among the weakest *COX2* signals (discussed below).

Deletions of other mt ribosomal protein genes resulted in intermediate splicing defects ranging between 41%- 56%. Compared to the 88% splicing displayed by the wild-type strain, these data suggest some mitoribosomal proteins play a role in aI5γ splicing.

3.2.1.2 Effect of the deletion of mitoribosomal proteins on bI1 splicing

In the Northern hybridization analysis in Fig. 3.3, the 8.4-kb primary transcript is not evident in either the wild-type or derivatives of that strain with deletions of mitoribosomal proteins. This suggests that processing of the primary *COB* transcript, unlike that of *COX1*, is not dependent on any of the tested mitoribosomal proteins. The 3.0-kb precursor (Pre-1) can be observed as the faint uppermost band in many of the mutants, although the 2.9-kb precursor (Pre-2) is more readily apparent. With the excision of the 0.8-kb bI1 intron, the mature *COB* transcript is 2.2 kb, similar in size to the *COX1* mRNA, and is observed as the lowest, most prominent band in the wild-type strain (lane 1).

Among the mitoribosomal proteins tested, the strongest bI1 defects were also those that exhibited the strongest defects in aI5γ splicing—Mrpl10 and Mrpl13, with 54% and 57% splicing, respectively (lanes 5 and 8). Deletion of Mrp1 produced a defect similar to that of Mrpl13 with 58% splicing (lane 4). *MRP1* has been shown to exhibit genetic interactions with *PET122*, which encodes a *COX3*-specific translational activator (Haffter et al. 1991).

Deletion of the genes of two mitoribosomal proteins, *IMG2* and, *MRPL11,* exhibited the highest ratios of bI1 splicing ability at 84% and 90%, respectively (Fig. 3.3, lanes 3 and 7). However, these two also exhibited severely reduced levels of RNA as observed by the weak *COB* and *COX2* hybridization signals.

In general, deletion of mitoribosomal proteins had a similar effect on bI1 splicing as on that on aI5γ, though less severe. The ratio of spliced to unspliced precursor is 99% in wild-type bI1 splicing, while the mean value exhibited by the tested deletion strains was 66% splicing, slightly better splicing than the observed 60% mean value for aI5γ with the same deletions.

3.2.1.3 Deletions of many mitoribosomal proteins cause a more severe COX2 processing defect in aI5γ-containing strains than in bI1-containing strains.

The intronless *COX2* mRNA is routinely used as a loading control in yeast mitochondrial studies. With the Phase II proteins having been chosen based in part on their deletion triggering cells to become petite, I exercised care to grow the cells for short periods of time. Nonetheless, many times, the Northern hybridizations detected only low levels of mtRNA, despite normalization of total whole cell RNA. Thus, it was particularly important to test for *COX2* levels, especially in cases such as those where hybridization signals were weak. Unexpectedly, the deletion of the genes of several mitoribosomal proteins also caused a processing defect in *COX2*, as seen in the lower panels of 3.2 and 3.3. To compensate for this effect, I used the total amount of *COX2*, both primary and mature, relative to that of wild-type for loading control values (% total:

WT, bottom panels in Fig 3.2 and Fig. 3.3). The weak *COX1* signals exhibited by *img2Δ* and *mrp1Δ* in lanes 3 and 4 of Fig. 3.2, and *img2Δ* and *mrpl11*Δ in lanes 3 and 7 of Fig. 3.3 are likely a result of the cells becoming ρ^- with the loss of the portion of the mt genome that includes *COX2*. This result was expected for *img2Δ*; its protein is known to be required for mt genome maintenance (Coppee et al. 1996). The signal is almost completely lacking in both its primary and mature form. Interestingly, deletion of most of the mitoribosomal proteins that cause a *COX1* processing defect also cause a similar processing defect in *COX2*.

In Fig. 3.4, a comparison of both *COX2* Northern hybridizations strains aI5γ (A) and bI1 (B) indicate that deletions in the aI5γ strains are associated with more severe *COX2* processing defects than in bI1 strains. Two values of *COX2* processing were measured: the percent processing taken as the ratio of mRNA to primary transcript + mRNA (upper value); and this percent processing normalized to wild-type processing (lower value). The mean percentage of *COX2* processing for the aI5γ null mutants was 54% wild type, compared to 79% wild type for the bI1 null strains, an indication that *COX2* processing may be more dependent on proper *COX1* splicing than on *COB*.

The difference, however, may also be, at least in part, a function of the processing efficiencies observed for the wild type of each strain (Fig. 3.4A and B, lanes 1). As seen in the first lanes of each blot, the wild-type aI5γ strain exhibited a 77% processing efficiency compared to the 91% splicing in the wild-type bI1 strain. Since the Cox2 protein is part of the cytochrome *c* oxidase multisubunit holoenzyme, it is possible that

COX2 processing and subsequent translation has a greater dependence on correct *COX1* splicing than on that of *COB.*

3.2.1.4 Deletion of some mitoribosomal proteins does not cause splicing defects

Intriguingly, four of the ribosomal proteins tested did not demonstrate a splice defect: Mrpl38, Sws2, Mrpl36 and Mrpl8. Results of the *mrpl38*Δ and *sws2*Δ strains are shown in the Northern hybridization analyses in Fig. 3.5, with the hybridization for *COX1* in the upper panel in (A), and that for *COB* in the upper panel in (B). Mrpl38 is a universally conserved protein whose bacterial homolog, L14, has been mapped to a central location between the peptidyl transferase and GTPase regions of the large ribosomal subunit (Davies et al. 1996). Sws2/Ynl081C is a putative ribosomal protein of the small subunit with similarities to the bacterial S13 which has been found to function as a control element for translocation of the mRNA-tRNA complex (Cukras et al. 2003).

Interestingly, the loss of neither Mrpl38 nor Sws2 caused a *COX2* processing defect (lower panels of Fig. 3.5A and B), suggesting that there may exist a correlation between proper splicing of the *COX1* and *COB* mRNAs and *COX2* processing.

Deletion of the *MRPL8* gene resulted in loss of mtRNA and consequently no Northern hybridization was possible. Mrpl8, homologous to bacterial ribosomal protein L17, is located near the mitoribosomal tunnel exit (Amunts et al. 2014).

3.2.2 Deletions of several tRNA synthetases cause a splicing defect

In addition to their role in protein synthesis in which amino acids are attached specifically to cognate tRNAs, the diverse group of aminoacyl tRNA-synthetases has

been co-opted to perform alternate activities in the cell including assisting in splicing of group I introns in the mitochondria (Martinis et al. 1999). To date, at least two such dual-functioning fungal mitochondrial splicing cofactor synthetases have been identified: leucyl-tRNA synthetase (LeuRS or Nam2) from *S. cerevisiae* and *S. douglasii* (Herbert et al. 1988; Labouesse 1990; Sarkar et al. 2012) and the tyrosyl-tRNA synthetase (TyrRS or Cyt18) from *Neurospora crassa* (Akins and Lambowitz 1987; Paukstelis and Lambowitz 2008). Both of these synthetases are group I splicing factors.

Here, several mitochondrial tRNA synthetases were tested for the effect of their deletion on aI5γ and bI1 splicing (Fig. 3.6): Mst1 (mt threonyl-tRNA synthetase), Msm1 (mt methionyl-tRNA synthetase), Msd1 (mt aspartyl-tRNA synthetase), Mse1 (mt glutamyl-tRNA synthetase), and Dia1 (probable mt seryl-tRNA synthetase). All exhibited a degree of defective splicing in aI5γ (Fig. 3.6A, lanes 6, 10, 13, 16, 9), while in most cases, the deletions also caused a processing defect of the 6.6-kb *COX1* primary transcript. There is a conspicuous difference in the *msm1Δ* and *msd1Δ* strains in that the *COX1* primary transcript containing the aI5γ intron is reduced (lanes 10 and 13) as compared to *mst*Δ , *mse*Δ and *dia4*Δ (lanes 6,16, and 19). To confirm the presence of the aI5γ intron in the *COX1* primary transcript, the membranes in Fig. 3.6A were stripped and re-probed with a ^{32}P-labeled DNA oligonucleotide complementary to the aI5γ intron (Fig. 3.6B). The presence of the 6.6-kb primary transcript corresponds to the primary transcript that includes unspliced aI5γ intron in A. With the exception of the *msd1Δ* strain, the processing defect of the *COX1* primary transcript can be seen in the I^0 strains,

indicating that the loss of these synthetases also impacts processing in strains lacking introns.

Deletion of these tRNA synthetases also caused splicing defects in bI1 (Fig. 3.6C, lanes 7, 11, 14, 17, 20). Additionally, the *dia4Δ*/aI5γ strain lost its *COB* RNA (lane 19).

3.2.3 Deletions of two translation elongation factors cause splicing defects

Within the yeast mitochondrion, there are three identified elongation factors, Mef1, Mef2 and Tuf1, of which I tested the latter two. Both Tuf1 and Mef2 are required for respiratory growth, protein synthesis and are essential for mitochondrial genome maintenance. Tuf1 is a G-protein that, when bound to GTP, binds to and delivers an aminoacylated-tRNA to the A-site of the ribosome. If the codon-anticodon pairing is correct, the ribosome acts as a GTPase activator and the GTP is hydrolyzed, releasing the inactive GDP-bound form of the protein.(Myers et al. 1985; Chiron et al. 2005). The Northern hybridization analyses in Fig. 3.7A show that *tuf1*Δ causes a strong defect in aI5γ splicing (lane 6) and a weaker bI1 splicing defect (Fig. 3.7B, lane 7). Remnants of the *COX1* primary transcript are also visible in all *tuf1*Δ strains.

Though Mef2 is defined as an elongation factor in the Saccharomyces Genome Database (SGD; yeastgenome.org, April 2015), there is some evidence to indicate that it is not involved in the GTP-dependent ribosomal translocation step during translation elongation (Welcsh et al. 1994). It has, however, been found to have involvement in ribosome recycling (Callegari et al. 2011). The negative effect of the deletion of Mef2 on the splicing of aI5γ and bI1 is observed in Fig. 3.7A, lane 10 and Fig. 3.7B, lane 11,

respectively. Though the deletion of this protein also caused a processing defect of the *COX1* primary transcript in most of the strains, the I^0 shows wild-type processing (Fig. 3.7A, lane 9), suggesting the presence of introns affects processing in *mef2Δ* strains.

3.2.4 Deletions of proteins that act on mt 21S rRNA or 15S rRNA cause splicing defects

Pet56/Mrm1 is a ribose methyltransferase that modifies a functionally critical, conserved nucleotide in mitochondrial 21S rRNA, the mitochondrially-encoded ribosomal RNA of the large mitoribosomal subunit (Sirum-Connolly and Mason 1993). In the Northern hybridization analyses in Fig. 3.8, the loss of Pet56 is seen to cause a strong defect in the splicing of aI5γ (A, lane 6) and a weak defect in splicing bI1 (B, lane 7).

According to the SGD, *YOR199w* and *YOR200w* are dubious ORFs that overlap *PET56* at its 5′end. As such, the result of their deletions would be expected to be similar to the defective splicing observed for *pet56*Δ. That is indeed the case for aI5γ splicing, as observed in Fig. 3.8A, lanes 10 and14; though not as evident for bI1 splicing (Fig. 3.8B, lanes 11 and 15). This difference suggests that the putative interactions of Pet56/Mrm1 with the aI5γ and bI1 introns occur at different domains of the protein, as would be expected.

There is a pronounced processing defect of the *COX1* primary transcript in the LSU strains (Fig. 3.8A, lanes 8, 12, and 16) that is especially evident in the *yor199w*Δ strain (lane 12). This effect suggests that processing of the *COX1* primary transcript is defective without the critical modification to the 21S rRNA normally provided by Pet56.

Ccm1/Rrg2/Dmr1 is a pentatricopeptide repeat (PPR) protein, required for the maintenance of the 15S rRNA, the mitochondrially-encoded ribosomal RNA of the small subunit (Lipinski et al. 2010; Puchta et al. 2010). Deletion of this gene caused a weak aI5γ splicing defect, though the total RNA was also apparently reduced as seen by the comparatively weaker 2.2-kb RNA band (Fig. 3.8A, lane 18). The *COX1* processing defect was observed to be more severe in the bI1 and LSU strains (top panel, lanes 19 and 20) than in others (lanes 17 and 18). Previous work had reported this protein to be required only for excision of group I introns aI4 in *COX1* and bI4 in *COB.* (Moreno et al. 2009; Lipinski et al. 2011), but not for aI5γ or bI1 as was observed here. This is likely due to their use of a different methodology (RT-PCR) or perhaps due to strain differences.

3.2.5 Deletions of some translational activators cause splicing defects

There are fifteen known translational activators critical for the expression of mitochondrial proteins within *S. cerevisiae*, with each of the eight mitochondrially-encoded genes having at least one translational activator (Herrmann et al. 2013). Of the fifteen identified translational activators, eleven were tested in Phase I of the screen. Deletion of each was found to cause either instability of the transcript or a splicing defect, though none specifically in aI5γ or bI1(Nyberg 2006). Here I have tested the remaining four: Aep1, Atp22, Sov1 and Pet309, all of which contain RNA-binding PPR motifs (Lipinski et al. 2011) (Fig. 3.9).

Peripherally associated with the mt inner membrane, Aep1 is a translational activator for *ATP9* (Payne et al. 1993), a gene encoding a component of the ATP synthase complex. The deletion of *AEP1* caused splicing defects in both aI5γ and bI1, though the effect on aI5γ was strong, while that on bI1 was weak (Fig. 3.9A, lane 6 and Fig. 3.9B, lane 7, respectively).

Atp22 is the translational activator for *ATP6* and *ATP8* (Herrmann et al. 2013), genes that also encode proteins for the ATP synthase complex. It is unknown whether this protein is an integral inner membrane protein or only peripherally associated with the inner mt membrane. The strong effect of its deletion on aI5γ splicing is seen in lane 9 of Fig. 3.9A, as compared to the weak defect observed for bI1 splicing in lane 10 of Fig. 3.9B. Unidentified bands that run more slowly than the *COB* mRNA are evident in all four strains (lanes 8-11).

Sov1 is described by the SGD (April 2015) as a protein of unknown function, but is categorized as a translational activator for *VAR1* by others (Sanchirico 1998; Herrmann et al. 2013). Taken as such, it is being grouped here with other translational activators. Var1 is the only mitochondrially-encoded ribosomal protein in yeast and is part of the mitoribosomal small subunit. The strong aI5γ splicing defect caused by *sov1*Δ is seen in lane 13 of Fig. 3.9A. The relatively weak bI1 splicing defect is seen in lane 14 of Fig. 3.9B.

Pet309 is the membrane-bound translational activator for *COX1* known to affect the stability of *COX1* primary transcripts (Manthey and McEwen 1995; Manthey et al. 1998). Due to a severe reduction in *COX1* RNA with deletion of this gene, testing its

effect on splicing required the use of three times the total RNA (3.6 µg) as compared to the other translational activators. The strong effect *pet309*Δ has on aI5γ splicing is seen in lane 17 of Fig. 3.9A. (Other unidentified RNA species that run more slowly than the mRNA are observed here as in *atp22*Δ and may be the result of non-specific cross-hybridization.) Lane 18 of Fig. 3.9B shows that *pet309*Δ causes no splicing defect in bI1.

Because the *COB* Northerns for *atp22*Δ and *pet309*Δ hybridized with an exon probe appear to have a very weak or non-existent bI1 splicing defects, all five membranes were stripped and re-probed for the bI1 intron using a ^{32}P-internally-labeled probe complementary to the intron itself (see Table 2.1). The results of those hybridizations are seen in Fig. 3.9C. With *aep1*Δ and *sov1*Δ, and to a far lesser degree, with *atp22*Δ, there remains a small amount of bI1-containing 2.9-kb precursor (lanes 7, 14, and 10, respectively), in contrast to none in the *pet309*Δ strain (lane 18). All four, however, show the excised 0.77 kb intron that is only faintly visible in wild-type. This band is reduced in *pet309*Δ (lane 18) relative to that of the other three (lanes 7, 10, and 14), despite having three times the total RNA, and therefore comparable to wild-type levels of excised bI1 (lane 3).

In conclusion, splicing of aI5γ was strongly impacted by the deletion of each of the tested translational activators, raising the possibility of an interconnected network among these proteins as discussed below. In contrast, bI1 splicing was only weakly affected, and then only by Aep1 and Sov1.

3.2.6 Novel functions observed for Pet 309 and Atp22

Pet309 (and to a lesser degree, Atp22) appeared to be specific for aI5γ splicing. To test for specificity and the possible effect of their deletion on other introns, the genes for these translational activators, plus that for Pet54, were knocked out of strains harboring introns other than aI5γ and bI1. These three strains, HRH421, HRH 524, and HRH422, obtained from the lab of Dr. Philip Perlman, are all in a 161-U7 background. Pet54, a translational activator for *COX3* (Herrmann et al. 2013) required for normal levels of *COX1* synthesis in an intronless strain (Shingu-Vazquez et al. 2010), and a known splicing factor for the group I intron aI5β (Costanzo et al. 1989), was used as a control.

Strain HRH421 contains only group II intron aI1 and strain HRH524 has only group II intron aI2. Both of these introns encode their own active maturases. (see Fig. 1.3). Strain HRH422 has three group I introns: aI4, bI4 and bI5. Intron aI4 encodes an inactive maturase but is aided instead by the active maturase encoded by bI4 that assists in the splicing of aI4 as well as itself (Rho and Martinis 2000). Splicing of both of these introns is aided by Nam2, a mt leucyl-tRNA synthetase (Labouesse 1990) and Ccm1(Moreno et al. 2009). Intron bI5 does not code for a maturase; its splicing is facilitated by Cbp2 (Gampel and Cech 1991). All of the mt introns are also aided in their splicing by the general RNA chaperone, Mss116.

The results of deleting the genes for Pet309, Atp22 and Pet54 in these strains are shown in the Northern hybridization analyses in Fig. 3.10A. All were performed with 3.6 μg total RNA. Lanes 1-7 are in strain HRH421 harboring only intron aI1. As seen in the

top panel, none exhibit defective splicing. However, the deletion of *PET309* destabilizes the transcript with only the single, maturase-containing intron, contradicting a previous report regarding the role of Pet309 in which the stability of a *COX1* transcript in *pet309*Δ strains was inversely related to the number of introns contained (Manthey and McEwen 1995). Lanes 8-13 are in the strain harboring only intron aI2. The deletion of *PET309* (lanes 9-10) is observed to destabilize the transcript, again with only a single, maturase-containing intron. With the deletion of *ATP22* and *PET54* in lanes 11-13, some minor bands of the sizes of the primary and precursor transcripts can be observed. Lanes 14-20 are in the strain harboring the group I intron aI4. Faint bands are visible in the *pet309*Δ strain; in the *atp22*Δ strain, a clear splicing defect is evident for this intron, while no defect is evident in the *pet54*Δ strain. To assess loading, particularly for the *pet309*Δ strains, all the membranes were stripped and re-probed with a ^{32}P-labeled DNA oligonucleotide complementary to *COX2*. The results are shown in Fig. 3.10B and confirm that loading is approximately equal.

The instability of the *COX1* transcripts containing introns aI1or aI2 when deleted for the *PET309* gene is in sharp contrast to the stability of the transcript containing only aI5γ, shown in Fig. 3.10C. In contrast to the results of Manthey and McEwen, here the data show that it is not the number of introns that are important to *COX1* stability—strains with aI1, aI2, or aI5γ each have only one intron— but rather whether those introns encode their own maturases. Those with intron-encoded maturases like aI1 and aI2 are dependent upon the translational activator role of Pet309, while aI5γ is not. The separate

functions of translation and stabilization of transcript are thought to function in two separate domains of Pet309 (Tavares-Carreón et al. 2008). While the translation function is not required for the maturase-lacking aI5γ intron, the loss of Pet309 results in a strong splicing defect. Thus, in addition to roles in translation and transcript stability, Pet309 may also be acting as a splicing factor specific for aI5γ.

Figure 3.11 shows the effect of *pet309*Δ, *atp22*Δ and *pet54*Δ on the splicing of *COB* group I introns bI4 and bI5. The blots were hybridized with the various ^{32}P-labeled probes as indicated beneath each. Pet309 and Pet54 do not appear to be playing a role either in splicing of these introns or in transcript stability (Fig. 3.11A, lanes 2-3, 6-7, 9-10, 13-14, 16-17, and 20-21). Atp22, however, does seem to be required for *COB* stability (lanes 4-5, 11-12, and 18-19). The loss of this protein causes a striking destabilization of the *COB* transcript not previously reported, suggesting that Atp22 may also be a translational activator for *COB.* As discussed earlier, bI4 encodes a maturase that it shares with aI4. With the destabilization of the *COB* transcript, it is likely that the aI4 splicing defects observed in Fig. 3.10A, lanes 17 and 18, are a result of not having this bI4 maturase.

To assess loading, the blots were stripped and re-probed with a ^{32}P-DNA oligonucleotide complementary to *COX2* (Fig. 3.11B). As noted with the hybridizations in Fig. 3.10, deletions of these proteins do not exhibit the *COX2* processing defect observed with the deletions of some mitoribosomal proteins.

3.2.7 Deletions of miscellaneous other proteins that cause splice defects

There were several other proteins tested that do not share a single category, yet their loss caused a splicing defect. These are shown together in Fig. 3.12.

Sls1 is a mitochondrial membrane protein thought to coordinate expression of mitochondrially-encoded genes. It may facilitate delivery of mRNA to membrane-bound translation machinery, also interacting with Nam1, the mt transcription factor (Bryan et al. 2002). Lane 5 of fig. 3.12A shows the stringent aI5γ splicing defect caused by *sls1*Δ. A bI1 defect is also evident (Fig. 3.12B, lane 7), though the defect is not as severe as that observed for aI5γ. There is no observable *COX1* processing defect.

Rrg1 is a protein of unknown function according to the SGD, though it has been described as essential for mt genome maintenance (Merz and Westermann 2009). Deletion of its gene caused splicing defects in both aI5γ and bI1 (Fig. 3.12A, lane 9 and B, lane 10). Some *COX1* processing defect is evident.

Atp5 is subunit 5 of the stator stalk of mitochondrial F1F0 ATP synthase (Devenish et al. 2000). Deletion of this protein also caused splicing defects in both aI5γ and bI1 (Fig. 3.12A, lanes 12-13 and B, lanes 14-15, respectively).

Oxa1 is a highly-conserved mitochondrial inner membrane insertase that interacts with the mitoribosomes. It mediates the insertion of both mitochondrial- and nuclear-encoded proteins from the matrix into the inner membrane by behaving as a pore-forming translocase regulated in a membrane potential and substrate-dependent manner (Krüger et al. 2012). Deletion of this protein caused strong splicing defects in both aI5γ and bI1

(Fig. 3.12A, lanes 18-19 and B, lanes 20-21, respectively). Note: the *atp5*Δ and *oxa1*Δ Northern hybridizations were performed by Kathryn Turner.

3.2.8 Pet309 may be part of a large complex involved in splicing

Of all the proteins tested, only Pet309 appeared to be specific for aI5γ splicing and as such warranted further testing. This *COX1* translational activator had previously been found to be part of 900-kDa complex that also included *COB* translational activators Cbp1 and Cbs2 (Krause et al. 2004).This complex has been proposed to link transcription to translation and thus may also affect splicing.

To identify other proteins that may associate with Pet309 and potential components of this putative complex, a commercially available BY4741 strain (GE Healthcare) in which a Tandem Affinity Purification (TAP) tag had been appended to the 3′ end of the chromosomal copy of Pet309 was used. An untagged isogenic strain was used as negative control. Purified mitochondria from 3 l cultures grown in YPR to an $O.D._{600} \approx 3.0$ were subjected to the TAP protocol described in Methods. Samples were run on a 4-12% bis-tris polyacrylamide gel (Life Technologies) and stained with Coomassie Brilliant Blue (Fig. 3.13). Isolated gel fragments from an identical gel run approximately 1 cm were submitted to the University of Texas at Austin Protein Facility for mass spectrometry analysis.

Although the tagged Pet309 sample contained many more proteins than the untagged sample, thereby suggesting enrichment of a complex, Pet 309 is not among them. It had been previously noted that disruption of mitochondria either by sonication or

by the use of detergents resulted in the fragmentation of Pet309 when tagged with HA (Krause et al. 2004), and may explain the inability to detect the naturally low-abundant protein here. Among the proteins identified in the tagged sample, however, was the RNA chaperone Mss116. Interestingly, Pet309 was among the proteins associated with RNA chaperone Mss116 in an aI5γ ρ^- strain tested in Chapter 7, where it will be discussed further.

Overexpression of Pet309 is likely not a suitable alternative strategy as previous work in overexpressing translational activators has resulted in the formation of aggregates (Weber and Dieckmann 1990).

3.2.9 Tested proteins that had no effect on splicing

The following are those proteins whose gene deletions did not cause a splicing defect in either aI5γ or bI1. Following each name is a brief description taken from the SGD. The Northern hybridizations indicated in parentheses can be found in the Appendix unless otherwise noted.

Abf2: Mitochondrial DNA-binding protein; involved in mitochondrial DNA replication

Adh3: Glucose-repressible alcohol dehydrogenase II

Aep3: Peripheral mitochondrial inner membrane protein; may facilitate use of in mitochondrial translation initiation

Dcs1: Non-essential hydrolase involved in mRNA decapping

Glo3: ADP-ribosylation factor GTPase activating protein (ARF GAP); involved in ER-Golgi transport

Gon1/Gem1: Outer mitochondrial membrane GTPase. No effect on bI1 splicing; lost *COX1* RNA

Grx5: Protein involved in the synthesis and assembly of Fe-S centers.

Inh1: Protein that inhibits ATP hydrolysis by the F1F0-ATP synthase

Kap123: Karyopherin beta; mediates nuclear import of ribosomal proteins prior to assembly into ribosomes and import of histones H3 and H4; localizes to the nuclear pore, nucleus, and cytoplasm

Lcb5: Minor sphingoid long-chain base kinase

Mrpl36: a mitoribosomal protein of the large subunit

Mrpl38: a mitoribosomal protein of the large subunit

Mtg1: Putative GTPase peripheral to the mitochondrial inner membrane; essential for respiratory competence, likely functions in assembly of the large mitoribosomal subunit

Mtg2: Putative GTPase; member of the Obg family

Nam1: Mt protein that interacts with an N-terminal region of mtRNA polymerase Rpo41 and couples RNA processing and translation to transcription

Nrp1: Putative RNA binding protein of unknown function

Pim1: ATP-dependent Lon protease; involved in degradation of misfolded proteins in mitochondria

Pkh2: Serine/threonine protein kinaseinvolved in sphingolipid-mediated signaling pathway that controls endocytosis

Qr17/Ydl104c: Protein involved in threonylcarbamoyl adenosine biosynthesis

Ssq1: Mitochondrial hsp70-type molecular chaperone

Sws2: a putative mitoribosomal protein of the small subunit

Ydr042: Putative protein of unknown function

Yhm1: Mitochondrial GTP/GDP transporter

Ynl170w: Dubious open reading frame; unlikely to encode a functional protein

Yta12: Mitochondrial inner membrane m-AAA protease component; mediates degradation of misfolded or unassembled proteins

3.2.10 Deletions of some proteins result in loss of mtRNA

Despite short incubation times, the deletion of several genes and the proteins they encode (listed below) caused severe loss of mtRNA resulting in poor hybridizations. Following each name is a brief description taken from the SGD.

Caf17: Involved in incorporating iron-sulfur clusters into proteins

Dem1/Exo5: Mitochondrial 5'-3' exonuclease and sliding exonuclease; required for mitochondrial genome maintenance

Gem1: Outer mt membrane GTPase, may coordinate mtDNA replication and growth, specific for *COX1*

Isa2: Protein required for maturation of mt Fe-S proteins

Mrpl8: mitoribosomal protein of the large subunit

Met7: required for methionine synthesis and for maintenance of mitochondrial DNA

Msu1/Dss1: 3'-5' exoribonuclease; component of the mitochondrial degradosome along with the ATP-dependent RNA helicase Suv3 (loss appears specific for *COB*)

Mtf1: mtRNA polymerase specificity factor, similar to bacterial sigma factor

Oct1: Mt intermediate peptidase; cleaves destabilizing N-terminal residues of a subset of proteins upon import

Rim 1: ssDNA-binding protein essential for mt genome maintenance

Rpo41: mt RNA polymerase; RNA lost in all strains but aI5γ

The results of all the deletions tested in this part of the study are summarized in Table 3.1.

3.2.11 An as-yet-unidentified mt genomic splicing factor?

Most of the proteins that caused a splicing defect were associated with either the mitoribosome or with translation, posing the question as to whether there may be an as-yet-unidentified splicing factor within the mt genome. One protein that appeared to be a good candidate was the putative protein, Rf1, discussed in section 3.1.2 and diagrammed in Fig. 3.1C. Rf1 has been annotated in the SGD as an uncharacterized maturase-like protein, since it is reported to have two very small introns (39 and 30 nt) and a variant LAGLIDADG motif (Foury et al. 1998). The LAGLIDADG motif has been found in at least one group II intron splicing factor, the pentatricopeptide repeat gene OTP51 (de Longevialle et al. 2008). Endonucleases with this motif have also been found to be encoded by free-standing ORFs not associated with introns (Lambowitz and Caprara 1999).

To test the possibility that the *RF1* transcript may not be properly processed from the *COX2/RF1* transcript (and thereby precluding the possibility of its translation), the

membranes used in Fig. 3.4 were stripped once again and re-probed for *RF1* with a ^{32}P-labeled oligonucleotide complementary to the 3´ end of the gene (see Fig. 3.1C). Since the *COX2* processing defect was more pronounced in the aI5γ strain, that membrane is shown. The *RF1* signal is seen only in the primary transcript, but there is no visible band where the 1.5 kb mRNA was expected in either the null or the wild-type strains. A more sensitive ^{32}P-internally-labeled PCR product was then used as a probe with similar results (Fig. 3.14C).

A recent study of the yeast mt transcriptome found that levels of the *RF1* RNA were extremely low (Turk et al. 2013). Thus, any future studies should perhaps try using much more RNA for Northern hybridizations, or perhaps use RT-PCR (reverse transcription-PCR) to test this intriguing putative protein. Future work to test any possible role of Rf1 in aI5γ and bI1 splicing might also involve the re-coding of the transcript to allow for centromeric, allotropic expression and subsequent mitochondrial import in splicing-defective strains. Similar methods were successfully employed for *COX2* (Cruz-Torres et al. 2012) and for the cytosolic expression of the bI4 maturase (Banroques et al. 1986).

3.3 DISCUSSION

Results of this portion of the study showed that with few exceptions, those genes whose deletion caused a splicing defect in aI5γ and bI1 were associated primarily with the mitoribosome or with mitochondrial translation. Previous studies in the *Saccharomyces cerevisiae* mitochondrial system have revealed a functional coupling of

transcription and translation at the inner mitochondrial membrane where the assembly of the oxidative phosphorylation machinery is initiated (Naithani et al. 2003; Rodeheffer and Shadel 2003; Krause et al. 2004; Shadel 2004). Of course, excision of introns must occur subsequent to transcription and prior to translation to ensure proper expression. Introns that encode their own maturases are clearly dependent upon functional mitoribosomes. Here, I show that two introns that do not encode maturases, aI5γ and bI1, also appear to be dependent upon functional mitoribosomes as well as upon proteins involved in mt translation.

While it is theoretically possible that an as-yet-unidentified splicing factor is encoded within the mt genome and is dependent upon the mitoribosomes for its translation and subsequent functionality, no evidence of that was found here.

Translational activators interact with the 5´ ends of newly transcribed RNAs guiding them to the mitoribosomes and are thus perfectly positioned to monitor splicing prior to translation. In 2003, Naithani *et al*. reported interactions between the translational activators for *COX1*, *COX2* and *COX3*. Later, translational activators for *COB* and *COX1* mRNAs, Cbp1 and Pet309 respectively, were shown to be associated in a high-molecular weight complex thought to link transcription to translation (Krause et al. 2004). The results presented here expand on this model, showing that Pet309 and translational activators for other mRNAs, Aep1, Sov1, and Atp22, strongly impact the splicing of aI5γ, possibly reflecting that a higher order of organization among these proteins is involved in aI5γ splicing. Two of these translational activators, Aep1 and Sov1, also impact bI1 splicing, albeit weakly. Finally, Atp22, a translational activator for the *ATP8/ATP6*

mRNA was found to be important to the stability of *COB* mRNA when harboring introns bI4 and bI5, thus linking components of the ATP synthase to *COB*.

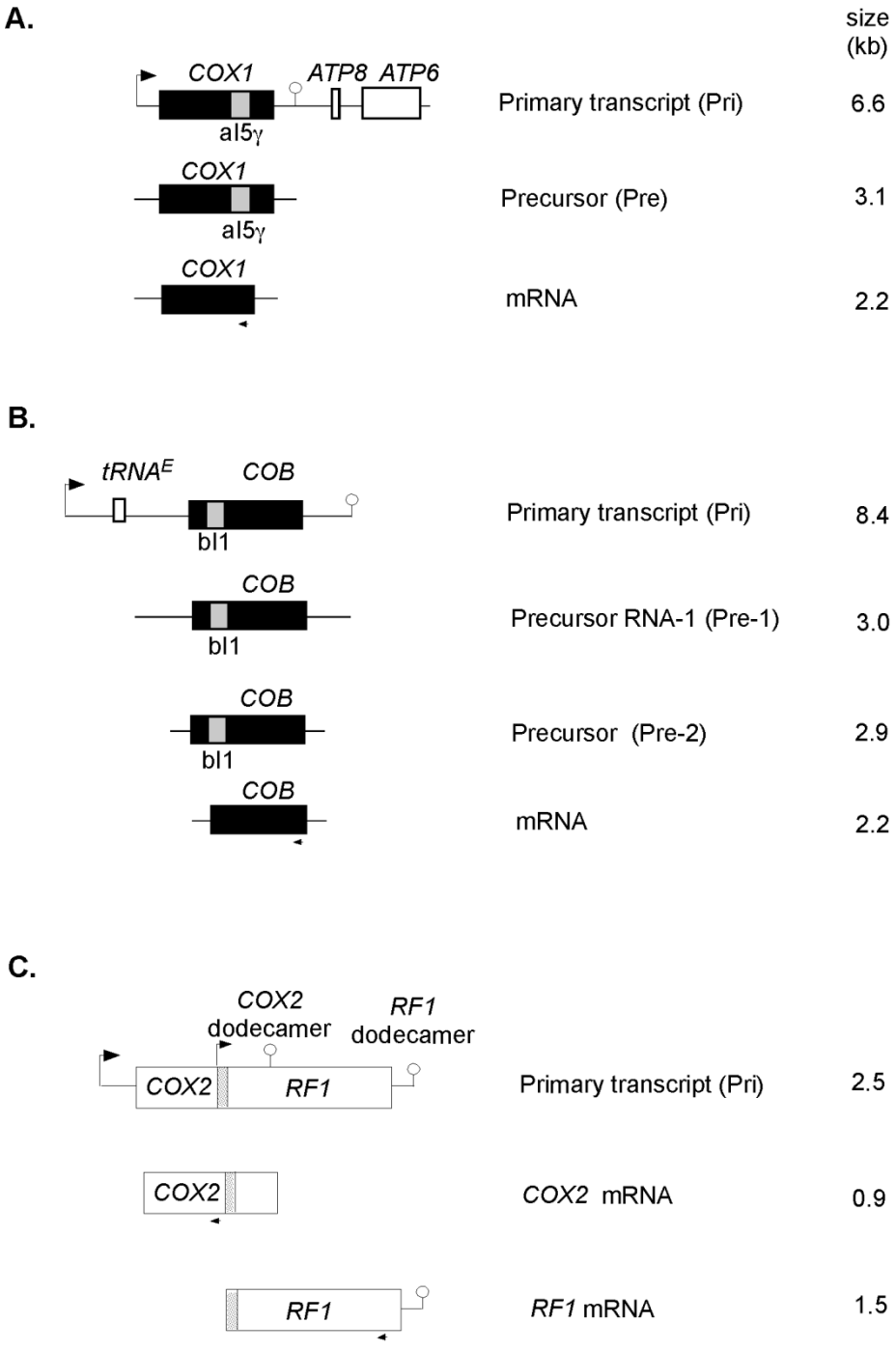

Figure 3.1: Processing pathways of *COX1*, *COB*, and *COX2* mRNAs

Figure 3.1 (continued): Processing pathways of *COX1*, *COB*, and *COX2* mRNAs

(A) Processing and splicing of the *COX1/ATP8/ATP6* primary transcript. The transcriptional start site of the *COX1* gene is indicated by a bent arrow, *COX1* exons are in black, and the aI5γ intron is in gray. A 6.6-kb primary transcript (Pri) is cleaved downstream of *COX1* to generate a 3.1-kb *COX1* precursor (Pre) from which the aI5γ intron is spliced to yield a mature 2.2-kb mRNA. (B) Processing and splicing of the primary $tRNA^{E}$-*COB* transcript. The position of the transcriptional start site upstream of $tRNA^{E}$ is indicated by a bent arrow. *COB* exons are in black, and the bI1 intron is in gray. An 8.4-kb primary transcript (Pri) is cleaved just downstream of the $tRNA^{E}$ gene generating an initial 3.0-kb precursor (Pre-1) transcript. A second cleavage reaction upstream of the *COB* gene then generates a second 2.9-kb precursor (Pre-2) from which the bI1 intron is spliced to yield a 2.2-kb mature mRNA. (C) Processing of the *COX2/RF* transcript. The transcriptional start site for the 2.5-kb *COX2-RF1* primary transcript is 54 bp upstream from the protein-coding gene. Endonucleolytic cleavage occurs just after the conserved dodecamer sequence, AAUAAUAUUCUU (lollipop), 75-nt downstream from the *COX2* stop codon. The 5´-coding region of *RF1* overlaps the 3´ region of *COX2* (stippled). Cleavage of *COX2* at its dodecamer sequence truncates the *RF1* transcript. Small arrows under the genes indicate the positions of ^{32}P-labeled DNA oligonucleotide probes used in Northern hybridizations.

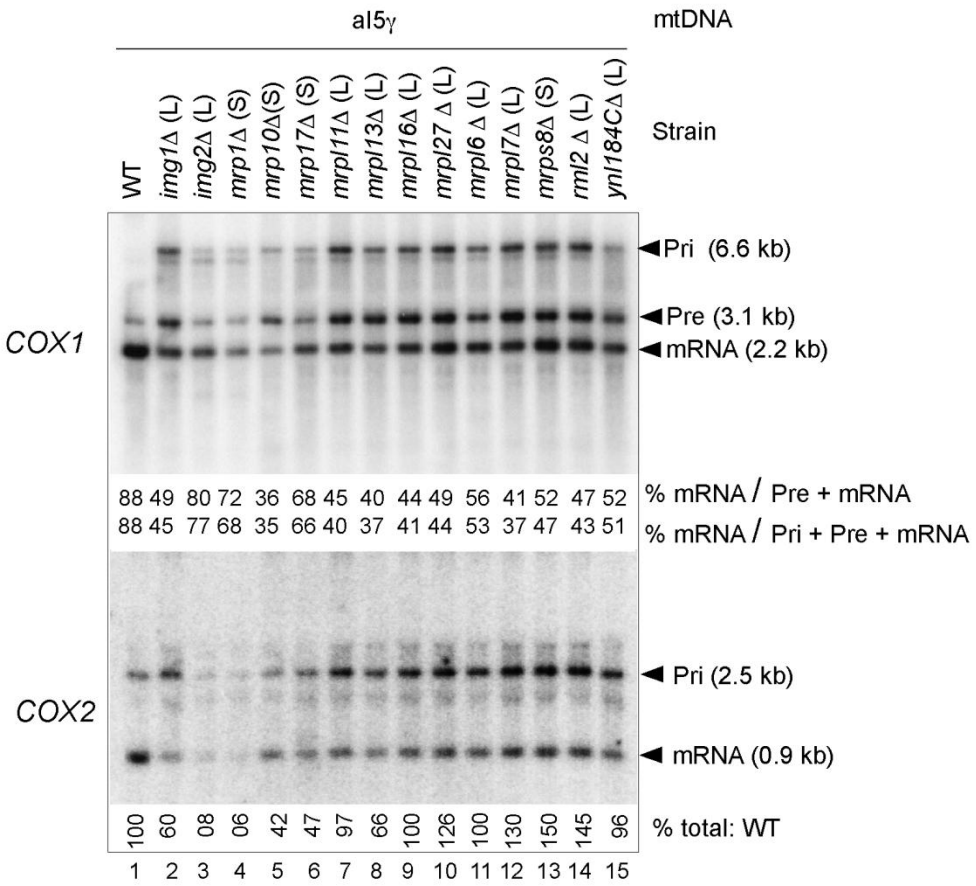

Figure 3.2: Northern hybridization analysis of aI5γ splicing in the single intron wild-type 161-U7/aI5γ and derivatives of that strain with deletions in mitoribosomal protein genes.

Figure 3.2 (continued): Northern hybridization analysis of aI5γ splicing in the single intron wild-type 161-U7/aI5γ and derivatives of that strain with deletions in mitoribosomal protein genes.

The blots show Northern hybridizations of wild-type strain 161-U7/aI5γ and derivatives of that strain in which the indicated mitoribosomal protein gene has been deleted. Strains were grown in YPR to an $O.D._{600}$ of about 0.8. Total cellular RNA was isolated, run in a 1.5% RNA-grade agarose gel, blotted onto a nylon membrane, and hybridized with a ^{32}P-labeled DNA oligonucleotide complementary to the *COX1* terminal exon (the small arrow below *COX1* in Fig. 3.1 A). The deleted mitoribosomal protein gene is indicated above each lane with the letter in parentheses indicating whether the protein is from the large (L) or small (S) ribosomal subunit. The *YNL184C* gene encodes an uncharacterized protein that overlaps mitoribosomal protein Mrpl19 (Hu et al. 2007). The primary and precursor transcripts are denoted as Pri and Pre, respectively. The percentage of spliced mRNA relative to mRNA + precursor RNA (upper value) or mRNA + precursor RNA + primary transcript (lower value) is indicated under each lane in the blot. After hybridization with the *COX1* exon probe, the blots were stripped and rehybridized with a probe complementary to the intronless *COX2* mRNA to assess loading (measured as the total of Pri + mRNA and normalized to the wild-type strain). Deletion of the mitoribosomal protein genes *IMG2* and *MRP1* (lanes 3-4) resulted in petites with deletions in the *COX2* gene.

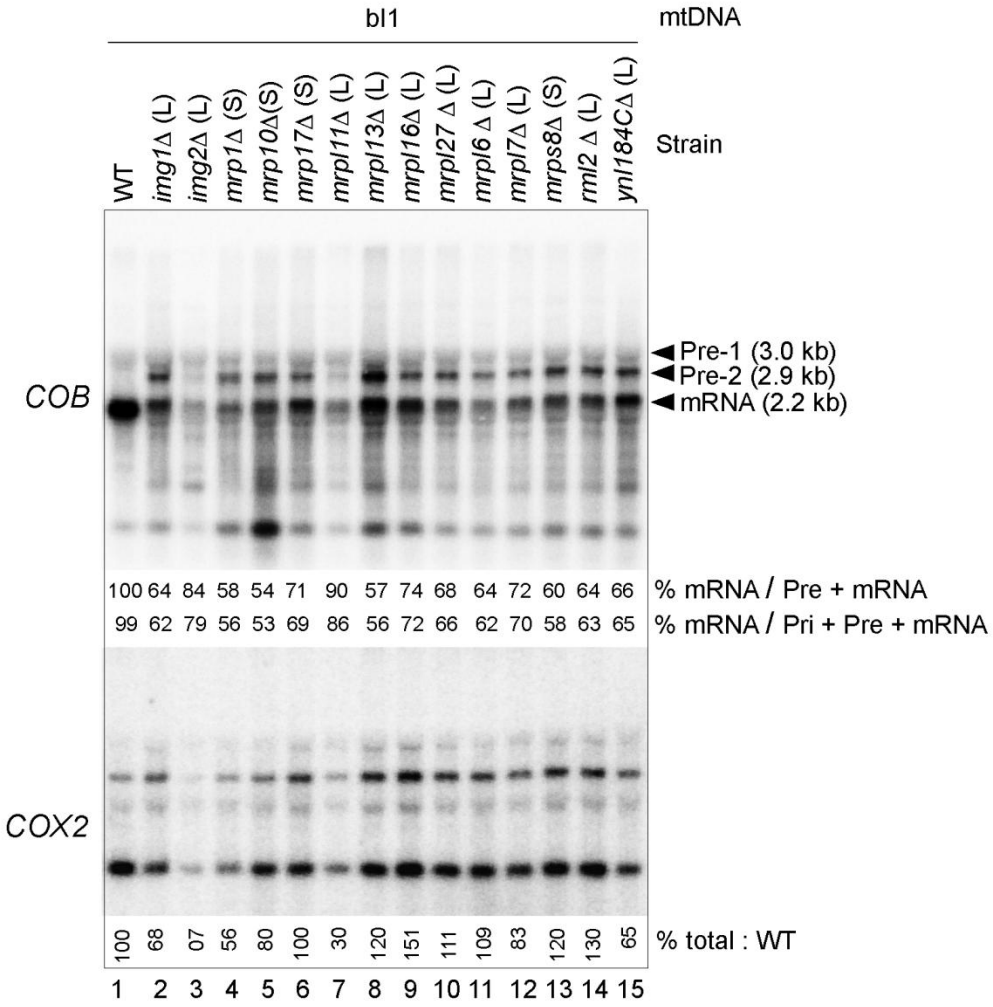

Figure 3.3: Northern hybridization analysis of bI1 splicing in the single intron wild-type 161-U7/bI1 and derivatives of that strain with deletions in mitoribosomal protein genes.

Figure 3.3 (continued): Northern hybridization analysis of bI1 splicing in the single intron wild-type 161-U7/bI1 and derivatives of that strain with deletions in mitoribosomal protein genes.

The blots show Northern hybridizations of wild-type strain 161-U7/bI1 and derivatives of that strain in which the indicated mitoribosomal protein gene has been deleted. Northern hybridizations were carried out as described in Fig. 3.2 but hybridized with a ^{32}P-labeled DNA oligonucleotide complementary to the *COB* terminal exon (small arrow below *COB* in Fig. 3.1B).

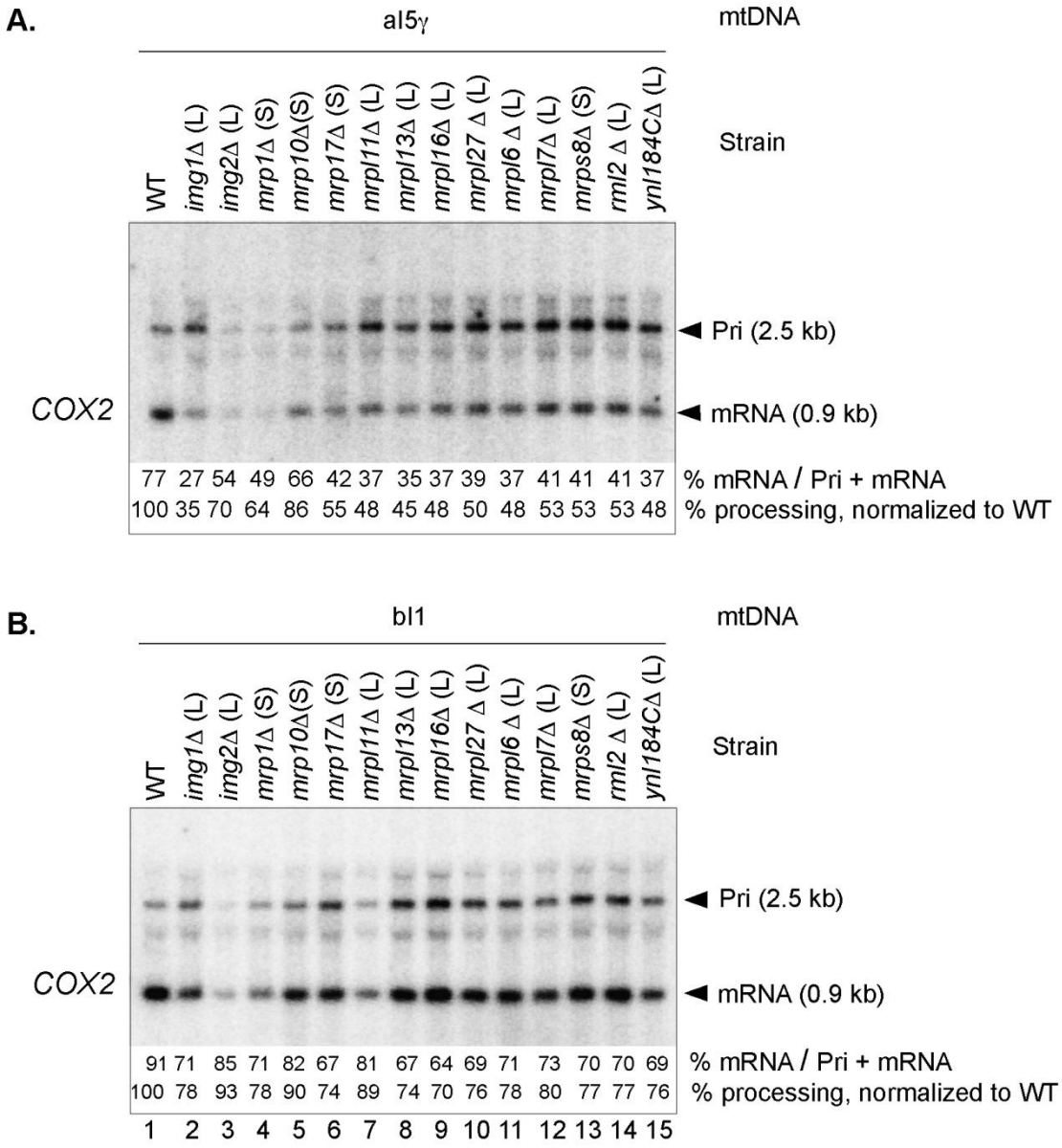

Figure 3.4: *COX2* processing defects caused by deletion of mitoribosomal protein genes are more severe in the aI5γ-containing strain than the bI1-containing strain.

Figure 3.4 (continued): *COX2* processing defects caused by deletion of mitoribosomal protein genes are more severe in the aI5γ-containing strain than the bI1-containing strain.

A comparison of the *COX2* Northern hybridizations from Figs. 3.2 and 3.3 for strains 161-U7/aI5γ (top) and 161-U7/bI1 (bottom) indicate that deletions of the mitoribosomal protein genes in the aI5γ-containing-strains result in greater *COX2* processing defects than in the bI1-containing strains. *COX2* processing was measured in two ways: as the percentage of mRNA relative to primary transcript + mRNA (upper value); and percent wild-type processing (lower value). The mean processing efficiency for *COX2* RNAs was 54% wild type in the aI5γ null mutants and 79% wild type in the bI1 null strains.

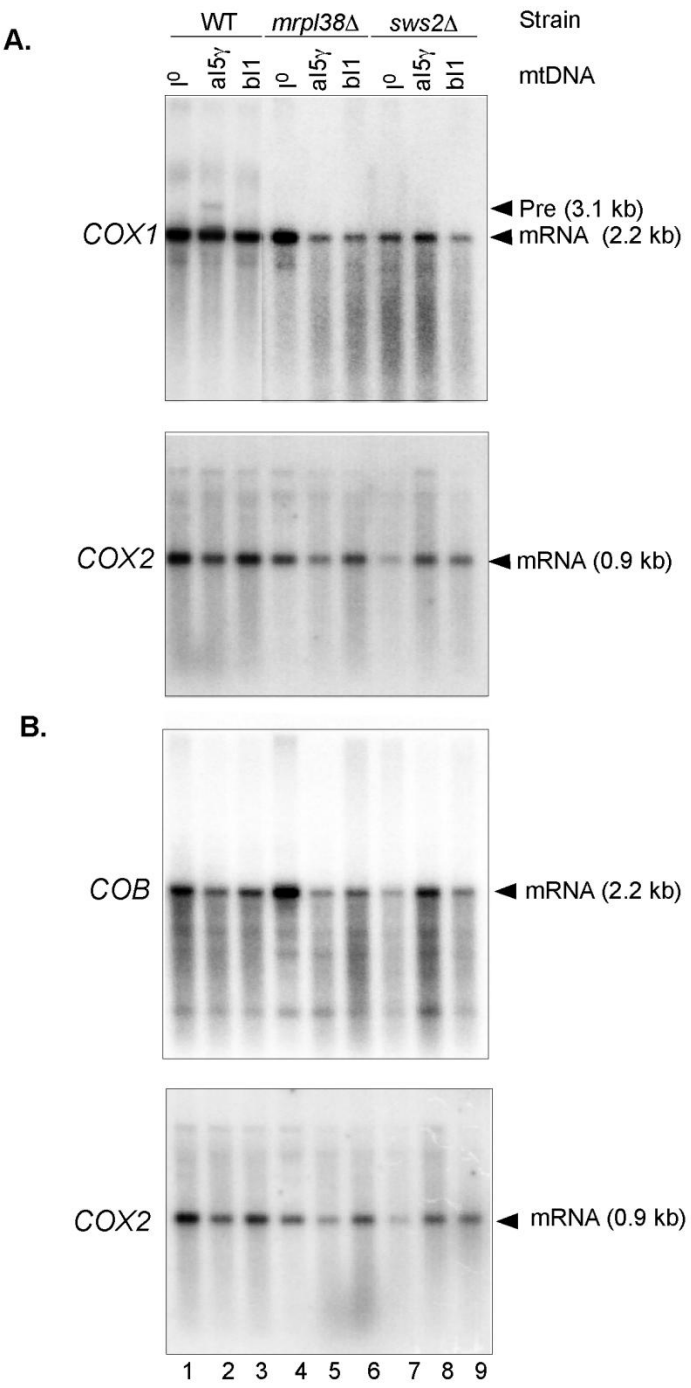

Figure 3.5: Northern hybridization analysis for strains with deletions of mitoribosomal protein genes that had no effect on aI5γ or bI1 splicing or on *COX2* processing.

Figure 3.5 (continued): Northern hybridization analysis for strains with deletions of mitoribosomal protein genes that had no effect on aI5γ or bI1 splicing or on *COX2* processing.

(A) The blots show Northern hybridizations of wild-type strain 161-U7 whose mtDNA contains either no introns (I^0) or single intron aI5γ or bI1 and derivatives of those strains in which mitoribosomal protein genes *MRPL38* and *SWS2* were deleted. Northern hybridizations were carried out as in Fig. 3.1 and probed with a ^{32}P-labeled DNA oligonucleotide complementary to the *COX1* terminal exon (top panel). After hybridization with the *COX1* exon probe, the blots were stripped and rehybridized with a probe complementary to the *COX2* mRNA (lower panel). (B) Strains are as in A, but hybridized with a ^{32}P-labeled DNA oligonucleotide complementary to the *COB* terminal exon. After hybridization with the *COB* exon probe, the blots were stripped and rehybridized with a probe complementary to the *COX2* mRNA to assess loading (lower panel).

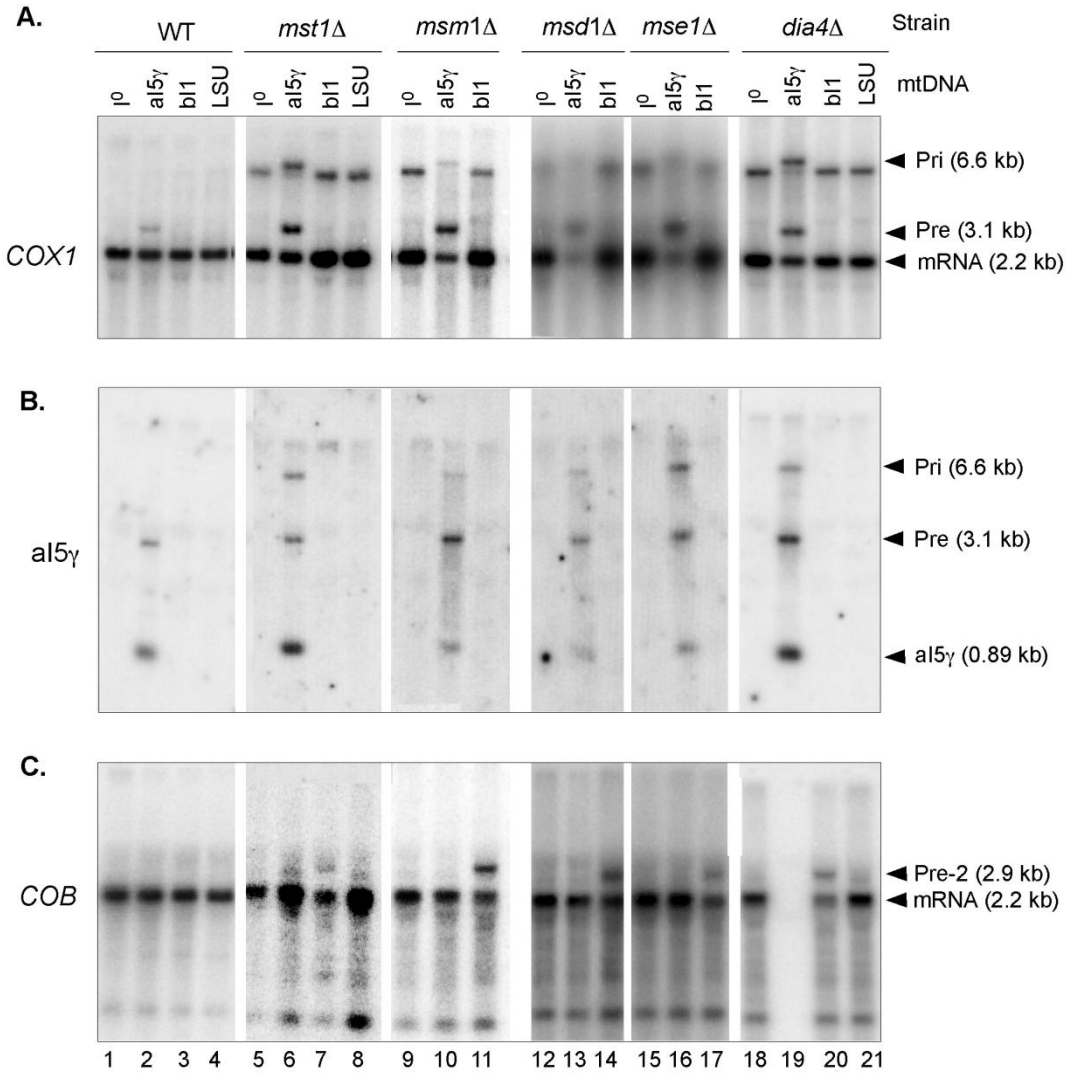

Figure 3.6: Northern hybridization analysis showing that deletions of mt aaRS genes cause aI5γ and bI1 splicing defects.

Figure 3.6 (continued): Northern hybridization analysis showing that deletions of mt aaRS genes cause aI5γ and bI1 splicing defects.

(A) The blots show Northern hybridizations of wild-type strain 161-U7 whose mtDNA contains either no introns, (I^0) or single introns aI5γ, bI1 or LSU and derivatives of each strain in which genes *MST1, MSM1, MSD1, MSE1* and *DIA4* have been deleted. Northern hybridizations were carried out as in Fig. 3.2 and probed for the *COX1* terminal exon.(B) Following hybridization with the *COX1* exon probe, the blots were stripped and rehybridized with a ^{32}P-labeled oligonucleotide complementary to the aI5γ intron. (C) Strains are as in A, but hybridized with a ^{32}P-labeled DNA oligonucleotide complementary to the *COB* terminal exon. Primary (Pri), Precursor (Pre), mature mRNA (mRNA), and aI5γ intron are indicated to the right of each panel.

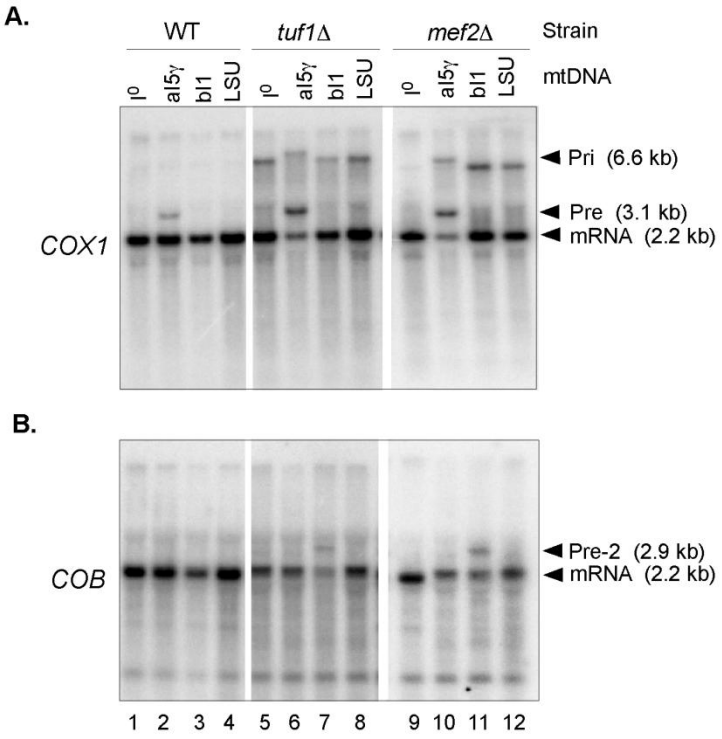

Figure 3.7: Northern hybridization analysis showing that deletions of mt elongation factor genes cause aI5γ and bI1 splicing defects.

(A) Northern hybridizations of wild-type strain 161-U7 whose mtDNA contains either no introns, (I^0) or single introns aI5γ, bI1, or LSU and derivatives of each strain in which genes *TUF1* and *MEF2* have been deleted. Northern hybridizations were carried out as in Fig. 3.2 and probed for the *COX1* terminal exon. (B) Strains are as in A, but hybridized with a ^{32}P-labeled DNA oligonucleotide complementary to the *COB* terminal exon. Primary (Pri), Precursor (Pre), and mature mRNA (mRNA) are indicated to the right of the panels.

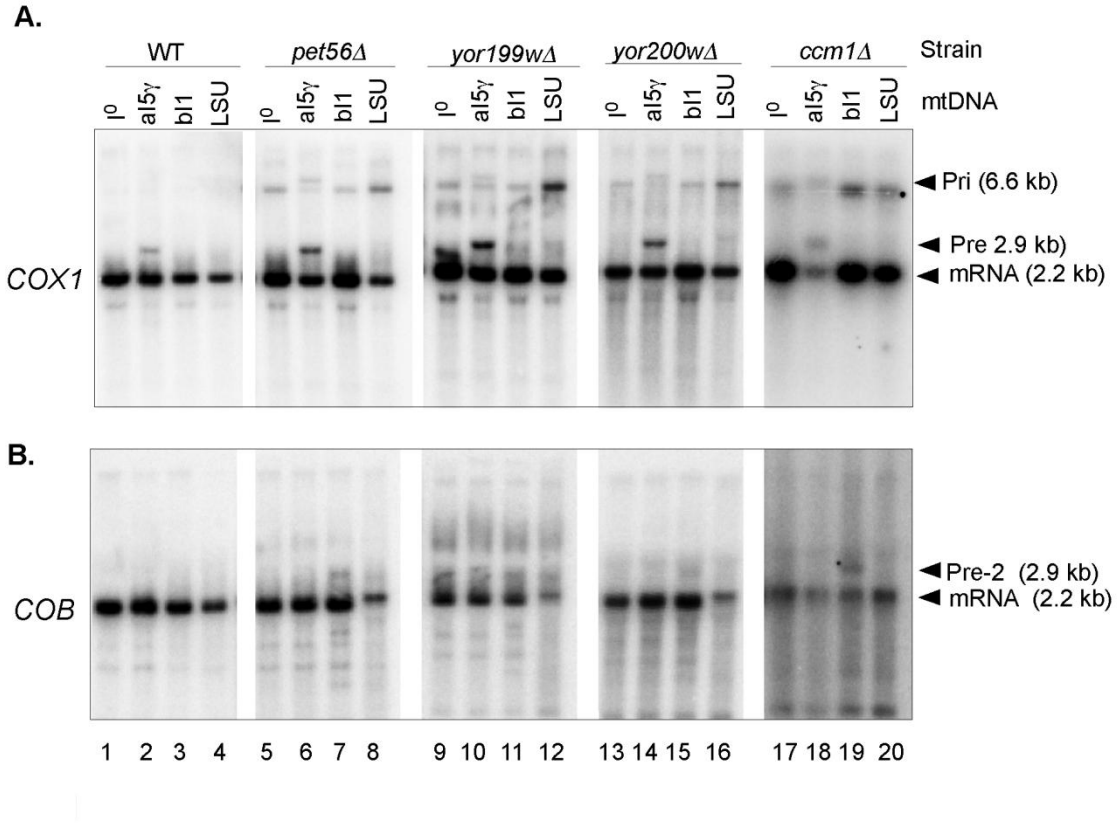

Figure 3.8: Northern hybridization analysis showing the effects on aI5γ and bI1 splicing with deletions of proteins that bind directly to the mt 21S rRNA or 15S rRNA.

(A) The blots show Northern hybridizations of wild-type strain 161-U7 whose mtDNA contains either no introns, (I^0) or the single introns aI5γ, bI1, or LSU and derivatives of each strain in which genes *PET56*, *YOR199w*, *YOR200w*, and *CCM/DMR1* have been deleted. Northern hybridizations were carried out as in Fig. 3.2 and probed with a ^{32}P-labeled DNA oligonucleotide complementary to the *COX1* terminal exon. (B) Strains are as in A, but hybridized with a ^{32}P-labeled oligonucleotide complementary to the *COB* terminal exon. Primary (Pri), Precursor (Pre), and mature mRNA (mRNA) are indicated to the right of the panels.

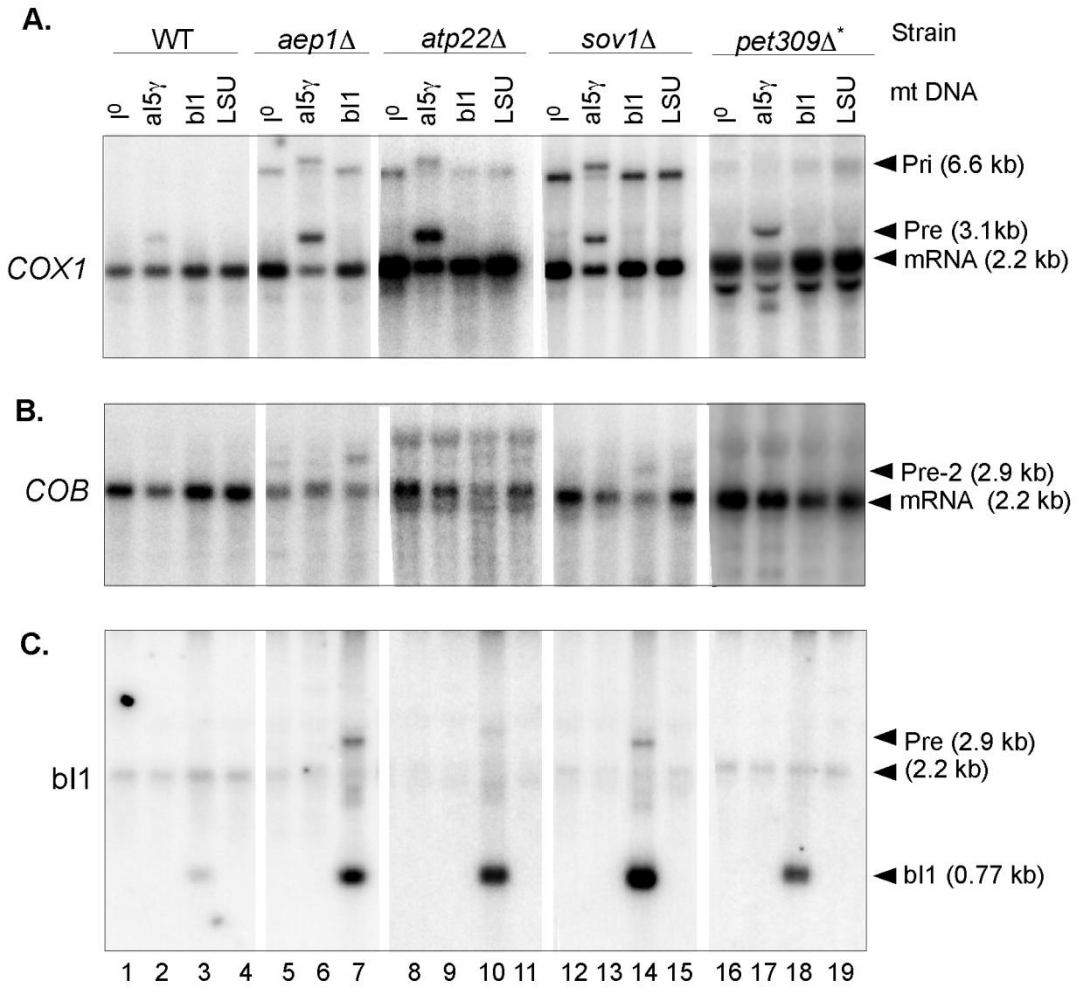

Figure 3.9: Northern hybridization analysis showing the effect on aI5γ and bI1 splicing with deletion of four mt translational activator/PPR proteins.

Figure 3.9 (continued): Northern hybridization analysis showing the effect on aI5γ and bI1 splicing with deletion of four mt translational activator/PPR proteins.

(A) The blots show Northern hybridizations of wild-type strain 161-U7 whose mtDNA contains either no introns, (I^0) or the single introns aI5γ, bI1, or LSU and derivatives of each strain in which genes for translational activator/PPR proteins *AEP1*, *ATP22*, *SOV1*, and *PET309* have been deleted. Northern hybridizations were carried out as in Fig. 3.2 except that the amount of total RNA for *pet309*Δ was tripled compared to other samples. Membranes were probed with a ^{32}P-labeled DNA oligonucleotide complementary to the *COX1* terminal exon. (B) Strains are as in A, but hybridized with a ^{32}P-labeled DNA oligonucleotide complementary to the *COB* terminal exon. (C) After hybridization with the *COB* exon probe, the blots were stripped and rehybridized with a probe complementary to the bI1 intron. Primary (Pri), Precursor (Pre), mature mRNA (mRNA), and bI1 intron are indicated to the right of the panels.

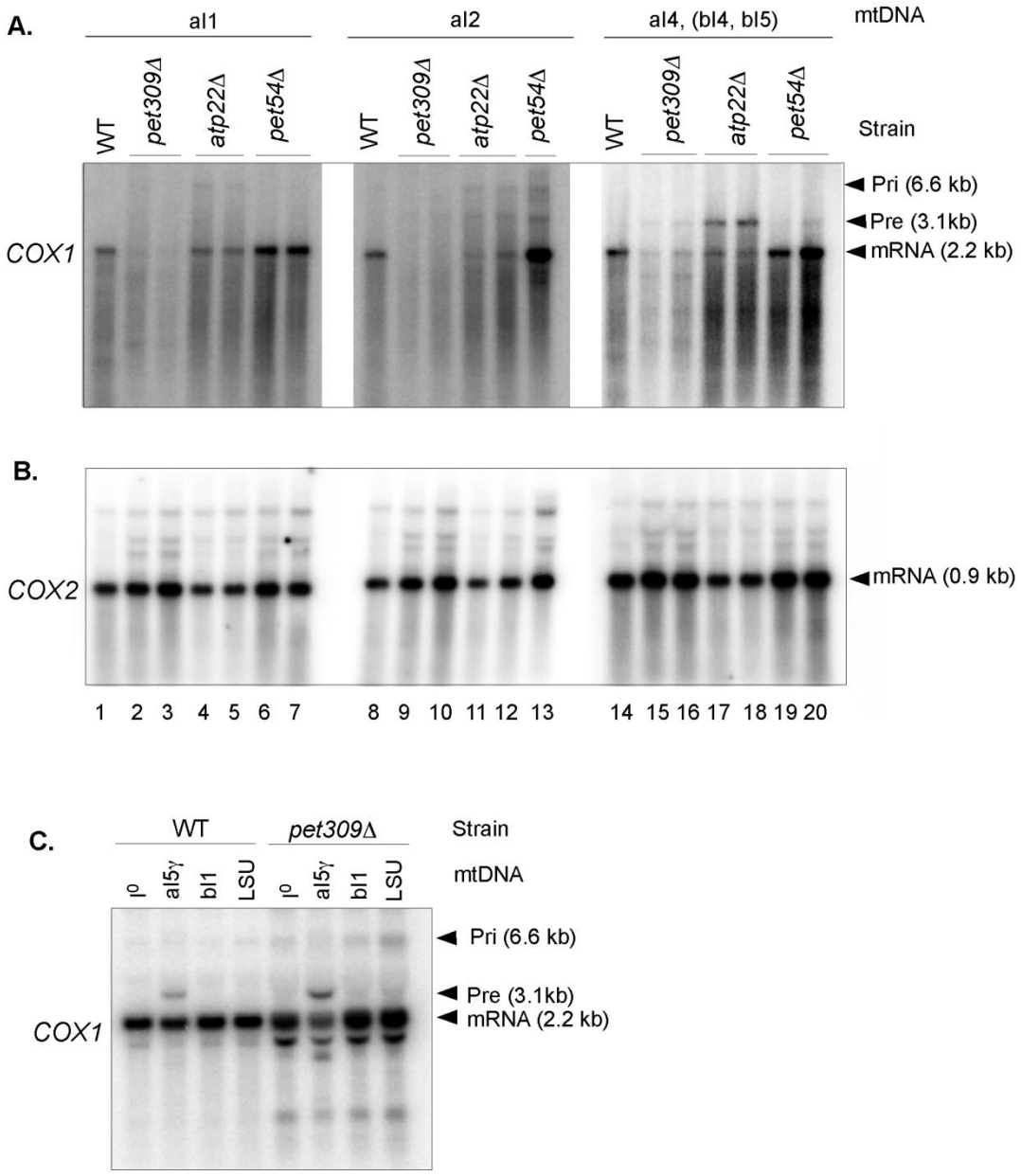

Figure 3.10: Northern hybridization analysis showing the effect of the deletion of three translational activators on the splicing of *COX1* introns aI1, aI2, aI4 and aI5γ.

Figure 3.10 (continued): Northern hybridization analysis showing the effect of the deletion of three translational activators on the splicing of *COX1* introns aI1, aI2, aI4 and aI5γ.

(A) The blots show Northern hybridizations of a wild-type 161-U7-derived strain whose mtDNA contains only introns aI1, aI2, or aI4 and mutants of each strain in which genes for *PET309*, *ATP22*, and *PET54* have been deleted. Northern hybridizations were carried out as in Fig. 3.2 except all mutants contain triple the amount of total RNA. Blots were probed for the *COX1* terminal exon. (B) Following hybridization, the blots were stripped and rehybridized with a probe complementary to the *COX2* mRNA. (C) Northern hybridizations of wild-type 161-U7-derived strains whose mtDNA contains either no introns (I^0) or the single intron aI5γ, bI1 or LSU and mutants of each strain in which the gene for *PET309* has been deleted. Northern hybridizations were carried out as in Fig. 3.2 except all mutants contain triple the amount of total RNA. Blot was probed with a ^{32}P-labeled DNA oligonucleotide complementary to the *COX1* terminal exon. Primary (Pri), Precursor (Pre), and mature mRNA (mRNA) are indicated to the right of the panels.

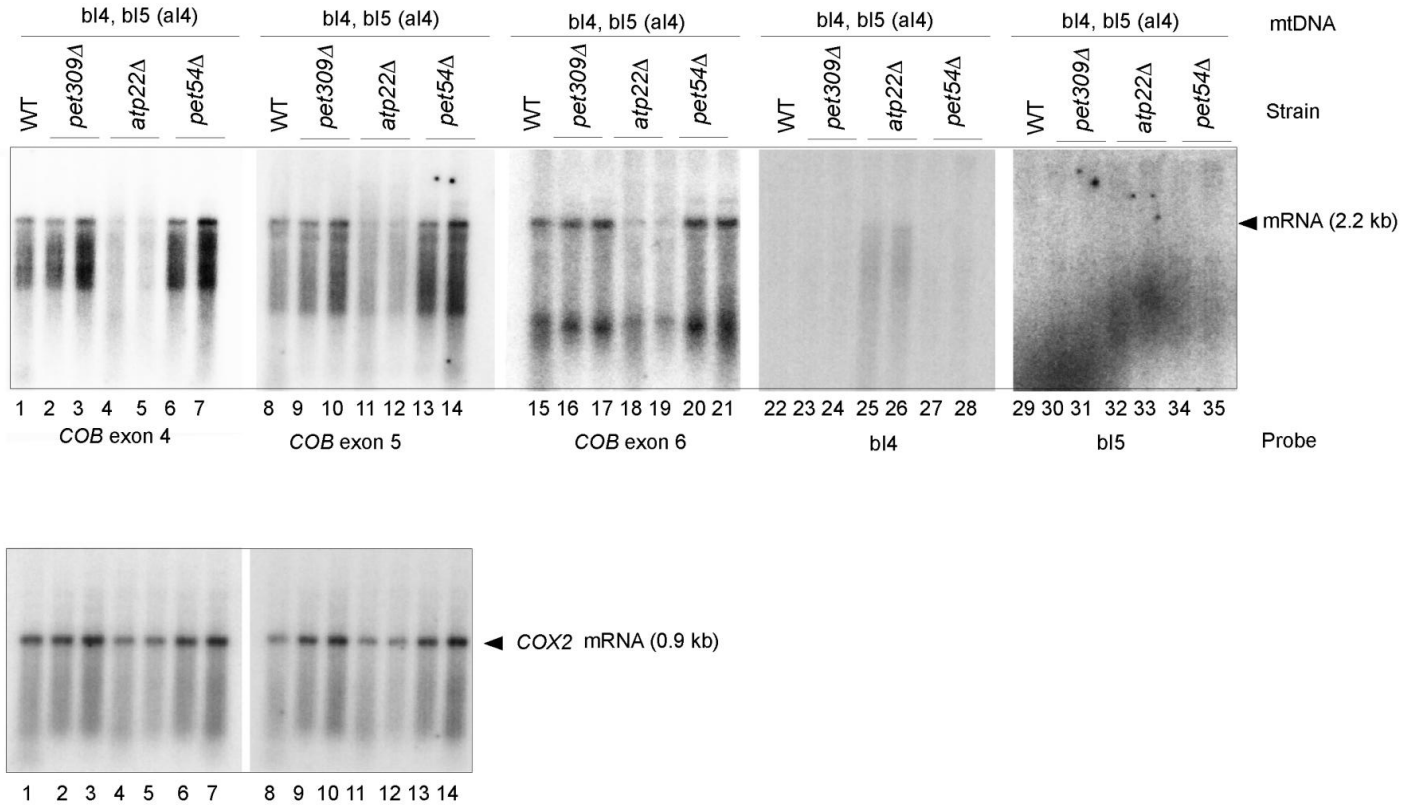

Figure 3.11: Northern hybridization analysis showing the effect of deletion of three translational activators on the splicing of group I introns bI4 and bI5.

Figure 3.11 (continued): Northern hybridization analysis showing the effect of deletion of three translational activators on the splicing of group I introns bI4 and bI5.

The blots show Northern hybridization analysis of wild-type 161-U7-derived strains whose mtDNA contains either intron bI4 or bI5 and mutants of each strain in which genes for *PET309*, *ATP22*, and *PET54* have been deleted. Northern hybridizations were carried out as in Fig. 3.2 except all mutants contain triple the amount of total RNA. Blots were probed for *COB* exons 4 and 5 (indicated below top panel), after which they were stripped and rehybridized with a probe complementary to the *COX2* mRNA (lower panels). Blots were re-stripped and re-probed for *COB* exon 6 and introns bI4, and bI5. Each blot was probed with a ^{32}P-labeled DNA oligonucleotide complementary to the exon or intron indicated. The mature mRNAs (mRNA) are indicated to the right of the panels.

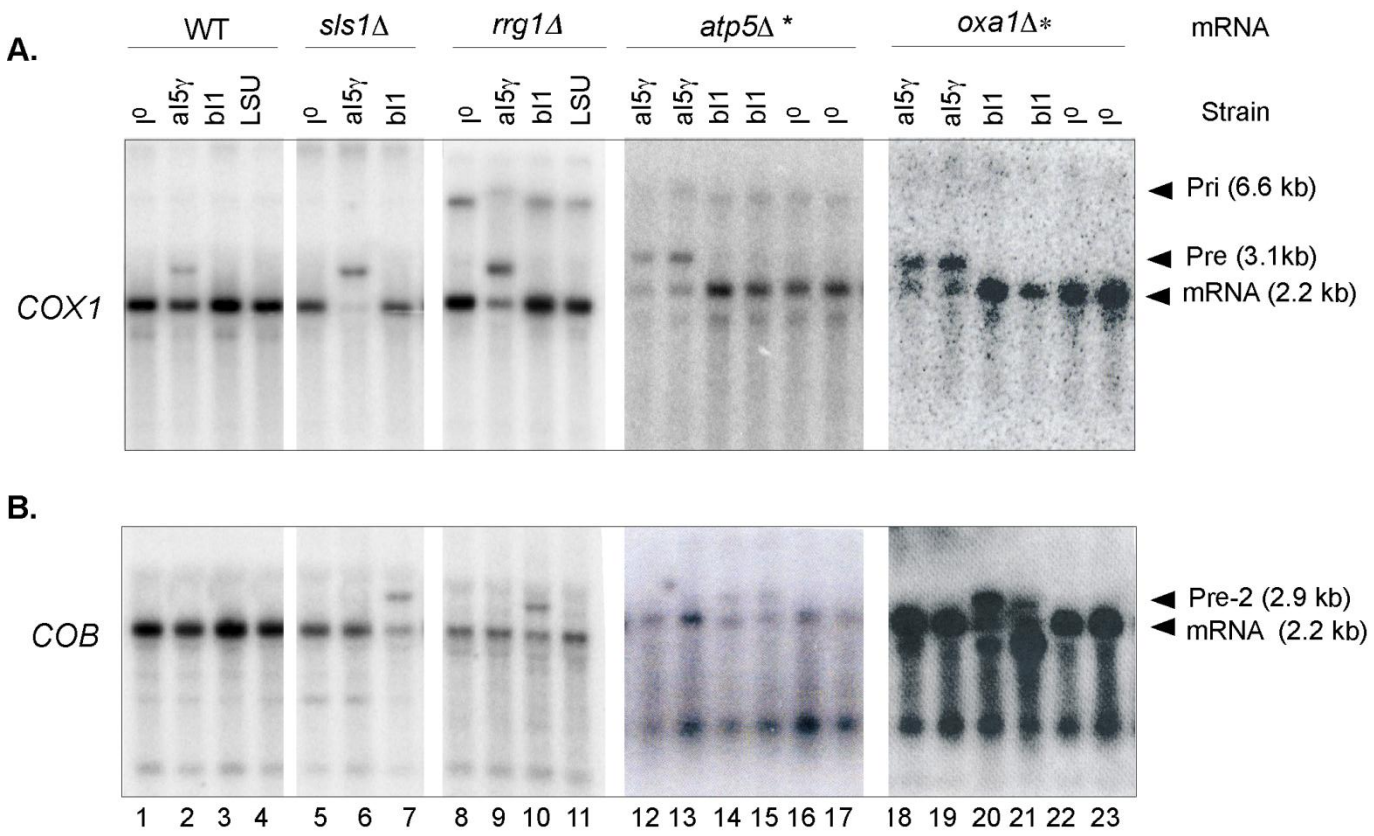

Figure 3.12: Northern hybridization analysis showing the effect of deletion of miscellaneous proteins on aI5γ and bI1 splicing.

Figure 3.12 (continued): Northern hybridization analysis showing the effect of deletion of miscellaneous proteins on aI5γ and bI1 splicing.

(A) The blots show Northern hybridizations of wild-type strain 161-U7 whose mtDNA contains either no introns, (I^0) or single introns aI5γ, bI1, or LSU and mutants of each strain in which genes *SLS1*, *YLR091w*, *MTG1*, *ATP5*, and *OXA1* have been deleted. Northern hybridizations were carried out as in Fig. 3.2 and probed for the *COX1* terminal exon. (B) Strains are as in A, but hybridized with a ^{32}P-labeled DNA oligonucleotide complementary to the *COB* terminal exon. Primary (Pri), Precursor (Pre), and mature mRNA (mRNA) are indicated to the right of the panels. Blots *atp5*Δ and *oxa1*Δ were performed by Kathryn Turner.

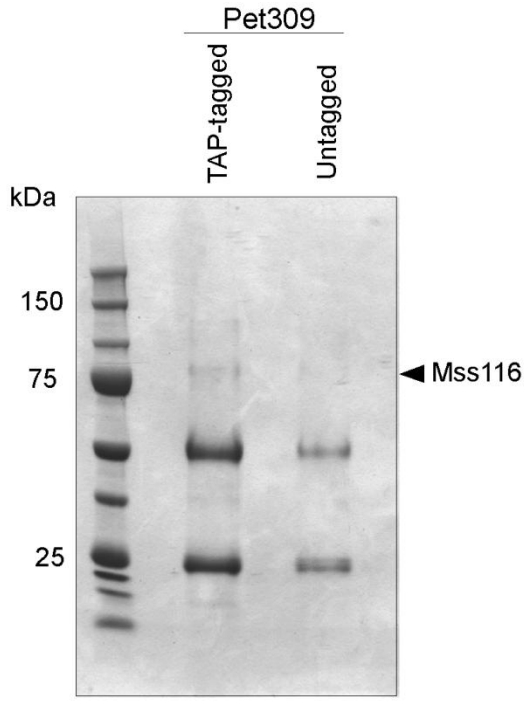

Figure 3.13: SDS-PAGE analysis resulting from TAP-tagged and untagged Pet309 pull-down assay.

Commercially available yeast strains BY4741 in which the chromosomal copy of *PET309* is untagged (WT) or TAP-tagged at the C-terminus (GE Healthcare) were grown to $O.D._{600} \approx 3.0$ in 3 l of YPR. Mitochondria were isolated and subjected to the Tandem Affinity Purification protocol as described in Methods. Aliquots from the tagged and untagged samples were separated in a 4-12% Bis-Tris polyacrylamide gel (Life Technologies) and stained with Coomassie Brilliant Blue. Mss116 is identified at the right, with sizes (kDa) indicated to left.

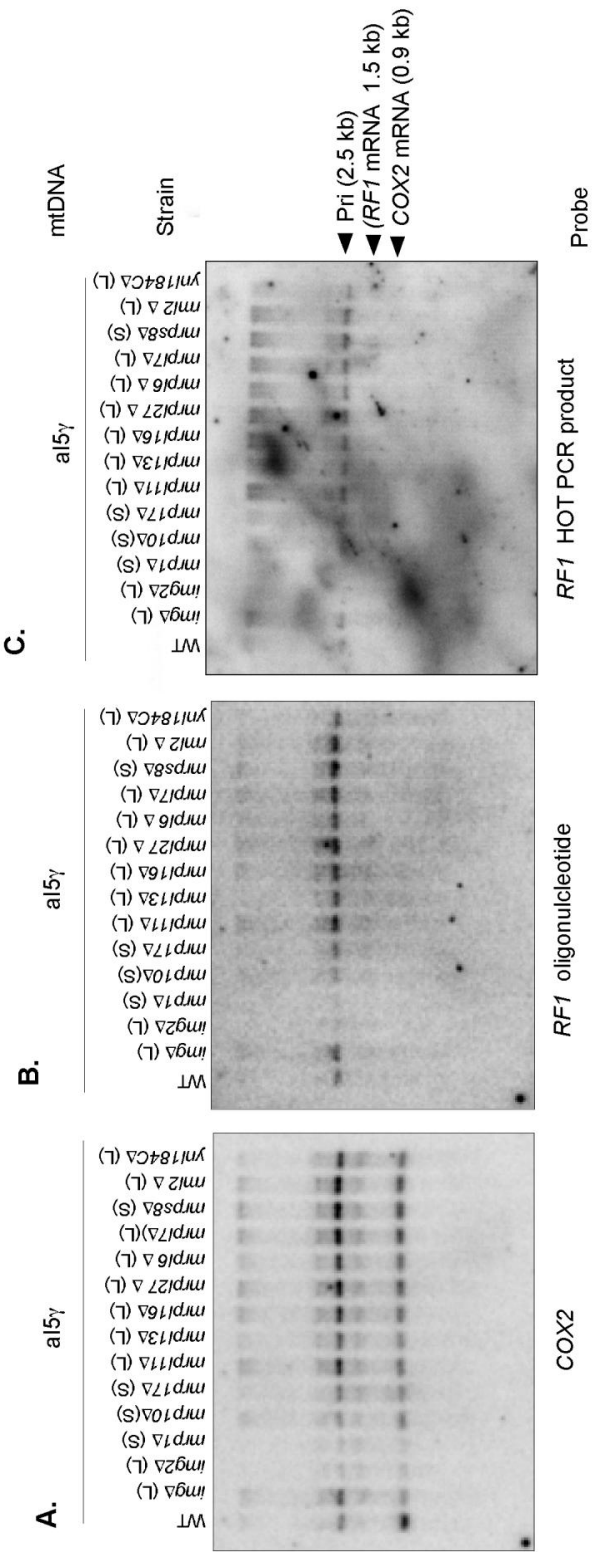

Figure 3.14: Northern hybridization analysis showing the effect of deletions of mitoribosomal protein genes on processing of the *RF1* transcript.

Figure 3.14(continued): Northern hybridization analysis showing the effect of deletion of mitoribosomal protein genes on processing of the *RF1* transcript.

(A) The *COX2* blot is the same one used in Fig. 3.2, which had been probed for the 3´ end of *COX2* RNA. The 2.5-kb primary transcript and 0.9-kb processed *COX2* transcript are indicated to the right of the figure. (B) The blot was stripped and re-probed for *RF1* with a ^{32}P-labeled DNA oligonucleotide complementary to the 3´ end of *RF1* RNA (small arrow beneath *RF1* in Fig. 3.1). (C) The blot was re-stripped and probed with a ^{32}P-internally-labeled PCR product complementary to the 3´ end of *RF1* RNA. The expected position of the processed 1.5-kb *RF1* transcript is indicated in parentheses to the right of the figure.

Ph II ID #	Systematic name	Gene	aI5γ defect	bI1 defect	Function/description
1	YCR046C	*IMG1*	+	+	Mt rp (L)
2	YCR071C	*IMG2*	+	+	Mt rp (L)
3	YDR347W	*MRP1*	+	+	Mt rp (S)
4	YDL045W-A	*MRP10*	+	+	Mt rp (S)
5	YKL003C	*MRP17*	+	+	Mt rp (S)
11	YDL202W	*MRPL11*	+	+	Mt rp (L)
12	YKR006C	*MRPL13*	+	+	Mt rp (L)
14	YBL038W	*MRPL16*	+	+	Mt rp (L)
19	YBR282W	*MRPL27*	+	+	Mt rp (L)
23	YBR122C	*MRPL36*	--	--	Mt rp (L)
25	YKL170W	*MRPL38*	--	--	Mt rp (L)
30	YPR100W	*MRPL51*	+	+	Mt rp (L)
31	YHR147C	*MRPL6*	+	+	Mt rp (L)
32	YDR237W	*MRPL7*	+	+	Mt rp (L)
33	YJL063C	*MRPL8*	0	0	Mt rp (L)
38	YMR158W	*MRPS8*	+	+	Mt rp (S)
40	YEL050C	*RML2*	+	+	Mt rp (L)
48	YNL081C	*SWS2*	--	--	MT rp (S) putative
49	YDR042C	*YDR042C*	--	--	Uncharacterized ORF
54	YNL184C	*(MRPL19)*	+	+	Uncharacterized ORF
57	YHR011W	*DIA4*	+	+	Probable mitochondrial seryl-tRNA synthetase
58	YPL104W	*MSD1*	+	+	Mitochondrial aspartyl-tRNA synthetase
59	YOL033W	*MSE1*	+	+	Mitochondrial glutamyl-tRNA synthetase
62	YGR171C	*MSM1*	+	+	Mitochondrial methionyl-tRNA synthetase
64	YKL194C	*MST1*	+	+	Mitochondrial threonyl-tRNA synthetase
65	YMR287C	*MSU1*	+	0	3'-5' exoribonuclease; component of the mitochondrial degradosome along with the ATP-dependent RNA helicase Suv3p
70	YOR201C	*PET56*	+	+	Ribose methyltransferase; modifies a functionally critical, conserved nucleotide in mitochondrial 21S rRNA
74	YBR163W	*DEM1*	0	0	Mitochondrial 5'-3' exonuclease and sliding exonuclease; required for mitochondrial genome maintenance
75	YOR199W	*YOR199W*	+	+	Dubious ORF
76	YOR200W	*YOR200W*	+	+	Dubious ORF
77	YFL036W	*RPO41*	0	0	Mitochondrial RNA polymerase

Table 3.1: Summary of the results of deletions in the single intron ρ^+ strains.

Table 3.1 (continued)

Ph II ID #	Systematic name	Gene	aI5γ defect	bI1 defect	Function/description
78	YDL044C	*NAM1*	--	--	Mitochondrial matrix protein that interacts with an N-terminal region of mitochondrial RNA polymerase (Rpo41p) and couples RNA processing and translation to transcription
79	YLR27W	*DCS1*	--	--	Hydrolase involved in mRNA decapping
80	YLR139C	*SLS1*	+	+	Coordinates expression of mitochondrially-encoded genes; may facilitate delivery of mRNA to membrane-bound translation machinery
81	YPL005W	*AEP3*	--	--	May facilitate use of unformylated tRNA-Met in mitochondrial translation initiation
82	YMR228W	*MTF1*	0	0	Mitochondrial RNA polymerase specificity factor
83	YMR064W	*AEP1*	+	+	Required for expression of the mitochondrial OLI1 gene encoding subunit 9 of F1-F0 ATP synthase
85	YJL102W	*MEF2*	+	+	Mitochondrial elongation factor involved in translational elongation
87	YMR097C	*MTG1*	--	--	Putative GTPase
89	YLR067C	*PET309*	+	--	Specific translational activator for the *COX1* mRNA
90	YMR066W	*SOV1*	+	+	Mitochondrial protein of unknown function
91	YOR187W	*TUF1*	+	+	Mitochondrial translation elongation factor
92	YKL134C	*OCT1*	0	0	Mitochondrial intermediate peptidase
94	YHR168W	*MTG2*	--	--	Putative GTPase; member of the Obg family
95	YER154W	*OXA1*	+	+	Mitochondrial inner membrane insertase; mediates the insertion of both mitochondrial- and nuclear-encoded proteins
98	YBL022C	*PIM1*	--	--	ATP-dependent Lon protease; involved in degradation of misfolded proteins in mitochondria
99	YDL104C	*QR17*	--	--	Essential for t6A modification of mitochondrial tRNAs
100	YLR369W	*SSQ1*	--	--	Mitochondrial hsp70-type molecular chaperone
101	YMR089C	*YTA12*	--	--	m-AAA protease that mediates degradation of misfolded or unassembled proteins and is also required for correct assembly of mitochondrial enzyme complexes
102	YMR072W	*ABF2*	--	--	Mitochondrial DNA-binding protein; involved in mitochondrial DNA replication and recombination
105	YOR241W	*MET7*	+	+	Folylpolyglutamate synthetase
112	YCR028C-A	*RIM1*	0	0	Single-stranded DNA-binding protein essential for mitochondrial genome maintenance; involved in mitochondrial DNA replication
114	YDL198C	*YHM1*	--	--	Mitochondrial GTP/GDP transporter; essential for mitochondrial genome maintenance
115	YMR083W	*ADH3*	--	--	Mitochondrial alcohol dehydrogenase isozyme III; involved in the shuttling of mitochondrial NADH to the cytosol under anaerobic conditions
117	YDR298C	*ATP5*	+	+	Subunit 5 of the stator stalk of mitochondrial F1F0 ATP synthase
121	YDR350C	*ATP22*	+	--	Specific translational activator for the mitochondrial ATP6 mRNA
122	YPL059W	*GRX5*	--	--	Hydroperoxide and superoxide-radical responsive glutathione-dependent oxidoreductase; mitochondrial matrix protein involved in the synthesis/assembly of iron-sulfur centers
124	YDL181W	*INH1*	--	--	Inhibits ATP hydrolysis by the F1F0-ATP synthase
125	YPR067W	*ISA2*	0	0	Required for maturation of mitochondrial [4Fe-4S] proteins

Table 3.1 (continued)

Ph II ID #	Systematic name	Gene	aI5γ defect	bI1 defect	Function/description
128	YLR091W	*YLR091W*	+	+	Unknown
132	YJR122W	*CAF17*	0	0	Involved in the incorporation of iron-sulfur clusters into mitochondrial aconitase-type proteins
138	YGR102C	*GTF1*	+	+	Subunit of the trimeric GatFAB AmidoTransferase(AdT) complex
139	YGR150C	*CCM1/ DMR1*	+	+	Mitochondrial 15S rRNA-binding protein; required for intron removal of *COB* and *COX1* pre-mRNAs
143	YPR116W	*YPR116W*	+	+	Uncharacterized; required for mitochondrial genome maintenance
148	YER122C	*GLO3*	--	--	ADP-ribosylation factor GTPase activating protein
151	YER110C	*KAP123*	--	--	Karyopherin beta; mediates nuclear import of ribosomal proteins prior to assembly into ribosomes and import of histones H3 and H4; localizes to the nuclear pore, nucleus, and cytoplasm
152	YLR260W	*LCB5*	--	--	Minor sphingoid long-chain base kinase
154	YOL100W	*PKH2*	--	--	Serine/threonine protein kinase
160	YAL048C	*GEM1/ GON1*	0	--	Outer mitochondrial membrane GTPase, subunit of the ERMES complex; potential regulatory subunit of the ERMES complex that links the ER to mitochondria
162	YDL167C	*NRP1*	--	--	Uncharacterized; predicted to be involved in ribosome biogenesis
163	YNL170W	*YNL170W*	--	--	Dubious ORF
NA	YMR063W	*RIM9*	+	--	Plasma membrane protein of unknown function

Table 3.1: Summary of the results of deletions in the single intron ρ^+ strains.

Phase II identification numbers as given in Phase I of the study (Nyberg, 2006) are given next to each systematic name and gene name. Splicing defects for aI5γ or bI1are indicated by +, wild-type splicing is indicated by--. Loss of RNA is indicated by 0. Description or function of the encoded protein is taken from the Saccharomyces Gene Database. Mitoribosomal proteins (Mt rp) are from large (L) or small subunit (S).

Chapter 4: Screen for nuclear-encoded splicing factors using yeast petite strains

4.1 BACKGROUND

4.1.1 Rationale: reducing the mitoribosomal background

Of the 72 candidate genes that were deleted in the initial Phase II screen described in the previous chapter, 54% displayed splicing defects in either aI5γ or both aI5γ and bI1—many more than were originally anticipated. As many of these proteins are associated with the mitoribosome or function in translation, it was possible that the splicing defects observed for deletions made in wild-type yeast strains could be secondary effects of disruption of mitoribosomes or inhibition of translation. We therefore shifted to using petite (ρ^-) strains that lack functional mitoribosomes and are unable to carry out mitochondrial protein synthesis. By using such strains, the expectation was that proteins that function directly in RNA splicing could be more readily identified.

4.1.2 Petite (ρ^-) strains

The petite phenotype is generally caused by the loss or mutation of nuclear- or mitochondrial-encoded genes involved in oxidative phosphorylation (Sherman 1965). The defective respiratory chain that results from such mutations prevents the cell from being able to grow on media containing only non-fermentable carbon sources, such as glycerol or ethanol. Though incapable of respiration, such cells are still capable of fermentation using carbon sources such as glucose or raffinose, resulting in the formation of small (petite) anaerobic colonies. Loss of portions of the mt genome also results in the

cell's inability to assemble functional mitoribosomes. It was the latter condition which made the use of petite strains valuable in this portion of the study, enabling the investigation of the splicing effects of other mt genes in a background free of functional mitoribosomes or mitochondrial protein synthesis.

4.2 RESULTS

4.2.1 Candidate protein determination by mass spectrophotometry

To identify additional candidates for testing, ribonucleoprotein (RNP) complexes from isolated mitochondria (see Methods) from each of the experimental strains were analyzed by mass spectrometry. The RNPs were prepared and the mass spectroscopy results were analyzed by Dr. Georg Mohr, a senior scientist in our lab. The strains tested included a wild-type strain harboring all twelve *COX1* and *COB* introns (strain $1^{+}2^{+}$), ρ^{-} and ρ^{+} strains harboring either the single intron aI5γ or bI1, and the intronless I^{0}/ρ^{+} strain. Each of the single-intron strains was tested by PCR and Northern hybridization to confirm its status as bearing only the intron of interest (not shown).

The spectral counts obtained from the mass spectroscopy data represented a general measure of abundance for each protein with higher numbers indicating more abundant proteins. However, the counts are also sensitive to the length of the proteins and the number of possible peptides that can be detected by MS/MS. The tabulated counts were determined by averaging three injections of each RNP. Abundant proteins showed less than 25% variation between injections, while less abundant proteins varied by several fold and were not considered. The spectral counts for each protein were

normalized to the total number of counts for each RNP to allow for comparison across strains. A second value, a Z-score, was also calculated for each protein, which indicated the number of standard deviations the spectral count was above or below the mean. Proteins with Z-scores greater than 3 were considered significant since Z-scores greater than 2.58 are generally equivalent to a 99% confidence level, p-value = 0.01 (Lu et al. 2007).

Preliminary comparisons of known splicing factors were found in greater abundance in the $1^{+}2^{+}$ strain as compared to the I^{0} strain and established the soundness of the method. Those proteins that were found to be enriched in the ρ^{-} over the ρ^{+} strains (as was the general splicing factor, Mss116) comprised the list of candidates to be tested for this portion of the study.

Of the eight proteins known to be encoded in the mt genome, four were detected in more than three RNPs: Atp6, Cox1, Cox2, and Var1. Interestingly, Rf1, also known as Q0255, or Orf1, was also detected. This is the maturase-like protein discussed previously in section 3.2.11.

Several translational activators were also among the enriched proteins in the ρ^{-} strains: Sov1 (translational activator for *VAR1*, enriched in bI1ρ^{-}), Atp22 (translational activator for *ATP8/6*, moderately enriched in aI5γ ρ^{-} and bI1 ρ^{-}), Pet54 (translational activator for *COX3*, moderately enriched in bI1 ρ^{-}), and Pet309 (translational activator for *COX1*, moderately enriched in bI1 ρ^{-}). All but Pet54 are pentatricopeptide repeat (PPR) proteins.

Several other proteins were highly enriched in the ρ^- strains but had previously been tested and their deletions caused either a weak or no splice defect in ρ^+ strains, or caused the cells to lose mtRNA: Rim1 (Appendix, Blot 39) , Rpo41 (Appendix, Blots 12 and 15), and Rmd9 (Phase I), and so were not tested further. The final candidate proteins and their functions, if known, are listed in Table 4.1, most of which had also been identified for analysis in Phase I and Phase II of the study.

4.2.2 Growth of petite strains

By necessity, ρ^- knock-out strains were grown for a longer period than were the ρ^+ strains in the initial part of the study (see Methods for details). When allowed to grow only to an $O.D._{600}$ of about 0.8-1.0 as were the initial ρ^+ strains, there were no clear differences in splicing observed between ρ^- knock-outs and ρ^- with wild-type nuclear backgrounds. By growing for 20 hours, however, differences in splicing patterns became apparent, though in several cases, the cells were not able to retain their mtDNA.

4.2.3 Deletions in ρ^- strains produce various effects

The Northern hybridization analyses in Fig. 4.1 show the effect on the splicing of aI5γ (A) and bI1 (B) with the deletions of several of the potential splicing candidates that had been determined by mass spectrometry. Some null mutants in the aI5γ strains exhibited variant colony phenotypes and are identified by the isolate number alongside the strain name which will be discussed in more detail below.

The wild-type ρ^+ strain and ρ^- strains are in lanes 1 and 2, respectively. The ρ^- strain with a wild-type nuclear background exhibits a splicing defect for both aI5γ (A) and bI1 (B), suggesting that the mitoribosome oe mitochondria protein synthesis may play a role in splicing these introns, albeit an indirect one. Additionally, the ρ^- strain appears be deficient in processing the primary *COX1* transcript (Pri).

4.2.3.1 Some deletions in ρ^- cause splice defects in aI5γ and loss of COB mtRNA

Several of the deletion strains exhibited a splicing defect in aI5γ, but lost the *COB* transcript in the bI1 strains: *aim10Δ*, *fmp38Δ*, *mrp10Δ*, and *atp22Δ* in Fig. 4.1A and B, lanes 3, 5, 7, and 11. *AIM10* encodes a putative prolyl-tRNA synthetase that when deleted, displays an elevated frequency of mitochondrial genome loss (Sentandreu et al. 1997) as observed here for *COB*. *FMP38/GEP3/MTG3* encodes an inner membrane protein required for mitochondrial ribosome small subunit biogenesis through the maturation of 15S rRNA (Paul et al. 2012). *MRP10* encodes a mitoribosomal protein from the small subunit whose deletion was observed to also cause aI5γ and bI1 splicing defects in the ρ^+ strains (upper panels in Figs. 3.2, and 3.3, lanes 5). *ATP22* encodes a specific translational activator for *ATP6/8* mRNA, encoding a subunit of the F1F0 synthase. Deletion of *ATP22* was observed earlier to destabilize the *COB* transcript in the presence of introns bI4 and bI5 in a ρ^+ strain (Fig. 3.11, lanes 4,5, 11, 12, 18, and 19) and to a lesser degree when only bI1 was present (Fig. 3.9B, lane 10).

Though strains *pet123Δ* and *rsm22Δ* did not entirely lose the COB transcript, they exhibited severe reductions in the *COB* RNA, suggesting it might be lost with longer

culturing (Fig. 4.1B, lanes 14 and 15, respectively). Both of these strains also exhibited aI5γ splicing defect (Fig. 4.1A, lanes 14 and 15). *PET123* encodes a mitoribosomal protein of the small subunit that exhibits genetic interactions with *PET122* which, in turn, encodes a *COX3* mRNA-specific translational activator (Haffter et al. 1991). *RSM22* also encodes a mitoribosomal protein of the small subunit that is predicted to be an S-adenosylmethionine-dependent RNA methyltransferase (Petrossian and Clarke 2009).

In summary, *COB* RNA was lost or greatly reduced with the loss of proteins of the small mitoribosomal subunit; a protein involved in small subunit biogenesis; the translational activator for *ATP6/8*; and a putative tRNA synthetase. These deletions also exacerbated the aI5γ splicing defect of the ρ^- wild-type strain.

4.2.3.2 Some deletions in ρ^- cause splice defects in both aI5γ and bI1

Some strains exhibited splicing defects beyond the baseline defect of the wild-type ρ^- strains. Strains *pet130Δ*, *pet54Δ*, and *mrh4Δ* exhibited exacerbated splicing defects in both aI5γ (Fig. 4.1A) and bI1 (Fig. 4.1B) (lanes 8, 12, and 17, respectively). Little is currently known about Pet130, other than it is required for respiratory growth (Petrossian and Clarke 2009). The observation that splicing of both aI5γ and bI1 is affected in the *pet130Δ* strain may, in part, explain that requirement. *PET54* encodes one of three translational activators for the *COX3* mRNA and acts as a splicing factor for the group I intron, aI5β, facilitating exon ligation (Costanzo et al. 1989; Kaspar et al. 2008). Mrh4 (lanes 17) is a mt ATP-dependent RNA helicase of the DEAD-box family that is required for assembly of the large subunit of the mitoribosomes. It binds to the large

subunit 21S rRNA and localizes to the matrix face of the mitochondrial inner membrane, associating with the large subunit precursor and with mature mitoribosomes (De Silva et al. 2013). Its deletion caused a severe splicing defect in bI1.

Thus, loss of a *COX3* translational activator and a DEAD-box RNA helicase associated with the large mitoribosomal subunit caused splicing defects for both aI5γ and bI1.

4.2.3.3 Some deletions in ρ⁻ cause splice defects in aI5γ but not in bI1

Deletions of three genes, *MRP17*, *PET309, and MRPS12* appear to cause splicing defects specific for aI5γ beyond that of the wild-type ρ^- strain, though not for bI1 (lanes 9, 13, and 16, respectively). Mrp17 is a mitoribosomal protein of the small subunit that exhibits genetic interactions with *PET122*, which encodes a *COX3*-specific translational activator (Haffter and Fox 1992). Pet309 is a translational activator for the *COX1* mRNA which localizes to the mitochondrial inner membrane (Manthey et al. 1998; Zamudio-Ochoa et al. 2014). As observed in the ρ^+ strain earlier, this protein appears to be specific for aI5γ (Figs. 3.10 and 3.11). In this ρ^- background, its role in translation activation is likely minimized and emphasizes its possible role as a splicing factor specific for aI5γ. Mrps12 is a mt protein with similarities to the *E. coli* S12 ribosomal protein (Gan et al. 2002) which has been identified as an subunit interface protein that assists rRNA in translocation (Cukras et al. 2003).

4.2.3.4 Some deletions in ρ⁻ exhibit wild-type splicing phenotype in aI5γ strains

Unexpectedly, three of the strains, *aep1Δ*, *sov1Δ*, and *aep3Δ* (Fig. 4.1A, lanes 4, 6, and 10) all exhibited a wild-type splicing phenotype for aI5γ. The colony color phenotype for these strains was not the same white color as the ρ^- parent strain, but cream, in contrast to the red color of the ρ^+ strains. For each of these deletions, bI1 splicing and color phenotype were similar to the ρ^- parent strain. All three proteins, Aep1, Sov1, and Aep3, contain PPR motifs (Lipinski et al. 2011). Additionally, Aep1 and Sov1 are translational activators for the *ATP9* and *VAR1* mRNAs, respectively (Herrmann et al. 2013) and Aep3 reportedly functions as an accessory initiation factor in mitochondrial protein synthesis (Lee et al. 2009).

The 161-U7 wild-type red phenotype is known to be caused by oxidation of a by-product of the adenine pathway (Jones and Fink 1982). In respiratory-deficient strains, this by-product is not oxidized, so that the colony phenotype remains white. Addition of excess adenine to the media bypasses the adenine pathway, preventing both the formation of the by-product and the red color. To test whether this pathway was influencing splicing, these strains were re-cultured with the addition of excess adenine (0.15 mg/ml). While the strains reverted to the white color phenotype, the excess adenine had no effect on splicing which remained as wild-type (not shown).

4.2.4 Testing other translational activators and PPR proteins

Since the strains displaying a wild-type splicing phenotype were either translational activators, PPR proteins, or both, I decided to test isolates of others that met

these criteria. The *pet54Δ* and *pet309Δ* strains in Fig. 4.1A were white colonies that exhibited splicing defects (lanes12 and 13), however, other knock-outs of these genes displayed the cream-colored phenotype, as did other isolates of *aep3Δ*, and *sov1Δ*; therefore these were also tested for their splicing abilities. The *atp22Δ* and *pet111Δ* strains all exhibited white phenotypes. Since protein products of these genes are both translational activators as well as PPR proteins, these mutants were included in the subsequent tests. A *cbp1Δ* strain was generated to be included, since Cbp1 is likewise a translational activator that contains PPR motifs (Lipinski et al. 2011; Herrmann et al. 2013) although Phase I of the screen had shown no splicing defect with the deletion of this protein.

In Fig. 4.2, two isolates each of *pet54Δ*, *cbp1Δ*, and *atp22Δ* were tested in both the aI5γ ρ^- (A) and bI1ρ^- (B) strains. The wild type ρ^+ and ρ^- strains of each blot are in lanes 1 and 2, respectively. Lanes 3 and 4 show the difference in splicing abilities in two isolates of *pet54Δ*, with the first exhibiting a more severe splicing defect than the wild type ρ^- strain, while the second exhibits a wild-type splicing ability comparable to ρ^+. In lanes 5 and 6 are the two isolates of *cbp1Δ*. Both exhibit a wild-type splicing phenotype. In lanes 7 and 8 are two *atp22Δ* isolates; both of which exhibit a stronger splicing defect than the wild type ρ^- strain. None of the deletions in the bI1ρ^- strains (B) exhibit any significant difference in splicing ability as compared to the wild type ρ^-. Both blots were stripped and re-probed with ^{32}P-labeled DNA oligonucleotides complementary to their respective introns. There appears to be residual intron in the primary transcripts (Pri) in

all the aI5γ ρ^- strains not observed in the ρ^+. The amount of precursor (Pre) is inversely proportional to the amount of excised intron (aI5γ).

Because no differences had been observed in the bI1ρ^- strains, the next set of Northern hybridizations were only tested in the aI5γ strains (Fig. 4.3). The wild type ρ^- strain is in lane 1. In lanes 2 and 3 are *aep3Δ* isolates, with the first exhibiting a near wild-type splicing phenotype, while the second is similar to the ρ^- parent strain, albeit with an apparent increased amount of unspliced and unprocessed primary transcript (Pri). In lanes 4 and 5 are two isolates of *pet309Δ*, with the first displaying a very strong splicing defect, while the second displays near-wild-type splicing. In lane 6 is a strain deleted for *OXA1*, which encodes an insertase associated with the mitoribosomes and is neither a translational activator nor a PPR protein. This control strain exhibits a severe splicing defect. In Fig. 4.3, lane 7 is another *pet54Δ* strain that again exhibits a wild-type splicing phenotype in contrast to the ones in Figs. 4.1A, lane 12 and 4.2A, lane 3. In Fig. 4.3, lanes 8 and 9 are two *pet111Δ* isolates, both exhibiting a more severe splicing defect than observed in the ρ^- parent strain. In lane 10 another *sov1Δ* isolate, that exhibits a strong splicing defect, in contrast to the one seen in Fig. 4.1, lane 6.

4.2.5 Re-confirming gene replacement in ρ^- mutants that exhibit wild-type splicing

Though each of the mutants used in these Northern hybridizations had been previously tested by PCR to check for gene replacement by a kanamycin antibiotic resistance cassette, here I re-tested those that gave mixed phenotypes: *pet309Δ*, *aep1Δ*, *sov1Δ*, and *aep3Δ*, also testing for the presence/absence of the gene of interest. Figure

4.4A diagrams the relative positions of the primers used to test for the presence of the gene (G) and to test for the presence of kanamycin cassette (K). In Fig. 4.4B, PCR products of the expected sizes are seen in the mutants only for those reactions amplifying the kanamycin cassette (K) (lanes 1, 3, 6, 8, 11, 13, 15, 18, 20, and 22). The gene (G) is only amplified in the control wild-type strain (WT, lanes 5, 10, 17, 24). In Fig. 4.4C, total RNA from each of the strains was tested by PCR for the presence of contaminating DNA, though none is found. These results confirm the replacement of the indicated gene with the kanamycin cassette.

4.2.6 ρ^- mutants are not ρ^+ contaminants

To test for the possibility that these may be ρ^+ knock-out contaminants, the blots from Fig. 4.1A and B were stripped and re-probed with a ^{32}P-labeled DNA oligonucleotide complementary to the *COX2* mRNA. Figure 4.5 shows the results for the aI5γ strains, with the original blot in panel A. The signal for the *COX2* mRNA is only visible for the ρ^+ strain in lane 1 of panel B, indicating that the remaining strains lack the *COX2* portion of the mt genome and therefore are petite. Similar findings are seen for the bI1 strains in Fig. 4.6 with the original blot shown in panel A. The signal for the *COX2* mRNA is only visible for the ρ^+ strain in lane 1 of panel B. This indicates that those strains exhibiting wild-type splicing are indeed ρ^-

4.2.7 Phenotype colors are stable

The finding that deletions in aI5γ ρ^- strains can sometimes lead to near-wild-type splicing suggests there may be alternate pathways to aI5γ splicing. Could alternate

pathways develop over time in splice-defective strains? To test this notion, the strains in Fig. 4.4 were streaked onto YPD/G416 agar plates and YPR/G418 agar plates and incubated at 30° C for 3 to 5 days. Several of the colonies were re-streaked onto fresh plates and incubated again at 30° C for another 3 to 5 days. This procedure was repeated two more times to look for a color change from white to cream indicating a change in splicing ability, but none was ever observed; the color phenotypes remained stable. This suggested that instead of multiple splicing pathways, there may be second-site suppressor mutations that rescued the splicing of aI5γ in the absence of both functional mitoribosomes and some translational activators or PPR proteins. This problem will remain for future studies.

4.3 DISCUSSION

The results of this portion of the study showed that mitoribosomal proteins and proteins involved in mt translation impacted the splicing of aI5γ and bI1 in strains lacking functional mitoribosomes or mitochondrial protein synthesis. This suggests that several of these proteins may be involved in functions other than translation, and/or perhaps that they are part of a larger complex involved in the splicing of these two introns.

The deletion of genes *PET130*, *PET54* and *MRH4* caused splicing defects in both aI5γ and bI1, with the deletion of DEAD-box protein *MRH4* having a severe impact on bI1 splicing. Deletion of other genes resulted in defective aI5γ splicing and loss or reduction of the *COB* RNA: *AIM10, FMP38, MRP10, ATP22, PET123*, and *RSM22*, suggesting that these proteins may participate in coordinating *COX1* splicing and *COB*

stability. In Chapter 3, deletion of *ATP22*, translational activator for ATP6, was seen to cause the instability of *COB*. Pet123 genetically interacts with *PET122* which encodes a translational activator for *COX3* (Haffter et al. 1991*)*. Loss of Cbp1, a translational activator known to be required for *COB* stability, exhibited a wild-type splicing phenotype in the ρ^- strain (this study) as well in the ρ^+(Nyberg 2006).

The deletion of three genes, *PET309*, *MRP17, and MRPS12* caused splicing defects for aI5γ, but not for bI1. A similar effect was observed when *PET309* was deleted in ρ^+ strains (Fig. 3.9) where its deletion was specific for aI5γ. Mrp17 and Mrps12 are both mitoribosomal proteins of the small subunit, the former known to exhibit genetic interactions with *COX3* translational activator Pet122 (Haffter and Fox 1992) which in turn, has been shown to interact with Pet309 (Naithani et al. 2003).

Along with Pet309, translational activators for other mRNAs, Aep1, Sov1, and Atp22, were shown in Chapter 3 to impact the splicing of aI5γ, suggesting these proteins may coordinate to regulate aI5γ splicing. In this part of the study, three of these translational activators were found to sometimes exhibit near wild-type splicing when deleted in aI5γ ρ^- strains, possibly due to second-site suppressor mutations. Loss of the fourth, Atp22, the translational activator for the *ATP6* mRNA, consistently caused an aI5γ splicing defect in both ρ^+ and ρ^- strains. Pet54, the translational activator for the *COX3* mRNA, did not impact aI5γ splicing in the ρ^+ strain, but its deletion sometimes caused a splicing defect in the ρ^- strain, and sometimes exhibited a wild-type splicing phenotype. Similarly, in Phase I of the study, Nyberg observed no splicing defect in aI5γ

with the deletion of *PET111* (although a strong defect was observed for aI5β). Here, its deletion exhibited wild-type splicing in the ρ^- strain. Loss of a translational activator for *COB*, Cbp1, did not impact splicing of either aI5γ or bI1 when tested in Phase I of the study. Here, deletion of its gene also exhibited a near wild-type splicing phenotype in the aI5γ ρ^- strain.

These results further support the idea that a higher order of organization exists among these proteins to regulate aI5γ splicing, possibly also including many of the ribosomal proteins. Alternatively, most of these translational activators have been identified as PPR proteins, well known for their interactions with RNA, so that it is also possible that the proteins are interacting with each others' mRNAs or with the rRNAs. Pet54, though not identified as a PPR protein, is recognized as a splicing factor for aI5β in addition to its role as translational activator for *COX3*, confirming the protein's ability to also interact with RNA. This protein is also required for the maintenance of normal levels of *COX1* synthesis in an intronless strain (Shingu-Vazquez et al. 2010).

It is unclear why deletions of several of the translational activator and/or PPR proteins would sometimes have a near-wild-type splicing phenotype. One possible explanation may be that these translational activators, in normal, wild-type backgrounds, would bind their respective mRNAs and/or mitoribosomal proteins or rRNAs, which in effect, sequesters these proteins thereby releasing a block on aI5γ splicing. Deletion of these proteins, along with the mitoribosomal proteins or rRNAs mimics this condition,

allowing near-wild-type splicing. It remains unclear why the results are not consistent, however. More work is required to understand this phenomenon.

Standard name	Gene name	Protein description/function
YDL045W-A	*MRP10*	Mitochondrial ribosomal protein of the small subunit; contains twin cysteine-x9-cysteine motifs; oxidized by Mia40p during import into mitochondria
YKL003C	*MRP17*	Mitochondrial ribosomal protein of the small subunit; MRP17 exhibits genetic interactions with PET122, encoding a *COX3*-specific translational activator
YOR158W	*PET123*	Mitochondrial ribosomal protein of the small subunit; PET123 exhibits genetic interactions with PET122, which encodes a *COX3* mRNA-specific translational activator
YKL155C	*RSM22*	Mitochondrial ribosomal protein of the small subunit; also predicted to be an S-adenosylmethionine-dependent methyltransferase
YNR036C	*YNR036C*	Mitochondrial protein; may interact with ribosomes based on co-purification experiments; similar to E. coli and human mitochondrial S12 ribosomal proteins
YGL064C	*MRH4*	Mitochondrial ATP-dependent RNA helicase of the DEAD-box family; required for assembly of the large subunit of mitochondrial ribosomes; binds to the large subunit rRNA, 21S_rRNA; localizes to the matrix face of the mitochondrial inner membrane and associates with the large subunit precursor and with mature ribosomes
YPL005W	*AEP3*	Peripheral mitochondrial inner membrane protein; may facilitate use of unformylated tRNA-Met in mitochondrial translation initiation; PPR protein (Lipinski, 2011)
YMR064W	*AEP1*	Translational activator for mitochondrial OLI1 gene; PPR protein (Lipinski, 2011)
YLR067C	*PET309*	Specific translational activator for the *COX1* mRNA; also influences stability of intron-containing COX1 primary transcripts; localizes to the mitochondrial inner membrane; contains seven pentatricopeptide repeats (PPRs)
YNR066W	*SOV1*	transcriptional activator for Var1 (Herrmann et al. 2013) PPR protein (Lipinski, 2011)
YDR350C	*ATP22*	Specific translational activator for the mitochondrial ATP6 mRNA, PPR protein (Lipinkski, 2011)
YOR205C	*MTG3/ FMP38*	Protein required for mitochondrial ribosome small subunit biogenesis; null mutant is defective in respiration and in maturation of 15S rRNA; protein is localized to the mitochondrial inner membrane; null mutant interacts synthetically with prohibitin (Phb1p)
YJL023C	*PET130*	Protein required for respiratory growth; the authentic, non-tagged protein is detected in highly purified mitochondria in high-throughput studies
YER087W	*YERO87W*	Protein with similarity to tRNA synthetases; non-tagged protein is detected in purified mitochondria; null mutant is viable and displays elevated frequency of mitochondrial genome loss
YGR222W	*PET54*	Mitochondrial inner membrane protein; binds to the 5' UTR of the *COX3* mRNA to activate its translation together with Pet122p and Pet494p; also binds to the *COX1* Group I intron AI5 beta to facilitate exon ligation during splicing
YLR382C	*NAM2*	Mitochondrial leucyl-tRNA synthetase; also has a direct role in splicing of several mitochondrial group I introns; indirectly required for mitochondrial genome maintenance
YLR139C	*SLS1*	Mitochondrial membrane protein; coordinates expression of mitochondrially-encoded genes; may facilitate delivery of mRNA to membrane-bound translation machinery
YPL029W	*SUV3*	ATP-dependent RNA helicase; component of the mitochondrial degradosome along with the RNase Dss1p; the degradosome associates with the ribosome and mediates RNA turnover; also required during splicing of the COX1 AI5_beta intron
YHR120W	*MSH1*	DNA-binding protein of the mitochondria; involved in repair of mitochondrial DNA; has ATPase activity and binds to DNA mismatches; has homology to E. coli MutS; transcription is induced during meiosis

Table 4.1: Potential splicing factors identified by mass spectroscopy.

Table 4.1(continued): Potential splicing factors identified by mass spectroscopy.

Ribonucleoproteins were prepared from isolated mitochondria from ρ^+ and ρ^- strains of 161-U7/aI5γ and 161-U7/bI1 and analyzed by mass spectrometry. Listed are those proteins which were enriched in the ρ^- strains. Systematic names, standard gene names and protein functions, when known, are given. The shaded area represents those proteins for which deletions in the ρ^- strains were not successful.

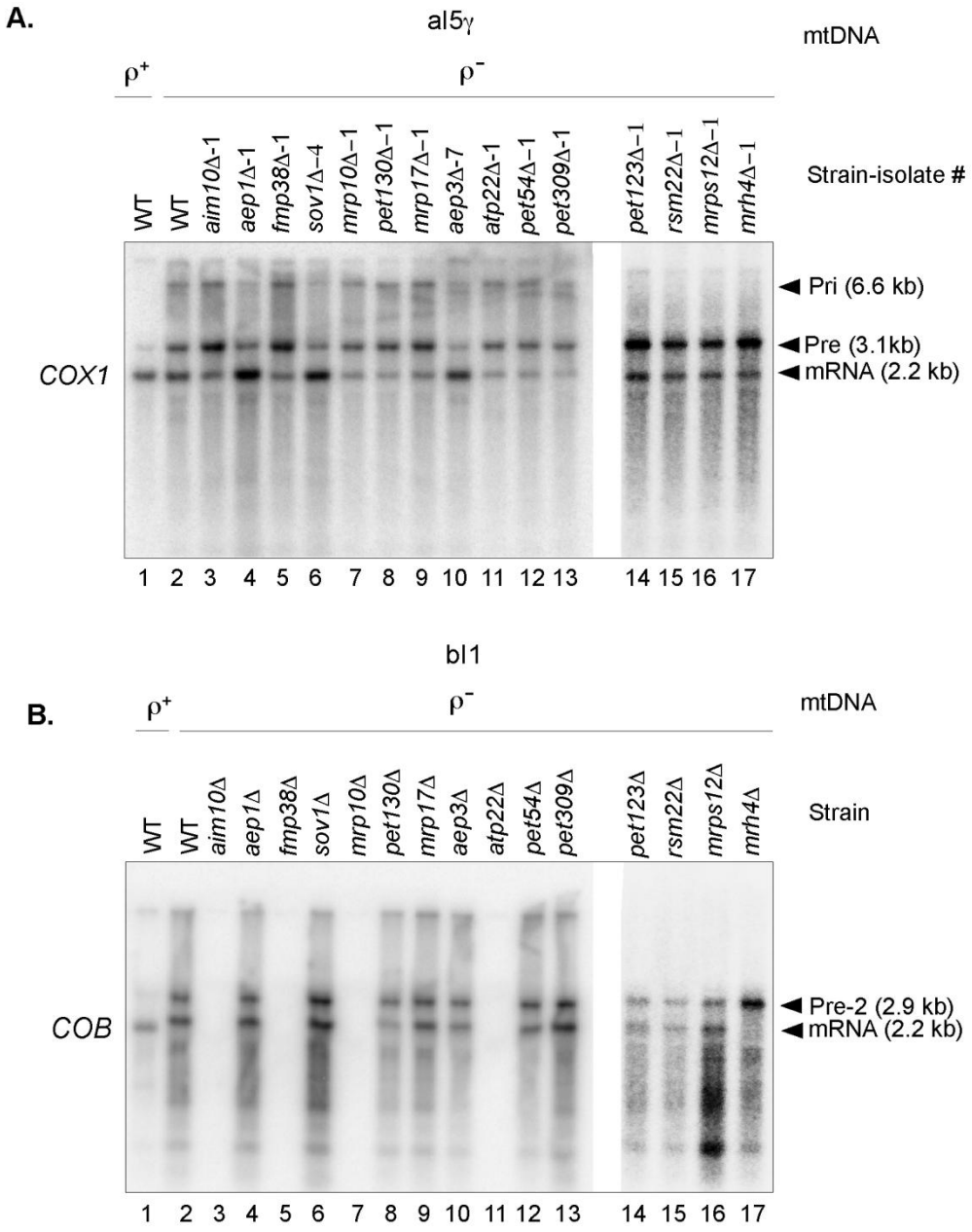

Figure 4.1: Northern hybridization analysis showing the effect of deletion of potential splicing factors identified by mass spectroscopy analysis in comparing single intron ρ^+ to ρ^- strains.

Figure 4.1(continued): Northern hybridization analysis showing the effect of deletion of potential splicing factors identified by mass spectroscopy analysis in comparing single intron ρ^+ to ρ^- strains.

(A) Northern hybridizations of wild-type strain 161-U7/aI5γ ρ^+ and ρ^- and derivatives of the petite strain in which the indicated gene has been deleted. Cells from freshly streaked plates were resuspended in YPR at a starting $O.D._{600}$ = 0.2 and allowed to grow for 20 h. Total cellular RNA was isolated, run in a 1.5% RNA-grade agarose gel, blotted onto a nylon membrane, and hybridized with a ^{32}P-labeled DNA oligonucleotide complementary to the *COX1* terminal exon. (B) Wild-type strain 161-U7/bI1 ρ+ and ρ- and derivatives of the petite strain in which the indicated gene has been deleted. Cells were cultured, RNA prepared and run as in A except the blot was hybridized with a ^{32}P-labeled DNA oligonucleotide complementary to the *COB* terminal exon. Primary (Pri), Precursor (Pre), and mature mRNA (mRNA) are indicated to the right of the panels.

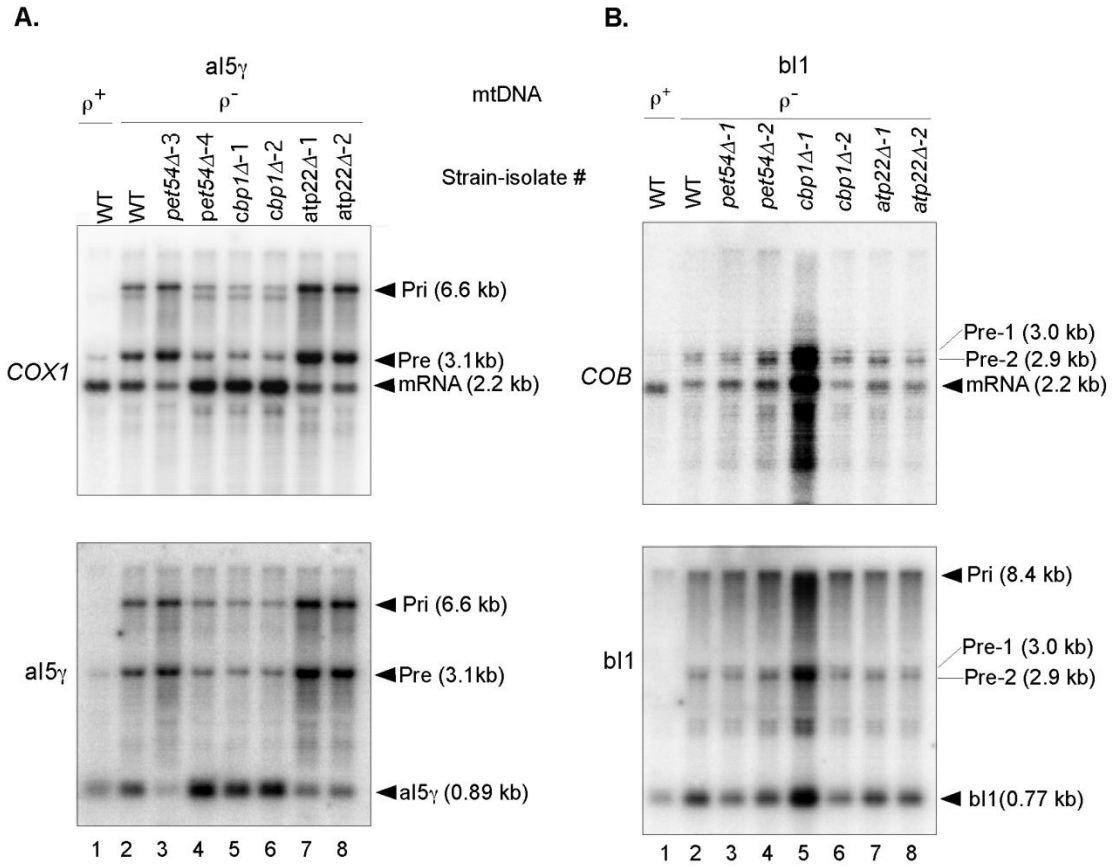

Figure 4.2: Northern hybridization analyses showing the effect on aI5γ and bI1 splicing in ρ^- strains with deletions of known translational activators.

(A) Northern hybridizations of wild-type (WT) strain 161-U7/aI5γ ρ^+ and ρ^- and derivatives of the petite strain in which the indicated gene has been deleted. Cells were cultured, RNA prepared and run as described in Fig. 4.1. Northern hybridization of the *COX1* exon (top panel) is as in Fig. 4.1. To probe for intron aI5γ, the membrane was stripped and rehybridized with a ^{32}-P-label DNA oligonucleotide complementary to aI5γ. (B) Wild-type (WT) strain 161-U7/bI1 ρ^+ and ρ^- derivatives of the petite strain in which the indicated gene has been deleted. Cells were cultured, RNA prepared and run as in Fig.4.1B. To probe for intron bI1, the membrane was stripped and rehybridized with a ^{32}-P-label DNA oligonucleotide complementary to the bI1 intron (bottom panel). Primary (Pri), Precursor (Pre), and mature mRNA (mRNA are indicated to the right of the panels.

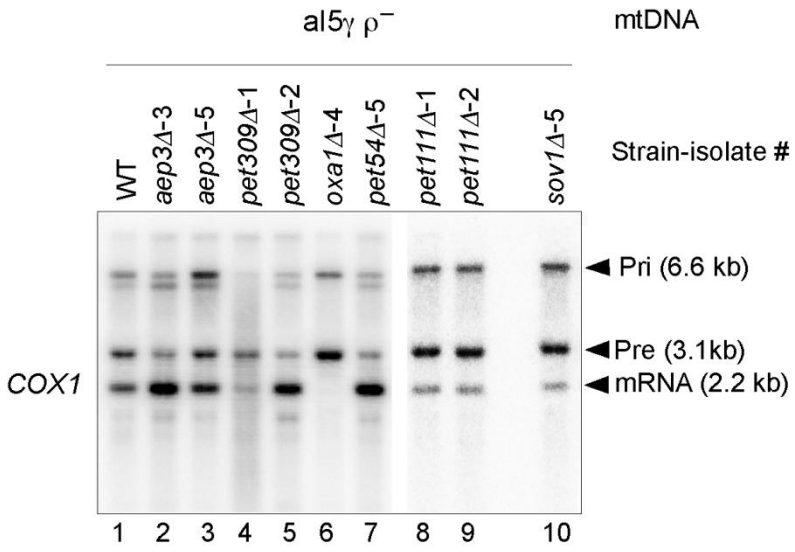

Figure 4.3: Northern hybridization analysis showing the effect on aI5γ splicing in ρ⁻ strains with deletions of other translational activator and PPR proteins.

Northern hybridization analysis of wild-type (WT) strain 161-U7/aI5g r- and derivatives of that strain in which the indicated gene has been deleted. Cells were cultured, RNA prepared and run and hybridized as in Fig. 4.1A. Primary (Pri), Precursor (Pre), and mature mRNA (mRNA are indicated to the right of the panels.

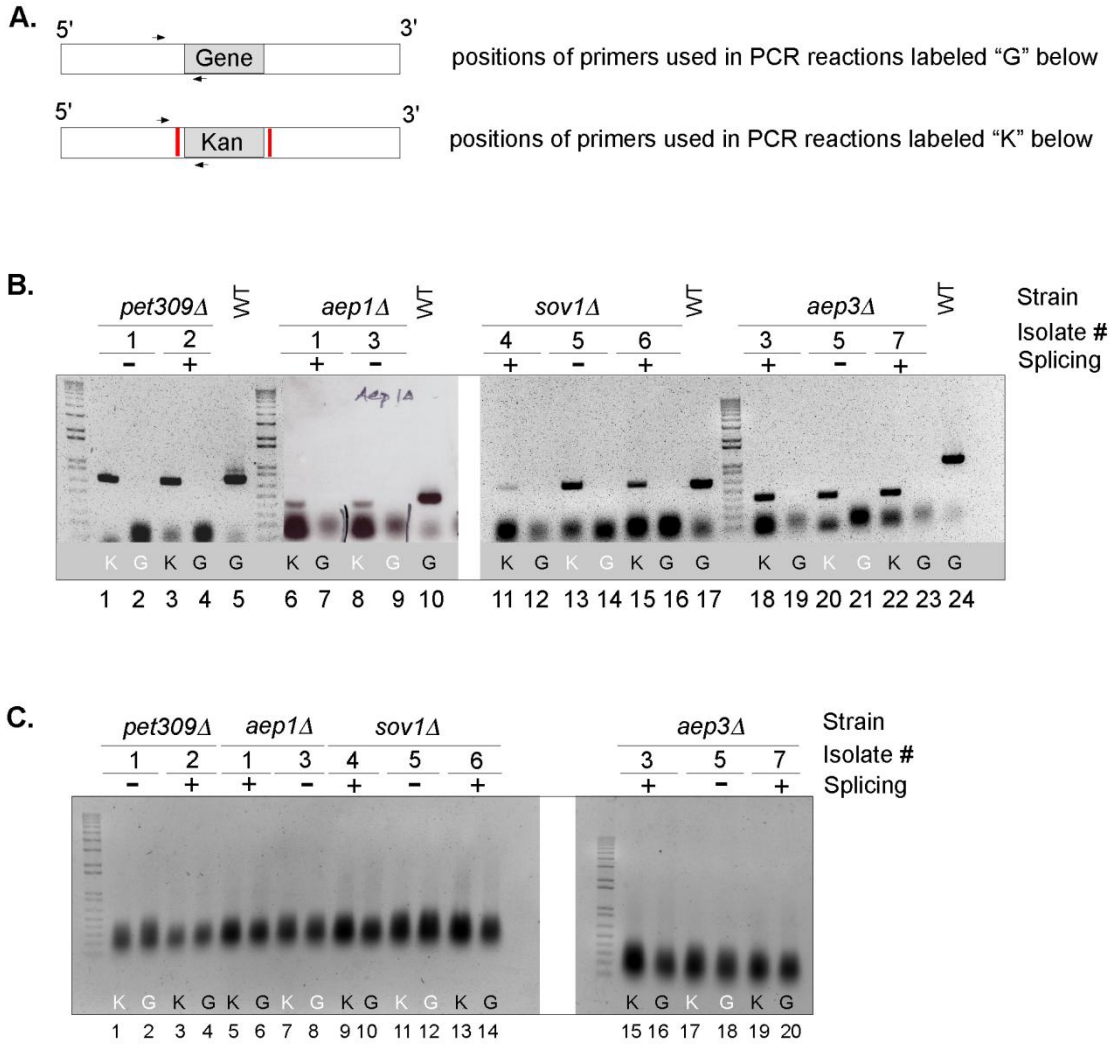

Figure 4.4: PCR analyses confirming gene replacement in 161-U7/aI5γ ρ^- strains with mixed splicing phenotypes.

Figure 4.4(continued): PCR analyses confirming gene replacement in 161-U7/aI5γ ρ^- strains with mixed splicing phenotypes.

(A) Relative positions of DNA primers (see Methods) used in B and C to test by PCR for gene replacement by a kanamycin resistance cassette. The boundaries of the transforming kanamycin cassette are indicated by red lines. Relative positions of primers used in testing for the presence of the gene (G) and kanamycin cassette (K) are shown. Forward primers (right-pointing arrows) were complementary to the region upstream of the cassette originally used for homologous recombination. Reverse primers (left-pointing arrows) were complementary to either the 5´ region within the gene or the kanamycin cassette. (B) Colony PCR analyses of freezer stocks. The deleted gene is indicated above sets of mutants with either wild-type (+) or defective (-) splicing phenotypes for each given isolate. Wild-type strains (WT) were used as controls. PCR reactions testing either for the presence of a kanamycin cassette (K) or the indicated gene (G) is indicated beneath each lane. White font indicates colonies are white; dark font indicates colonies are cream-colored when grown on YPD/G418 agar plates. (C) PCR analyses of isolated whole-cell RNA from each of the isolates, using the same conditions as in B.

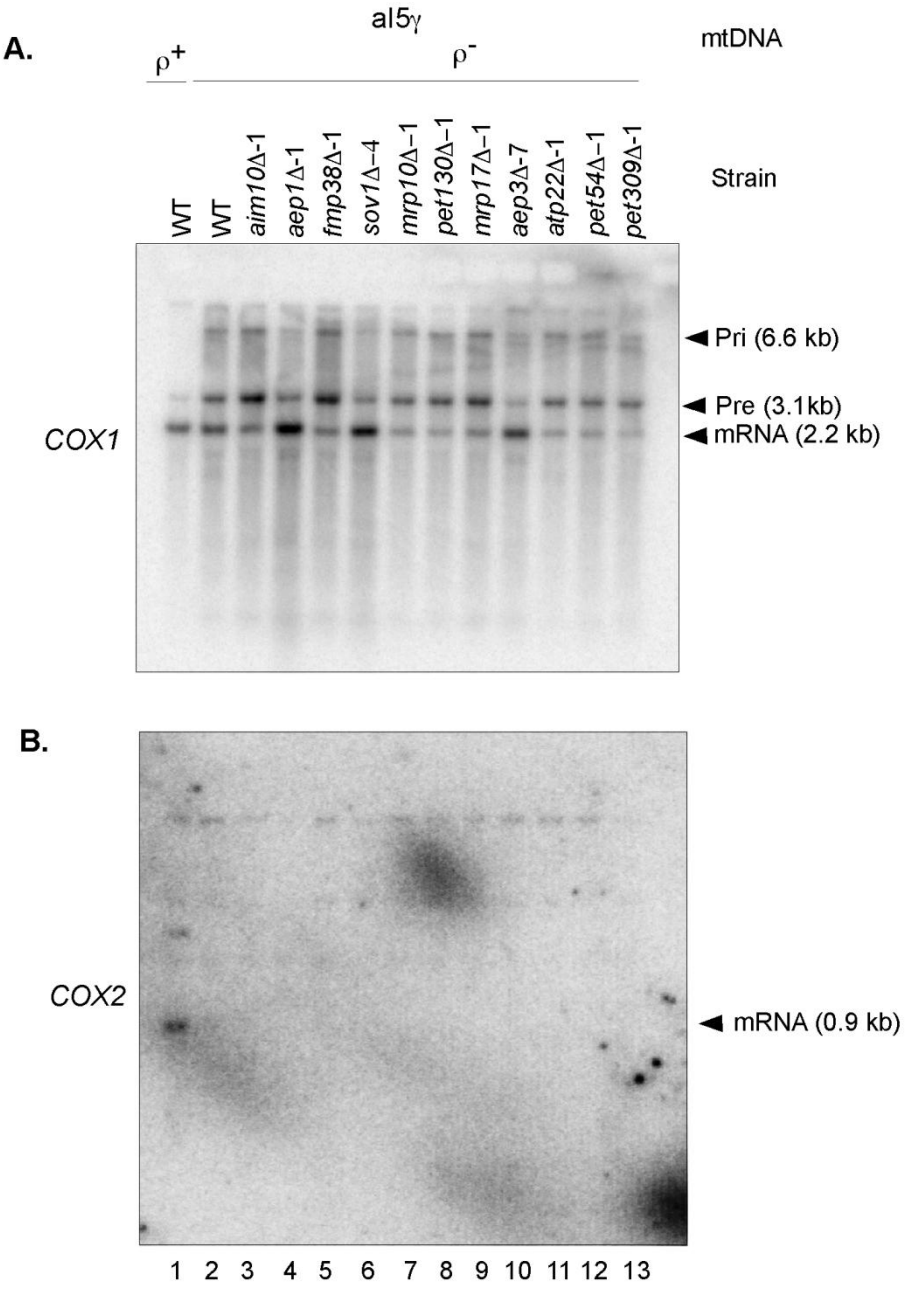

Figure 4.5: Northern hybridization analysis confirming ρ^- status of 161-U7/aI5γ ρ^- strains.

(Top) Blot from Figure 4.1A (lanes 1-13) was stripped and rehybridized (bottom) with a ^{32}P-labeled DNA oligonucleotide complementary to the *COX2* mRNA. Primary (Pri), Precursor (Pre), and mature mRNA (mRNA) are indicated to the right of the panels.

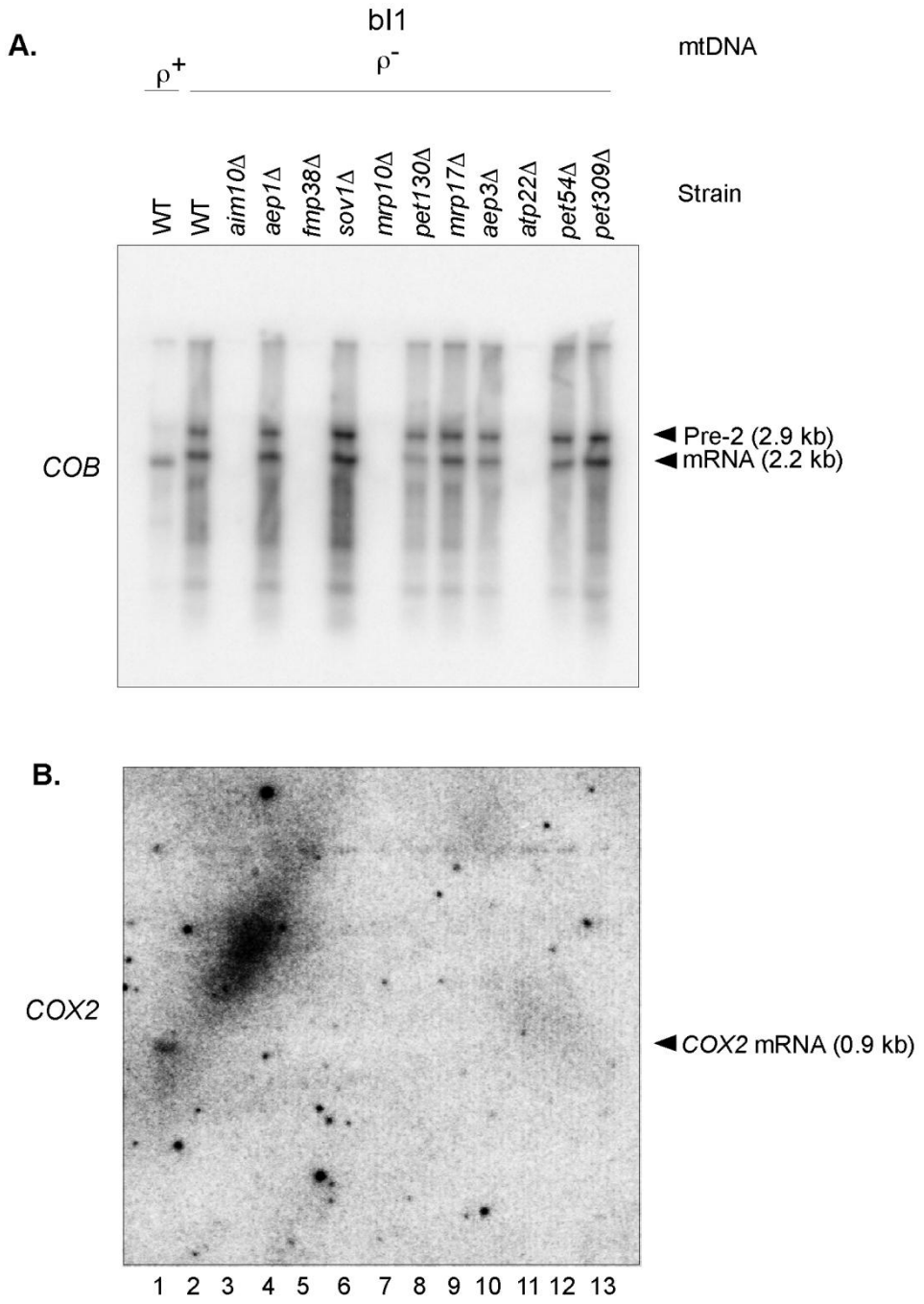

Figure 4.6: Northern hybridization analysis confirming ρ^- status of 161-U7/bI1 ρ^- strains.

(Top) Blot from Figure 4.1B (lanes 1-13) was stripped and rehybridized (bottom) with a ^{32}P-labeled DNA oligonucleotide complementary to the *COX2* mRNA. Primary (Pri), Precursor (Pre), and mature mRNA (mRNA) are indicated to the right of the panels.

Chapter 5: Oxa1 plays a role in aI5γ and bI1 splicing

5.1 BACKGROUND

5.1.1 Rationale

The screen for mt intron splicing factors discussed in Chapters 3 and 4 identified Oxa1 as a protein potentially required for aI5γ and bI1 splicing (Fig 3.12A, lanes 22-23; Fig. 3.12B, lanes 23-24; Fig. 4.3, lane 6). These interesting results prompted further exploration of the possibility that Oxa1 might function as a splicing factor for aI5γ and bI1. The results of these investigations form the basis of this chapter.

5.1.2 Structure and function of Oxa1

A member of the highly-conserved Oxa1/YidC/Alb3 protein family, Oxa1 is found in the inner membranes of yeast mitochondria (Funes et al. 2011). All members of this family function as insertases, that is, proteins that assist in the insertion of hydrophobic proteins into membranes. In the case of Oxa1, the protein assists with the inner membrane insertion of the highly hydrophobic proteins encoded by the mt genome; however, nuclear-encoded proteins imported into the mitochondrion are also assisted by Oxa1 (Hildenbeutel et al. 2012). Some evidence suggests that translocation of the hydrophobic proteins is facilitated by the formation of a pore composed of Oxa1 dimers (Kohler et al. 2009; Krüger et al. 2012).

Oxa1 has 5 transmembrane domains positioned within the mitochondrial inner membrane with an N-out, C-in orientation (Hell et al. 1997; Funes et al. 2011) (Fig.5.1A). These transmembrane domains comprise the hydrophobic core of the protein

and are so well conserved that the region may be functionally interchanged among Oxa1, YidC and Alb3 (Jiang et al. 2003; Funes et al. 2009). Linking the first two transmembrane domains is a feature common to all insertases, the Loop 1 region that extends into the matrix which is thought to contribute to ribosome binding (Lemaire et al. 2000). A second Oxa1 domain, less common among insertases, is the C-terminal domain (CTD) that also protrudes into the matrix and interacts with the mt ribosome and possibly with the nascent polypeptides to increase the efficiency of the insertion process (Jia et al. 2003; Szyrach et al. 2003; Kohler et al. 2009). The yeast CTD is thought to form an amphipathic α-helix with one positively-charged and one hydrophobic surface characteristic of a coiled-coil structure that has been shown to be both required and sufficient for binding the mt ribosome to the mt inner membrane (Kohler et al. 2009). Previous studies in the multi-intron yeast strain W303 have shown that deletion of either of these domains individually does not prevent growth on glycerol, while deletion of both domains, does. (Lemaire et al. 2000).

Crosslinking experiments indicate that Oxa1 dimers localize above the ribosome polypeptide exit tunnel allowing the direct insertion of nascent and highly hydrophobic mitochondrially-encoded proteins into the hydrophobic inner membrane (Jia et al. 2003; Szyrach et al. 2003; Kohler et al. 2009; Keil et al. 2012). (Fig. 5.1B). This raises the possibility that the splicing defect observed due to the loss of Oxa1 may be a result of an indirect effect on another yet-unidentified protein dependent on this function. However, other proteins have been shown to also participate in protein insertion within the mitochondrion, so that Oxa1 is not necessarily absolutely essential for this process

(Dimmer and Rapaport 2012). Except for Cox2, all mt translation products can integrate into the membrane in the absence of Oxa1, although with reduced efficiencies (Altamura et al. 1996; He and Fox 1997; Hamel et al. 1998; Lemaire et al. 2000).

5.1.3 The processing of the 21S rRNA transcript

The rRNA of the mitochondrial large subunit (LSU) is the 21S rRNA. The polycistronic 6.7-kb primary transcript of the 21S rRNA gene includes the non-coding genes of the mitochondrial tRNAs for threonine, cysteine and histidine (Turk et al. 2013) (Fig.5.2). Following 3′ processing, the resulting precursor is 4.4 kb which, with the excision of the 1.1-kb intron, matures to the final 3.3-kb rRNA (Merten et al. 1980). In some of the Northern hybridizations that follow, these RNAs were visualized by using a ^{32}P-labeled DNA oligonucleotide complementary to the exon of the LSU/rRNA (small arrow below *LSU* in Fig. 5.2)

5.2 RESULTS

5.2.1 Splicing defects in *oxa1Δ* strains are observed in aI5γ and bI1, but not ω

During the general screen, Oxa1 was among many proteins knocked out in four different ρ^+ strains: 161-U7/aI5γ, 161-U7/bI1, 161-U7/ $I^0$and 161-U7/ω (see Methods). The Northern hybridizations in Figure 5.3 compiles several deletion strains in which the blots were hybridized with ^{32}P-labeled DNA oligonucleotides complementary to either the terminal exons of *COX1*, *COB*, or *LSU/* 21s rRNA. In each blot, wild type is in lane 1. The strong splicing defect produced by the deletion of the general RNA chaperone, Mss116, is clearly observed in lane 2 of all three hybridizations. Deletion of three

mitoribosomal proteins in lanes 3-5 follow, each exhibiting a defect less extreme than that of Mss116, for both aI5γ and bI1 splicing, though no splicing defect is evident for ω. The gene *YNL184C* encodes an uncharacterized protein whose deletion causes splicing defect patterns (lanes 6) similar to those of the mitoribosomal proteins. *GTF1* encodes a subunit of the trimeric GatFAB AmidoTransferase (AdT) complex (Barros et al. 2011). Its deletion in lanes 7 causes no splicing defect in any of the three introns. Similarly, deletion of *KAP123*, which encodes a cytoplasmic protein that facilitating nuclear import of ribosomal proteins prior to assembly into ribosomes (Rout et al. 1997), has no impact on the splicing of any of the introns (lanes 8). The *oxa1Δ* strains in lanes 9 exhibited strong splicing defects for the group II introns aI5γ and bI1,though no defect is seen for the group I intron ω. This result prompted two questions: (1) Is the defective splicing a result of Oxa1's close association to the mitoribosomes? (2) Is Oxa1 a splicing factor specific to group II introns, or more particularly, to aI5γ and bI1?

5.2.2 Splicing defects are exacerbated in oxa1Δ ρ- strains grown in YPR

To address the first question, *OXA1*was deleted in aI5γ and bI1 single-intron petite (ρ^-) strains to reduce the background effect of the mitoribosomes These strains lack functional mitoribosomes and exhibit a diminished ability to splice both aI5γ and bI1 even with a wild-type nuclear genotype as observed in Chapter 4.

The Northern hybridizations in Fig. 5.4 show the effect of deletion of *OXA1* in single intron ρ^- strains compared to deletions in single intron ρ^+ and intronless I^0 strains. The intronless control shows little difference between wild type and *oxa1Δ* (Fig. 5.6A

and B, lanes 1-2), suggesting that Oxa1's effect may be limited to strains with introns. In the ρ^+ strains, the effect of deleting *OXA1* is particularly apparent in the aI5γ strain as compared to the bI1 (5.3 A and B, lanes 3-4). In the ρ^- strains, deleting *OXA1* exacerbates the splicing defects in both aI5γ and bI1strains when compared to ρ^- wild type, with virtually all of the RNA in precursor form and none as spliced mRNA (Fig. 5.4, A and B, lanes 6). This suggested that Oxa1 may be playing a role in splicing, even in the absence of functional mitoribosomes.

5.2.3 Loss of Oxa1 impacts splicing in aI5γ and bI1 more than in other tested mt introns

The next question to be addressed was whether Oxa1 is required specifically for the splicing of group II introns aI5γ and bI1. To test this, I first attempted to knock out *OXA1* in a 1^+2^+ wild-type strain harboring all 12 group I and II introns in *COX1* and *COB*. While *OXA1* knock-outs were relatively easily obtained in single-intron strains aI5γ and bI1, two attempts to replace *OXA1* with the kanamycin resistance cassette in the 1^+2^+ wild-type strain resulted in only two transformants. In culture, these quickly became petite resulting in loss of mtRNA that consequently resulted in Northern hybridizations of poor quality. As an alternative, I chose to use the three strains, HRH421, HRH524 and HRH422, previously used in Chapter 3. For clarity, they will be briefly described again here.

Strain HRH421 has only the group II intron, aI1. This intron encodes its own active maturase and requires RNA chaperone, Mss116 for proper splicing. Strain

HRH524 only has group II intron aI2. It also encodes its own active maturase and requires Mss116. Strain HRH422 has 3 group I introns: aI4, bI4 and bI5. Intron aI4 encodes an inactive maturase but is aided instead by the active maturase encoded by bI4 that assists in the splicing of itself and aI4 (Rho and Martinis 2000). Besides Mss116, splicing of both of these introns is aided by Nam2, a mt leucyl-tRNA synthetase (Labouesse 1990). Intron bI5 does not code for a maturase; its splicing is facilitated by Cbp2 as well as Mss116.

In Figure 5.5 A, *COX1* group II introns aI5γ, aI1, and aI2, as well as group I intron aI4 are compared. The intronless strain I^0 is used as control (lanes 1-2). In marked contrast to aI5γ in lanes 4 and 6, introns aI1, aI2, and aI4 (lanes 8, 10, 12) show no dependence on Oxa1 for splicing. Similarly, *COB* group I introns bI4 and bI5 (in B, lane 8) do not exhibit any evident splicing defect except with darker contrast, during which a faint band corresponding to the size of unspliced bI5 (also 2.9 kb) becomes visible. This faint band is distinctly different from the pronounced defect observed for bI1 in lanes 4 and 6. Thus, Oxa1 did not have any marked effect on any of the group I introns tested, and among the group II introns, Oxa1 appears to be more important to those without maturases; i.e. aI5γ and bI1. It is interesting to note that despite the close relationship between Oxa1 and the mitoribosome, deletion of the insertase has little noticeable effect on the expression of the intron-encoded maturases of aI1 and aI2 as observed by their near-wild-type splicing. One possible explanation is the hydrophilic maturases are not reliant on Oxa1's insertase function.

5.2.4 Oxa1 mutants suggest aI5γ and bI1 splicing is influenced by the protein's insertase activity

With much of Oxa1 buried within the mt inner membrane, the two domains that extend into the matrix would seem to be those likely involved in splicing. In 2004, Lemaire, *et al*. designed a series of Oxa1 mutants to test the functions of its various domains (Lemaire et al. 2004). Here, I reconstructed these mutants to investigate how each might contribute to intron splicing. Figure 5.6A illustrates the locations of amino acid residues (designated by asterisks) within the Oxa1 protein topology that were used in constructing mutants in Fig. 5.6B. The untagged and myc-tagged wild-type sequences are diagrammed in (i) and (ii), respectively. One mutant has a large portion of Loop 1 removed (iii); one has most of the CTD removed (iv); and one has both regions removed (v). All were myc-tagged for possible subsequent Western blotting. Previous studies have shown that Oxa1 tolerates C-terminal tagging well (Reif et al. 2005; Jia et al. 2009; Stoldt et al. 2012). Each of the constructs was cloned into centromeric plasmid pRS416 and transformed into a strain in which the chromosomal copy of *OXA1* had been replaced by a kanamycin resistance cassette. Selection required use of a uracil$^-$ defined media; here I used Hartwell's Complete (HC) with 2% glucose as carbon source. Cultures were grown in HC lacking uracil with 2% raffinose as carbon source to minimize the effect of glucose repression (see Methods). These complementation mutants were then tested by Northern hybridization for the effect they had on the splicing of aI5γ and bI1.

Following scanning with a phosphorimager, the Northern hybridizations in Figures 5.7 and 5.8 were analyzed using GelQuant software (BioChem Lab Solutions) to

determine the percentage of spliced mRNA. Ratios of mRNA to mRNA + precursor RNA (upper value) or to mRNA + precursor + primary transcript (lower value) are indicated as percent spliced mRNA under each lane in the blot. Intronless strain I^0 served as negative control.

5.2.4.1 Effect of loss of two Oxa1 domains on aI5γ splicing

The effects on aI5γ splicing are shown in Fig. 5.7A. Both of the *oxa1Δ*/ aI5γ ρ^+ and ρ^- strains exhibited a severe splicing defect (lanes 9 and 16) that is rescued by complementation with wild type (lanes 10-11 and 17-18). Comparable splicing ability by the untagged and myc-tagged wild-type complements showed little interference by the myc tag: in the ρ^+ strains (79% and 73%, respectively) and in the ρ^- strains (86% and 84%, respectively). This corroborates previous work showing that C-terminal tagging is well tolerated by Oxa1 (Reif et al. 2005). Complementation by the Δ Loop 1 (ΔL1-myc) had little effect on splicing in ρ^+ (86%, lane 12). In contrast, this mutant did not rescue the splicing defect in the aI5γ ρ^- strain to the extent it did in the ρ^+ strain (70% spliced mRNA, lane 19), suggesting that the presence of the ribosome can somewhat compensate for the lack of Loop 1. Complementation with ΔCTD Oxa1 mutant protein (ΔCTD-myc) rescued the splice defect in both ρ^+ and ρ^- strains (lanes 13 and 20), which exhibited similar splicing abilities at 84% and 83%, respectively. This indicates that the tail region is not critical for aI5γ splicing. Complementing with the double-deletion mutant (ΔL1/CTD-myc), however, showed a strong synergistic splicing defect in both ρ^+ and ρ^- strains with only 57% and 51% splicing (lanes 14 and 21), respectively. Thus, though

neither the Loop 1 nor the CTD domains appeared critical to splicing on their own, loss of both domain did cause an aI5γ splicing defect. This defect, however, was not as severe as that observed in the ρ^+ and ρ^- null mutant complements which exhibited only 26% and 35% splicing (lanes 9 and 16), respectively. This suggests that the remaining core transmembrane insertase domain that contributes most significantly to the proper splicing of aI5γ.

5.2.4.2 Effect of loss of two Oxa1 domains on bI1 splicing

The effects on bI1 splicing by the Oxa1 complementation mutants are shown in Fig 5.8A. Two values for the percent splicing were determined: as the ratio of mRNA to Precursors 1, 2 and the mRNA (top value) and the second (lower value) as the ratio of mRNA to precursors 1, 2 (Pre-1 and Pre-2 combined), mRNA and the primary transcript (Pri). Interestingly, remnants of the *COB* primary transcript are only evident for the empty vector and wild-type complements (lanes 9-11), but not for the ΔL and ΔCTD mutant complements (lanes 12- 14 and 19-21). Therefore, in the results and discussion below, only the top value will be considered. Also evident are several unidentified RNAs (*), which run faster than the mRNA but slower than the bI1 intron that likely represent splicing intermediates containing the intron and exon. These latter RNAs may represent different configurations of the excised lariat, and nonetheless were not considered in the determination of percent splicing.

A comparison of the ρ^+ and ρ^- wild types in lanes 8 and 15 shows a slight splicing defect in the ρ^- strain (82% as compared to 100% for ρ^+). As in the previous set of

complementing proteins, the myc tag appears to have no adverse effect on splicing. This is clearly observed by comparing the splicing abilities of the ρ^+ wild-type untagged and tagged complementing proteins, both with 94% splicing (lanes 10 and 11); and the ρ^- untagged and tagged wild type with 79% and 80% splicing, respectively (lanes 17 and 18).

Interestingly, with only 32% splicing, the ρ^+ null mutant (lane 9) exhibits a stronger splicing defect than the ρ^- strain (lane 16) with 58%. Complementation by the ΔL1-myc mutants rescues both: 93% splicing for ρ^+ (lane 12) and 84% for ρ^- (lane 19), suggesting that the Loop 1 domain is not essential for bI1 splicing. Similarly, complementing with the ΔCTD-myc mutants also allows both ρ^+ and ρ^- strains to regain near-wild-type splicing at 95% and 80%, respectively (lanes 13 and 20), also suggesting that this domain is not essential for splicing. Complementation with the double-deletion mutant complement (ΔL1/CTD-myc) rescues splicing only to 63%, accompanied by a sharp drop in *COB* RNA (lane 14). Unexpectedly, the ρ^- strain is not as severely affected as is the ρ^+ strain. In this case, complementation with ΔL1/CTD-myc (though not as restorative as complementation with either ΔL1 or ΔCTD individually) restores splicing to 76%. Complementation with ΔL1/CTD-myc still maintains levels of splicing greater than those of the null mutants (compare lanes 14 to 9 and 21 to 16).

To assess equal loading, both the aI5γ and bI1 blots were stripped and rehybridized with a ^{32}P-labeled DNA oligonucleotide complementary to the intronless

COX2 mRNA (Figs. 5.7B and 5.8B). There is no observable *COX2* message for the petites, as expected (lanes 15-21).

5.2.4.3 Loss of Oxa1 up-regulates 21S rRNA

Because of Oxa1's interaction with the large mitoribosomal subunit, and to test for the presence of a second portion of the mt genome, the membranes were re-stripped and rehybridized for the mitochondrially-encoded *21S rRNA* of the large subunit using a ^{32}P-labeled DNA oligonucleotide (Figs. 5.7C and 5.8C). Unexpectedly, the wild-type ρ^+ strains have very low levels of *21S rRNA* (lanes 1 and 8), while the *oxa1Δ* strains which were complemented with the empty vectors have strong signals (lanes 2 and 9). It seems plausible that in the wild-type strains, the *21S rRNA* is bound within the mitoribosomes, so that little free RNA remains. Without Oxa1, however, *21S rRNA* appears to be upregulated, perhaps to signal the biogenesis of more mitoribosomes. However, a similar effect is not observed for the 15S rRNA of the small subunit (Figs. 5.7D and 5.8D) in which the levels are approximately equal.

Neither the 21S nor the 15S rRNAs are seen in the aI5γ and bI1 ρ^- strains, confirming their lack of assembled mitoribosomes (lanes 15-21).

5.2.5 Type of media appears to affect splicing

One of the other unexpected results of these experiments was the large amount of mRNA visible in the ρ^- wild-type and *oxa1Δ* mutant strains (Fig. 5.7A and Fig. 5.8A, lanes 15 and 16). This is in contrast to the more severe splicing defects observed previously when grown in similar conditions, but with YPR media (Fig. 5.4A and B,

lanes 6; and Fig. 5.5A and B, lanes 5 and 6). Since the complementing mutants in these experiments were expressed in plasmids that required minimal media lacking uracil for selection, it seemed possible that the strains required more time to exhibit a splicing defect. To test this idea, strains used in Fig. 5.7A, lanes 15 and 16, (*oxa1Δ*/aI5γ ρ^+ and ρ^-) were cultured in HC/Ura$^-$ media with 2% raffinose over a course of 60 h. Samples of each were taken at 20, 24, 36, and 60 h and total RNA prepared as before. Insufficient RNA was available in the time-zero sample, so cells were obtained instead by scraping them from the starting HC/Ura$^-$/raffinose agar plates. Northern hybridization analyses in Fig. 5.9 show that even at 60 h, there is no complete splice defect when grown in this media compared to the splicing defect usually observed at 20 h when grown in YPR.

5.2.6 General RNA chaperone, Mss116 is not dependent on Oxa1

Thus, for both aI5γ and bI1, complementation with the double-deletion mutant ΔL1/CTD-myc caused a defect that was less severe than the null, but more severe than either single deletion. This implies that the remainder of Oxa1, that is, the core domain that functions as an insertase, may be involved in the splicing of these introns. It is unclear whether this effect is direct, or whether an as-yet-unidentified protein dependent upon Oxa1 may be responsible. Previous studies have shown that besides mitochondrial-encoded proteins, some nuclear-encoded mitochondrial inner-membrane proteins are also dependent upon Oxa1 for proper membrane insertion (He and Fox 1997; Hell et al. 1997; Szyrach et al. 2003; Bohnert et al. 2010).

It appeared unlikely that Mss116 would be this unidentified protein since wild-type splicing was observed in Fig. 5.5 in several of the *oxa1Δ* mutants that harbor other introns. Nonetheless, it seemed prudent to confirm this hypothesis by Western blotting. Wild-type 161-U7aI5γ and three of its derivatives were tested for the presence of Mss116: *oxa1*Δ, *mrp1*Δ, and *img1*Δ. Cultures of each were grown with shaking at 30° C to $O.D._{600}$ = 1.0 in 50 ml of either YPD or YPR. Whole-cell protein was isolated as described in Methods. Proteins were separated on 4-12% bis-tris mini gels (Life Technologies) with one gel being stained using Coomassie Brilliant Blue and the second used for overnight transfer to PVDF membrane for Western blotting (see Methods).

In Figure 5.10, the *oxa1*Δ strain (lanes 3-4) is flanked by the wild-type (WT) in lanes 1-2, and mitoribosomal protein deletion strains *mrp1Δ* and *img1Δ* in lanes 5-8. Wild type shows all the Mss116 protein in its fully-mature state at 72 kDa. Deletion of the two mitochondrial ribosomal proteins Mrp1 and Img1 (lanes 5-8) show significant amounts of precursor Mss116 (76 kDa), though the mature protein is in quantities comparable to wild type. The *oxa1*Δ strain in lanes 3 and 4, shows only minimal amounts of precursor evident in addition to the mature Mss116 in quantities comparable to wild-type. This indicates that deletion of *OXA1* has little impact on mitochondrial importation of Mss116.

5.3 DISCUSSION

The yeast insertase Oxa1 appeared to be critical for aI5γ and bI1 splicing during the general screen in Chapter 3 and when tested in a petite (ρ^-) strain in Chapter 4. It is

described in the SGD as required for genome maintenance, though this statement is only inferred from genetic and mutant interactions (website accessed March 2015). Here, I show that the mt genome is stable in *oxa1Δ* strains that have few or no introns, though the $1^{+}2^{+}$ *oxa1Δ* strain did rapidly become ρ^{0}, further suggesting the protein may play a role in splicing.

Deletion of *OXA1* in ρ^{-} strains elicited a severe splice defect in both aI5γ and bI1 introns when grown in YPR media. This splicing defect was specific for these two introns when compared to group I and group II introns aI1, aI2, aI4, bI4 and bI5.

To test which specific domains within *OXA1* might be most involved in splicing, the effect of the loss of the two domains that extend into the matrix (Loop 1 and the C-terminal domain) were tested. This involved complementation with mutants expressed on a plasmid that required minimal media for selection. The two Oxa1 domains contributed somewhat to the splicing efficiency, but the main contributor was the core insertase domain. This result suggests that there are other yet-unidentified splicing factors that rely on Oxa1's insertase function, very likely membrane-bound proteins. Testing confirmed that the general RNA chaperone Mss116 is not reliant on Oxa1.

When grown in minimal HC media, there was no severe splicing defect in the *oxa1Δ* aI5γ ρ^{-} strain as when it was cultured in YPR, suggesting that Oxa1 is not critical for splicing when the growth rate is slow. One possible explanation for this observation may be that during slow growth, the introns may fold into their catalytic conformations independently of Oxa1, with other proteins known to also have less efficient insertase

functions, like Oxa2, assisting in positioning splicing factors into the inner membrane. In rapidly-growing cells, Oxa1 may indirectly assist in splicing by positioning splicing factors into the inner membrane via its efficient insertase function.

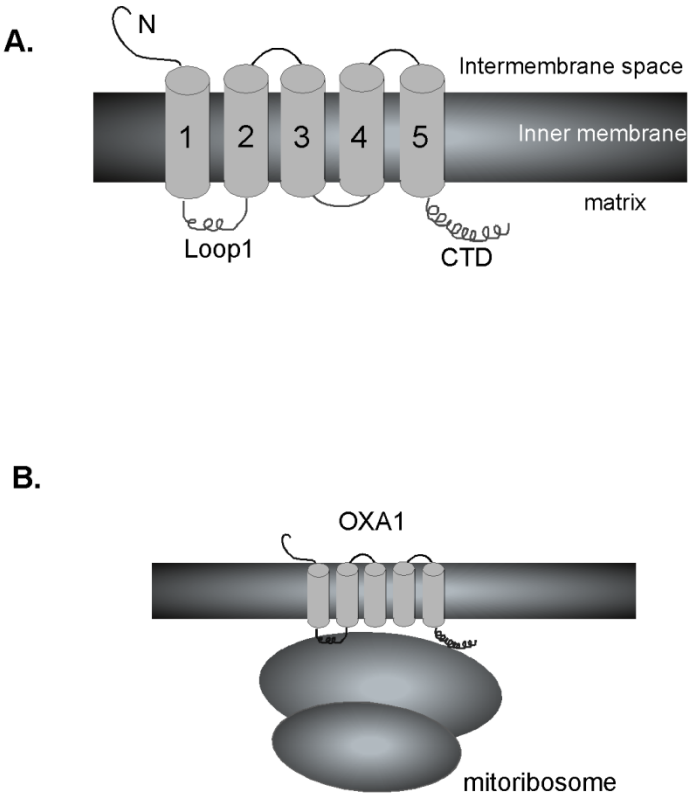

Figure 5.1: The yeast mitochondrial insertase, Oxa1

(A) A model of a monomer of Oxa1 depicting its N-out, C-in orientation with respect to the mt inner membrane (adapted from Bonnefoy, *et al*., 2009). Five transmembrane domains comprise the core of the protein. Two domains, Loop 1 and the C-terminal domain (CTD) extend into the mitochondrial matrix and are being tested here for their contribution to splicing. (B) Both Loop 1 and the CTD interact with the mt ribosome near its tunnel exit. The CTD forms an amphipathic α-helix with one positively charged and one hydrophobic surface that has been found to help bind the mt ribosome to the inner membrane surface, adapted from Funes, et al. 2009.

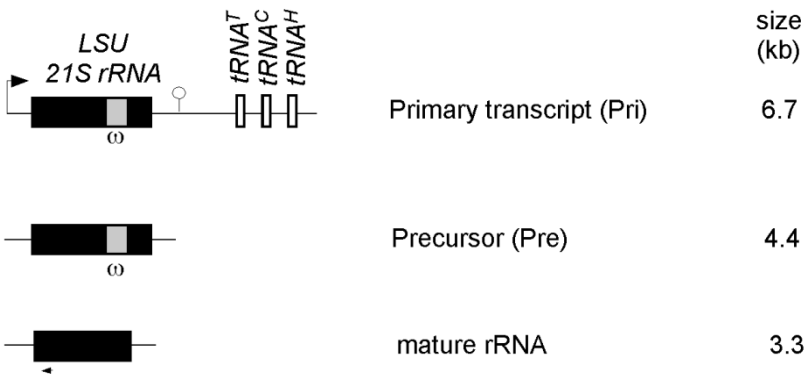

Figure 5.2: Processing pathway of the 21s rRNA of the large subunit (LSU)

Processing and splicing of the 21S rRNA/tRNA^T/tRNA^C/tRNA^H primary transcript. The transcriptional start site of the *21S rRNA* gene is indicated by a bent arrow,the 21S rRNA non-coding exons are in black, and the ω intron is in gray. A 6.7-kb primary transcript (Pri) is cleaved downstream of 21S rRNA at the dodecamer sequence (lollipop) to generate a 4.4-kb 21S rRNA precursor (Pre) from which the 1.1-kb ω intron is spliced to yield the 3.3-kb mature 21S rRNA

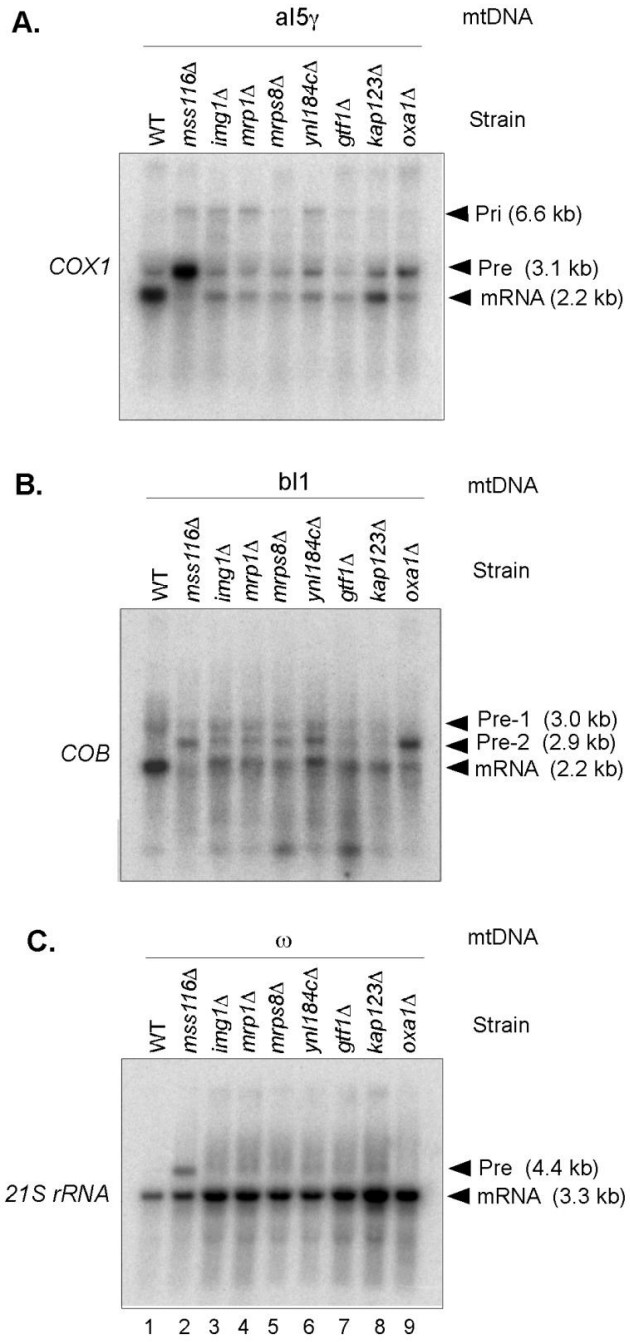

Figure 5.3: Northern hybridization analyses comparing the effect on splicing in 3 different ρ^+ strains: aI5γ, bI1 and LSU (ω).

Figure 5.3 (continued): Northern hybridization analyses comparing the effect on splicing in 3 different ρ^+ strains: aI5γ, bI1 and LSU (ω).

(A) Northern hybridizations of wild-type strain 161-U7/aI5γ ρ^+ and derivatives of that strain in which the indicated gene has been deleted. Strains were grown in YPR to an $O.D._{600}$ of about 0.8. Total cellular RNA was isolated, run in a 1.5% RNA-grade agarose gel, blotted onto a nylon membrane, and hybridized with a ^{32}P-labeled DNA oligonucleotide complementary to the *COX1* terminal exon. The primary, precursor, and mature mRNA transcripts are denoted as Pri, Pre, and mRNA, respectively. (B) Northern hybridizations of wild-type strain 161-U7/bI1 ρ^+ and derivatives of that strain in which the indicated gene has been deleted. Strains were grown, RNA isolated and run as in (A). Blots were hybridized with a ^{32}P-labeled DNA oligonucleotide complementary to the *COB* terminal exon. Primary (Pri), precursors 1 and 2 (Pre-1 and Pre-2), and mature mRNA (mRNA) are indicated to the right of the panel. (C) Northern hybridizations of wild-type strain 161-U7/ω ρ^+ and derivatives of that strain in which the indicated gene has been deleted. Strains were grown, RNA isolated and run as in (A). Blots were hybridized with a ^{32}P-labeled DNA oligonucleotide complementary to the *LSU* terminal exon. Precursor and mature mRNA transcripts are denoted as Pri and mRNA to the right of the panel.

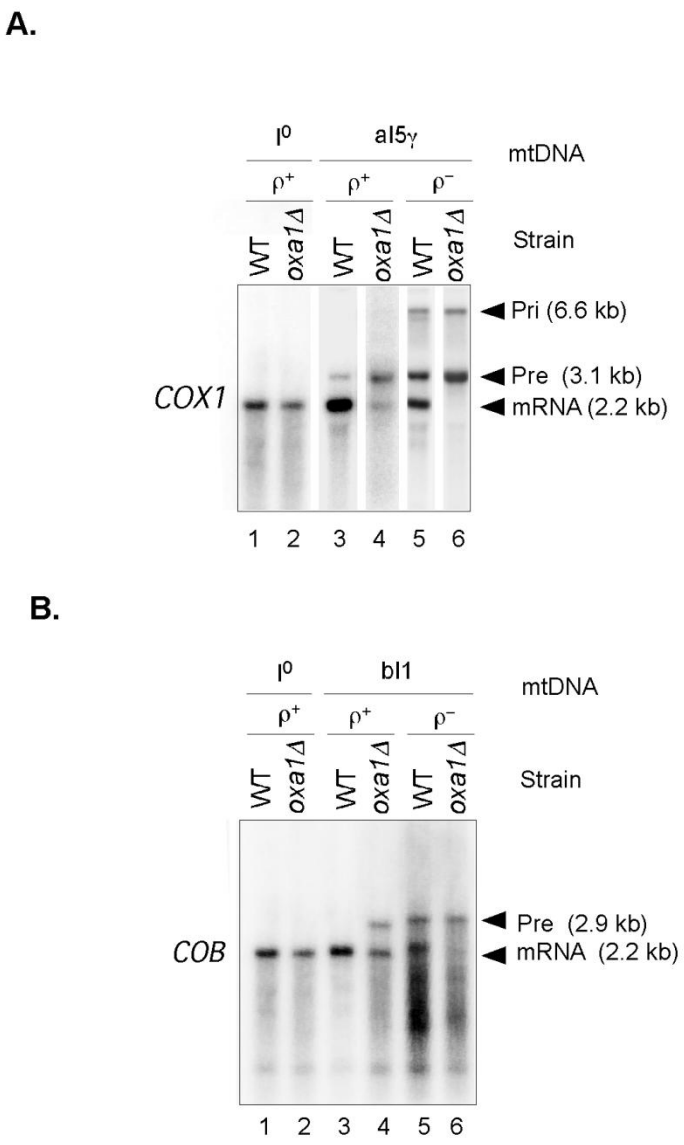

Figure 5.4: Northern hybridization analyses. Deletion of *OXA1* exacerbates splicing defects in single-intron petite strains grown in YPR.

Figure 5.4(continued): Northern hybridization analyses. Deletion of *OXA1* exacerbates splicing defects in single-intron petite strains grown in YPR.

Northern hybridizations of wild-type strains 161-U7/I^0 ρ^+, 161-U7/aI5γ ρ^+ or 161-U7/aI5γ ρ^- and derivatives of those strains in which *OXA1* has been deleted. Strains were grown, RNA isolated, run, blotted and hybridized as in Fig. 5.2A. Primary (Pri), precursor (Pre), and mature mRNA (mRNA) are indicated to the right of the panel. (B) Northern hybridizations of wild-type strains 161-U7/I^0 ρ^+ or 161-U7/bI1 ρ^+ and 161-U7/bI1 ρ^- and derivatives of those strains in which *OXA1* has been deleted. Strains were grown, RNA isolated, run, blotted as in Fig. 5.2A. Blots were hybridized with a ^{32}P-labeled DNA oligonucleotide complementary to the *COB* terminal exon. Primary (Pri), precursors 1 and 2 (Pre-1 and Pre-2), and mature mRNA (mRNA) are indicated to the right of the panel.

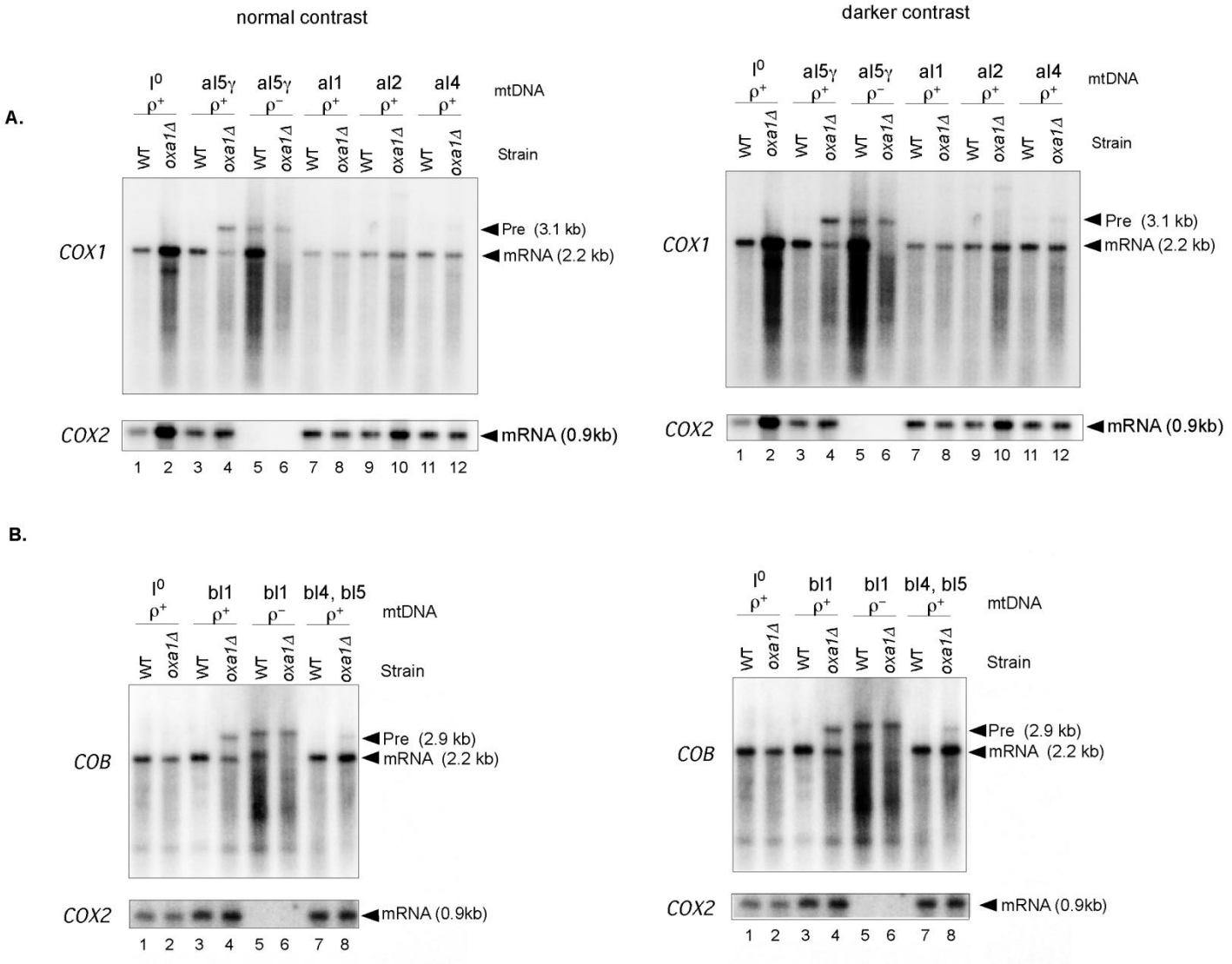

Figure 5.5: Northern hybridization analyses. Group II introns aI5γ and bI1 are more dependent on Oxa1 for splicing than are other introns tested.

Figure 5.5 (continued): Northern hybridization analyses. Group II introns aI5γ and bI1 are more dependent on Oxa1 for splicing than are other introns tested.

Northern hybridizations of wild-type strains 161-U7/I^0 ρ^+, 161-U7/aI5γ ρ^+, 161-U7/aI5γ ρ^- 161-U7/aI1 ρ^+, 161-U7/aI2 ρ^+ and 161-U7/aI4 ρ^+ and derivatives of those strains in which *OXA1* has been deleted. Strains were grown, RNA isolated, run, blotted and hybridized as in Fig. 5.2A. Precursor (Pre) and mature mRNA (mRNA) are indicated to the right of the panel. To better visualize the fainter bands, the image is duplicated with greater contrast to the right. To assess loading, the blot was stripped and rehybridized with a ^{32}P-labeled DNA oligonucleotide probe complementary to *COX2*. (B) Northern hybridizations of wild-type strains 161-U7/I^0 ρ^+, 161-U7/bI1 ρ^+, 161-U7/bI1 ρ^-, 161-U7/bI4/bI5 ρ^+, and derivatives of those strains in which *OXA1* has been deleted. Strains were grown, RNA isolated, run, blotted as in Fig. 5.2A. Blots were hybridized with a ^{32}P-labeled DNA oligonucleotide complementary to the *COB* terminal exon. Precursor 2 (Pre-2), and mature mRNA (mRNA) are indicated to the right of the panel. To better visualize the fainter bands, the image is duplicated with greater contrast to the right. To assess loading, the blot was stripped and rehybridized with a ^{32}P-labeled DNA oligonucleotide probe complementary to *COX2*.

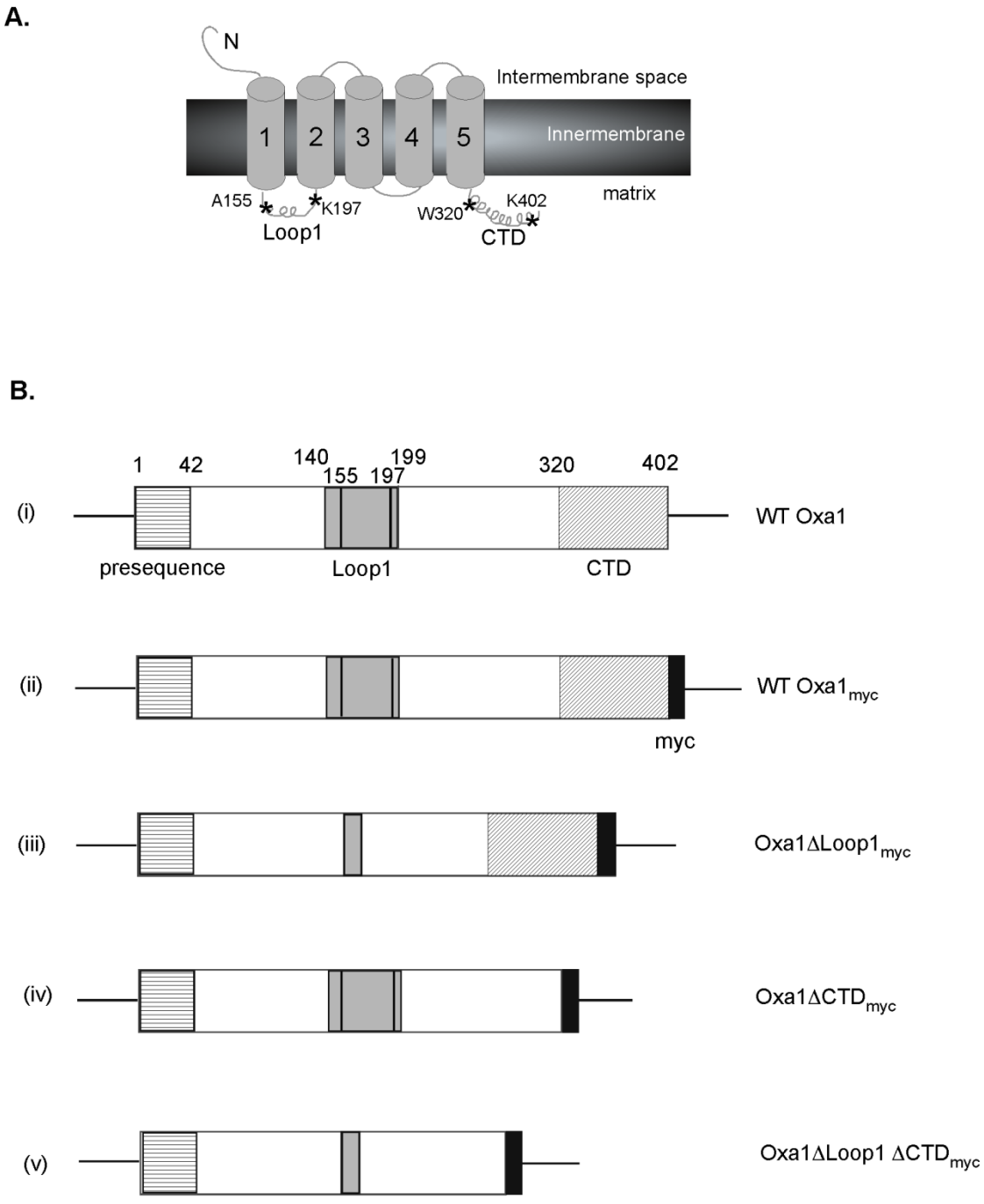

Figure 5.6: Wild-type yeast Oxa1 and Oxa1 mutant constructs.

Figure 5.6 (continued): Wild-type yeast Oxa1 and Oxa1 mutant constructs. (After Lemaire, et al. 2004).

(A) Locations of amino acid residues (designated by asterisks) within the Oxa1architecture used in constructing mutants in (B) below. (B) Complementation mutants engineered to test the effect on splicing of the deletion of Loop 1 and CTD individually and together. (i) Wild-type Oxa1with domains key to this study labeled below the diagram and their boundary residues numbered above. (ii) Wild-type Oxa1 with a C-terminal myc tag added after residue K402 (iii) Oxa1ΔLoop1$_{myc}$ was constructed by deleting the portion of Loop 1 from A155 to K197. A C-terminal myc tag follows K402. (iv) Oxa1ΔCTD$_{myc}$ was constructed by deleting the C-terminal domain from W320 to K402. The myc tag follows residue 319. (v) Oxa1ΔLoop1ΔCTD$_{myc}$ was constructed by deleting both Loop 1 and CTD as in (iii) and (iv). Each was cloned into a centromeric plasmid pRS416 and transformed into a strain in which the chromosomal copy of *Oxa1* had been replaced by a Kan^{R} cassette.

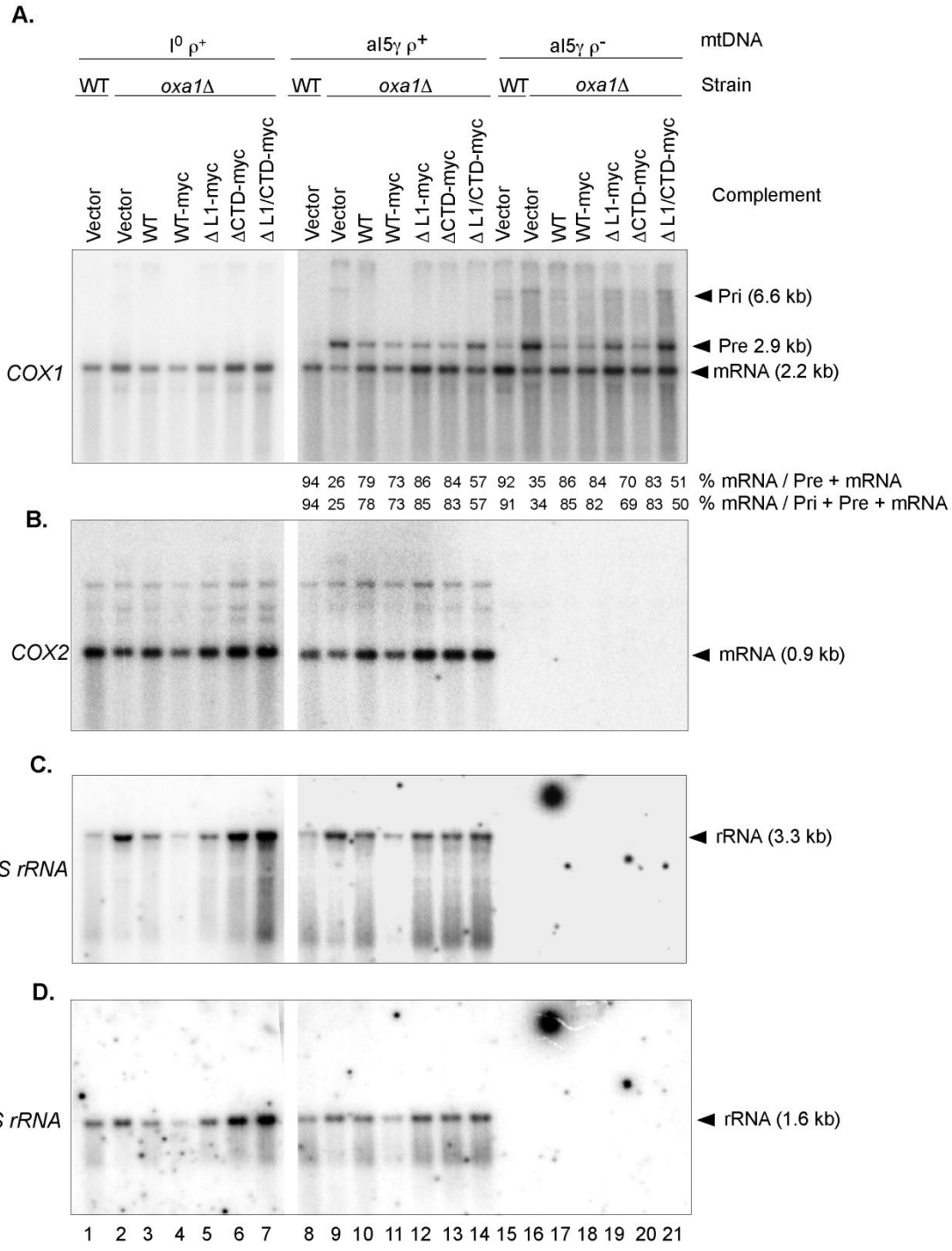

Figure 5.7: Northern hybridization analyses. Complementation of aI5γ splicing defects by Oxa1 mutants expressed on centromeric plasmid pRS416.

Figure 5.7(continued): Northern hybridization analyses. Complementation of aI5γ splicing defects by Oxa1 mutants expressed on centromeric plasmid pRS416.

Northern hybridizations of wild-type strains 161-U7/I^0 ρ^+, 161-U7/aI5γ ρ^+ or 161-U7/aI5γ ρ^- and derivatives of those strains in which *OXA1* has been deleted and complemented by Oxa1 variants expressed from plasmid pRS416. Constructs are as described in Fig. 5.5B. Vector is empty pRS416; L1 is Loop 1. Starter cultures of $O.D._{600} = 0.2$ were grown in Hartwell's Complete liquid media with 2% raffinose but lacking uracil at 30°C for 20 hours. RNA was isolated, run, blotted and hybridized as in Fig. 5.2A. Precursor (Pre) and mature mRNA (mRNA) are indicated to the right of the panel. Following scanning with a phosphorimager, the percentage of spliced mRNA was determined using GelQuant software (BioChem Lab Solutions). Ratios of mRNA to mRNA + precursor RNA (upper value) or to mRNA + precursor + primary transcript (lower value) are indicated under each lane in the blot. To assess loading, the blot was stripped and rehybridized with a ^{32}P-labeled DNA oligonucleotide probe complementary to *COX2*. To test for levels of *21S rRNA*, the blot was stripped once again and rehybridized with a ^{32}P-labeled DNA oligonucleotide probe complementary to that RNA.

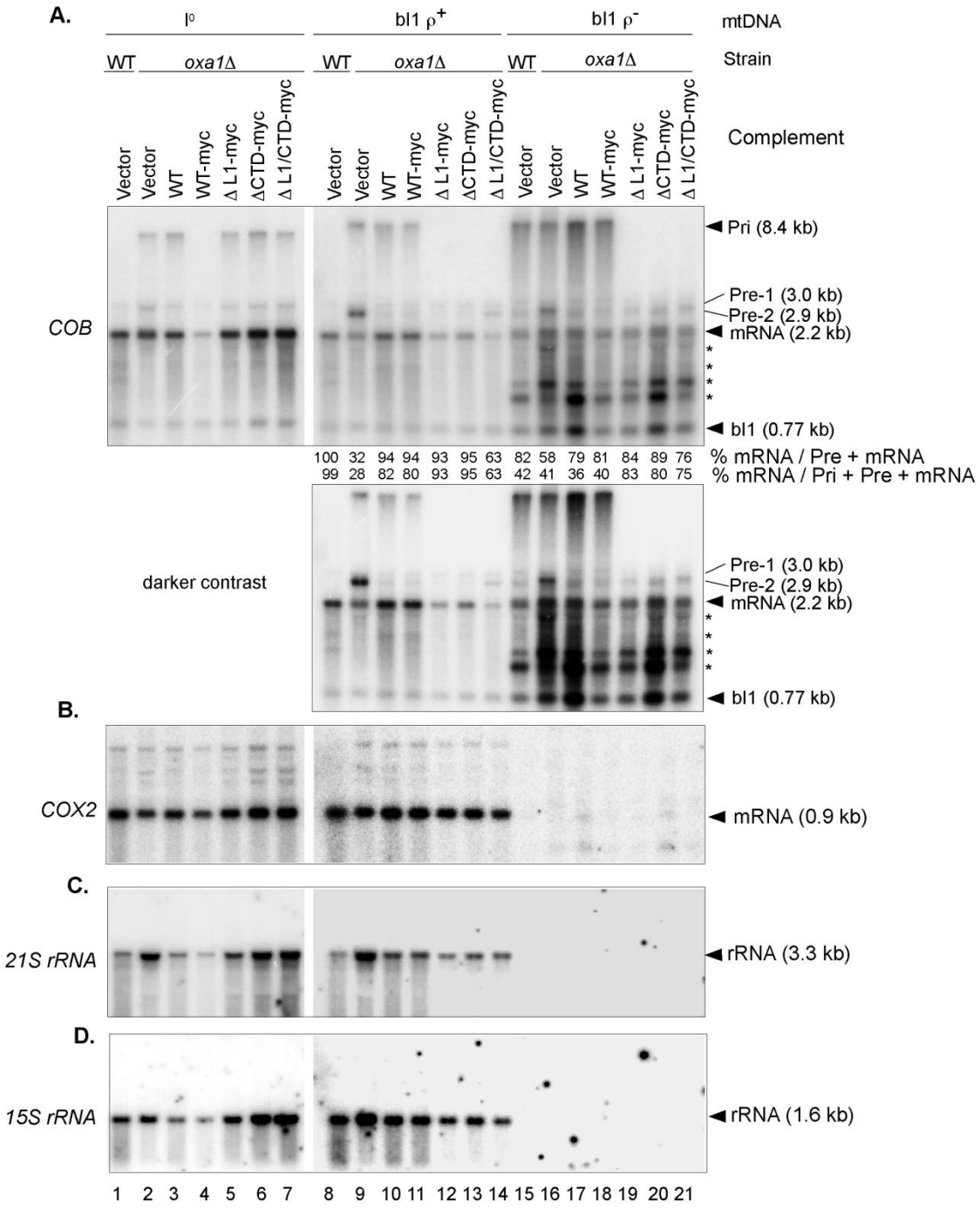

Figure 5.8: Northern hybridization analyses. Complementation of bI1 splicing defects by Oxa1 mutants expressed on centromeric plasmid pRS416.

Figure 5.8 (continued): Northern hybridization analyses. Complementation of bI1 splicing defects by Oxa1 mutants expressed on centromeric plasmid pRS416.

Northern hybridizations of wild-type strains 161-U7/I^0 ρ^+, 161-U7/bI1 ρ^+ or 161-U7/bI1 ρ^- and derivatives of those strains in which *OXA1* has been deleted and complemented by Oxa1 variants expressed from plasmid pRS416. Constructs are as described in Fig. 5.5B. Vector is empty pRS416; L1 is Loop 1. Cells were cultured as in Fig. 5.6. RNA was isolated, run, blotted and hybridized as in Fig. 5.2A. Primary, precursor 1, precursor 2, mature mRNA and intron bI1 are denoted as Pri, Pre-1, Pre-2, mRNA, and bI1 to the right of the panel. Unidentified RNAs are indicated by asterisks. Following scanning with a phosphorimager, the percentage of spliced mRNA was determined using GelQuant software (BioChem Lab Solutions). Ratios of mRNA to mRNA + precursor RNA (upper value) or to mRNA + precursor + primary transcript (lower value) are indicated under each lane in the blot. To assess loading, the blot was stripped and rehybridized with a ^{32}P-labeled DNA oligonucleotide probe complementary to *COX2*. To test for levels of *21S rRNA*, the blot was stripped once again and rehybridized with a ^{32}P-labeled DNA oligonucleotide probe complementary to that RNA.

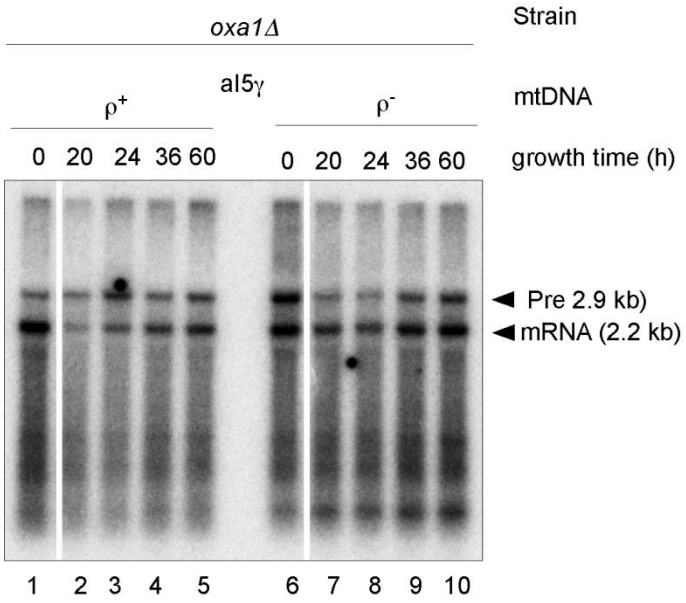

Figure 5.9: Northern hybridization analyses. Time course of 161-U7/aI5γ ρ^+ and 161-U7/aI5γ ρ^- derivatives in which *OXA1* has been deleted and complemented with empty vector pRS416.

Strains are those in Fig. 5.6, lanes 9 and 16, grown in Hartwell's Complete minimal media, lacking uracil with 2% raffinose for the number of hours indicated at the top of each lane on the blot with the exception of time zero. To obtain sufficient RNA for Northern hybridization, the time zero sample was scraped from HC/Ura-/raffinose agarose plates. RNA was isolated, run, blotted and hybridized as in Fig. 5.2A.

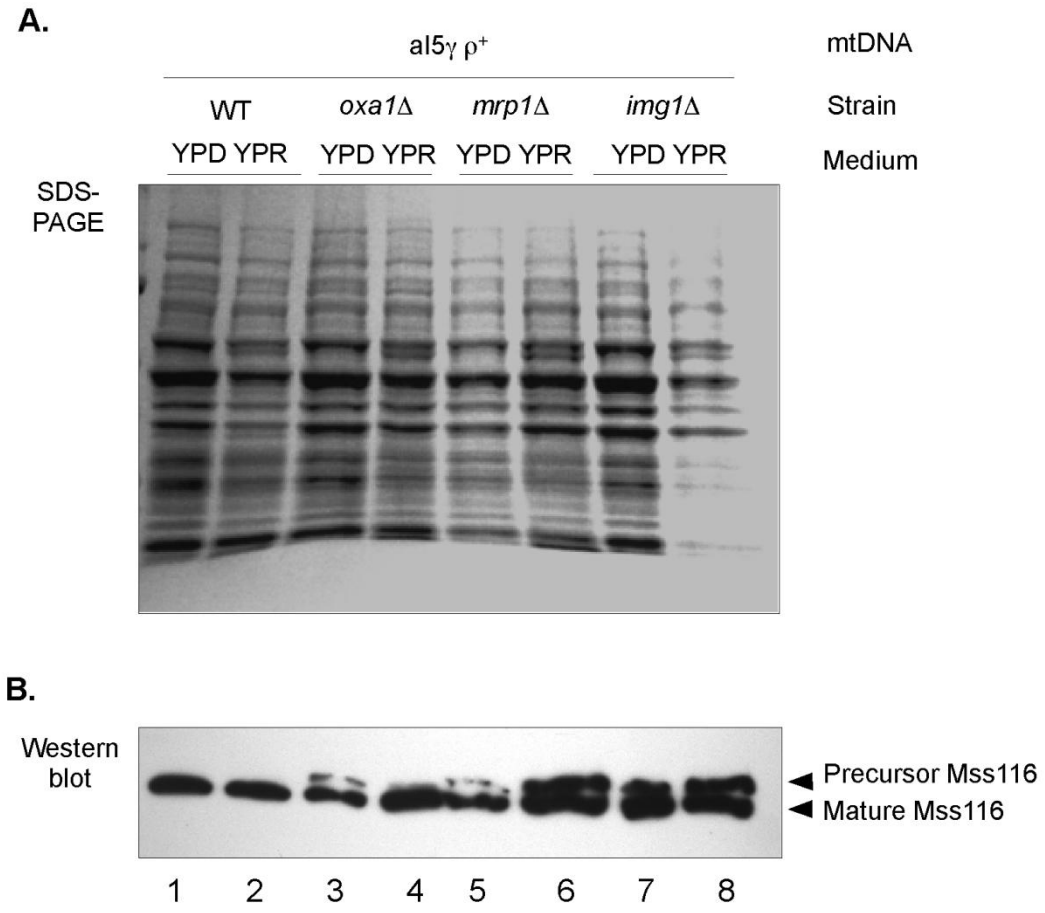

Figure 5.10: SDS-PAGE and Western blot comparing the effect on Mss116 with the deletion of three different proteins

The strains analyzed were wild-type 161-U7/aI5γ ρ^+ and derivatives of that strain in which genes for the insertase *OXA1*, or mitoribosomal proteins *MRP1* and *IMG1* were deleted. Strains were grown at 30° C in 50 ml of either Yeast Peptone Dextrose (YPD) or Yeast Peptone Raffinose (YPR) as indicated above each lane. TCA-precipitated proteins were separated on a 0.1% SDS/4-12% polyacrylamide gel and (A) stained with Coomassie Brilliant Blue or (B) transferred to a Sequi-Blot™ PVDF membrane (Bio-Rad) and probed with an antibody an Mss116 antibody.

Chapter 6: Mne1 is a component of the mitochondrial splicing apparatus responsible for processing group I intron aI5β

6.1 Background

Nuclear-encoded protein Mne1 had previously been reported to be a mitochondrial protein in a large-scale localization study (Huh et al. 2003). It was first identified as a possible splicing factor for the group I intron aI5β in strain BY4741 during the Phase I portion of the screen (Nyberg 2006). In 2008, deletion of *MNE1* was found to cause cells to exhibit a drug sensitivity similar to that of *cox* mutants and to have a specific impairment in cytochrome C oxidase assembly (Hillenmeyer et al. 2008).

Here, I further investigated the splicing abilities of this protein within a derivative of strain W303 received from the lab of Roland Lill (Kispal et al. 1999) in collaboration with the lab of Dennis Winge at the University of Utah Health Sciences Center (Watts et al. 2011). Strain W303 is a derivative of strain S288c with genotype *MAT*a/*MAT*α /*leu2-3,112 trp1-1 can1-100 ura3-1 ade2-1 his3-11*.

6.2 Results

Mne1 Functions in aI5γ Intron Splicing

Northern analyses were carried out with total RNA isolated from W303 wild-type and *mne1*Δ strains harboring a *COX1* with seven confirmed mtDNA introns (Fig. 6.1). Strains were grown at 30 °C in 50 ml of YP with 2% raffinose to an $O.D._{600}$ = 0.8-1.0. Total RNA was run on a 1.2% agarose gel with RNA-grade 1× TAE buffer (40 mM Tris

acetate, 1 mM EDTA), pH 8, at RT and blotted overnight onto a nylon membrane. The ^{32}P-labeled DNA oligonucleotides complementary to the *COX1* terminal exon or to each intron used for the analyses are listed in Table 2.1.

Hybridization with the *COX1* exon 6 probe shows a 2.2-kb mature *COX1* mRNA in the wild-type strain (Fig. 6.1B, lane 1). This band is greatly diminished in *mne1*Δ cells where, instead, two larger bands of about 3.8 and 6.3 kb are apparent (lane 2). Intron-specific probes for the three *COX1* group II introns show that splicing of the aI1, aI2, and aI5γ introns is not affected in the absence of Mne1 (lanes 4, 6, and 16*).* The spliced aI3, aI4, and aI5β introns are not visible in the Northern blots and appear to be unstable in mitochondria (1.4 kb signals seen in lanes 7-10, 13, and 14 are most likely cross-hybridization to the 15S rRNA). Strong hybridization signals running just below the large ribosomal subunit band with the aI3 and aI4 intron probes are detected in the wild-type strain and suggest that these bands represent the splicing intermediates containing the single introns and exons. The same band is also visible with the exon probe in the wild-type strain in lane 1. These aI3 and aI4 splicing intermediates are greatly reduced in the *mne1*Δ strain (lanes 8and 10). However, with both probes we see a signal for a 6.3-kb band also seen with the *COX1* exon probe. This suggests that this band contains more than one unspliced intron. The aI5α probe shows little difference between the wild-type and *mne1*Δ cells with the exception of a slightly more intense band running below the small ribosomal subunit rRNA, which is possibly the excised aI5α intron (lane 12). The greatest difference in hybridization signals is seen with the aI5β probe (lane 14). The

strongest signal (at 3.8 kb) in the *mne1*Δ strain co-migrates with the large ribosomal subunit band and most likely represents a *COX1* RNA that has all introns removed except aI5β. A second signal is detected for an RNA of about 6.3 kb, which co-migrates with the signals seen for the aI3 and aI4 intron probes. This suggests that the 6.3-kb band represents multiple RNA species that all contain the aI5β intron and also aI3 and/or aI4.

6.3 DISCUSSION

Mne1 is shown to be an important accessory factor in the splicing of *COX1* precursor RNA through the removal of the aI5β intron. Splicing of the aI5β intron is known to require at least 5 other proteins including Mrs1, Mss18, Mss116, Pet54, and Suv3 (Seraphin et al. 1988; Valencik et al. 1989; Bousquet et al. 1990; Huang et al. 2005; Turk and Caprara 2010). In *S. cerevisiae* strain S288c, the aI5β intron is not in frame with the upstream exon, so that its intron-encoded maturase appears to require alternative splicing to place it in-frame (Turk et al. 2013). This alternative splicing requirement may offer one explanation for the need of multiple splicing factors for this intron in derivatives of strain S288c such as W303 and BY4741.

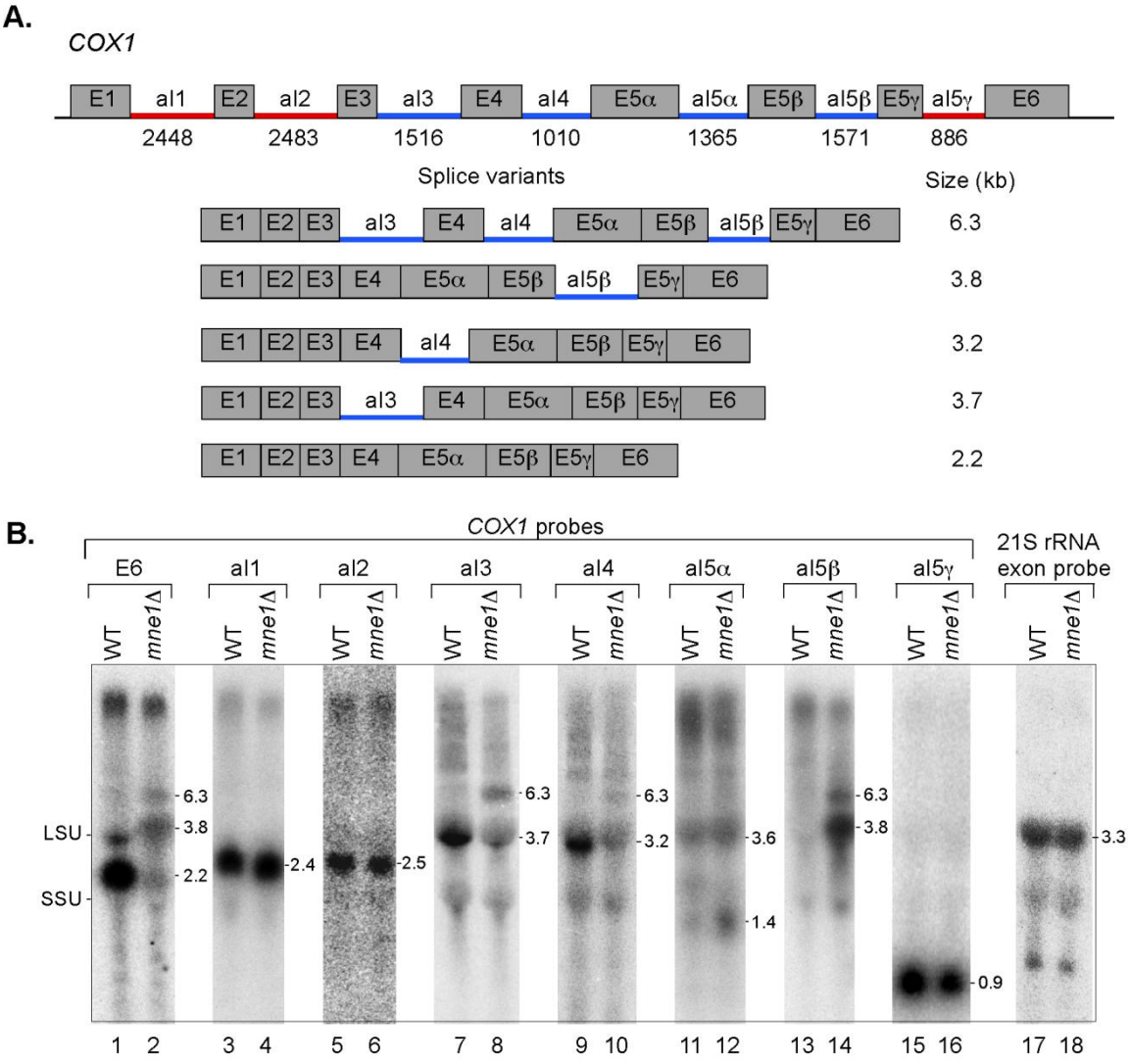

Fig. 6.1: Northern hybridization analysis of *COX1* introns in WT and *mne1*Δ cells in strain W303.

Fig. 6.1(continued): Northern hybridization analysis of *COX1* introns in WT and *mne1*Δ cells in strain W303.

(A) Schematic showing the molecular organization of the *COX1* gene from the wild-type strain (top), with the size of each intron (in nt) given below its name. Group I introns are indicated by a blue line and group II introns by a red line. Splice variants containing either single or multiple introns aI3, aI4 and /or aI5β are shown below. The size (kb) of each variant is indicated to the right. (B) Northern hybridization analysis. Strains of wild-type W303 or derivatives in which *MNE1* had been deleted were grown in YPR to an $O.D._{600}$ = 0.8-1.0. Total cellular RNA was isolated, run in a 1.2% RNA-grade agarose gel, blotted onto a nylon membrane, and hybridized with a ^{32}P-labeled DNA oligonucleotide complementary to the *COX1* terminal exon, or *COX1* introns aI1, aI2, aI3, aI4, aI5α-γ and 21S rRNA exon 1 as detailed in Table 2.1. The numbers to the right of each Northern panel indicate the approximate size of the indicated transcripts in kb. The positions of the large and small ribosomal rRNAs are indicated as *LSU* and *SSU*, respectively, on the left.

Chapter 7: General RNA Chaperone, Mss116

7.1 BACKGROUND

The *S. cerevisiae* DEAD-box protein Mss116 (Fig. 7.1) is involved in many processes within the yeast mitochondrion, among which is intron splicing where Mss116 promotes the efficient splicing of all thirteen mt group I and group II introns (Huang et al. 2005). Previous studies from the Lambowitz lab indicated that Mss116 functions as a general RNA chaperone that uses its ATP-dependent RNA-unwinding activity to disrupt stable RNA secondary and tertiary structures that are kinetic traps during RNA folding (Huang et al. 2005; Halls et al. 2007 ; Del Campo et al. 2009; Mallam et al. 2012). Other findings from both the Lambowitz and Pyle laboratories indicated that Mss116 could also promote some splicing steps in an ATP-independent manner (Solem et al. 2006; Halls et al. 2007) with the Pyle lab suggesting that such ATP-independent functions play a major role in the splicing of the group II intron aI5γ (Solem et al. 2006). In this section, I used mutational analysis to investigate ATP-dependent and -independent roles of Mss116 in group II intron splicing *in vivo,* as well as the impact on splicing of mutations in conserved helicase motifs involved in RNA binding and the coupling of ATP hydrolysis to RNA unwinding (Fig. 7.1B). I also investigated the minimal amount of Mss116 required to promote group II intron splicing *in vivo* and used TAP-tagging to look for proteins that interact with Mss116 *in vivo*. My findings provide insight into the mechanism of action of Mss116 in promoting group II intron splicing *in vivo*.

7.2 RESULTS

7.2.1 Temperature does not compensate for loss of Mss116 in aI5γ splicing *in vivo*

To test whether Mss116 was required for aI5γ splicing in *S. cerevisiae in vivo* at temperatures outside of its optimal growth temperature of 30° C, I cultured strains at 25° C, 30° C and 37° C. The strains tested were 161-U7/aI5γ, 161-U7/I^0, and derivatives of those strains in which *MSS116* had been deleted. Each strain was grown in 50 ml of YPR at the indicated temperatures to $O.D._{600}$ = 0.8-1.0. Total RNA was isolated and run on a 1.5% agarose gel as described in Methods. The Northern hybridization analysis in Fig. 7.2 compares the abilities of wild-type and *mss116Δ* strains to promote the splicing of aI5γ at 25°C, 30°C and 37°C (lanes 1-6). In the wild-type strain, splicing at all three temperatures is efficient with very little unspliced precursor remaining (lanes 1-3), although at 37°, there is a slight reduction in the amount of mRNA as compared to the other temperatures. Interestingly, there is no comparable reduction of mRNA at 37° in the intronless strain, I^0 (lane 9). In contrast to wild type, the transcripts in all the *mss116Δ*/aI5γ strains remain as unspliced precursor at each of the three temperatures. This indicates that Mss116 is required at these temperatures as well as at 30° C (lanes 4-6). Additionally, there is also a notable reduction in RNA at 37°. In the I^0 control strains, the reduction in RNA at the elevated temperature is seen only in the *mss116Δ* strain in lane 12. Together, these data show that high temperatures do not compensate for the loss of Mss116's splicing activity for aI5γ *in vivo*.

7.2.2 The splicing activity of Mss116 mutants correlates with ATP-dependent RNA unwinding activity

For most of its functions, Mss116, like other DEAD-box proteins, uses ATP-dependent RNA unwinding to promote RNA structural transitions. However, the Pyle

lab, using mutants K158R, K158A (motif I) and SAT/AAA (motif III) along with the mt group II intron aI5γ as a substrate for their *in vitro* experiments, reported that ATP-dependent helicase activity is not required for Mss116-stimulated splicing of aI5γ and that Mss116 facilitates the folding of this intron primarily by stabilizing a folding intermediate (Solem et al. 2006; Karunatilaka et al. 2010). To address the apparent inconsistencies in the understanding of this mechanism, we conducted more in-depth studies (Potratz et al. 2011).

Motif I, also known as the Walker A motif, forms a phosphate-binding loop (P-loop) found in many nucleotide-binding proteins (Walker et al. 1982; Sarastea et al. 1990). The signature pattern of the motif is the tripeptide glycine, lysine and threonine (GKT) of which the lysine (K) residue is crucial for nucleotide-binding, forming a pocket that binds the β- and γ-phosphates of the NTP (Hanson and Whiteheart 2005). Mutations in this region of other DEAD-box proteins reduce or eliminate ATPase activity (Pause, EMBO, 1992). In Mss116, this critical lysine is K158 (Fig. 7.1B).

Motif III, whose conserved amino acid sequence is S-A-T (Fig. 7.1A and B), lies at the interface of D1 and D2 in the protein's closed conformation and is involved with communication between D1 and D2, possibly bridging ATP interactions to RNA binding (Story et al. 2001; Banroques et al. 2010).

To investigate the function of motifs I and III in promoting the splicing of group II intron aI5γ *in vivo,* I engineered the centromere (CEN) plasmid pRS416 to express wild-type Mss116 and mutants K158R, K158A, or SAT/AAA. These plasmids were then

transformed into a 161-U7 *mss116*Δ yeast strain harboring only mt intron aI5γ and grown at 30° in Hartwell Complete media minus uracil (HC/Ura$^-$) with 2% raffinose to $O.D._{600}$ = 1.5 (see Methods). Using this non-repressing fermentable carbon source allowed examination of splicing even in mutants with strongly defective Mss116.

The Northern hybridization analysis in Fig. 7.3A compares the abilities of wild-type and Mss116 mutant strains to promote splicing of intron aI5γ. The blot was hybridized with a ^{32}P-labeled DNA oligonucleotide probe complementary to the *COX1* terminal exon. As expected, the wild-type strain with a functional chromosomal copy of *MSS116*, spliced aI5γ efficiently, yielding a predominant band corresponding to mature *COX1* mRNA (lane 1), while the predominant band that accumulated in the *mss116*Δ strain was unspliced precursor RNA (lane 2). Complementation of the splicing defect by expression of wild-type Mss116 from the CEN plasmid effectively restored aI5γ splicing to near wild-type levels (lane 3). In contrast, the K158A and K158R mutants were unable to complement splicing of aI5γ substantially above the low residual level in the *mss116*Δ strain (null phenotype; lanes 4 and 5). Complementation with the K158A mutant allowed for a very small increase in spliced mRNA that paralleled the small amount of residual ATPase activity described by the Pyle group (Solem et al. 2006). The SAT/AAA mutant gave an intermediate phenotype, with approximately equal amounts of spliced mature mRNA and unspliced precursor (lane 6). The mutant proteins were expressed at or near the level of wild-type Mss116 as verified by Western blot (Fig. 7. 2B). These results are in good agreement with previous experiments using strains with multiple *COX1* and *COB*

introns showing that K158A and other motif I mutants gave a null phenotype, while the SAT/AAA mutant gave an intermediate phenotype for the splicing of all mitochondrial group I and group II introns examined (Huang et al. 2005; Bifano et al. 2010).

Taken together, these experiments showed that Mss116 mutants K158A, K158R and SAT/AAA promote splicing *in vivo* to levels that correlate with their ATP-dependent RNA-unwinding activities. The K158 mutants had essentially no RNA-unwinding activity, while the motif III mutant retained partial RNA unwinding activity (Potratz et al. 2011). These results indicated that, although DEAD-box proteins play multiple roles in RNA folding, the physiological function of Mss116 in aI5γ splicing includes a requirement for ATP-dependent local unfolding, allowing a nonfunctional RNA structure to convert into functional, catalytic RNA.

7.2.3 Effect of mutations in motif III on mitochondrial intron splicing in vivo

Our understanding of motif III was further refined by Northern and Western analyses of *in vivo* splicing activity of functional variants identified by high-throughput genetic selection and unigenic evolution method (Mohr et al. 2011). In this set of experiments, a plasmid library of motif III mutants was transformed into the multi-intron strain 161-U7 *mss116*Δ/$1^{+}2^{+}$ harboring the twelve group I and group II introns from the *COX1* and *COB* genes. Those variants able to grow on glycerol, a non-fermentable carbon source, were identified as having functional motif III mutants (Fig. 7.1B). These variants were then grown at 30° in HC/Ura^{-} media with 2% raffinose to an $O.D._{600} \approx 1.5$. Aliquots of the culture were reserved for whole cell TCA protein preparation for

immunoblots and the remainder was used for total cellular RNA isolation (see Methods). Northern blots of whole cell RNAs from the different strains were hybridized with ^{32}P-labeled DNA oligonucleotides complementary to either the *COX1* or *COB* terminal exon. The membranes were then stripped and rehybridized with a probe complementary to the *COX2* RNA to assess equal loading.

The Northern blots in Fig. 7.4A show that the SAT mutants that support growth on glycerol also promote splicing of *COX1* or *COB* introns, albeit to different degrees. In lane 1, the wild-type strain exhibits a splicing phenotype in which the predominant band is the mature mRNA, in both the *COX1* and *COB* strains. In contrast to the splicing phenotype of *COX1* in the single-intron aI5γ strain seen in Northern hybridizations in previous chapters, multiple bands are evident in this multi-intron strain. In lane 2, the *mss116*Δ strain exhibits a severe splicing defect of both *COX1* and *COB*, with no evident spliced mature mRNA. Complementation with wild-type *MSS116* in lanes 3, rescues the defects in splicing both introns, displaying splicing patterns similar to those observed in lane 1. The AAA mutant in lane 4, produced no observable mature mRNAs, as expected from its severely impaired glycerol-growth phenotype. A comparison of the splicing phenotypes of the SAT/AAA mutant in this multi-intron strain with that in the single intron strain in Fig. 7.3A, lane 6, clearly shows the more extreme splicing defect the mutation has on a strain with multiple introns.

Unexpectedly, several of the novel motif III variants demonstrated near-wild-type efficiency in promoting splicing in both *COX1* and *COB* intron (FAT, GGT, LCT, and

SST; lanes 6, 8, 11 and 12). DAC and GIG in lanes 5 and 9 displayed moderate splicing efficiency, with GST and GAV displaying progressively weaker splicing efficiencies (lanes 10 and 7, respectively). Interestingly, though the latter two variants displayed weak efficiencies in splicing *COX1* introns, they both displayed moderate efficiencies in splicing introns within the *COB* gene. Western blots showed that all of the variant proteins were expressed from the CEN plasmid at levels comparable to that of the wild-type protein (Fig.7.4B).

The variability allowable in Mss116 motif III is greater than that observed in previous studies of other DEAD-box proteins, including Ded1 where similar codon randomization was done separately for the first and third positions (Banroques et al. 2010). The fully or moderately functional Mss116 variants break the consensus sequence pattern of alcohol-small amino acid-alcohol at different sites along each of the three positions, with the moderately functional variant GIG violating this consensus at all three positions. Although the four strongest variants all share the final threonine, this amino acid at the third position is not itself sufficient for efficient splicing as seen by the weak splicing of the GST variant, nor is it essential as observed in the moderate splicing of the DAC variant. Interestingly, the almost fully functional FAT variant places a large phenylalanine side chain at a position where it would not easily fit in the crystal structure of Mss116 in its closed state.

Our observations of permissible amino acid substitutions indicate that: (1) the putative H-bonds between the hydroxyls of S305 and T307 and residues in motifs II and VI in the crystal structure are not essential for splicing activity; (2) A306 and T307 can

be substituted with residues having similarly-sized nonpolar or uncharged polar side chains; and (3) S305 can tolerate substitutions with larger side chains (F, D, L, H, M, Q). The larger degree of variation observed for the Mss116 motif III mutants as compared to that observed in other work (Banroques et al. 2010) may be a result of the simultaneous randomization of the codons. Alternatively, Mss116 may be less dependent upon motif III interactions than are other DEAD-box proteins due to its higher RNA-binding affinity (Rudolph et al. 2006; Mohr et al. 2008). Nonetheless, the strong splicing defect observed in the AAA mutant, particularly in the multi-intron strain, argues that motif III is required for Mss116 splicing activity.

7.2.4. Effect of mutations in the Mss116 RNA-binding tract on splicing of mitochondrial introns in vivo

The crystal structure of Mss116 identified several amino acid residues along the helicase core and the CTE that contacted U10 RNA suggesting these residues may serve a potentially critical function (Del Campo and Lambowitz 2009). Although the helicase core contacted residues U3-U10, U9 and U10, it displayed only weak electron densities, indicating mobility in those positions. Contacts with U3-U8 were made mainly through residues in the conserved motifs and were part of an RNA-binding tract spanning core domains 1 and 2, similar to that seen in other DEAD-box protein structures (Del Campo and Lambowitz 2009). However, structures of Mss116 and other DEAD-box proteins provide only a static picture of these contacts with little insight into their relative contributions to RNA binding or intron splicing. Here, I investigated variants in the

RNA-binding motifs Ic, IV and the recently identified Post II (at D280, downstream of motif II) (Fig. 7.1B) (Mohr et al. 2011).

In the unigenic evolution analysis, seven of the residues identified as contacting U10 RNA in the crystal structure were invariant (R190, T242, R245, D248, D280, R415, T433), while one (K384) showed only the conservative substitution to R. These residues were further assessed by randomizing the codons for each and then selecting for functional mutants by growth on glycerol. The analysis showed that a number of amino acid residues whose side chains make ionic or H-bond contacts with the RNA are conserved, while residues that make main-chain contacts could often be replaced by non-synonymous residues that could make the same contacts. I tested the effect on splicing in six of these mutants: T242P, R245A, D248V, D280I, D280S, and K384G (Fig. 7.5A). The splicing abilities for five of these mutants (lanes 4, 6, 7, 8 and 9) were similar to that of the wild-type strain (lane 1) and correlated well with glycerol growth which was also similar to wild type (not shown). The one striking exception was R245A which grew only weakly on glycerol and exhibited a severe splicing defect (lane 5); strongly suggesting that the aliphatic, positively charged side chain of arginine plays a key role is mt intron splicing.

The correlated Western blot in Fig. 7.5B reveals near wild-type levels of protein expression for all the variants with the exception of mutant D248V (lane 6) which exhibited about a 3-fold reduction in expression level as compared to wild-type, yet maintained near wild-type splicing ability.

These findings show that in all functional variants, an α-helix is predicted to be maintained despite the amino acid sequence changes.

7.2.5. Analysis of N-terminal and C-terminal truncations *in vivo*

Flanking D1 and D2 are the upstream N-terminal extension (NTE) and the downstream α-helical C-terminal extension (CTE) and the unstructured, basic C-tail (Fig. 7.1A). In crystal studies of Mss116, the C-tail was not visible, an indication of the flexibility of that domain (Del Campo and Lambowitz 2009). However, by using a different method, small angle X-ray scattering (SAXS), visualization of flexible regions and thus the full-length Mss116 protein was possible. Data collected with SAXS by others in our lab had indicated that the NTE projects outward and away from the RNA-binding D1 and that the C-tail may act as a tether to bind nonspecifically to different portions of large RNAs, perhaps enabling the helicase core to sample nearby regions for RNA unwinding (Mallam et al. 2011).

The CTE is known to be necessary for Mss116 activity, since mutations within the region destabilize and inactivate the protein (Del Campo and Lambowitz 2009). The cause for this was made clear when our lab obtained X-ray crystal structures of truncated Mss116 (ΔC-tail), illustrating that the CTE interacts extensively with D2. A wedge helix within the CTE, together with another in motif Ic, caused RNA crimping that is thought to help induce strand separation (Del Campo and Lambowitz 2009).

Previous studies in our lab of a CTE mutant (Δ569) showed its splicing ability to be suboptimal (Mohr et al. 2008). Here, I re-examined this mutant and investigated the

impact on splicing with the deletion of the NTE, of the C-tail (Δ598), and of both domains simultaneously using the constructs diagrammed in Fig. 7.6.

The strains analyzed were wild-type 161-U7/$1^{+}2^{+}$ and *mss116Δ*/$1^{+}2^{+}$ containing the CEN plasmid vector pRS416 alone or expressing either the wild-type Mss116 or the N- or C- terminal truncation mutants. Cultures were grown as described in section 7.2.2. The Northern hybridizations in Figure 7.7A show multiple bands indicative of the multiple introns contained in these strains. In lane 1 is the wild-type *MSS116*/$1^{+}2^{+}$ strain transformed with CEN plasmid vector pRS416 showing wild-type splicing. In lane 2 is the *mss116Δ*/$1^{+}2^{+}$ strain also transformed with the empty vector where no mature mRNA was evident in either the *COX1* or *COB* transcript. Complementation with wild-type Mss116 expressed from pRS416 rescued the splicing defects in both *COX1* and *COB*, although a prominent band of incompletely spliced transcript just smaller than the primary transcript is evident for *COB* (lane 3). Complementation with either the ΔNTE mutant (lane 4), the ΔC-tail mutant (lane 5) or the mutant with deletion of both domains (lane 6) each rescued the splicing defects in both *COX1* and *COB*, as predicted from prior *in vitro* studies showing that splicing is primarily dependent upon domains D1 and D2 (Mallam et al. 2012). In lane 7, complementation with the Δ569 mutant rescued splicing, but only partially as the amounts of both *COX1* and *COB* mature mRNAs were reduced as compared to wild type. To confirm uniform loading, each blot was stripped and rehybridized with a ^{32}P-labeled DNA oligonucleotide complementary to *COX2*. In all cases, splicing was sufficient to support growth on glycerol (data not shown).

In the Western blot in Fig. 7.7B, the truncated mutant Mss116 proteins are the expected sizes. Interestingly, despite the similar levels of splicing ability, the levels of Mss116 varied widely. This is especially evident in comparing the single truncation mutant ΔNTE (lane 4) or ΔC-tail (lane 5) to the double mutant ΔNTE + ΔC-tail (lane 6). The loss of the NTE region reduces the protein signal to 25% wild type, whereas the ΔC-tail protein level is comparable to that of wild type (1.1-fold difference). The combination of both of these truncations, however, results in a severely reduced level of Mss116 (8% wild type; lane 6).

To assess loading, the lower portion of the blot was probed with porin antibody, which confirmed that similar levels of total protein had been loaded. The reduction in signals may be a result of increased protein degradation of the more severely mutated, and perhaps more unstable, proteins. Alternatively, the truncations my reflect loss of epitope recognition sites for the Mss116 polyclonal antibody. This possibility will be addressed below.

7.2.6. Determining the efficiency of anti-Mss116 antibody recognition of wild-type and truncated mutant Mss116 proteins

The apparent low levels of Mss116 seen in Figs. 7.5, lane 6 and 7.7, lane 6, suggested that very little Mss116 was required to support wild-type levels of splicing of the *COX1* and *COB* introns. While loss of epitope recognition sites for the D248V mutant would not be expected, the same is not true for the double truncation mutant ΔNTE + ΔC-tail discussed in the previous section.

In Fig. 7.8A, the Western blot shows samples of the full-length and truncated

proteins each at concentrations of 2, 3, 4, and 5 nM. Image acquisition was with a FluorChemHD2 camera (Cell Biosciences) and densitometry was performed with GelQuant software (BioChemLabSolutions.com) to obtain signal values for each band and their corresponding local backgrounds. Background values were subtracted from the corresponding band values to obtain the corrected signal value at each concentration. The ratio of the signal for the wild-type protein compared to that of the double-truncation mutant was calculated at each concentration. A mean ratio of 2.2 was determined as the average efficiency of Mss116 antibody recognition of wild-type to mutant Mss116 epitopes.

In the Western blot in Fig. 7.7B, the ΔNTE + ΔC-tail signal is 8% wild type, indicating an apparent 12.5-fold decrease in protein level compared to wild type. Correcting for loss of epitope recognition sites in the truncation mutant, I calculate that the actual decrease in protein level in the mutant is 12.5/2.2 = 5.7-fold, or approximately six-fold lower than wild type. Thus, Mss116 is capable of promoting splicing at levels at least 6 times lower than those normally found in wild-type cells.

7.2.7 Modifying the *in vivo* expression of Mss116

The results in the section above suggested that reduced levels of Mss116 are sufficient for near wild-type splicing. To investigate the minimum amount of wild-type Mss116 required for splicing, I attempted to reduce levels of Mss116 expression using two different methods.

7.2.7.1 Modulating Mss116 expression using a family of TEF promoters

The first method involved cloning the *MSS116* ORF behind a family of yeast Translation Elongation Factor (TEF) promoters which had been engineered to vary in strength for the expression of exogenous proteins in yeasts and were provided to us by the lab of Dr. Hal Alper (Alper et al. 2005). The plasmids were transformed into a 161-U7-*mss116Δ*/$1^{+}2^{+}$ strain and grown in YPR at 30° C to $O.D._{600}$ = 1. Approximately 60 µg of total TCA-precipated protein were separated by SDS-PAGE, transferred to a PVDF membrane and immunoblotted. The weakest promoter of the set, TEF2 (Fig. 7.9 lane 4), however, gave expression levels that were considerably higher than those of the native *MSS116* promoter (lane 3), so a second method was devised.

7.2.7.2 Modulating Mss116 expression by mutating the MSS116 promoter

In this second method, portions of the *MSS116* putative promoter were deleted within plasmid pHRH197 to regulate Mss116 expression levels. Previous work had shown that the region 710 bp upstream of the Mss116 ATG was able to drive expression in this plasmid (Huang et al. 2005). This -710 sequence was analyzed by the online software Promoter Scan (http://www-bimas.cit.nih.gov/molbio/proscan/) to search for key promoter elements. A predicted TATA box (at -501, relative to the ATG) and transcriptional start site (TSS) (at -472, relative to the ATG) were located in the region flanked by two ClaI restriction sites (Fig. 7.10A).

To delete the region flanked by the two ClaI sites (-704 and -356), plasmid pHRH197 was digested with ClaI and religated by standard methods. This mutant was

then used as the template for the remaining deletion constructs which were engineered by stitch PCR to add different promoter segments using primers listed in Table 2.1. Sequence-verified plasmids were cloned into digested pHRH197 with selection on LB/Amp^{R} plates. Plasmids were transformed into the 161-U7/1^{+}2^{+} WT or 161-U7/1^{+}2^{+} *mss116*Δ strain using the yeast transformation protocol described in Methods. Cultures were grown at 30° in 30 ml HC/ Ura^{-} media, with 2% raffinose as carbon source to O.D.$_{600}$ = 1.0.

The Western blot in Fig. 7.11B shows the variation in Mss116 expression levels achieved by the *MSS116* promoter mutations. Lane 1 show the level of expression from the wild-type genomic copy of *MSS116,* while lane 2 shows lack of Mss116 expression in the *mss116*Δ transformed with an empty vector, pHRH197. Complementation of the *mss116Δ* strain with Mss116 expressed from the CEN plasmid with the full 710 bp 5´ UTR restores expression to wild-type levels (lane 3). Unexpectedly, deletion of the putative TATA box and TSS regions (Δ-704/-356) in lane 4 did not cause a significant decrease in expression. Similarly, deletion of the -704/-314 region permitted wild-type expression (lane 5). Significant reductions in expression levels were seen with the deletions of -307/ -61 and -704/ -61 regions in lanes 6 and 7, respectively. As expected, deletion of the entire promoter region, -704 to -1 entirely eliminated Mss116 expression (lane 8).

Interestingly, but not unexpectedly, based on observations in preceding sections, the splicing abilities of Mss116 with reduced expression remained similar to wild type for both *COX1* and *COB* transcripts (Fig. 7.11A, lanes 6 and 7). The mutant promoter in lane

6, Δ-307/-61, provided the lowest level of expression that gave wild-type levels of aI5γ and bI1 splicing and will be used in estimating the minimum amount of Mss116 required for splicing.

7.2.8 Estimating the minimum amounts of Mss116 needed for mt intron splicing

To estimate the amounts of Mss116 in the wild-type and the most reduced samples (Δ -307/-61) (Fig. 7.11B, lanes 3 and 6), protein preparations from known volumes of each were analyzed by Western blot alongside a series of known concentrations of purified Mss116 (Fig. 7.12A). The concentration of the wild-type sample was diluted by 50% to prevent oversaturation of signal. The standards were diluted Mss116 that had been overexpressed in *E. coli* and purified to homogeneity. The stock concentration was determined by Bradford assay and confirmed by Qubit® 2.0 Fluorometer (Life Technologies). Using GelQuant.NET software (BiochemLabSolutions.com) to measure signal intensities, concentrations of the wild-type and mutant samples were calculated by simple linear regression derived from the standard curve (Fig. 7.12B). Independent trials gave a mean value of 1.7 nM (σ = 0.1) for the promoter mutant sample, and 2.4 nM for the 50% wild-type sample. Cell number/ml was estimated using a hemocytometer and associated $O.D._{600}$ values. From this, estimates for the number of cells loaded for each sample were obtained. The protein concentrations obtained from the standard curve were then converted from nM to pmol/μl, and then multiplied by the volume loaded in μl. The resulting value in pmol was converted to moles and multiplied by Avogadro's constant to obtain an estimate of the

number of Mss116 molecules loaded. Using this method and correcting for the 50% wild-type sample used, the estimated value for wild-type Mss116 was calculated to be approximately 96,000 molecules per cell.

The Saccharomyces Genome Database reports the estimated amounts of wild-type Mss116 to be 10,300 molecules/cell, a figure derived from work in the lab of Dr. Jonathan Weissman (Ghaemmaghami et al. 2003). There are several possible explanations for the almost ten-fold disparity between my value and that of Ghaemmaghami, *et al.* with the most likely causes being the use of different strains, methods and carbon sources.

In the previous study, the values were obtained by TAP-tagging the open reading frame and expressing it from its natural chromosomal location in yeast strain BY4741. Extracts containing TAP-fusion proteins were then analyzed by Western blot using an anti-CBP antibody. Here, I used an untagged molecule expressed from a CEN plasmid in strain 161-U7. The protein expression was measured using a polyclonal antibody specific for Mss116.

The type of carbon source used is another variable that could explain the discrepancy in values. It is well documented that the use of glucose as a carbon source suppresses mitochondrial gene expression, sometimes referred to as the "Crabtree effect" (Crabtree 1928; Thomson et al. 2005). In contrast to the glucose used in rich media by Ghaemmaghami, *et al*., I used raffinose, a carbon source that does not cause this suppression. It is plausible that the differences in these values reflect the differences in Mss116 expression with and without glucose suppression.

From my estimate of 96,000 molecules per cell for wild-type Mss116, we can now return to Figs. 7.5, 7.7, and 7.11 to extrapolate the reduced values of the mutants observed in which significant reduction in Mss116 signal was accompanied by near-wild-type splicing. The full length D248V mutant seen in Fig. 7.5, lane 6 had about a 3.5-fold reduction in Mss116 signal compared to wild type, or about 27,000 molecules per cell. In Fig. 7.7, lane 6, the Mss116 ΔNTE+ ΔC-tail truncation mutant showed a 6-fold reduction compared to wild-type which translates to approximately 16,000 molecules per cell, whereas in Fig. 7.11, lane 6, the 6.7-fold reduction translates to about 14, 000 molecules per cell.

In *S. cerevisiae*, mtDNA has been estimated to be about 15% of the total DNA content of the cell, or about 25-50 copies of 75-kb mt genomes per haploid cell (Williamson 1976; Williamson 2002). Taking the estimated number of Mss116 molecules per cell at 96,000 and the range of 25- 50 mt genomes per cell, this translates to between 1900 and 3800 molecules of Mss116 per mt genome. Using the SGD value of 10,300 molecules per cell would be equivalent to about 200-400 molecules of Mss116 per mt genome. Thus, with or without glucose suppression, Mss116 appears to be very abundant so that even at reduced levels, there are sufficient molecules present to produce a wild-type splicing phenotype.

7.2.9. Other proteins associated with Mss116

It is now well understood that Mss116 interacts with RNAs as substrates in fulfilling its many functions. What is not known, however, is with which other *proteins*

Mss116 may interact, especially during intron splicing. Toward that end, this part of the study was designed to identify those proteins that associate with Mss116.

Tandem Affinity Purification (TAP-tag) has become a standard method of pulling down protein complexes associated with a TAP-tagged protein of interest (Rigaut et al. 1999; Puig et al. 2001). A prior TAP-tag analysis of tagged wild-type Mss116 in the 161-U7/$1^{+}2^{+}$ strain had shown that it is associated with multiple mitoribosomal proteins of both the large and small ribosomal subunits (Huang 2004); however, a strain lacking introns was not tested. This result raised the question: How would the population of proteins be altered in an intronless strain where Mss116 is not required for splicing?

7.2.9.1 Identifying proteins associated with TAP-tagged Mss116 in multi-intron and intronless strains

To address the question above, wild-type Mss116 was TAP-tagged at the C-terminus as diagrammed in Fig. 7.13 and cloned into CEN plasmid pRS416. Plasmids expressing TAP-tagged and untagged Mss116 (pHRH197, (Huang 2004)) were then transformed into strains 161-U7*mss116Δ*/$1^{+}2^{+}$, which harbors the twelve group I and group II mt introns of *COX1* and *COB*, and into 161-U7 *mss116Δ* /I^{0}, an isogenic, intronless strain. Mitochondria were isolated from each strain grown in 1 l cultures of HC/Ura^{-} media with 2% raffinose at 30° C to $O.D._{600} \approx 3$ as detailed in Methods. The TAP protocol was followed as described in Methods with the following exception: the calmodulin beads were washed in either the standard 200 mM KCl or the less stringent 170 mM KCl wash buffer prior to elution. The beads were boiled in 30 µl loading dye for 2 min to release the bound proteins. Half of each boiled sample was then separated in a 4-

12% polyacrylamide SDS gel (Fig. 7.14). The other half was run for approximately 1 cm in an identical gel, with the single band being excised for mass spectroscopy analysis at the University of Texas at Austin Protein Facility.

The protein gel in Fig. 7.14A shows proteins associated with the tagged (lane 1) and untagged Mss116 (lane 2) in the I^0 strain with the 200 mM salt wash. Lanes 3 and 4 show the proteins associated with tagged and untagged Mss116 in the 1^+2^+ strain.

Table 7.1 lists the proteins identified by mass spectroscopy with the 200 mM salt wash. The spectral count for each protein was normalized to that of the total sample. No proteins were detected in the untagged samples, although bands of 51 and 28 kDa were evident in the gel for the untagged I^0 strain (Fig. 7.14, lane 2). These bands may be residual TEV protease or contaminating *E. coli* proteins from the TEV protease isolation that would not be identified in an *S. cerevisiae* database. The proteins were listed in decreasing order of the fold change of the abundance of protein in the 1^+2^+ strain over the I^0 strain (right-hand column). The list of proteins is comprised of 15 proteins other than Mss116 and was very similar for both strains. The data are shown graphically in Fig. 7.15, where the proteins to the left on the X-axis are those most enriched in the 1^+2^+ strain. The heights of the bars relative to each other reflect the fold change of the 1^+2^+ strain (red) over the I^0 strain (green) for each protein.

Other than mitoribosomal proteins, two other proteins (highlighted in yellow in Table 7.14 and Fig. 7.15) were also pulled down with Mss116: the cytoplasmic helicase Ded1 (Senissar et al. 2014) and the *COB* processing protein and bI5 splicing factor, Cbp2 (Gampel et al. 1989). Though Ded1 was found to be about 5 times more abundant in the

1^+2^+ strain than in the I^0 strain and may be a contaminant associated with the mitochondrial outer membrane, it is known to be essential for translation initiation on cytoplasmic ribosomes in *S. cerevisiae* (Iost et al. 1999). However, upregulation of Ded1 due to retrograde signaling for the import of other mt proteins and the possibility that some proportion of Ded1 functions within mitochondria cannot be disregarded. Cbp2 was found to be slightly more abundant in the I^0 strain than in the 1^+2^+, but it is unclear if this difference is significant.

To identify proteins that might be more tenuously associated with Mss116 as possible components of a less stable complex, the final salt wash concentration in the TAP protocol was reduced from the standard 200 mM to 170 mM (Fig. 7.14B). With this change, many more proteins were identified (Table 7.2). As in Table 7.1, the proteins were ordered by the fold change of the normalized spectral counts of the 1^+2^+ strain over those for the I^0. These data are graphed in Fig. 7.16, with those proteins enriched in the 1^+2^+ strain to the left of the X-axis. Although most of the proteins were again mitoribosomal proteins from the large subunit, several other non-ribosomal proteins were identified (yellow highlight). The heights of the bars relative to each other reflect the fold change of the 1^+2^+ strain (red) over the I^0 strain (green). The protein with the greatest fold change over I^0 was an uncharacterized protein, Yer077C that when tested in Phase I was found to cause no splice defect (Nyberg 2006). Other proteins found more abundantly in the 1^+2^+ strain were Mgm101, Mrm1, Aim23, and Oms1. Mgm101 is a protein required for mtDNA damage repair and for mt genome maintenance (Chen et al. 1993). Mrm1/Pet56 methylates a conserved nucleotide in mt 21S rRNA (Sirum-Connolly and

Mason 1993) and its deletion was found in Chapter 3 to cause splicing defects in both aI5γ and bI1. Aim23 is a mt translation initiation factor (Kuzmenko et al. 2014). Oms1 is a multicopy repressor of defects caused by mutations in Oxa1 (Lemaire et al. 2004). As in the more stringent 200 mM salt wash, Cbp2 was again found to be associated with the tagged Mss116; however, under these less stringent wash conditions, it was more abundant in the $1^{+}2^{+}$ than in the I^{0}. In addition to mitoribosomal proteins from the large subunit, proteins from the small subunit were also found in the less stringent wash.

Table 7.3 is a compilation of the proteins identified in the experiments under both sets of conditions, along with the proteins identified in a previous study in which the final salt wash was 200 mM KCl (Huang 2004). Here, the proteins are ordered by their molecular weights, with "Y" (Yes) signifying the identification of that protein in the indicated experiment. With few exceptions, the proteins are mitoribosomal proteins, and where there is agreement in all three sets, the mitoribosomal proteins are often those located near the ribosomal tunnel exit (Mrpl3, Mrpl4, Mrpl22, and Mrpl40), a region of the mitoribosome known to be enriched with mitochondria-specific proteins and rRNA (Amunts et al. 2014). Other mitoribosomal proteins found in all sets were Yml6, and Mrpl15.

Considered together, the data above show that Mss116 appears to associate primarily with mitoribosomal proteins with relatively few differences observed between an intronless strain and one containing 12 mt introns.

7.2.9.2 Identifying proteins associated with TAP-tagged Mss116 in single-intron petite strains

Because of the large number of mitoribosomal proteins being identified as associated with the tagged Mss116 in the ρ^+ strains, this next set of experiments was conducted in single-intron petite strains which lack functional mitoribosomes to reduce their background effect. The strains were tested previously (Figs. 5.7 and 5.8) and lack 21S and 15S rRNAs. Plasmids expressing TAP-tagged and untagged wild-type Mss116 were transformed into ρ^+ and ρ^- strains of 161-U7*mss116Δ*/aI5γ and 161-U7*mss116Δ*/bI1. Cultures were grown, mitochondria isolated and treated as described in 7.2.8a.

The resulting proteins were separated in a 4-12% SDS polyacrylamide gel and stained with Coomassie Brilliant Blue (Fig. 7.17). In lanes 1-4 are the proteins associated with the TAP-tagged Mss116 in the four tested strains. Mss116 is clearly evident. In lanes 5-8 are the protein bands that represent the background in these strains, most of which are seen in both the tagged and untagged strains.

7.2.9.2a Identifying proteins associated with Mss116 in aI5γ strains

Table 7.4 lists the proteins identified by mass spectroscopy in TAP-tagged and untagged Mss116 in 161-U7/aI5γ ρ^+ and ρ^- strains. The proteins are in decreasing order of the fold change observed for the corrected ρ^+ over the corrected ρ^- strains. Corrected values were determined by subtracting the background untagged spectral count from the tagged value for each protein. Thus ordered, the proteins that are at the top of the list (fold change greater than 1) are those that were more abundant in the ρ^+ strain than the ρ^- strain, possibly highlighting those proteins that allow efficient splicing in the former

strain that are lacking in the latter. Conversely, the proteins at the bottom of the list (fold change = 0; not found in ρ^+) are those proteins that may be enriched in the ρ^- strains over the mitoribosomal background. Non-ribosomal proteins are highlighted in yellow at both ends of the list.

Unexpectedly, the values for Mss116 were much higher in the single intron strains than had been observed previously for either the 1^+2^+ or intronless strains. Though the reason for this is unclear, the Mss116 values dwarf those of the remaining proteins so that they are excluded from the graph in Fig. 7.18.

The graph is arranged with proteins enriched in the aI5γ ρ^+ strain (blue) to the left on the X-axis, and those enriched in the ρ^- strain (red) to the right with each portion of the graph enlarged in Figures 7.19 and 7.20 for clarity. Mitoribosomal proteins of the large subunit are predominantly represented in the ρ^+ strain that are absent from the ρ^- although several non-mitoribosomal proteins are also identified (yellow highlight). Among these are Yme2, a protein that assists in maintaining mt nucleoid structure and number; Pet127, a protein with a role in 5´-end processing of mtRNAs (Haffter and Fox 1992); Yhm2, a protein that associates with mt nucleoids and plays a role in replication and segregation of the mt genome (Thorsness and Fox 1993); Mrm1/Pet56, a protein that methylates a critical nucleotide in mt 21S rRNA (Sirum-Connolly and Mason 1993) and whose deletion was found in Chapter 3 to cause splicing defects in both aI5γ and bI1; and several proteins associated with the electron transport chain: Yhb1, Mir1, Pet9, Nde1 (Luttik et al. 1998; Reinders et al. 2007; Azuma et al. 2008; Tkach et al. 2012).

Among the proteins enriched in the aI5γ ρ^- strain were many cytoplasmic ribosomal proteins from both large and small subunits. Others included Ded1, a putative cytoplasmic DEAD-box protein also identified above; Tim44, a protein involved in protein import to the mitochondrion; aI5β splicing factors Mne1 and Suv3; bI5 splicing factor Cbp2; Aep3, a PPR protein involved in mt translation initiation; Rmd9, a PPR protein that may play a role in delivering mtRNAs to the mitoribosomes, and whose overexpression can compensate for the loss of Oxa1; and PPR protein and translational activator Pet309.

The presence of Cbp2 and Pet309 echoes the results from the Dieckmann lab in which these two proteins, together with Cbp1, were associated in a high-molecular weight complex that linked transcription to translation (Krause et al. 2004). Interestingly, here Cbp2 and Pet309 are associated with Mss116, with splicing factors for aI5β, and with PPR proteins Rmd9, Suv3, and Aep3 which are known to interact with RNAs. More recently, these proteins were found together complexed with mitoribosomal proteins (Kehrein et al. 2015).

7.2.9.2b Identifying proteins associated with Mss116 in the bI1 strains

Table 7.5 lists the proteins identified in the ρ^+ and ρ^- 161-U7/bI1 strains, listed in order of decreasing fold change of ρ^+ over ρ^-. Unlike the situation in the aI5γ strains, where Mss116 was found at levels more than double in aI5γ ρ^- than those in aI5γ ρ^+, in bI1, the situation was reversed, with the bI1ρ^+ strain having more than double the amount of Mss116 compared to the bI1ρ^-. Nonetheless, the levels of Mss116 in the bI1 strains

were also very high, dwarfing the levels of the remaining proteins. For that reason, Mss116 is not graphed in Fig. 7.21. On the left side of the X-axis are those proteins that were enriched in the bI1 ρ^+ strain (blue), and on the right, those enriched in the bI1 ρ^- strain (red). Each portion of the graph is enlarged for clarity in Figures 7.22 and 7.23.

As was the case with the aI5γ strains, the predominant proteins in the bI1 ρ^+ that are lacking in the bI1 ρ^- are the mitoribosomal proteins of the large subunit, most of which are identical to those identified in the aI5γ ρ^+ strain. With the varied levels of Mss116, the implication is that there is no direct relationship between the levels of Mss116 and these mitoribosomal proteins.

Several other proteins identified in the aI5γ ρ^+ strain were also identified in the bI1 ρ^+ strain: Mrm1, Ybh1, Mir1, and Nde1. Additional non-ribosomal mitochondrial proteins enriched in the bI1 ρ^+ strain but not in the aI5γ ρ^+ that may be involved specifically in bI1 splicing were: Mrx4/Ypl168W, an uncharacterized protein that associates with the mitoribosome (Kehrein et al. 2015); Rrg9, a protein of unknown function whose deletion causes loss of mtDNA (Merz and Westermann 2009); Fmp52, a protein of unknown function that localizes to the mt outer membrane (Dardalhon et al. 2007); Yil077C, a putative protein of unknown function detected in highly purified mitochondria (Reinders et al. 2006) , and Mgr1, a subunit of the mt protease complex that degrades misfolded mt proteins (Dunn et al. 2006).

Many small subunit mitoribosomal proteins were enriched in the bI1 ρ^- strain, in contrast to the aI5γ ρ^- strain, as was PPR protein and aI4 and bI4 splicing factor, Ccm1.

Other non-ribosomal proteins enriched in the bI1 ρ^- strain were Cyt1 and Qcr2, both associated with the electron transport chain (Dorsman and Grivell 1990; Schneider and Guarente 1991); Ilv5, a protein with a role in maintaining mtDNA (Macierzanka et al. 2008); and Pdb1, a component of the pyruvate dehydrogenase complex (Miran et al. 1993).

Few of the proteins enriched in the aI5γ ρ^- strains were also enriched in the bI1 ρ^- strain, suggesting the possibility that each petite may signal the cell for the import of specific proteins.

In both petite strains, many of the enriched proteins were involved in respiration and could be contaminants or may serve dual functions to also play a role in splicing.

7.2.9.3 TAP pull-down of Mss116 in strain 161-U7/1$^+$2$^+$ following RNase treatment

The large number of mitoribosomal proteins that appeared to be associated with Mss116 raised the question as to whether the helicase was interacting with the mitoribosomal proteins themselves or perhaps this observation was an artifact of the helicase's association with the ribosomal RNA. To test this possibility, the 161-U7 *mss116Δ*/1$^+$2$^+$ strain containing a plasmid expressing TAP-tagged Mss116 was cultured and the mitochondria isolated as described in section 7.2.8a. In this set of experiments, however, the mitochondrial experimental sample was treated with 60 µl RNase A (Thermo Scientific) to a final concentration of 0.2 mg/ml and the control sample with 60 µl of solubilization buffer immediately following the standard solubilization step (see

Methods). Both were incubated at 30° C for 10 min before proceeding with the remainder of the TAP protocol.

Samples were separated on a 4-12% gradient gel and stained with Coomassie Brilliant Blue (Fig. 7.20). In lane 1, the sample without the RNase treatment, Mss116 remains clearly apparent. The RNase-treated sample in lane 2, however, has lost almost all of its Mss116, suggesting that Mss116 may be interacting with and stabilized by rRNA. The level of mitoribosomal proteins is also diminished compared to the untreated sample. The 23- kDa band is not degraded, however, an indication that contaminating proteases are not responsible for the loss of Mss116. The results are consistent with the possibility that Mss116 may be interacting with the rRNAs and not the mitoribosomal proteins.

7.3 Discussion

The general RNA chaperone Mss116 functions in splicing the mitochondrial group I and group II introns in *S. cerevisiae.* This study provided greater insight into the mechanics of this role, provided estimates of the protein's abundance, and identified proteins that are associated with the helicase.

Permissible amino acid substitutions throughout Mss116 aided our understanding of the protein's mechanism of action: substitutions indicated that the RNA bend induced by the helicase core depends on ionic and hydrogen-bonding interactions with the bound RNA. The functionally important regions included those containing conserved sequence motifs involved in ATP and RNA binding or interdomain interactions, as well as

previously unidentified regions that may function in protein-protein interactions. Also identified were two conserved regions-one the previously noted post II region in the helicase core, and the other in the CTE-that may help displace or sequester the opposite RNA strand during RNA unwinding. The *in vivo* splicing analysis of the Mss116 SAT/AAA mutant in the single intron strain provided strong evidence that splicing ability is directly related to ATPase function.

Estimates for the amount of Mss116 were determined. The protein appears to be very abundant with an estimated 96,000 molecules per cell or between 1900 and 3800 molecules of Mss116 per mt genome. With such a plentiful protein, reduction to 15% of its wild-type levels was still found to be sufficient in supporting wild-type splicing in the 161-U7/$1^{+}2^{+}$ strain.

Pull-down experiments indicated that many proteins appear to interact with TAP-tagged Mss116. Chief among these were mitoribosomal proteins; however, RNase treatment disrupted many of these interactions, suggesting that Mss116 is primarily associated with the rRNAs. One intriguing explanation for these results may have Mss116 interacting with rRNAs as a means to monitor the status of the mitoribosome, thereby linking splicing to translation.

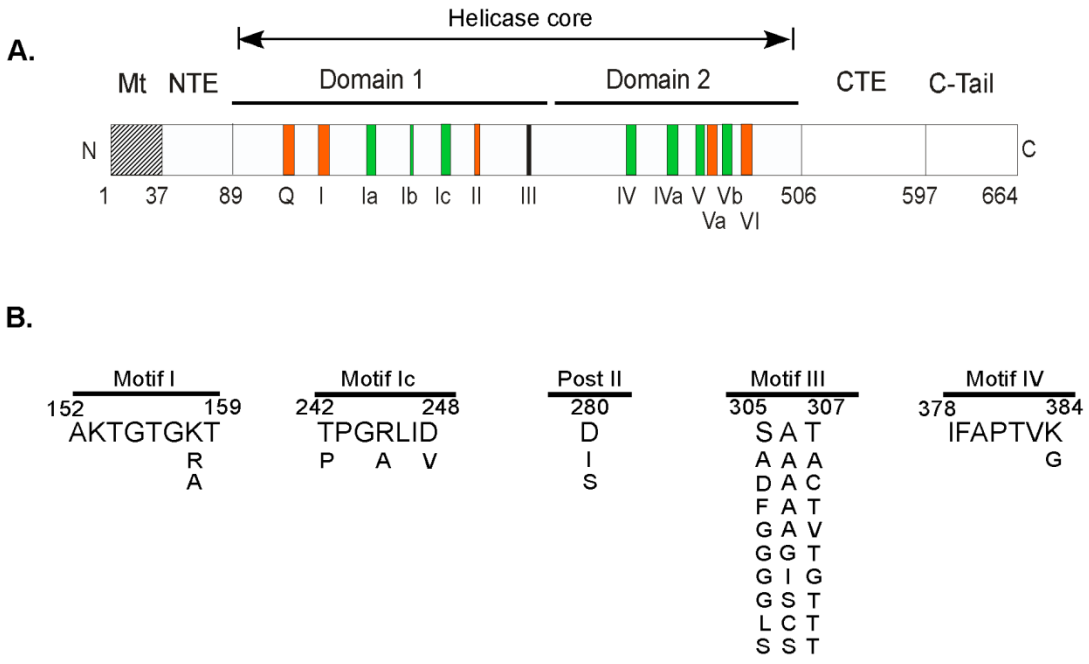

Figure 7.1: Key features of wild-type Mss116 and the mutants investigated in this study.

(A) Diagram of Mss116 showing domain architecture as described in Fig. 1.5. Motifs colored orange interact with ATP; those colored green interact with ssRNA. Motif III, in black, does not contact either ATP or RNA, but is involved with bridging domains 1 and 2. (B) Mss116 mutants investigated in this study. The wild-type sequence for each motif is indicated at the top between numbered boundary amino acids, with mutations analyzed in this research listed below the wild-type sequences.

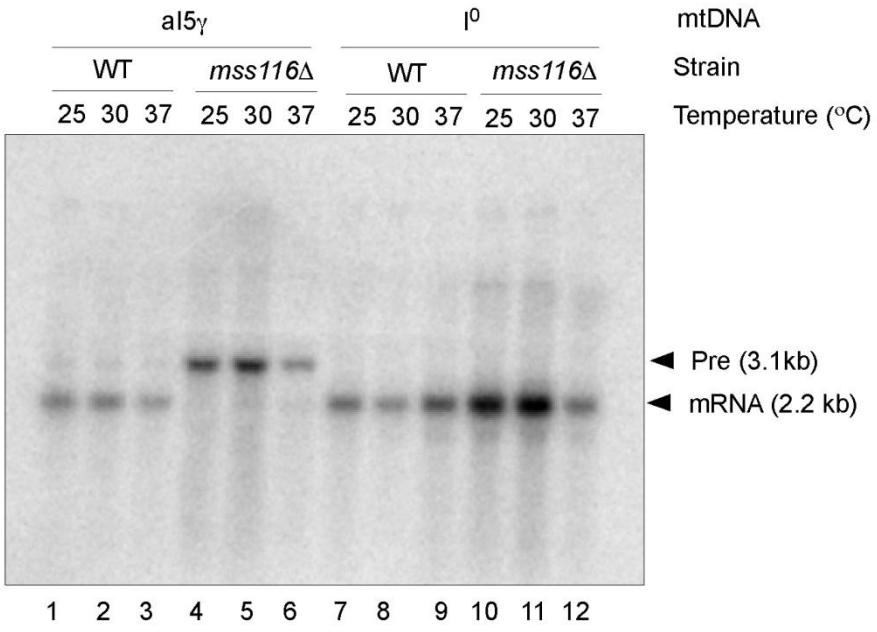

Figure 7.2: Northern hybridization analysis comparing the abilities of wild-type strains and derivatives of those strains in which *MSS116* has been deleted to promote splicing of group II intron aI5γ at 3 different temperatures.

The strains analyzed were wild-type (WT) 161-U7/aI5γ, 161-U7/I^0 and derivatives of those strains in which *MSS116* has been deleted. Strains were grown in 30 ml YPR at 25°C, 30°C, and 37°C to $O.D._{600} \approx 1.0$. Total cellular RNA was isolated for each sample and 1.0 µg run in a 1.5% RNA-grade agarose gel, blotted onto a nylon membrane, and hybridized with a ^{32}P-labeled DNA oligonucleotide complementary to the *COX1* terminal exon (small arrow below *COX1* in Fig. 3.3A). Precursor (Pre) and mature mRNA (mRNA) are indicated to the right of the panel.

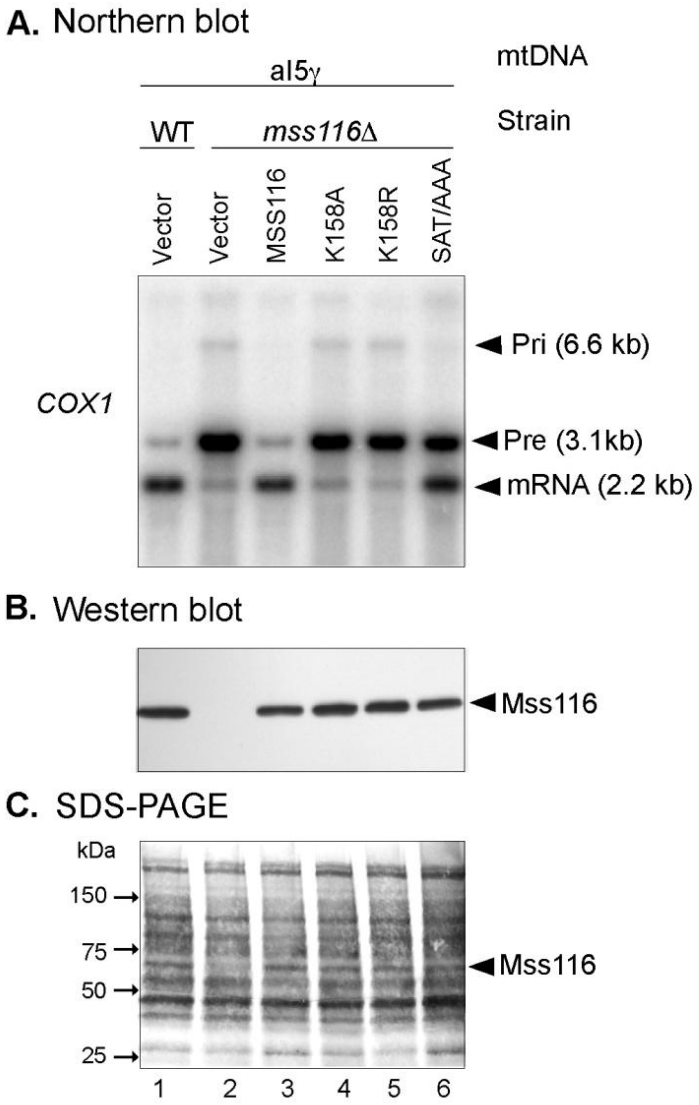

Figure 7.3: Northern hybridization analysis and correlated Western blot analyses comparing the abilities of wild-type and K158 and SAT/AAA mutant Mss116 proteins to promote the splicing of group II intron aI5γ.

Figure 7.3(continued): Northern hybridization analysis and correlated Western blot analyses comparing the abilities of wild-type and K158 and SAT/AAA mutant Mss116 proteins to promote the splicing of group II intron aI5γ.

(A) Northern hybridization analysis. The strains analyzed were wild-type (WT) 161-U7/aI5γ and mss116Δ/aI5γ containing the CEN plasmid vector pRS416 or CEN plasmids expressing wild-type Mss116 or the indicated mutants. Strains were grown in HC/Ura$^-$/raffinose liquid media (see Methods) to $O.D._{600}$ = about 1.0. Total cellular RNA was isolated, 1.0 µg run in a 1.5% RNA-grade agarose gel, blotted onto a nylon membrane, and hybridized with a ^{32}P-labeled DNA oligonucleotide complementary to the *COX1* terminal exon (the small arrow below *COX1* in Fig. 3.1 A). Lane 1, wild-type 161-U7/aI5γ (WT) transformed with CEN plasmid pRS416 (empty vector); lane 2, *mss116*Δ/aI5γ transformed with CEN plasmid pRS416 (empty vector); lanes 3–6, *mss116*Δ/aI5γ transformed with CEN plasmids expressing Mss116 mutants K158A, K158R, and SAT/AAA (B) Western blot. The blot shows TCA-precipitated proteins (~60 µg) from the same strains as in A, separated in a 0.1% SDS 4–20% polyacrylamide gradient gel, transferred to a Sequi-Blot™ PVDF membrane (Bio-Rad) and probed with an anti-Mss116 antibody. (C) The Western blot was stripped and stained with AuroDye Forte (GE Healthcare) to confirm equal loading. The numbers to the left of the gel in (B) and (C) indicate the positions of size markers (Precision Plus Protein Dual Color Standards; Bio-Rad).

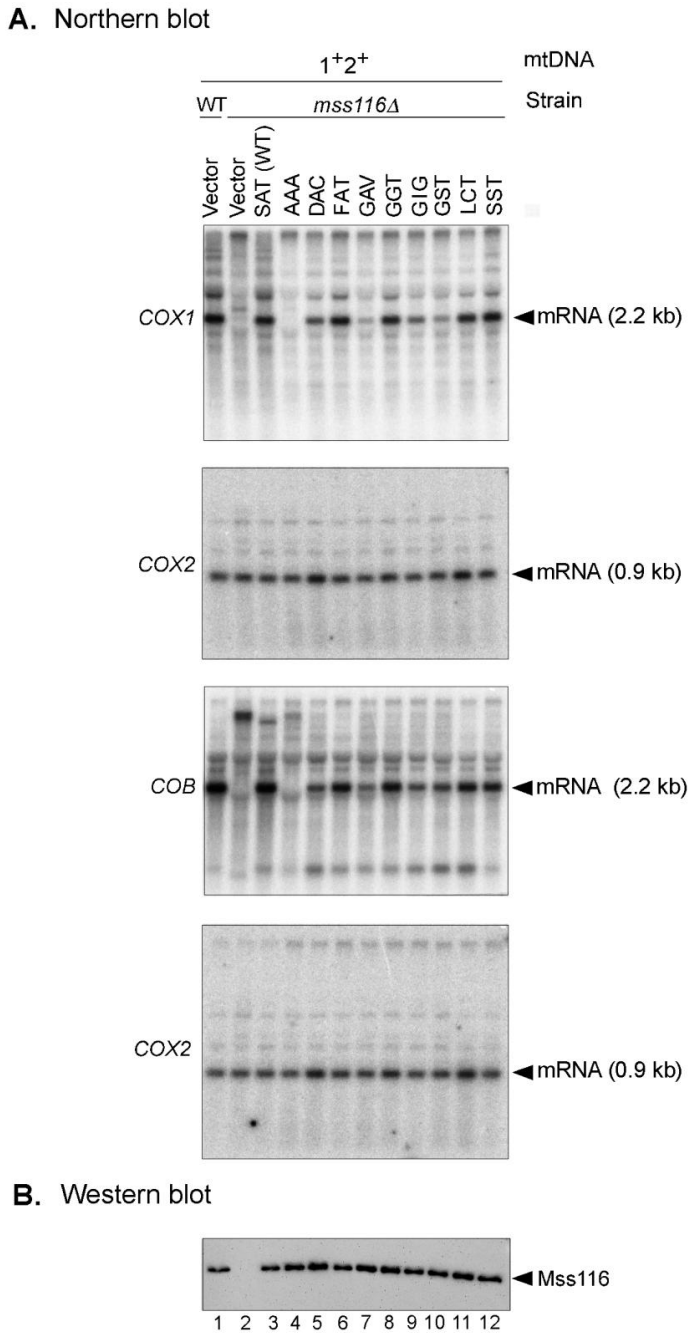

Figure 7.4: Northern hybridization analysis and correlated Western blot analyses comparing the abilities of wild-type and motif III mutant Mss116 proteins to promote mt intron splicing in strain 161-U7 *mss116*Δ/$1^{+}2^{+}$.

Figure 7.4 (continued): Northern hybridization analysis and correlated Western blot analyses comparing the abilities of wild-type and motif III mutant Mss116 proteins to promote mt intron splicing in strain 161-U7 *mss116*Δ/1^+2^+.

The strains analyzed were wild-type (WT) 161-U7/1^+2^+ and *mss116*Δ/1^+2^+ containing the CEN plasmid vector pRS416 or CEN plasmids expressing wild-type Mss116 or the indicated motif III mutants. Strains were cultured as in Fig. 7.2. (A) Northern hybridization analysis. The blots show whole-cell RNAs from the indicated strains separated in a 1.5% agarose gel, blotted onto a nylon membrane, and hybridized with ^{32}P-labeled oligonucleotide probes complementary to the *COX1* or *COB* terminal exon. The blots were then stripped and rehybridized with a probe for the intronless *COX2* gene to assess equal loading. (B) Western blot. The blot shows TCA-precipitated proteins from the same cultures as in A, separated in a 0.1% SDS/4–12% polyacrylamide gradient gel, transferred to a Sequi-Blot™ PVDF membrane (Bio-Rad), and probed with anti-Mss116 antibody.

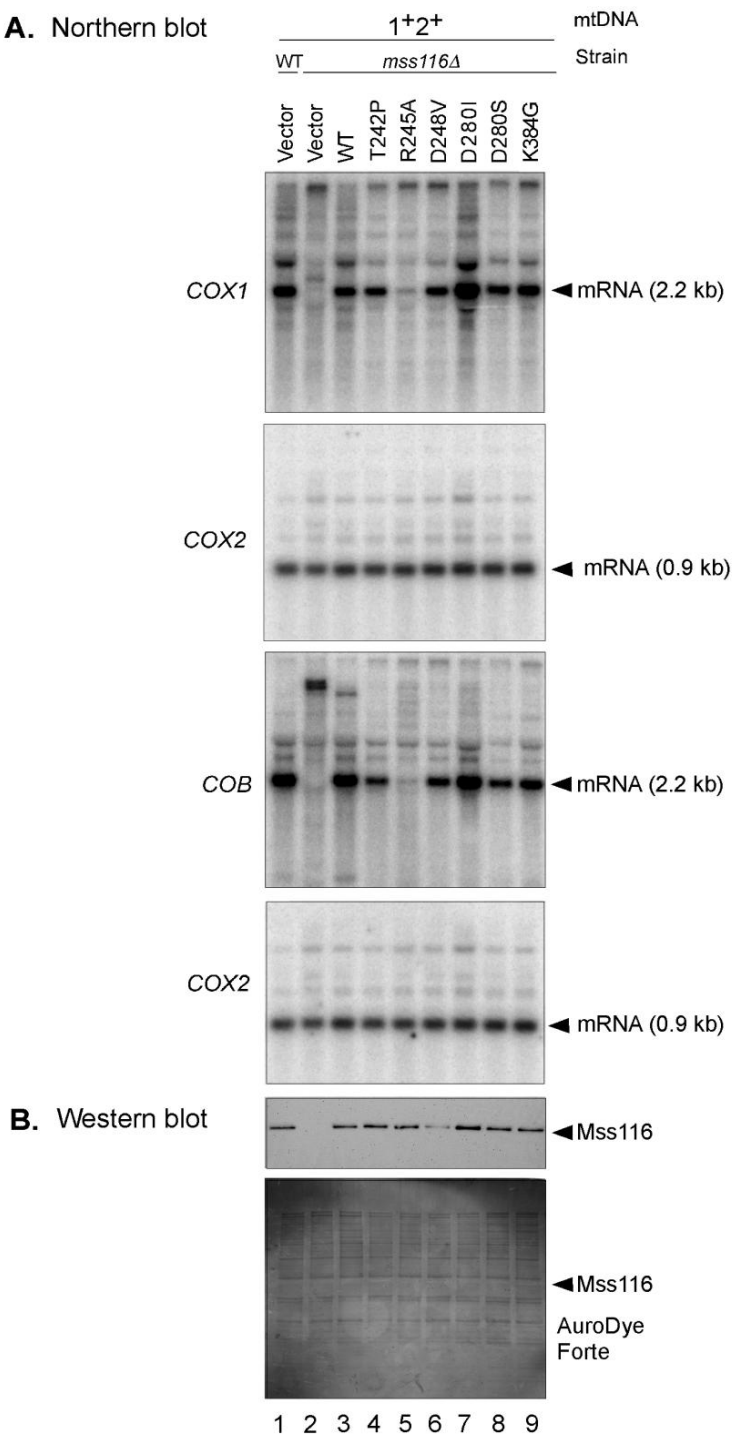

Figure 7.5: Northern hybridization analysis and correlated Western blot analyses comparing the abilities of wild-type and Mss116 RNA-binding tract mutant proteins derivatives to promote mt intron splicing in strain 161-U7 *mss116*Δ/$1^{+}2^{+}$.

Figure 7.5(continued): Northern hybridization analysis and correlated Western blot analyses comparing the abilities of wild-type and Mss116 RNA-binding tract mutant proteins derivatives to promote mt intron splicing in strain 161-U7 *mss116*Δ/1^+2^+.

The strains analyzed were wild-type 161-U7/1^+2^+ (WT) and *mss116Δ*/1^+2^+ containing the CEN plasmid vector pRS416 or CEN plasmids expressing WT Mss116 or the indicated mutant. Strains were cultured as in Fig. 7.2. (A) Northern hybridization analysis. Whole-cell RNAs from the indicated strains were separated in a 1.5% agarose gel, blotted onto a nylon membrane and hybridized with ^{32}P-labeled probes for *COX1*, *COB* and *COX2*, as described in the legend of Figure 7.3. (B) Western blot. TCA-precipitated proteins from the same strains were separated in a 0.1% SDS/4–12% polyacrylamide gradient gel, transferred to a Sequi-Blot™ PVDF membrane (Bio-Rad) and probed with anti-Mss116 antibody. After imaging, the membrane was stripped of antibodies and stained with AuroDye Forte to confirm equal loading.

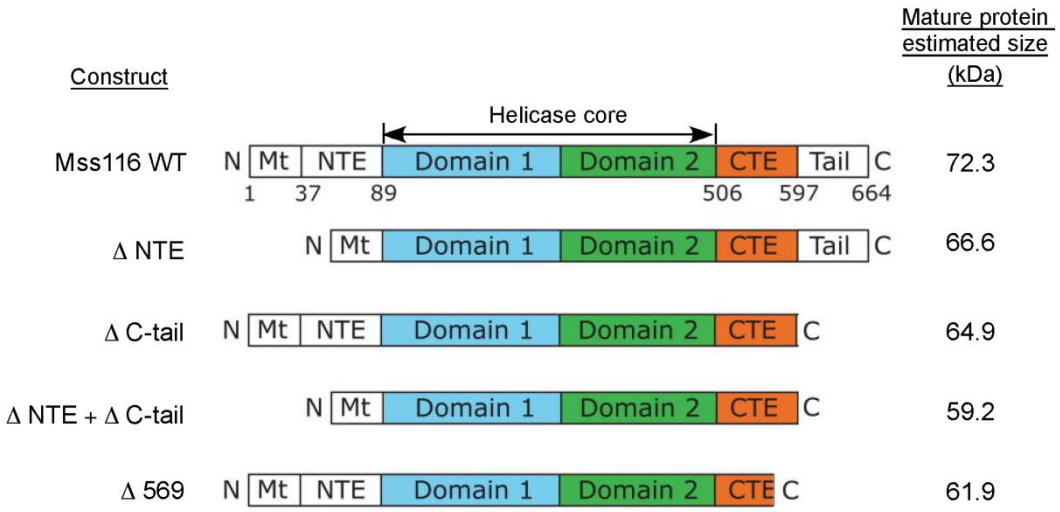

Figure 7.6: Schematic of Mss116 N-and C-terminal truncation mutants.

Wild-type Mss116 and truncation mutants. The protein is identified to the left of the schematic, and the size (kDa) of the mature protein is indicated to the right. (The cleaved mitochondrial target sequence, Mt, is not included in the size estimate of the mature protein.). Amino acid residues at the boundaries between different regions are numbered below the wild-type schematic.

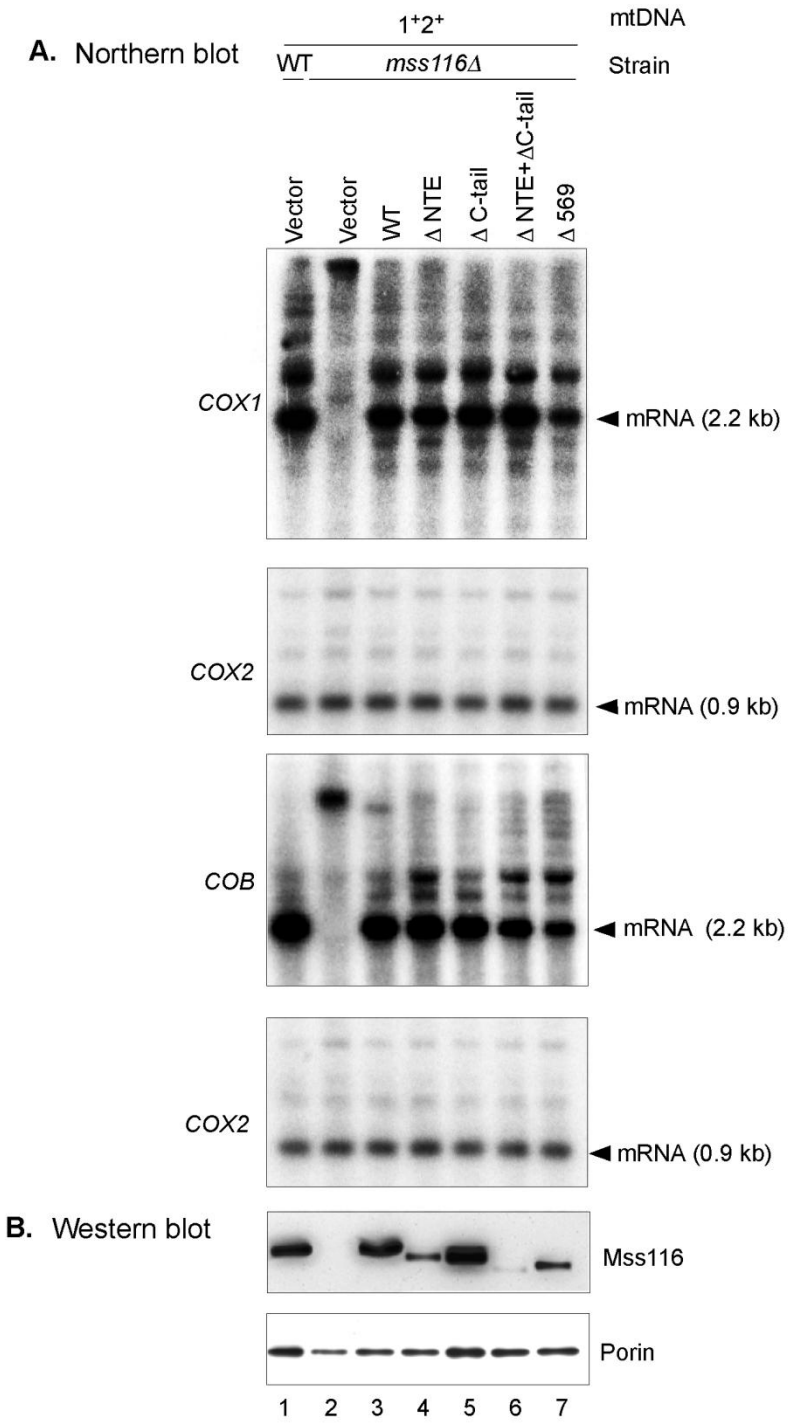

Figure 7.7: Northern hybridization and correlated Western blot analyses comparing the abilities of wild-type and Mss116 truncation mutants to promote mt intron splicing in strain 161-U7 *mss116*Δ/$1^{+}2^{+}$.

Figure 7.7 (continued): Northern hybridization and correlated Western blot analyses comparing the abilities of wild-type and Mss116 truncation mutants to promote mt intron splicing in strain 161-U7 *mss116*Δ/1^+2^+.

The strains analyzed were wild-type 161-U7/1^+2^+ and *mss116Δ*/1^+2^+ containing the CEN plasmid vector pRS416 or CEN plasmids expressing WT Mss116 or the indicated N- or C- terminal truncation mutants. Strains were cultured as described in Fig. 7.2. (A) Northern hybridization analysis. Whole-cell RNAs from the indicated strains were separated in a 1.5% agarose gel, blotted onto a nylon membrane, and hybridized with ^{32}P-labeled probes for *COX1*, *COB* and *COX2*, as described in the legend of Figure 7.3. (B) Western blot. TCA-precipitated proteins from the same cultures as in (A) were separated in a 0.1% SDS/4–12% polyacrylamide gradient gel and transferred to a Sequi-Blot™ PVDF membrane (Bio-Rad). The membrane was cut along the 50 kDa marker, and the upper portion of the membrane probed with anti-Mss116 antibody and the lower portion with anti-porin antibody for use as loading control.

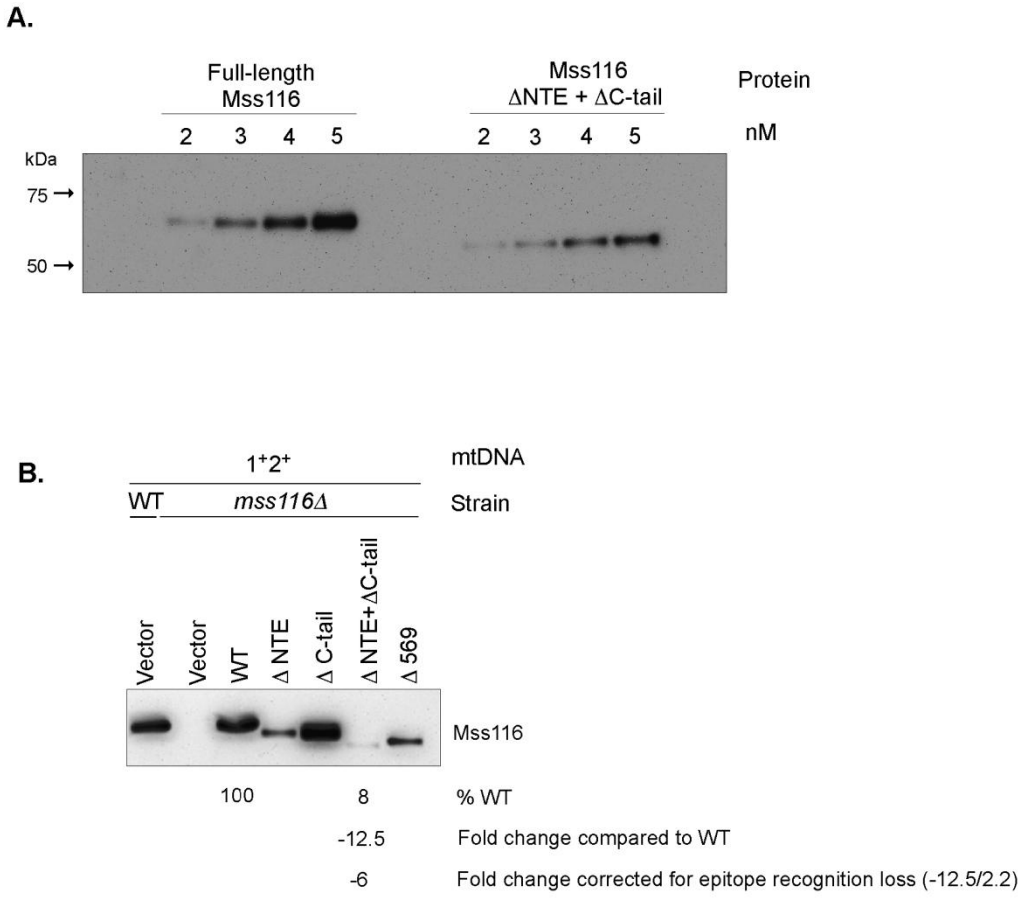

Figure 7.8: Estimating the efficiency of anti-Mss116 antibody recognition of wild-type and truncated Mss116 proteins.

(A) Western blot.. Known concentrations (nM) of purified full-length and truncated Mss116 (ΔNTE + ΔC-tail) proteins shown in Fig. 7.6 were separated in a 0.1% SDS/4–12% polyacrylamide gradient gel, transferred to a Sequi-Blot™ PVDF membrane (Bio-Rad), and probed with an anti-Mss116 antibody. Image acquisition was with a FluorChemHD2 camera (Cell Biosciences) and densitometry was performed with GelQuant.NET software (BioChemLabSolutions.com). (B) Western blot from Fig. 7.7B with the level of expression of Mss116 ΔNTE + ΔC-tail relative to that of the wild-type protein without (% WT and fold change compared to WT) and with correction for the efficiency of antibody recognition (fold change corrected for epitope recognition). Band intensity levels were measured with GelQuant.NET software.

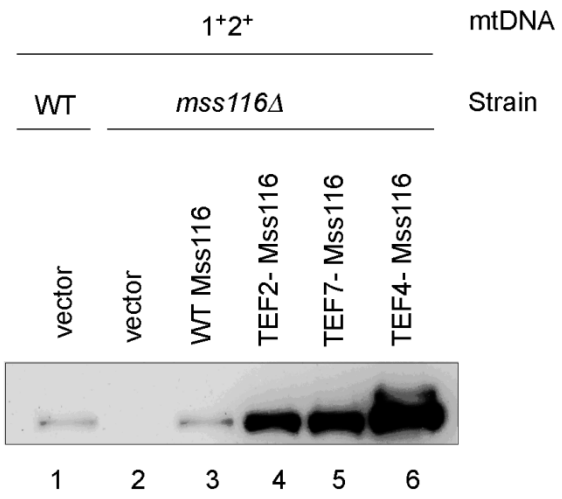

Figure 7.9: Western blot showing modulation of Mss116 protein expression by TEF promoter mutations.

The strains analyzed were WT 161-U7/1^+2^+ and *mss116Δ*/1^+2^+ containing the plasmid vector p416 or the indicated pRS416-TEF-Mss116 plasmids, in order of increasing promoter strength (Alper et al. 2005). TCA-precipitated proteins were separated in a 0.1% SDS/4–12% polyacrylamide gradient gel, transferred to a Sequi-Blot™ PVDF membrane (Bio-Rad), and probed with anti-Mss116 antibody.

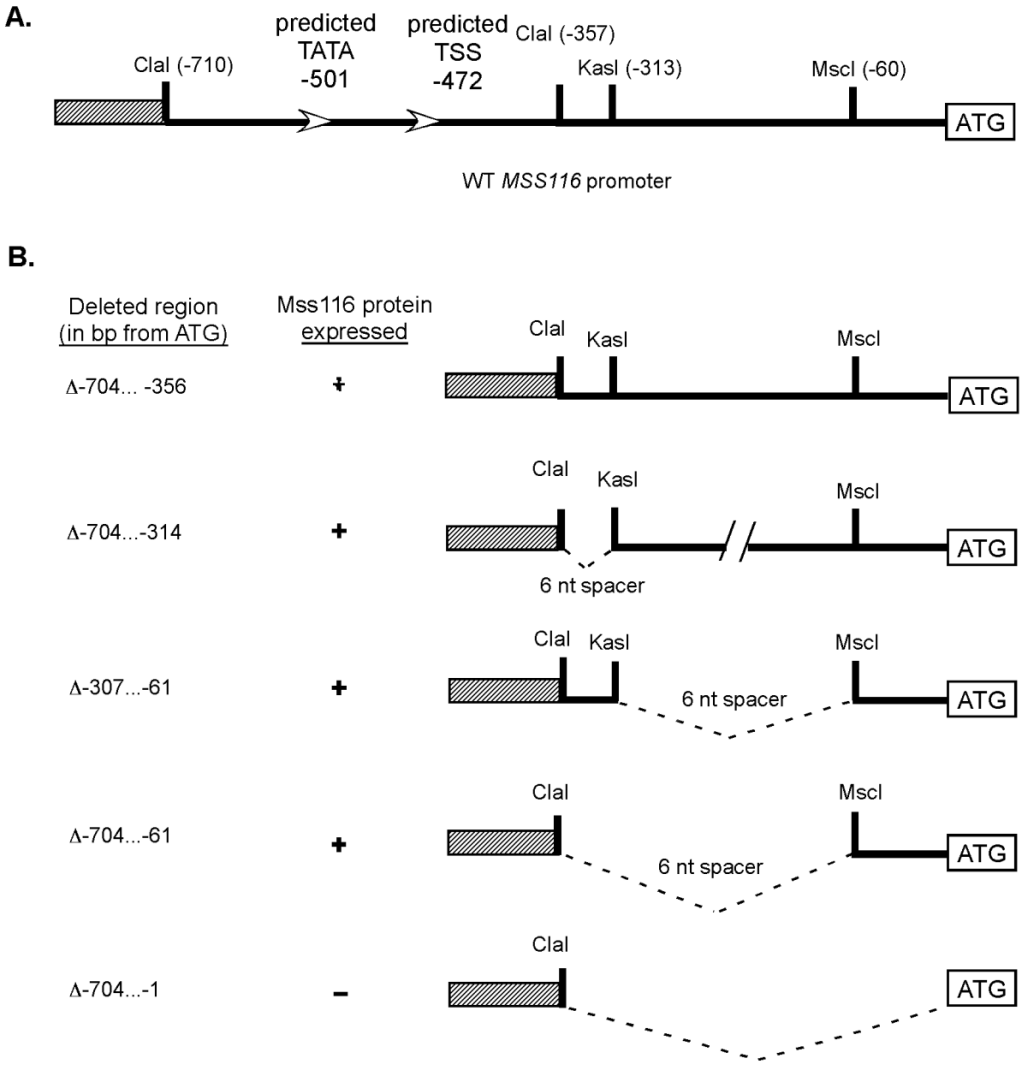

Figure 7.10: Constructs used for modulating Mss116 expression by *MSS116* promoter mutations.

(A) Wild-type *MSS116* promoter. Landmark restriction sites and their distances in bp from the ATG initiation codon are indicated in parentheses. The white arrowheads mark putative TATA box and transcriptional start site (TSS) as predicted by Promoter Scan software. (B) Promoter mutants used to alter the level of Mss116 expression. Deleted regions of the promoter are given to the left in bp from the ATG. Presence or absence of protein expression by each mutated promoter is indicated by + or – .

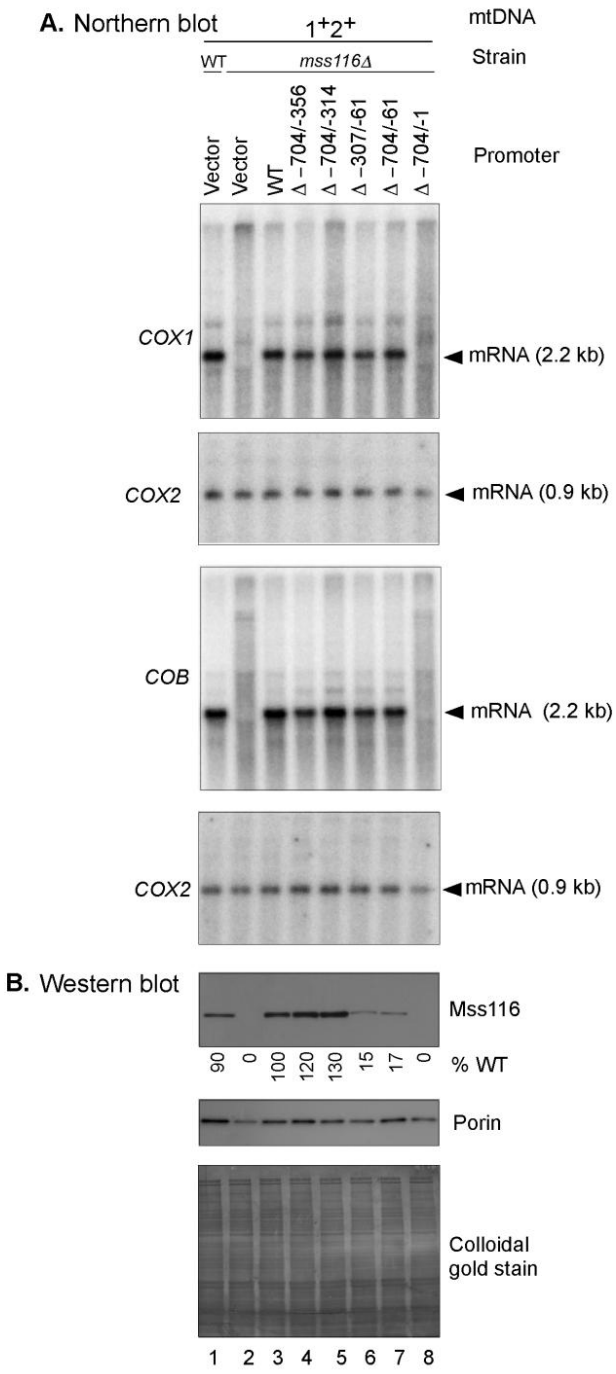

Figure 7.11: Northern hybridization analysis and correlated Western blot analyses comparing the ability of Mss116 expressed from a plasmid at various levels to promote mt intron splicing in strain 161-U7*mss116*Δ/$1^{+}2^{+}$.

Figure 7.11(continued): Northern hybridization analysis and correlated Western blot analyses comparing the ability of Mss116 expressed from a plasmid at various levels to promote mt intron splicing in strain 161-U7*mss116*Δ/$1^{+}2^{+}$.

The strains analyzed were wild-type 161-U7/$1^{+}2^{+}$ (WT) and *mss116Δ*/$1^{+}2^{+}$ containing the CEN plasmid vector pRS416 or CEN plasmids expressing wild-type Mss116 with the WT promoter or the indicated promoter mutations as diagrammed in Fig. 7.10. Strains were cultured as in Fig. 7.3. (A) Northern hybridization analysis. Whole-cell RNAs from the indicated strains were separated in a 1.5% agarose gel, blotted onto a nylon membrane, and hybridized with ^{32}P-labeled probes complementary to the *COX1* or *COB* terminal exon. (B) Western blots. TCA-precipitated proteins from the same cultures as in (A) were separated in a 0.1% SDS/4–12% polyacrylamide gradient gel and transferred to a Sequi-Blot™ PVDF membrane (Bio-Rad). The membrane was cut along the 50 kDa marker, and the upper portion of the membrane was probed with anti-Mss116 antibody and the lower portion with anti-porin antibody for use as loading control. After imaging, blots were stripped and stained with Gold Colloidal Stain (Bio-Rad) to confirm equal loading.

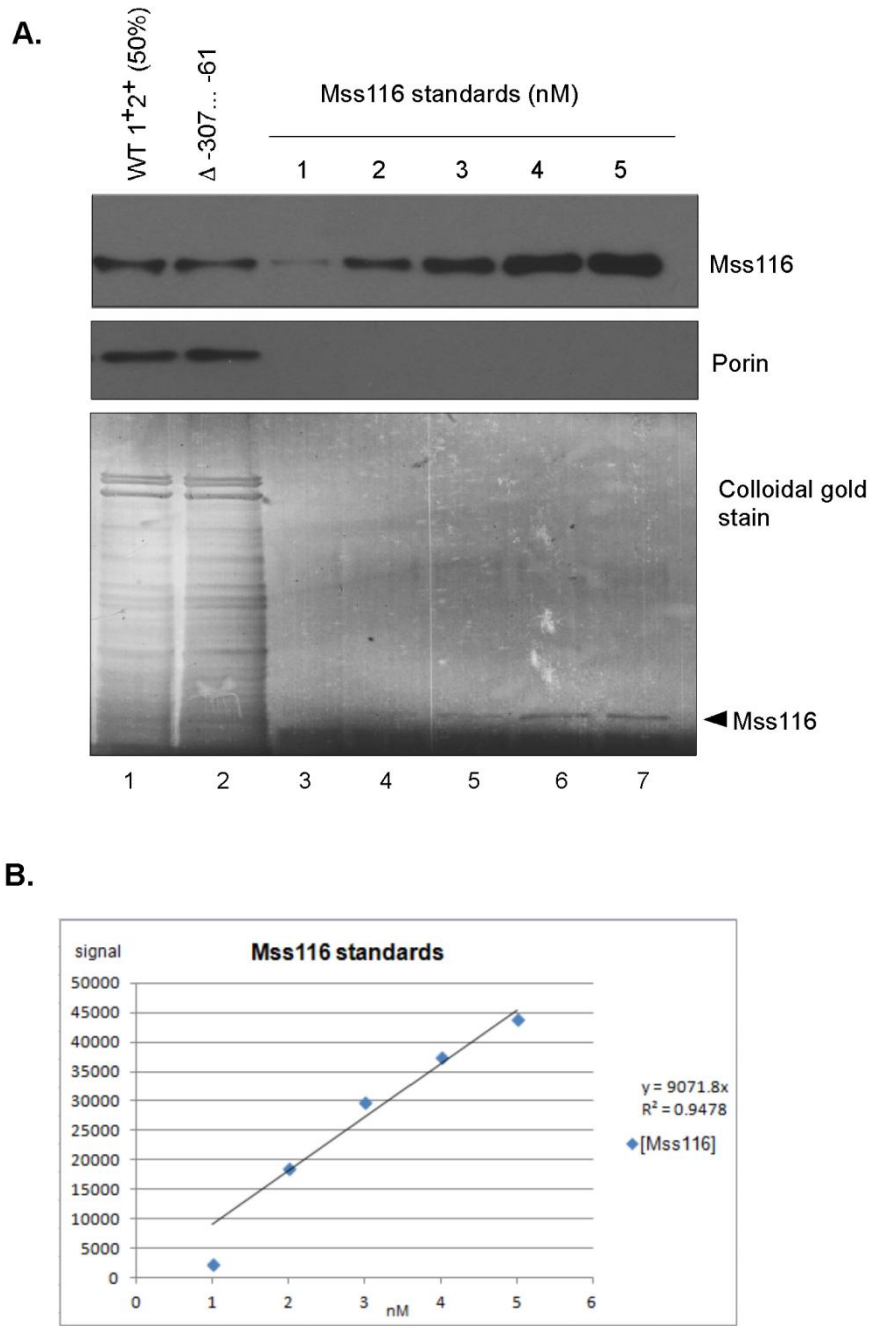

Figure 7.12: Quantification of Western blots to estimate levels of Mss116 expression in strains with wild-type and mutant promoters.

Figure 7.12(continued): Quantification of Western blots to estimate levels of Mss116 expression in strains with wild-type and mutant promoters.

(A) Western blot. Wild-type (WT) and mutant promoter mutant Δ -307/-61 strains were run alongside known concentrations (nM) of purified Mss116 in a 0.1% SDS/4–12% polyacrylamide gradient gel and transferred to a Sequi-Blot™ PVDF membrane (Bio-Rad). The membrane was cut along the 50 kDa marker, and the upper portion of the membrane was probed with anti-Mss116 antibody and the lower portion with anti-porin antibody for use as loading control. After imaging, the upper blot was stripped of antibodies and stained with Colloidal Gold Stain (Bio-Rad) to assess loading. The location of the Mss116 band is indicated to the right. (B) Linear regression of Western blot in (A) used in determining the formula for calculating the concentrations of the tested proteins. Image acquisition was with a FluorChemHD2 camera (Cell Biosciences) and densitometry was performed with GelQuant.NET (biochemlabsolutions.com).

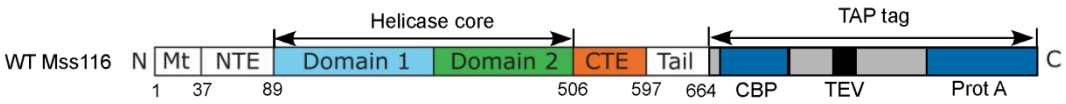

Figure 7.13: TAP-tagged Mss116 construct.

Schematic of wild-type Mss116 protein with a C-terminal in-frame TAP tag expressed in CEN plasmid pRS416. Features of Mss116 are as described in Fig. 7.6. The Tandem Affinity Purification (TAP) tag consists of two affinity modules, Protein A and Calmodulin Binding Protein (CBP) separated by a Tobacco Etch Virus (TEV) protease-cleavable sequence (Puig et al. 2001).

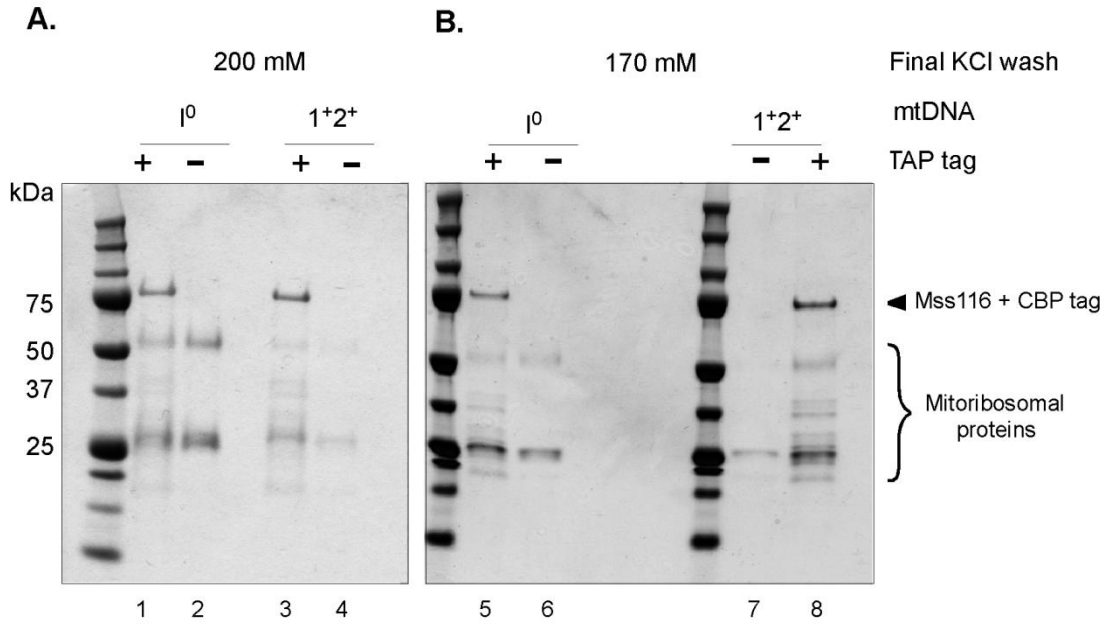

Figure 7.14: SDS polyacrylamide gel showing proteins associated with TAP-tagged and untagged Mss116 in strains 161-U7*mss116*Δ/1^+2^+ and 161-U7 *mss116*Δ/I° using a standard 200 mM KCl final salt wash.

(A). Strains used were 161-U7*mss116*Δ/1^+2^+ (1^+2^+) and 161-U7 *mss116*Δ/I° (I^0) expressing TAP-tagged (+) or untagged (-) Mss116 from CEN plasmid vector pRS416. Strains were cultured in 1 l of HC/Ura^- media with 2% raffinose at 30°C to $O.D._{600}$ = 3. Isolated mitochondria were subjected to the TAP protocol as described in Methods using the standard final bead wash of 200 mM KCl. Beads were boiled for 2 min in loading dye to release bound proteins. Half of the sample was separated in a 4-12% polyacrylamide gel and stained with Coomassie Brilliant Blue. (B) Strains wee cultured, mitochondria isolated and subjected to the TAP protocol as in A except for using a final bead wash of 170 mM KCl. Tagged Mss116 and other proteins are identified to the right.

			Normalized Spectrum count				
			TAP-tagged		Untagged		
Protein	**UniProt Accession #**	**MW (kDa)**	**I^0**	**1^+2^+**	**I^0**	**1^+2^+**	**1^+2^+ fold change over I^0**
ATP-dependent RNA helicase DED1 GN=DED1	DED1	66	2	10	0	0	5
54S ribosomal protein L1, mitochondrial GN=MRPL1	RM01	31	2	9	0	0	4.5
54S ribosomal protein RML2, mitochondrial GN=RML2	RML2	44	3	7	0	0	2.3
54S ribosomal protein L3, mitochondrial GN=MRPL3	RM03	44	7	14	0	0	2
54S ribosomal protein L15, mitochondrial GN=MRPL15	RM15	28	0	2	0	0	2
54S ribosomal protein YmL6, mitochondrial GN=YML6	RL4P	32	7	13	0	0	1.86
54S ribosomal protein L11, mitochondrial GN=MRPL11	RM11	29	6	7	0	0	1.17
54S ribosomal protein L8, mitochondrial GN=MRPL8	RM08	27	2	2	0	0	1
ATP-dependent RNA helicase MSS116, mitochondrial GN=MSS116	**MS116**	76	132	120	0	0	0.91
54S ribosomal protein L40, mitochondrial GN=MRPL40	RM40	34	11	9	0	0	0.82
54S ribosomal protein L35, mitochondrial GN=MRPL35	RM35	43	4	3	0	0	0.75
54S ribosomal protein L41, mitochondrial GN=MRP20	RM41	31	4	2	0	0	0.5
COB pre-mRNA-processing protein 2, splicing factor GN=CBP2	**CBP2**	74	4	1	0	0	0.25
54S ribosomal protein L4, mitochondrial GN=MRPL4	RM04	37	12	2	0	0	0.17
54S ribosomal protein L22, mitochondrial GN=MRPL22	RM22	35	5	0	0	0	0
54S ribosomal protein L9, mitochondrial GN=MRPL9	RM09	30	3	0	0	0	0

Table 7.1: Proteins associated with TAP-tagged Mss116 in strains 161-U7mss116Δ/1^+2^+ and 161-U7 *mss116Δ*/I° using final bead wash of 200 mM KCl.

Table 7.1(continued): Proteins associated with TAP-tagged Mss116 in strains 161-U7 *mss116Δ*/$1^{+}2^{+}$ and 161-U7 *mss116Δ*/I° using final bead wash of 200 mM KCl.

Strains are as in 7.14A. Samples were run approximately 1 cm in a 4-12% polyacrylamide gel and stained with Coomassie Brilliant Blue. The single band for each sample was excised and sent to the University of Texas at Austin Protein Facility where it was processed and subjected to mass spectroscopic analysis. (Details in Methods). Proteins were identified by comparison to the UniProt database for *S. cerevisiae*. Spectral counts for each protein were normalized to the count for the total sample. Untagged values were subtracted from the TAP-tagged value to obtain a background-corrected value. The ratio of corrected $1^{+}2^{+}$ to I^{0} values was calculated to estimate enrichment in the intron-containing strain over the intronless strain ($1^{+}2^{+}$ fold change over I^{0}). Proteins are listed in decreasing order of the fold change. Mss116 and known splicing factor Cbp2 are in bold. Non-ribosomal proteins are highlighted in yellow. The UniProt Accession identification number (UniProt Accession #) and the molecular weight in kDa (MW) are indicated for each protein.

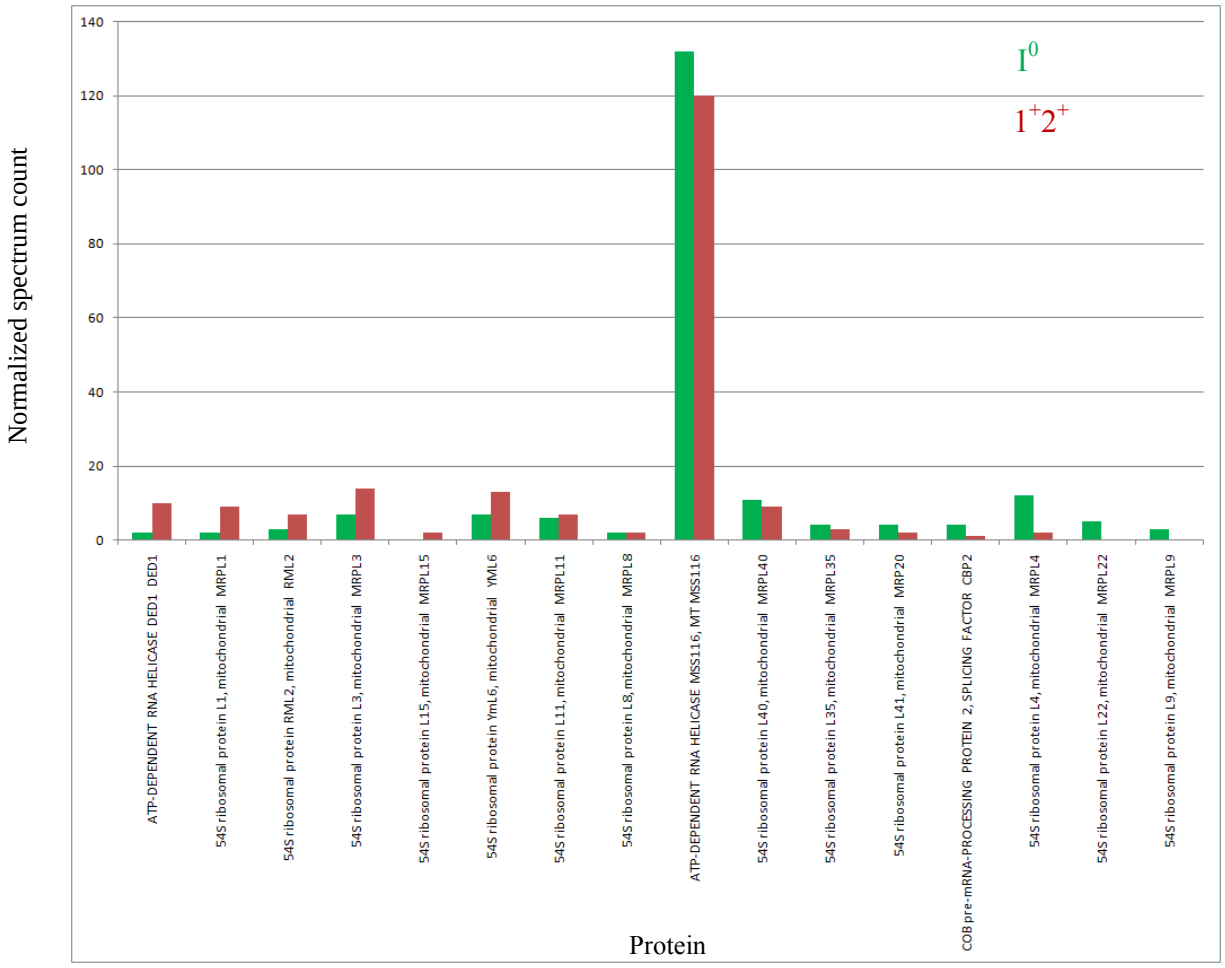

Figure 7.15: Proteins associated with Mss116 in strains 161-U7*mss116Δ*/1+2+ and 161-U7 *mss116Δ*/I° using final bead wash of 200 mM KCl.

Graphical representation of the data in Table 7.1. The height of the bars relative to each other represents the fold change of the corrected, normalized spectral count of the $1^{+}2^{+}$ strain (red) over the I^{0} strain (green). The proteins are listed in order of decreasing $1^{+}2^{+}$ to I^{0} fold change. Non-ribosomal proteins are labeled in all capital letters.

			Normalized Spectrum count				
			TAP-tagged		Untagged		
Protein	**UniProt Accession #**	**MW (kDa)**	**I^0 TAP**	**1^+2^+ TAP**	**I^0**	**1^+2^+**	**1^+2^+ fold change over I^0**
Uncharacterized protein YER077C GN=YER077C	YEQ7	80	1	16	0	0	16
37S ribosomal protein NAM9, mitochondrial GN=NAM9	NAM9	56	1	13	0	0	13
54S ribosomal protein L8, mitochondrial GN=MRPL8	RM08	27	0	12	0	0	12
Mitochondrial genome maintenance protein MGM101 GN=MGM101	MG101	30	1	8	0	0	8
rRNA methyltransferase, mitochondrial GN=MRM1	MRM1	46	2	12	0	0	6
Altered inheritance of mitochondria protein 23, mitochondrial GN=AIM23	AIM23	41	0	6	0	0	6
40S ribosomal protein S9-B GN=RPS9B	RS9B	22	1	5	0	0	5
40S ribosomal protein S24-A GN=RPS24A	RS24A	15	0	5	0	0	5
Ribosomal protein VAR1, mitochondrial GN=VAR1	RMAR	47	2	9	0	0	4.5
COB pre-mRNA processing protein 2, splicing factor GN=CBP2	**CBP2**	74	0	4	0	0	4
Methyltransferase OMS1, mitochondrial GN=OMS1	OMS1	56	8	23	2	0	3.83
37S ribosomal protein PET123, mitochondrial GN=PET123	RTPT	36	3	11	0	0	3.67
37S ribosomal protein S23, mitochondrial GN=RSM23	RT23	51	8	26	0	0	3.25
37S ribosomal protein S17, mitochondrial GN=MRPS17	RT17	28	4	12	0	0	3
37S ribosomal protein S5, mitochondrial GN=MRPS5	RT05	35	3	9	0	0	3
54S ribosomal protein L16, mitochondrial GN=MRPL16	RM16	27	2	6	0	0	3
37S ribosomal protein S16, mitochondrial GN=MRPS16	RT16	14	3	8	0	0	2.67
37S ribosomal protein S9, mitochondrial GN=MRPS9	RT09	32	2	5	0	0	2.5
54S ribosomal protein L35, mitochondrial GN=MRPL35	RM35	43	18	38	0	0	2.1
54S ribosomal protein L49, mitochondrial GN=MRPL49	RN49	18	5	10	0	0	2
37S ribosomal protein MRP1, mitochondrial GN=MRP1	RT01	37	5	10	0	0	2
37S ribosomal protein S24, mitochondrial GN=RSM24	RT24	37	4	8	0	0	2
54S ribosomal protein MRP49, mitochondrial GN=MRP49	RM49	16	2	4	0	0	2
54S ribosomal protein L9, mitochondrial GN=MRPL9	RM09	30	14	27	0	0	1.93
60S ribosomal protein L4-A GN=RPL4A	RL4A	39	6	11	0	0	1.83
54S ribosomal protein L36, mitochondrial GN=MRPL36	RM36	20	4	7	0	0	1.75
60S ribosomal protein L8-B GN=RPL8B	RL8B	28	4	7	0	0	1.75
37S ribosomal protein S35, mitochondrial GN=MRPS35	RT35	40	5	8	0	0	1.6

Table 7.2: Proteins associated with TAP-tagged Mss116 in strains 161-U7*mss116*Δ/1^+2^+ and 161-U7 *mss116*Δ/I° using final bead wash of 170 mM KCl.

Table 7.2 (continued)

Protein	UniProt Accession #	MW (kDa)	I^0 TAP	1^+2^+ TAP	I^0	1^+2^+	1^+2^+ fold change over I^0
ATP-dependent RNA helicase MSS116, mitochondrial GN=MSS116	**MS116**	76	19	30	0	0	1.58
Biotin synthase, mitochondrial GN=BIO2	BIOB	42	5	6	1	0	1.5
37S ribosomal protein RSM28, mitochondrial GN=RSM28	RSM28	41	8	12	0	0	1.5
54S ribosomal protein L23, mitochondrial GN=MRPL23	RM23	18	8	12	0	0	1.5
54S ribosomal protein L7, mitochondrial GN=MRPL7	RM07	33	6	9	0	0	1.5
40S ribosomal protein S4-A GN=RPS4A	RS4A	29	2	3	0	0	1.5
54S ribosomal protein L2, mitochondrial GN=MRP7	RM02	43	19	28	0	0	1.47
54S ribosomal protein L41, mitochondrial GN=MRP20	RM41	31	13	19	0	0	1.46
54S ribosomal protein L24, mitochondrial GN=MRPL24	RM24	30	20	29	0	0	1.45
54S ribosomal protein L3, mitochondrial GN=MRPL3	RM03	44	42	59	0	0	1.4
54S ribosomal protein L25, mitochondrial GN=MRPL25	RM25	19	8	11	0	0	1.38
54S ribosomal protein L13, mitochondrial GN=MRPL13	RM13	30	14	19	0	0	1.36
54S ribosomal protein L20, mitochondrial GN=MRPL20	RM20	22	15	20	0	0	1.33
54S ribosomal protein L28, mitochondrial GN=MRPL28	RM28	17	12	16	0	0	1.33
54S ribosomal protein L1, mitochondrial GN=MRPL1	RM01	31	22	29	0	0	1.32
54S ribosomal protein L22, mitochondrial GN=MRPL22	RM22	35	24	32	0	0	1.3
54S ribosomal protein YmL6, mitochondrial GN=YML6	RL4P	32	20	26	0	0	1.3
37S ribosomal protein MRP51, mitochondrial GN=MRP51	RT51	39	7	9	0	0	1.29
54S ribosomal protein L33, mitochondrial GN=MRPL33	RM33	10	7	9	0	0	1.29
40S ribosomal protein S8-B GN=RPS8B	RS8B	22	7	9	0	0	1.29
54S ribosomal protein L40, mitochondrial GN=MRPL40	RM40	34	26	32	1	0	1.28
54S ribosomal protein L17, mitochondrial GN=MRPL17	RM17	32	13	15	0	0	1.15
54S ribosomal protein RML2, mitochondrial GN=RML2	RML2	44	21	23	0	0	1.09
54S ribosomal protein L4, mitochondrial GN=MRPL4	RM04	37	22	23	0	0	1.05
54S ribosomal protein IMG2, mitochondrial GN=IMG2	IMG2	16	9	9	0	0	1
54S ribosomal protein L15, mitochondrial GN=MRPL15	RM15	28	9	9	0	0	1
54S ribosomal protein L27, mitochondrial GN=MRPL27	RM27	16	7	7	0	0	1
37S ribosomal protein S7, mitochondrial GN=RSM7	RT07	28	6	6	0	0	1
37S ribosomal protein S12, mitochondrial GN=MRPS12	RT12	17	4	4	0	0	1
37S ribosomal protein MRP4, mitochondrial GN=MRP4	RT04	44	4	4	0	0	1
40S ribosomal protein S6-A GN=RPS6A	RS6A	27	3	3	0	0	1
54S ribosomal protein L51, mitochondrial GN=MRPL51	RM51	16	13	12	0	0	0.92
54S ribosomal protein IMG1, mitochondrial GN=IMG1	IMG1	19	16	14	0	0	0.88

Protein	**UniProt Accession #**	**MW (kDa)**	**I^0 TAP**	**1^+2^+ TAP**	**I^0**	**1^+2^+**	**1^+2^+ fold change over I^0**
ADP,ATP carrier protein 2 GN=PET9	ADT2	34	9	5	0	0	0.56
54S ribosomal protein L11, mitochondrial GN=MRPL11	RM11	29	5	1	0	0	0.2
Mitochondrial DNA replication protein YHM2 GN=YHM2	YHM2	34	3	0	0	0	0

Table 7.2(continued): Proteins associated with TAP-tagged Mss116 in strains 161-U7*mss116*Δ/1^+2^+ and 161-U7 *mss116*Δ/I° using final bead wash of 170 mM KCl.

Strains are as in 7.14B. Samples were treated and analyzed as in Table 7.1. Proteins are listed in decreasing order of the 1^+2^+ to I^0 fold change. Mss116 and known splicing factor Cbp2 are in bold. Non-ribosomal proteins are highlighted in yellow. The UniProt Accession identification number (UniProt Accession #) and the molecular weight in kDa (MW) are indicated for each protein.

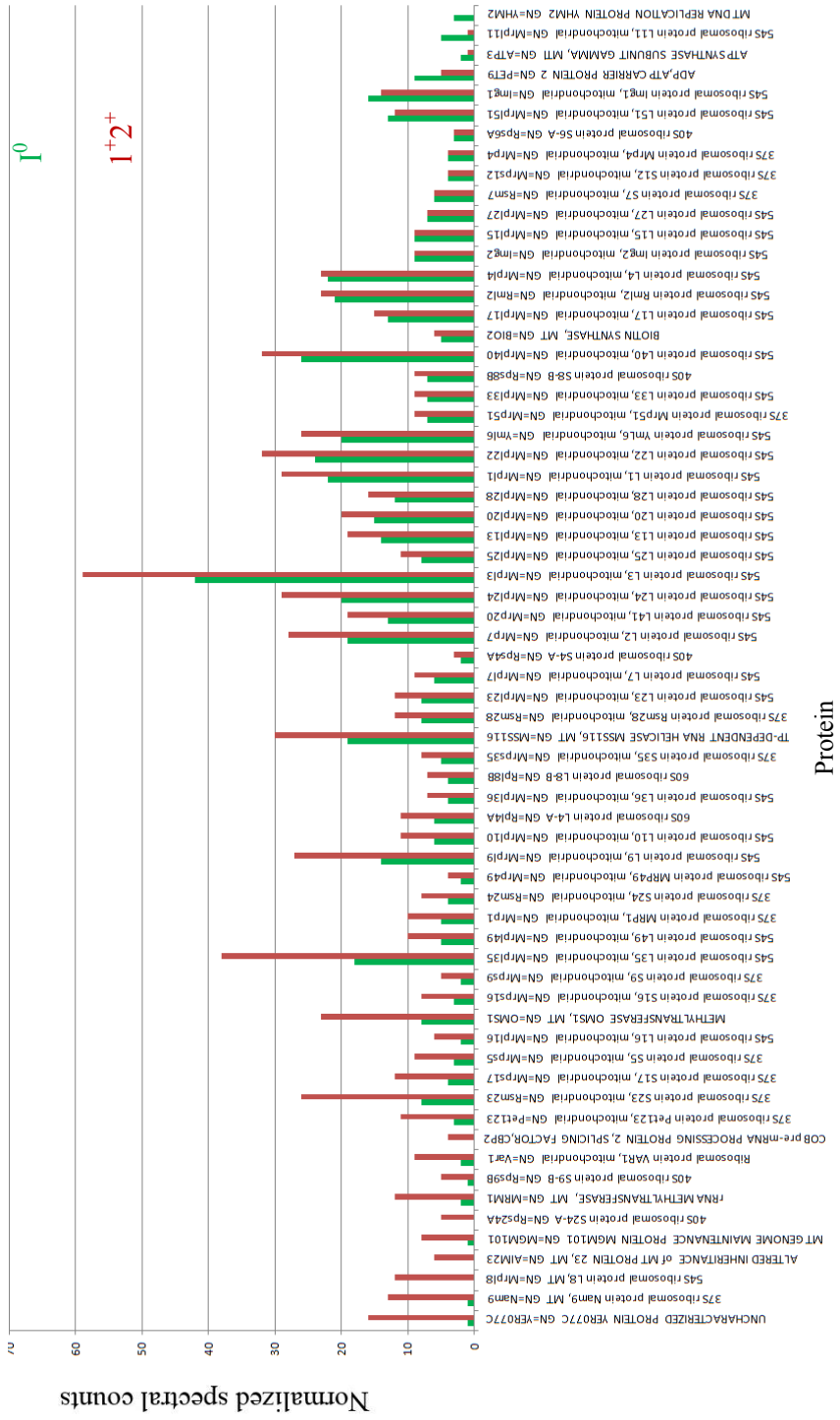

Figure 7.16: Proteins associated with TAP-tagged Mss116 in strains 161-7*mss116*Δ/$1^{+}2^{+}$ and 161-U7 *mss116*Δ/I° using final bead wash of 170 mM KCl.

Figure 7.16 (continued): Proteins associated with TAP-tagged Mss116 in strains 161-U7*mss116*Δ/$1^{+}2^{+}$ and 161-U7 *mss116*Δ/I° using final bead wash of 170 mM KCl.

Graphical representation of the data in Table 7.2. The height of the bars relative to each other represents the fold change of the corrected, normalized spectral count of the $1^{+}2^{+}$ strain (red) over the I^{0} strain (green). The proteins are listed in order of decreasing $1^{+}2^{+}$ to I^{0} fold change with proteins to the left on the X-axis more enriched in the $1^{+}2^{+}$ strain. Non-ribosomal proteins are labeled in all capital letters.

Protein name	MW (kDa)	200 mM KCl	170 mM KCl	Huang, 2004
Uncharacterized protein YER077C GN=YER077C	80		Y	
ATP-dependent RNA helicase MSS116, mitochondrial GN=MSS116	76	Y	Y	Y
COB pre-mRNA-processing protein 2, splicing factor GN=CBP2	74	Y	Y	
ATP-dependent RNA helicase DED1 GN=DED1	66	Y		
tRNA (guanine(26)-N(2))-dimethyltransferase, mitochondrial GN=TRM1	64		Y	
Methyltransferase OMS1, mitochondrial GN=OMS1	56		Y	
37S ribosomal protein NAM9, mitochondrial GN=NAM9	56		Y	
37S ribosomal protein S23, mitochondrial GN=RSM23	51		Y	Y
Ribosomal protein VAR1, mitochondrial GN=VAR1	47		Y	
rRNA methyltransferase, mitochondrial GN=MRM1	46		Y	
54S ribosomal protein L3, mitochondrial GN=MRPL3 , tunnel exit	44	Y	Y	Y
54S ribosomal protein RML2, mitochondrial GN=RML2	44	Y	Y	
37S ribosomal protein MRP4, mitochondrial GN=MRP4	44		Y	Y
54S ribosomal protein L35, mitochondrial GN=MRPL35	43	Y	Y	
54S ribosomal protein L2, mitochondrial GN=MRP7	43		Y	
Biotin synthase, mitochondrial GN=BIO2	42		Y	
37S ribosomal protein RSM28, mitochondrial GN=RSM28	41		Y	
Altered inheritance of mitochondria protein 23, mitochondrial GN=AIM23	41		Y	
37S ribosomal protein S35, mitochondrial GN=MRPS35	40		Y	
37S ribosomal protein MRP51, mitochondrial GN=MRP51	39		Y	Y
60S ribosomal protein L4-A GN=RPL4A	39		Y	
54S ribosomal protein L4, mitochondrial GN=MRPL4 , tunnel exit	37	Y	Y	Y
37S ribosomal protein MRP1, mitochondrial GN=MRP1	37		Y	
37S ribosomal protein S24, mitochondrial GN=RSM24	37		Y	
54S ribosomal protein L10, mitochondrial GN=MRPL10	36		Y	
37S ribosomal protein PET123, mitochondrial GN=PET123	36		Y	
54S ribosomal protein L22, mitochondrial GN=MRPL22 , tunnel exit	35	Y	Y	Y
37S ribosomal protein S5, mitochondrial GN=MRPS5	35		Y	
54S ribosomal protein L40, mitochondrial GN=MRPL40 , tunnel exit	34	Y	Y	Y
ADP,ATP carrier protein 2 GN=PET9	34		Y	Y
ATP synthase subunit gamma, mitochondrial GN=ATP3	34		Y	
Mitochondrial DNA replication protein YHM2 GN=YHM2	34		Y	
54S ribosomal protein L7, mitochondrial GN=MRPL7	33		Y	
37S ribosomal protein S28, mitochondrial GN= MRPS28	33			Y
54S ribosomal protein YmL6, mitochondrial GN=YML6	32	Y	Y	Y
54S ribosomal protein L17, mitochondrial GN=MRPL17	32		Y	
37S ribosomal protein S9, mitochondrial GN=MRPS9	32		Y	Y
54S ribosomal protein L41, mitochondrial GN=MRP20, tunnel exit	31	Y	Y	
54S ribosomal protein L1, mitochondrial GN=MRPL1	31	Y	Y	
37 S ribosomal protein Rsm25, mitochondrial GN=RSM25	31			Y
54S ribosomal protein L24, mitochondrial GN=MRPL24	30		Y	
54S ribosomal protein L9, mitochondrial GN=MRPL9	30	Y	Y	
54S ribosomal protein L13, mitochondrial GN=MRPL13, tunnel exit	30		Y	Y
Mitochondrial genome maintenance protein MGM101 GN=MGM101	30		Y	
37S ribosomal protein Rsm26, mitochondrial GN=RSM26	30			Y
40S ribosomal protein S4-A GN=RPS4A	29		Y	
54S ribosomal protein L11, mitochondrial GN=MRPL11	29	Y	Y	
54S ribosomal protein L15, mitochondrial GN=MRPL15	28	Y	Y	Y

Table 7.3: Compilation of those proteins associated with Mss116 in 3 different experiments.

Protein name	MW (kDa)	200 mM	170 mM	Huang, 2004
60S ribosomal protein L8-B GN=RPL8B	28		Y	
37S ribosomal protein S7, mitochondrial GN=RSM7	28		Y	
37S ribosomal protein S17, mitochondrial GN=MRPS17	28		Y	
54S ribosomal protein L16, mitochondrial GN=MRPL16	27		Y	
54S ribosomal protein L8, mitochondrial GN=MRPL8	27	Y	Y	
40S ribosomal protein S6-A GN=RPS6A	27		Y	
54S ribosomal protein L20, mitochondrial GN=MRPL20	22		Y	Y
40S ribosomal protein S8-B GN=RPS8B	22		Y	
40S ribosomal protein S9-B GN=RPS9B	22		Y	
54S ribosomal protein L36, mitochondrial GN=MRPL36	20		Y	
54S ribosomal protein IMG1, mitochondrial GN=IMG1	19		Y	Y
54S ribosomal protein L25, mitochondrial GN=MRPL25	19		Y	
54S ribosomal protein L49, mitochondrial GN=MRPL49	18		Y	
54S ribosomal protein L23, mitochondrial GN=MRPL23	18		Y	
54S ribosomal protein L28, mitochondrial GN=MRPL28	17		Y	
37S ribosomal protein S12, mitochondrial GN=MRPS12	17		Y	
54S ribosomal protein IMG2, mitochondrial GN=IMG2	16		Y	
54S ribosomal protein L51, mitochondrial GN=MRPL51	16		Y	Y
54S ribosomal protein L27, mitochondrial GN=MRPL27, tunnel exit	16		Y	
54S ribosomal protein MRP49, mitochondrial GN=MRP49	16		Y	
40S ribosomal protein S24-A GN=RPS24A	15		Y	
37S ribosomal protein S16, mitochondrial GN=MRPS16	14		Y	
54S ribosomal protein L33, mitochondrial GN=MRPL33	10		Y	

Table 7.3(continued): Compilation of those proteins associated with Mss116 in 3 different experiments

Proteins identified as being associated with TAP-tagged Mss116 from Tables 7.1 (200 mM) and 7.2 (170 mM) alongside results previously reported (Huang 2004). Proteins are listed in descending order of their molecular weights in kDa (MW). Mss116 and known splicing factor Cbp2 are in bold.

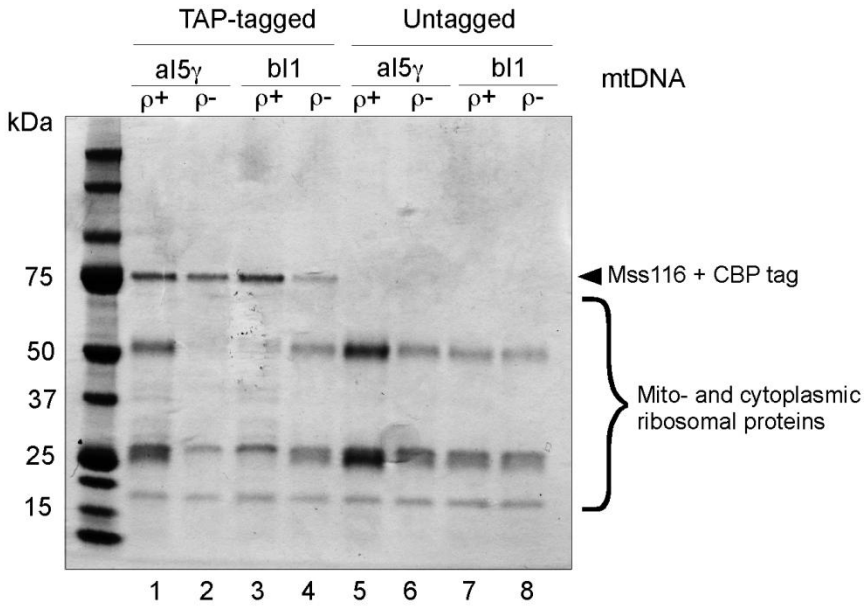

Figure 7.17: SDS polyacrylamide gel showing proteins associated with TAP-tagged and untagged Mss116 in ρ^+ and ρ^- strains of 161-U7*mss116Δ*/aI5γ and 161-U7*mss116Δ*/bI1.

The ρ^+ and ρ^- strains of 161-U7*mss116Δ*/aI5γ and 161-U7*mss116Δ*/bI1 expressing TAP-tagged and untagged Mss116 from CEN plasmid vector pRS416 were cultured as in Fig. 7.14. Mitochondria were isolated and subjected to the TAP protocol as in 7.14A. Mss116 and other proteins are identified to the right.

			Normalized Spectrum count **aI5γ**				
			TAP-tagged		Untagged		
Protein	**UniProt Accession #**	**MW (kDa)**	**aI5γ ρ^+**	**aI5γ ρ^-**	**aI5γ ρ^+**	**aI5γ ρ^-**	**ρ^+ fold change over ρ^-**
54S ribosomal protein L3, mitochondrial GN=MRPL3	RM03	44	65	0	0	0	65
54S ribosomal protein L10, mitochondrial GN=MRPL10	RM10	36	44	0	0	0	44
54S ribosomal protein L40, mitochondrial GN=MRPL40	RM40	34	36	1	0	0	36
54S ribosomal protein RML2, mitochondrial GN=RML2	RML2	44	35	0	0	0	35
54S ribosomal protein IMG1, mitochondrial GN=IMG1	IMG1	19	33	0	0	0	33
54S ribosomal protein YmL6, mitochondrial GN=YML6	RL4P	32	31	0	0	0	31
54S ribosomal protein L24, mitochondrial GN=MRPL24	RM24	30	28	0	0	0	28
54S ribosomal protein L13, mitochondrial GN=MRPL13	RM13	30	27	0	0	0	27
54S ribosomal protein L4, mitochondrial GN=MRPL4	RM04	37	26	0	0	0	26
54S ribosomal protein L41, mitochondrial GN=MRP20	RM41	31	23	0	0	0	23
54S ribosomal protein L8, mitochondrial GN=MRPL8	RM08	27	22	0	0	0	22
54S ribosomal protein L23, mitochondrial GN=MRPL23	RM23	18	21	0	0	0	21
54S ribosomal protein L49, mitochondrial GN=MRPL49	RN49	18	20	0	0	0	20
54S ribosomal protein L20, mitochondrial GN=MRPL20	RM20	22	19	0	0	0	19
54S ribosomal protein L31, mitochondrial GN=MRPL31	RM31	16	16	0	0	0	16
54S ribosomal protein L51, mitochondrial GN=MRPL51	RM51	16	16	0	0	0	16
54S ribosomal protein L9, mitochondrial GN=MRPL9	RM09	30	15	0	0	0	15
54S ribosomal protein L27, mitochondrial GN=MRPL27	RM27	16	15	0	1	0	15
54S ribosomal protein L15, mitochondrial GN=MRPL15	RM15	28	14	0	0	0	14
54S ribosomal protein L33, mitochondrial GN=MRPL33	RM33	10	12	0	0	0	12
Mitochondrial escape protein 2 GN=YME2	YME2	97	10	1	0	0	10
54S ribosomal protein L25, mitochondrial GN=MRPL25	RM25	19	14	2	0	0	7
54S ribosomal protein L1, mitochondrial GN=MRPL1	RM01	31	27	4	0	0	6.75
54S ribosomal protein L22, mitochondrial GN=MRPL22	RM22	35	20	3	0	0	6.67
37S ribosomal protein S23, mitochondrial GN=RSM23	RT23	51	6	0	1	0	6
54S ribosomal protein L16, mitochondrial GN=MRPL16	RM16	27	6	0	0	0	6
Flavohemoprotein GN=YHB1	FHP	45	6	0	0	0	6
54S ribosomal protein MRP49, mitochondrial GN=MRP49	RM49	16	6	1	0	0	6

Table 7.4: Proteins associated with Mss116 in ρ^+ and ρ^- strains of 161-U7*mss116Δ*/aI5γ.

Table 7.4 (continued)

Protein	UniProt Accession #	MW (kDa)	aI5γ ρ^+ TAP	aI5γ ρ^- TAP	aI5γ ρ^+	aI5γ ρ^-	ρ^+ fold change over ρ^-
54S ribosomal protein IMG2, mitochondrial GN=IMG2	IMG2	16	11	2	0	0	5.5
54S ribosomal protein L11, mitochondrial GN=MRPL11	RM11	29	5	0	0	0	5
Mitochondrial DNA replication protein YHM2 GN=YHM2	YHM2	34	5	0	0	0	5
Mitochondrial phosphate carrier protein GN=MIR1	MPCP	33	8	2	0	0	4
Uncharacterized protein YPL168W GN=YPL168W	YP168	49	3	0	0	0	3
37S ribosomal protein S7, mitochondrial GN=RSM7	RT07	28	3	0	0	0	3
37S ribosomal protein MRP51, mitochondrial GN=MRP51	RT51	39	3	0	0	0	3
37S ribosomal protein S24, mitochondrial GN=RSM24	RT24	37	3	0	0	0	3
ADP,ATP carrier protein 2 GN=PET9	ADT2	34	14	4	2	0	3
37S ribosomal protein MRP1, mitochondrial GN=MRP1	RT01	37	8	3	0	0	2.67
54S ribosomal protein L12, mitochondrial GN=MNP1	MNP1	21	5	2	0	0	2.5
External NADH-ubiquinone oxidoreductase 1, mitochondrial GN=NDE1	NDH1	63	4	2	0	0	2
Threonine dehydratase, mitochondrial GN=ILV1	THDH	64	5	3	1	1	2
Protein FMP52, mitochondrial GN=FMP52	FMP52	25	7	3	2	0	1.67
54S ribosomal protein L32, mitochondrial GN=MRPL32	RM32	21	9	6	0	0	1.5
Putative mitochondrial translation system component PET127 GN=PET127	PT127	93	11	8	0	0	1.38
54S ribosomal protein L36, mitochondrial GN=MRPL36	RM36	20	14	11	0	0	1.27
rRNA methyltransferase, mitochondrial GN=MRM1	MRM1	46	5	4	0	0	1.25
Uncharacterized mitochondrial membrane protein FMP10 GN=FMP10	FMP10	28	6	5	0	0	1.2
Protein MLP2 GN=MLP2	MLP2	195	1	0	0	3	1
Mitochondrial inner membrane i-AAA protease supercomplex subunit MGR1 GN=MGR1	MGR1	47	3	3	0	0	1
54S ribosomal protein L2, mitochondrial GN=MRP7	RM02	43	51	54	0	0	0.94
54S ribosomal protein L35, mitochondrial GN=MRPL35	RM35	43	42	49	0	0	0.86
54S ribosomal protein L28, mitochondrial GN=MRPL28	RM28	17	12	14	0	0	0.86
54S ribosomal protein L7, mitochondrial GN=MRPL7	RM07	33	10	13	0	0	0.77
40S ribosomal protein S6-A GN=RPS6A	RS6A	27	3	4	0	0	0.75
54S ribosomal protein L17, mitochondrial GN=MRPL17	RM17	32	19	27	0	0	0.7
Sphingolipid long chain base-responsive protein PIL1 GN=PIL1	PIL1	38	14	20	0	0	0.7
60S ribosomal protein L19-A GN=RPL19A	RL19A	22	4	6	0	0	0.67
Methyltransferase OMS1, mitochondrial GN=OMS1	OMS1	56	26	41	1	0	0.61
Acetolactate synthase catalytic subunit, mitochondrial GN=ILV2	ILVB	75	3	5	0	0	0.6
Phosphatidate phosphatase APP1 GN=APP1	APP1	66	17	32	1	0	0.5

Table 7.4 (continued)

Protein	UniProt Accession #	MW (kDa)	aI5γ ρ^+ TAP	aI5γ ρ^- TAP	aI5γ ρ^+	aI5γ ρ^-	ρ^+ fold change over ρ^-
ATP-dependent RNA helicase MSS116, mitochondrial GN=MSS116	**MS116**	76	438	964	22	2	0.45
40S ribosomal protein S5 GN=RPS5	RS5	25	2	5	0	0	0.4
60S ribosomal protein L18-A GN=RPL18A	RL18A	21	3	8	0	0	0.38
Prohibitin-1 GN=PHB1	PHB1	31	4	12	0	0	0.33
60S ribosomal protein L13-B GN=RPL13B	RL13B	23	4	13	0	0	0.31
60S ribosomal protein L3 GN=RPL3	RL3	44	5	18	0	0	0.28
60S ribosomal protein L20-A GN=RPL20A	RL20A	20	3	13	0	0	0.23
60S ribosomal protein L8-B GN=RPL8B	RL8B	28	3	13	0	0	0.23
Uncharacterized protein YER077C GN=YER077C	YEQ7	80	4	19	0	0	0.21
60S ribosomal protein L27-A GN=RPL27A	RL27A	16	2	10	0	0	0.2
ATPase expression protein 3 GN=AEP3	AEP3	70	1	5	0	0	0.2
ATP-dependent RNA helicase DBP2 GN=DBP2	DBP2	61	2	11	0	0	0.18
60S ribosomal protein L28 GN=RPL28	RL28	17	2	11	0	0	0.18
Cytochrome c1, heme protein, mitochondrial GN=CYT1	CY1	34	2	11	0	0	0.18
Heat shock protein 78, mitochondrial GN=HSP78	HSP78	91	4	17	1	0	0.18
Heat shock protein 60, mitochondrial GN=HSP60	HSP60	61	4	24	0	1	0.17
60S ribosomal protein L16-A GN=RPL16A	RL16A	22	1	6	0	0	0.17
Protein CBP3, mitochondrial GN=CBP3	CBP3	39	4	13	2	0	0.15
COB pre-mRNA-processing protein 2, splicing factor GN=CBP2	**CBP2**	74	6	36	1	1	0.14
60S ribosomal protein L2-A GN=RPL2A	RL2A	27	1	7	0	0	0.14
40S ribosomal protein S13 GN=RPS13	RS13	17	1	7	0	0	0.14
40S ribosomal protein S8-A GN=RPS8A	RS8A	22	1	7	0	0	0.14
60S ribosomal protein L7-A GN=RPL7A	RL7A	28	2	15	0	0	0.13
60S ribosomal protein L4-A GN=RPL4A	RL4A	39	4	31	0	0	0.13
ATP synthase subunit alpha, mitochondrial GN=ATP1	ATPA	59	4	32	0	0	0.13
Splicing factor MNE1 GN=MNE1	**MNE1**	77	1	8	0	0	0.13
60S ribosomal protein L15-A GN=RPL15A	RL15A	24	1	9	0	0	.11
Aconitate hydratase, mitochondrial GN=ACO1	ACON	85	1	9	0	0	0.11
60S ribosomal protein L25 GN=RPL25	RL25	16	1	10	0	0	0.10
40S ribosomal protein S4-A GN=RPS4A	RS4A	29	1	13	0	0	0.08
Heat shock protein SSC1, mitochondrial GN=SSC1	HSP77	71	2	32	0	1	0.06
60S ribosomal protein L21-A GN=RPL21A	RL21A	18	1	16	0	0	0.06
ATP synthase subunit beta, mitochondrial GN=ATP2	ATPB	55	1	26	0	0	0.04
Mitochondrial import inner membrane translocase subunit TIM44 GN=TIM44	TIM44	49	0	4	0	0	0

Table 7.4 (continued)

Protein	**UniProt Accession #**	**MW (kDa)**	**aI5γ ρ^+ TAP**	**aI5γ ρ^- TAP**	**aI5γ ρ^+**	**aI5γ ρ^-**	**ρ^+ fold change over ρ^-**
40S ribosomal protein S3 GN=RPS3	RS3	27	0	4	0	0	0
Cytochrome B pre-mRNA-processing protein 6 GN=CBP6	CBP6	19	0	5	0	0	0
ATP-dependent RNA helicase, splicing factor SUV3, Mt GN=SUV3	**SUV3**	84	0	5	0	0	0
37S ribosomal protein S28, mitochondrial GN=MRPS28	RT28	33	0	5	0	0	0
40S ribosomal protein S0-A GN=RPS0A	RSSA1	28	0	5	0	0	0
Elongation factor Tu, mitochondrial GN=TUF1	EFTU	48	0	6	0	0	0
Potassium-activated aldehyde dehydrogenase, mitochondrial GN=ALD4	ALDH4	57	0	6	0	0	0
60S ribosomal protein L17-A GN=RPL17A	RL17A	21	0	6	0	0	0
60S ribosomal protein L36-B GN=RPL36B	RL36B	11	0	7	0	0	0
Pentatricopeptide repeat-containing protein PET309, mitochondrial GN=PET309	PT309	113	0	7	0	1	0
60S ribosomal protein L12-A GN=RPL12A	RL12A	18	0	7	0	0	0
60S ribosomal protein L33-B GN=RPL33B	RL33B	12	0	7	0	0	0
40S ribosomal protein S11-A GN=RPS11A	RS11A	18	0	7	0	0	0
Altered inheritance of mitochondria protein 36, mitochondrial GN=AIM36	AIM36	29	0	7	0	0	0
40S ribosomal protein S19-A GN=RPS19A	RS19A	16	0	7	0	0	0
40S ribosomal protein S7-B GN=RPS7B	RS7B	22	0	7	0	0	0
40S ribosomal protein S17-A GN=RPS17A	RS17A	16	0	7	0	0	0
Dihydrolipoyllysine-residue acetyltransferase component of pyruvate dehydrogenase complex, mitochondrial GN=LAT1	ODP2	52	0	8	0	0	0
40S ribosomal protein S2 GN=RPS2	RS2	27	0	8	0	0	0
40S ribosomal protein S9-B GN=RPS9B	RS9B	22	0	8	0	0	0
Nucleolar protein 3 GN=NPL3	NOP3	45	0	8	0	0	0
60S ribosomal protein L6-B GN=RPL6B	RL6B	20	0	9	0	1	0
60S ribosomal protein L14-B GN=RPL14B	RL14B	15	0	9	1	0	0
ATP-dependent RNA helicase DED1 GN=DED1	DED1	66	0	9	1	0	0
60S ribosomal protein L1-A GN=RPL1A	RL1A	24	0	9	0	0	0
60S acidic ribosomal protein P0 GN=RPP0	RLA0	34	0	10	0	0	0
37S ribosomal protein S22, mitochondrial GN=RSM22	RT22	72	0	10	0	0	0
40S ribosomal protein S24-A GN=RPS24A	RS24A	15	0	10	0	0	0
Biotin synthase, mitochondrial GN=BIO2	BIOB	42	0	11	0	0	0
60S ribosomal protein L35-A GN=RPL35A	RL35A	14	0	14	0	0	0
Protein RMD9, mitochondrial GN=RMD9	RMD9	75	0	17	1	0	0

Table 7.4 (continued): Proteins associated with Mss116 in ρ^+ and ρ^- strains of 161-U7*mss116Δ*/aI5γ.

Strains are as in Fig. 7.17 (lanes 1, 2, 5 and 6) and were analyzed as in Table 7.1. Untagged values were subtracted from the TAP-tagged value to obtain a background-corrected value for each protein. The ratio of corrected ρ^+ to ρ^- values was calculated to estimate enrichment in wild-type strain over the petite strain (ρ^+ fold change over ρ^-). Proteins are listed in decreasing order of the fold change. Proteins at the bottom of the list are those found only in ρ^-. Non-ribosomal proteins are highlighted in yellow. Mss116 and known splicing factors are in bold. The UniProt Accession identification number (UniProt Accession #) and the molecular weight in kDa (MW) are indicated for each protein.

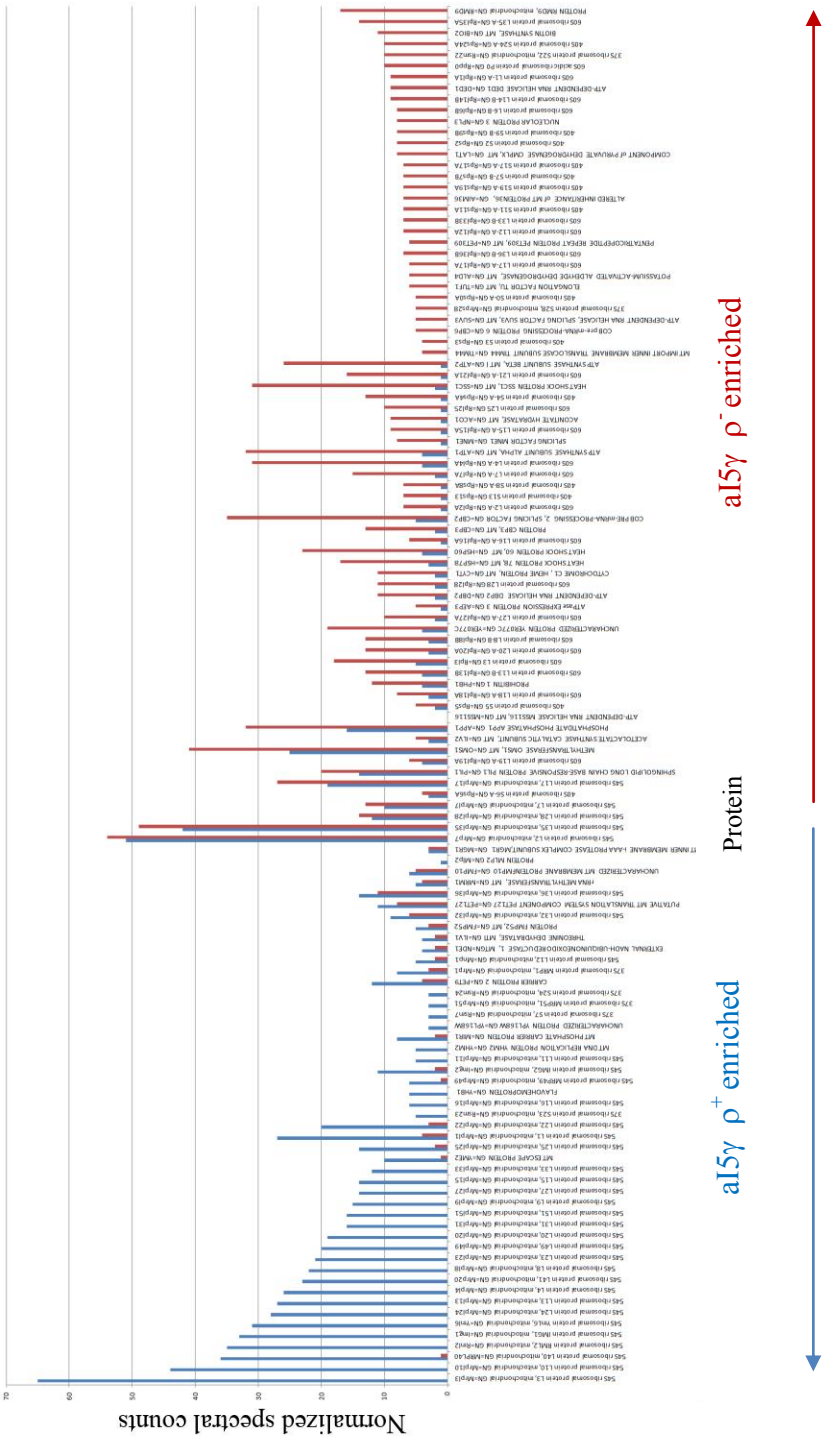

Fig. 7.18 : Proteins associated with Mss116 in ρ^+ and ρ^- strains of 161-U7*mss116Δ*/aI5γ.

Fig. 7.18 (continued): Proteins associated with Mss116 in ρ^+ and ρ^- strains of 161-U7*mss116Δ*/aI5γ.

Graphical analysis of data in Table 7.4. The height of the bars relative to each other represents the fold change of the correct, normalized spectral count of the aI5γ ρ^+ strain (blue) over the aI5γ ρ^- strain (red). The proteins are listed in order of decreasing aI5γ ρ^+ to aI5γ ρ^- fold change with proteins to the left on the X-axis more enriched in the aI5γ ρ^+ strain and those to the right more enriched in the aI5γ ρ^- strain. Each section of the graph is enlarged in subsequent Figures 7.19 and 7.20. Due to the very large values obtained for Mss116, the bars are not included for the protein.

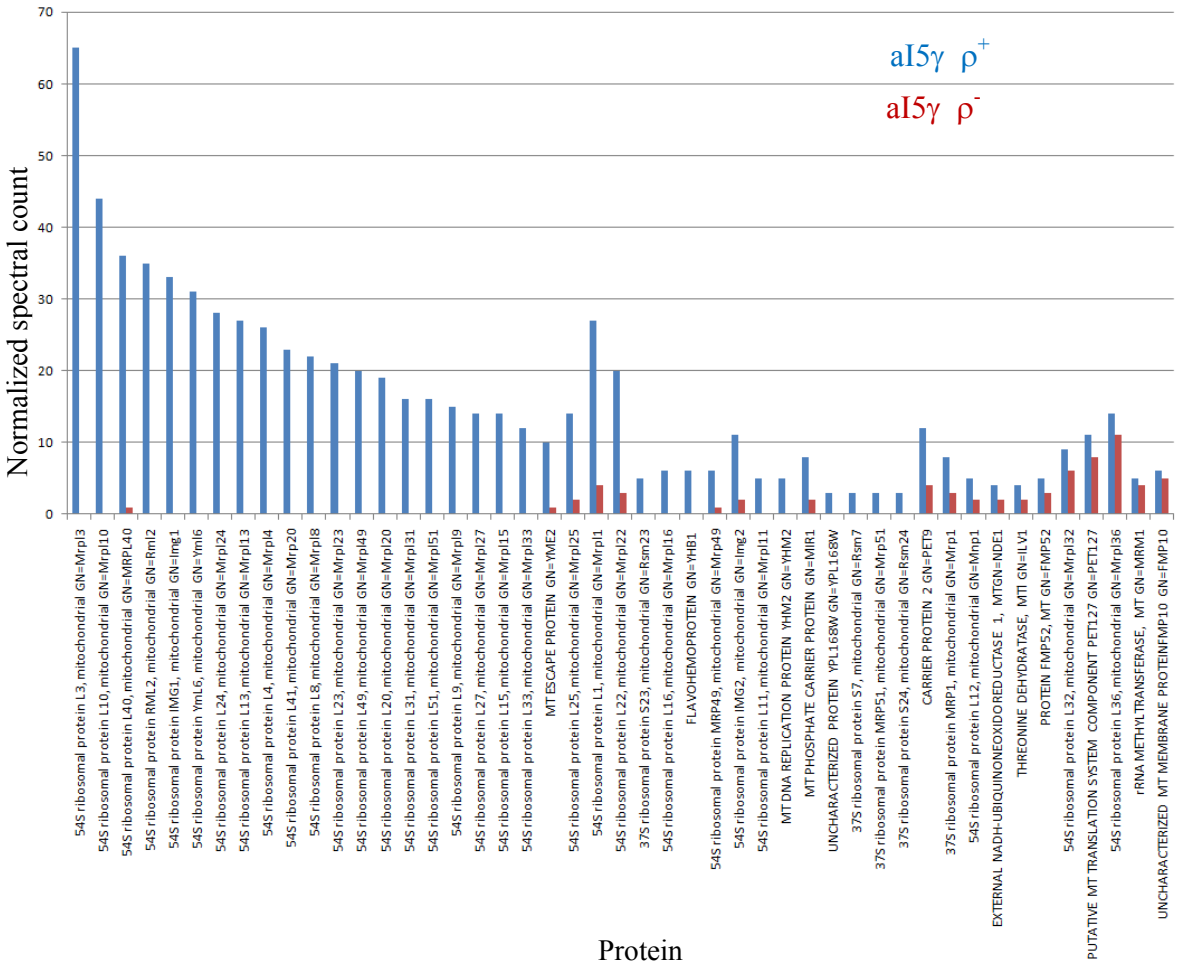

Fig. 7.19: Proteins that were associated with TAP-tagged Mss116 enriched in a 161-U7*mss116Δ*/aI5γ ρ^+ strain

Enlarged view of the ρ^+ enriched portion of the graph in Fig. 7.18. Non-ribosomal proteins are labeled in all capital letters.

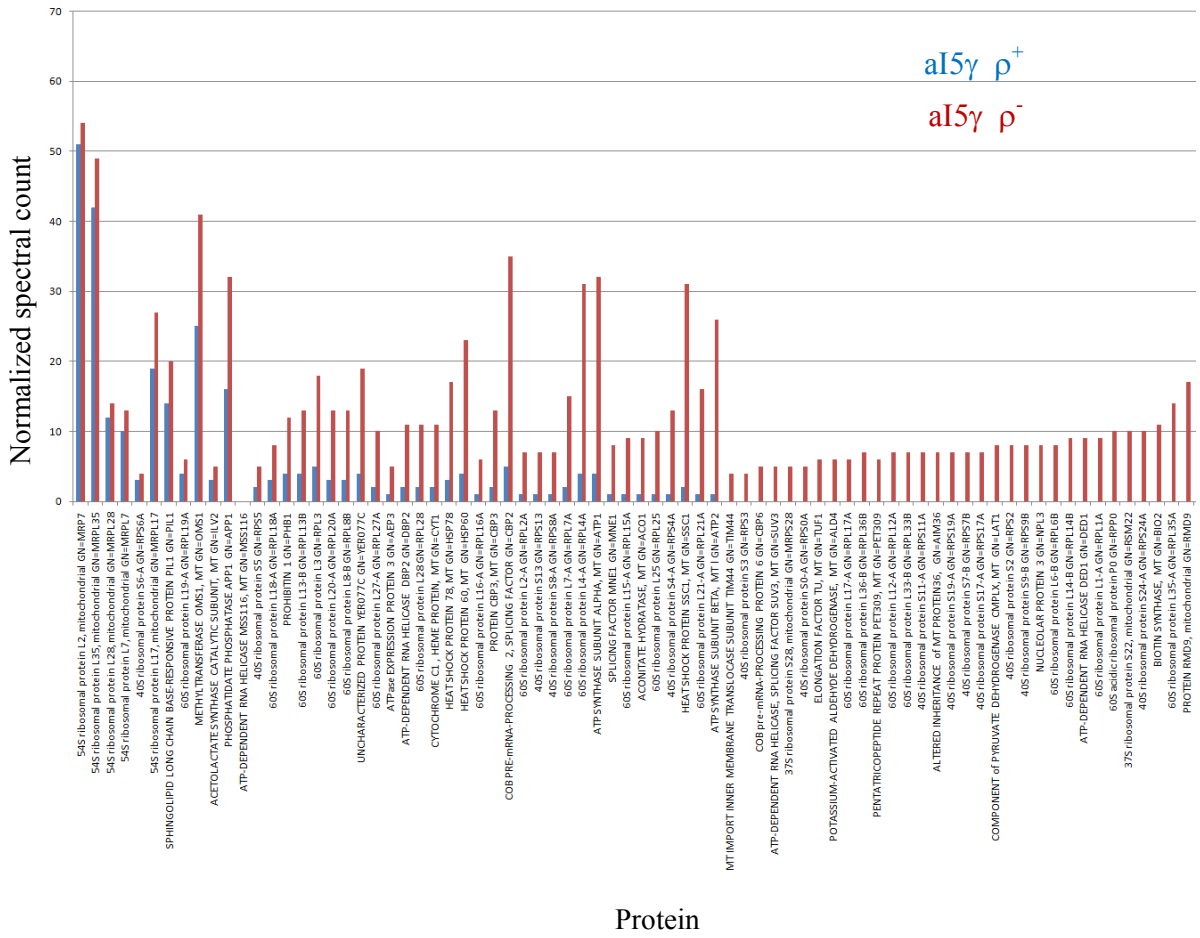

Fig. 7.20: Proteins that were associated with TAP-tagged Mss116 enriched in a 161-U7*mss116Δ*/aI5γ ρ⁻ strain

Enlarged view of the ρ⁻ enriched portion of the graph in Fig. 7.18. Non-ribosomal proteins are labeled in all capital letters.

			Normalized Spectrum count bI1				
			TAP-tagged		Untagged		
Protein	**UniProt Accession #**	**MW (kDa)**	**bI1 ρ^+**	**bI1 ρ^-**	**bI1 ρ^+**	**bI1ρ^-**	**ρ^+ fold change over ρ^-**
54S ribosomal protein L3, mitochondrial GN=MRPL3	RM03	44	61	0	0	0	61
54S ribosomal protein L10, mitochondrial GN=MRPL10	RM10	36	48	0	0	0	48
54S ribosomal protein L24, mitochondrial GN=MRPL24	RM24	30	42	0	0	0	42
54S ribosomal protein L4, mitochondrial GN=MRPL4	RM04	37	38	0	0	0	38
54S ribosomal protein L40, mitochondrial GN=MRPL40	RM40	34	46	0	0	0	34
54S ribosomal protein RML2, mitochondrial GN=RML2	RML2	44	34	0	0	0	34
54S ribosomal protein IMG1, mitochondrial GN=IMG1	IMG1	19	34	0	0	0	34
54S ribosomal protein L8, mitochondrial GN=MRPL8	RM08	27	28	0	1	0	28
54S ribosomal protein YmL6, mitochondrial GN=YML6	RL4P	32	26	0	0	0	26
54S ribosomal protein L13, mitochondrial GN=MRPL13	RM13	30	25	0	0	0	25
54S ribosomal protein L20, mitochondrial GN=MRPL20	RM20	22	24	0	0	1	24
54S ribosomal protein L22, mitochondrial GN=MRPL22	RM22	35	20	0	1	0	20
54S ribosomal protein L9, mitochondrial GN=MRPL9	RM09	30	19	0	1	0	19
54S ribosomal protein L15, mitochondrial GN=MRPL15	RM15	28	19	0	0	0	19
54S ribosomal protein L23, mitochondrial GN=MRPL23	RM23	18	18	0	0	0	18
54S ribosomal protein L49, mitochondrial GN=MRPL49	RN49	18	18	0	0	0	18
Mitochondrial escape protein 2 GN=YME2	YME2	97	16	0	0	0	16
54S ribosomal protein L51, mitochondrial GN=MRPL51	RM51	16	16	0	0	0	16
54S ribosomal protein L25, mitochondrial GN=MRPL25	RM25	19	15	0	0	0	15
54S ribosomal protein L41, mitochondrial GN=MRP20	RM41	31	15	0	0	0	15
54S ribosomal protein L11, mitochondrial GN=MRPL11	RM11	29	15	0	0	0	15
37S ribosomal protein RSM28, mitochondrial GN=RSM28	RSM28	41	14	0	0	0	14
54S ribosomal protein L16, mitochondrial GN=MRPL16	RM16	27	13	0	0	0	13
54S ribosomal protein L31, mitochondrial GN=MRPL31	RM31	16	13	0	0	0	13
54S ribosomal protein L1, mitochondrial GN=MRPL1	RM01	31	25	2	0	0	12.5
54S ribosomal protein IMG2, mitochondrial GN=IMG2	IMG2	16	21	2	0	0	10.5
54S ribosomal protein L33, mitochondrial GN=MRPL33	RM33	10	9	0	0	0	9
54S ribosomal protein L27, mitochondrial GN=MRPL27	RM27	16	8	0	0	1	8
CDP-diacylglycerol--glycerol-3-phosphate 3-phosphatidyltransferase GN=PGS1	PGPS1	59	8	0	0	0	8

Table 7.5: Proteins associated with Mss116 in ρ^+ and ρ^- strains of 161-U7mss116Δ/bI1.

Table 7.5 (continued):

Protein	**UniProt Accession #**	**MW (kDa)**	**bI1 ρ^+ TAP**	**bI1 ρ^- TAP**	**bI1 ρ^+**	**bI1 ρ^-**	**ρ^+ fold change over ρ^-**
54S ribosomal protein MRP49, mitochondrial GN=MRP49	RM49	16	8	0	0	0	8
Uncharacterized protein YPL168W GN=YPL168W	YP168	49	8	0	0	0	8
Mitochondrial phosphate carrier protein GN=MIR1	MPCP	33	10	1	2	0	8
60S ribosomal protein L20-A GN=RPL20A	RL20A	20	8	1	0	0	8
Flavohemoprotein GN=YHB1	FHP	45	6	0	0	1	6
Required for respiratory growth protein 9, mitochondrial GN=RRG9	RRG9	25	6	0	0	0	6
60S ribosomal protein L13-A GN=RPL13A	RL13A	23	6	1	0	0	6
54S ribosomal protein L12, mitochondrial GN=MNP1	MNP1	21	11	2	0	0	5.5
Histone H4 GN=HHF1	H4	11	5	0	1	0	5
Ribosomal protein VAR1, mitochondrial GN=VAR1	RMAR	47	5	0	0	0	5
Mitochondrial homologous recombination protein 1 GN=MHR1	MHR1	27	5	1	0	0	5
60S ribosomal protein L8-B GN=RPL8B	RL8B	28	5	1	0	0	5
54S ribosomal protein L36, mitochondrial GN=MRPL36	RM36	20	11	2	2	0	4.5
Protein FMP52, mitochondrial GN=FMP52	FMP52	25	10	2	1	0	4.5
Uncharacterized protein YIL077C GN=YIL077C	YIH7	37	4	0	0	0	4
Mitochondrial inner membrane i-AAA protease supercomplex subunit MGR1 GN=MGR1	MGR1	47	9	2	1	0	4
60S ribosomal protein L18-A GN=RPL18A	RL18A	21	4	1	0	0	4
rRNA methyltransferase, mitochondrial GN=MRM1	MRM1	46	9	3	0	0	3
External NADH-ubiquinone oxidoreductase 1, mitochondrial GN=NDE1	NDH1	63	6	2	0	0	3
54S ribosomal protein L35, mitochondrial GN=MRPL35	RM35	43	50	19	0	0	2.63
ATP-dependent RNA helicase MSS116, mitochondrial GN=MSS116	**MS116**	76	811	315	8	10	2.63
60S ribosomal protein L19-A GN=RPL19A	RL19A	22	5	2	0	0	2.5
54S ribosomal protein L17, mitochondrial GN=MRPL17	RM17	32	22	10	0	0	2.2
54S ribosomal protein L32, mitochondrial GN=MRPL32	RM32	21	8	5	0	1	2
Sphingolipid long chain base-responsive protein PIL1 GN=PIL1	PIL1	38	22	12	0	0	1.83
Uncharacterized protein YER077C GN=YER077C	YEQ7	80	11	6	0	0	1.83
Phosphatidate phosphatase APP1 GN=APP1	APP1	66	36	20	1	0	1.75
54S ribosomal protein L7, mitochondrial GN=MRPL7	RM07	33	12	7	0	0	1.71
Uncharacterized mitochondrial membrane protein FMP10 GN=FMP10	FMP10	28	5	5	0	2	1.67
54S ribosomal protein L2, mitochondrial GN=MRP7	RM02	43	51	36	0	0	1.41
Methyltransferase OMS1, mitochondrial GN=OMS1	OMS1	56	44	32	0	0	1.38

Table 7.5 (continued):

Protein, general name	**UniProt Accession #**	**MW (kDa)**	**bI1 ρ^+ TAP**	**bI1 ρ^- TAP**	**bI1 ρ^+**	**bI1 ρ^-**	**ρ^+ fold change over ρ^-**
Protein CBP3, mitochondrial GN=CBP3	CBP3	39	9	9	0	2	1.29
54S ribosomal protein L28, mitochondrial GN=MRPL28	RM28	17	15	12	0	0	1.25
Acetolactate synthase catalytic subunit, mitochondrial GN=ILV2	ILVB	75	6	5	1	1	1.25
60S ribosomal protein L7-B GN=RPL7B	RL7B	28	5	6	0	0	0.83
60S ribosomal protein L4-A GN=RPL4A	RL4A	39	15	19	0	0	0.79
Aconitate hydratase, mitochondrial GN=ACO1	ACON	85	3	4	0	0	0.75
Prohibitin-1 GN=PHB1	PHB1	31	9	9	4	2	0.71
37S ribosomal protein S23, mitochondrial GN=RSM23	RT23	51	9	12	1	0	0.67
Heat shock protein 78, mitochondrial GN=HSP78	HSP78	91	6	11	0	1	0.6
37S ribosomal protein S22, mitochondrial GN=RSM22	RT22	72	9	14	1	0	0.57
40S ribosomal protein S5 GN=RPS5	RS5	25	4	7	0	0	0.57
COB pre-mRNA-processing protein 2, splicing factor GN=CBP2	**CBP2**	74	12	15	5	2	0.54
37S ribosomal protein S7, mitochondrial GN=RSM7	RT07	28	8	14	1	0	0.5
37S ribosomal protein MRP1, mitochondrial GN=MRP1	RT01	37	12	25	0	0	0.48
37S ribosomal protein MRP4, mitochondrial GN=MRP4	RT04	44	6	13	0	0	0.46
37S ribosomal protein S25, mitochondrial GN=RSM25	RT25	31	2	6	0	1	0.4
37S ribosomal protein NAM9, mitochondrial GN=NAM9	NAM9	56	4	11	0	0	0.36
Altered inheritance of mitochondria protein 36, mitochondrial GN=AIM36	AIM36	29	2	5	1	2	0.33
37S ribosomal protein MRP51, mitochondrial GN=MRP51	RT51	39	5	15	0	0	0.33
60S ribosomal protein L28 GN=RPL28	RL28	17	3	9	0	0	0.33
37S ribosomal protein S9, mitochondrial GN=MRPS9	RT09	32	3	10	0	0	0.33
Heat shock protein SSC1, mitochondrial GN=SSC1	HSP77	71	17	46	5	2	0.27
40S ribosomal protein S17-A GN=RPS17A	RS17A	16	1	5	0	0	0.2
37S ribosomal protein S8, mitochondrial GN=MRPS8	RT08	17	2	12	0	0	0.17
37S ribosomal protein PET123, mitochondrial GN=PET123	RTPT	36	2	13	0	0	0.15
60S ribosomal protein L21-A GN=RPL21A	RL21A	18	1	7	0	0	0.14
37S ribosomal protein MRP17, mitochondrial GN=MRP17	RT06	15	1	8	0	0	0.13
37S ribosomal protein MRP13, mitochondrial GN=MRP13	RT13	39	1	8	0	0	0.13
ATP synthase subunit beta, mitochondrial GN=ATP2	ATPB	55	5	48	0	0	0.10
ATP synthase subunit alpha, mitochondrial GN=ATP1	ATPA	59	7	53	3	5	0.08
37S ribosomal protein S16, mitochondrial GN=MRPS16	RT16	14	1	15	0	0	0.07

Protein, general name	**UniProt Accession #**	**MW (kDa)**	**bI1 ρ^+ TAP**	**bI1 ρ^- TAP**	**bI1 ρ^+**	**bI1 ρ^-**	**ρ^+ fold change over ρ^-**
37S ribosomal protein S35, mitochondrial GN=MRPS35	RT35	40	1	16	0	1	0.07
Heat shock protein 60, mitochondrial GN=HSP60	HSP60	61	2	28	1	1	0.04
Cytochrome c1, heme protein, mitochondrial GN=CYT1	CY1	34	7	9	7	5	0
Mitochondrial group I intron splicing factor CCM1 GN=CCM1	**CCM1**	101	0	4	0	0	0
40S ribosomal protein S3 GN=RPS3	RS3	27	0	4	0	0	0
Ketol-acid reductoisomerase, mitochondrial GN=ILV5	ILV5	44	0	5	0	0	0
Mitochondrial peculiar membrane protein 1 GN=MPM1	MPM1	28	0	5	0	0	0
Cytochrome b-c1 complex subunit 2, mitochondrial GN=QCR2	QCR2	40	1	6	1	0	0
60S ribosomal protein L35-A GN=RPL35A	RL35A	14	0	6	0	0	0
37S ribosomal protein MRP21, mitochondrial GN=MRP21	RT21	20	0	6	0	0	0
Biotin synthase, mitochondrial GN=BIO2	BIOB	42	1	7	2	0	0
Pyruvate dehydrogenase E1 component subunit beta, mitochondrial GN=PDB1	ODPB	40	0	8	0	0	0
37S ribosomal protein S28, mitochondrial GN=MRPS28	RT28	33	0	26	0	0	0
Inhibitory regulator protein IRA2 GN=IRA2	IRA2	352	0	2	4	1	0
Prohibitin-2 GN=PHB2	PHB2	34	2	4	4	1	0

Table 7.5 (continued): Proteins associated with Mss116 in ρ^+ and ρ^- strains of 161-U7*mss116Δ*/bI1.

Strains are as in Fig. 7.17, lanes 3, 4, 7 and 8 and were analyzed as in Table 7.1. Untagged values were subtracted from the TAP-tagged value to obtain a background-corrected value for each protein. The ratio of corrected bI1ρ^+ to bI1ρ^- values was calculated to estimate enrichment in wild-type strain over the petite strain (ρ^+ fold change over ρ^-). Proteins are listed in decreasing order of the fold change. Proteins at the bottom of the list are those found only in ρ^-. Non-ribosomal proteins are highlighted in yellow. Mss116 and known splicing factors are in bold. The UniProt Accession identification number (UniProt Accession #) and the molecular weight in kDa (MW) are indicated for each protein.

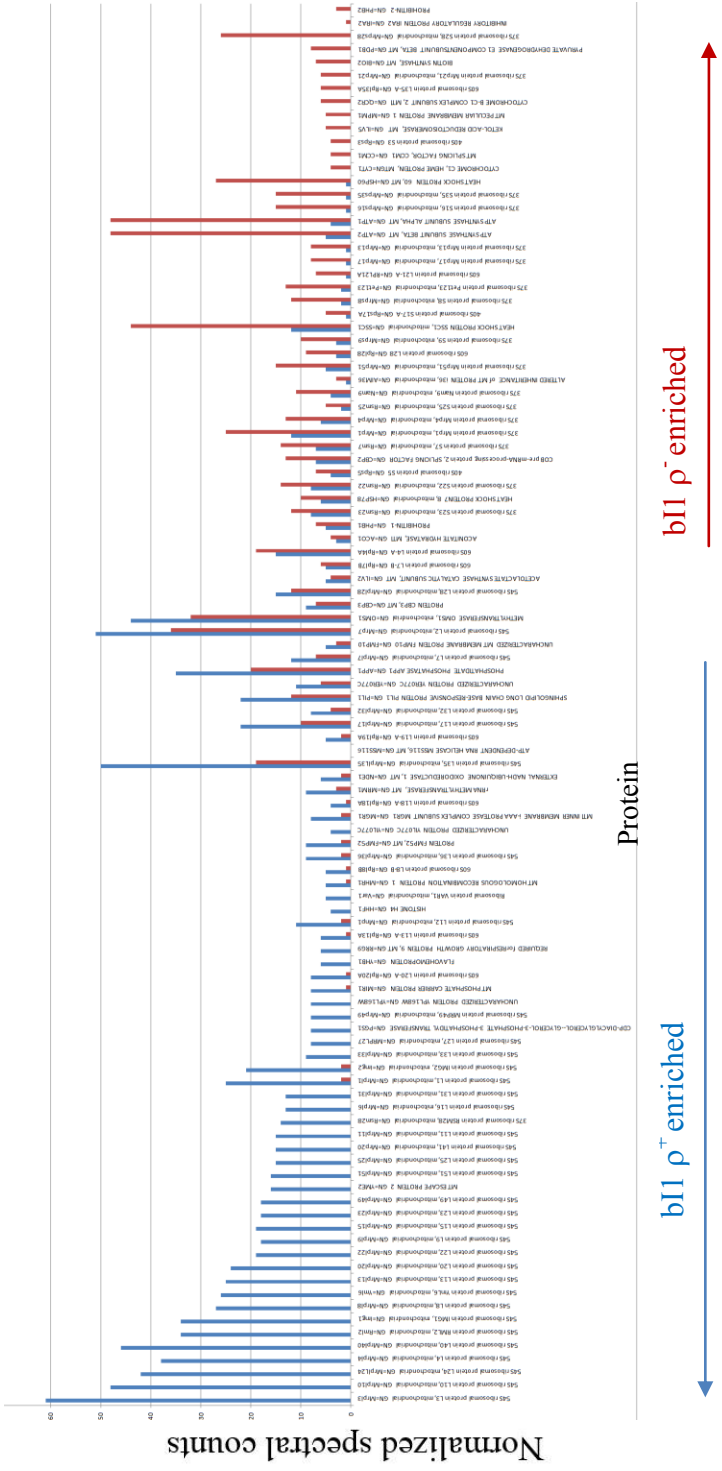

Figure 7.21: Proteins associated with Mss116 in ρ^+ and ρ^- strains of 161-U7*mss116*Δbl1.

Figure 7.21 (continued): Proteins associated with Mss116 in ρ^+ and ρ^- strains of 161-U7*mss116Δ*/bI1.

Graphical analysis of data in Table 7.5. The heights of the bars relative to each other represent the fold change of the correct, normalized spectral count of the bI1 ρ^+ strain (blue) over the bI1 ρ^- strain (red). The proteins are listed in order of decreasing bI1 ρ^+ to bI1 ρ^- fold change with proteins to the left on the X-axis more enriched in the bI1 ρ^+ strain and those to the right more enriched in the bI1 ρ^- strain. Enlargements of the graph are in Figures 7.22 and 7.23. Due to the very large values obtained for Mss116, the bars are not included for the protein.

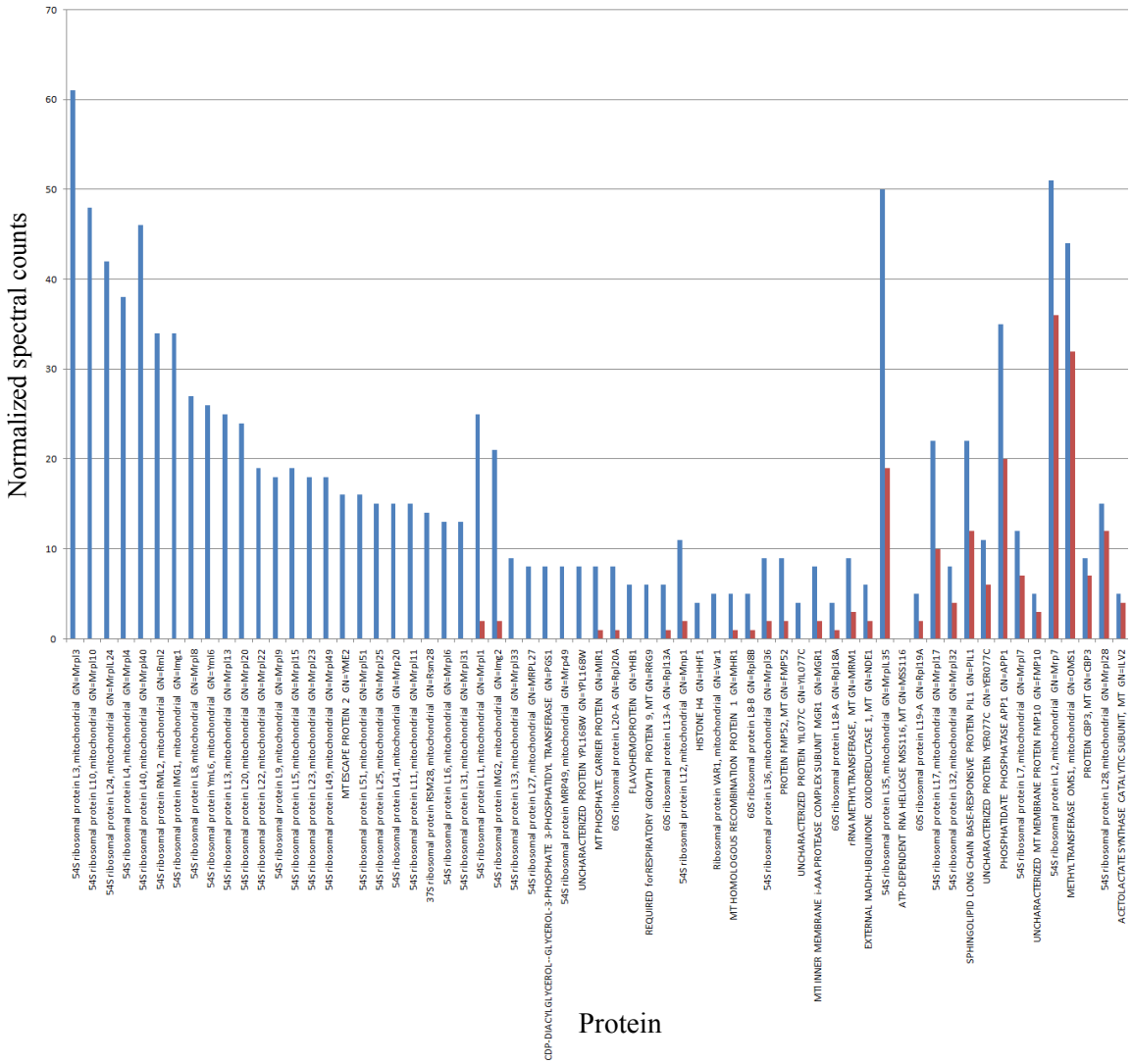

Figure 7.22: Proteins that were associated with TAP-tagged Mss116 enriched in a 161-U7 *mss116Δ*/bI1 ρ^+ strain

Enlarged view of the ρ^- enriched portion of the graph in Fig. 7.21. Non-ribosomal proteins are labeled in all capital letters.

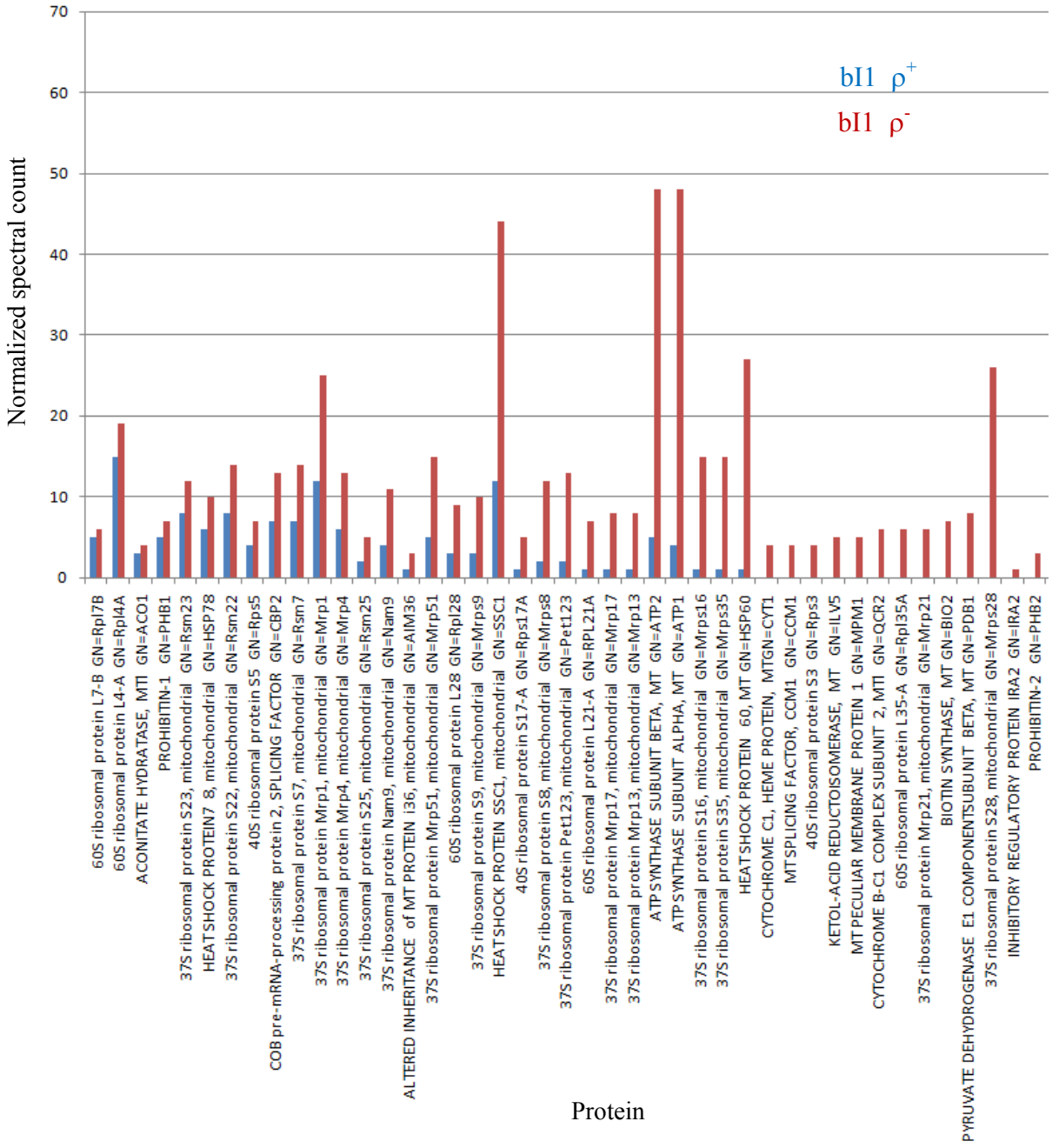

Figure 7.23: Proteins that were associated with TAP-tagged Mss116 enriched in a 161-U7 *mss116Δ*/bI1 ρ+ strain

Enlarged view of the ρ- enriched portion of the graph in Fig. 7.21. Non-ribosomal proteins are labeled in all capital letters.

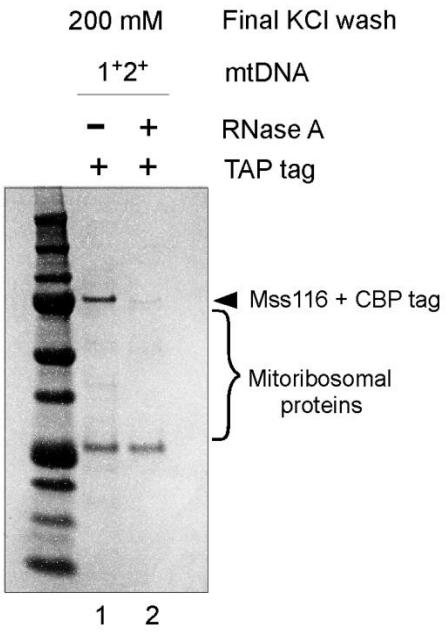

Figure 7.24: SDS polyacrylamide gel showing proteins associated with TAP-tagged Mss116 with and without RNase treatment.

The strain tested was 161-U7*mss116Δ*/$1^{+}2^{+}$ with TAP-tagged Mss116 expressed from plasmid vector pRS416. Cells were cultured and mitochondria were isolated as in Fig. 7.14. Mitochondrial pellets were solubilized as described in Methods with the following exception: to the experimental sample was added 60 µl RNase A and to the control sample 60 µl additional solubilization buffer. Each was incubated at 30°C for 10 min prior to proceeding with the remainder of the TAP protocol. Samples were separated on a 4-12% gradient gel and stained with Coomassie Brilliant Blue.

Conclusions

It has long been recognized that yeast mitochondrial intron splicing and functionality of the mitoribosomes are linked (Rodeheffer and Shadel 2003). The most common view has been that without functional mitoribosomes, intron-encoded maturases cannot be translated, thereby blocking splicing (Pel and Grivell 1993).

Here, I provided evidence that non-functional mitoribosomes and proteins involved in translation also negatively impact the *in vivo* splicing of introns that lack intron-encoded maturases. Interestingly, this splicing defect was sometimes circumvented: in the absence of functional mitoribosomes and certain proteins (primarily translational activators and/or PPR proteins), splicing was observed to proceed to completion, exhibiting a wild-type phenotype, presumably via second-site suppressor mutations. Further studies are necessary to ascertain the nature of these mutations.

Three of the translational activators for components of the cytochrome c oxidase holoenzyme (Pet 309 for *COX1*, Pet111 for *COX2*, and Pet122 and Pet494 for *COX3*) have previously been shown to be membrane-bound (McMullin and Fox 1993; Manthey et al. 1998; Green-Willms et al. 2001; Naithani et al. 2003), leading to the notion that the translational activator proteins could be topographically organized on the surface of the inner membrane so that synthesis of proteins Cox1, Cox2, and Cox3 would be co-localized to facilitate assembly of the core of the holoenzyme (Naithani et al. 2003; Gruschke and Ott 2010). Translational activators for *COB* and *COX1* mRNAs, Cbp1 and

Pet309 respectively, had also been shown to be associated in a high-molecular weight complex thought to link transcription to translation (Krause et al. 2004).

The results presented here expand on this model, showing that Pet309 and translational activators for other mRNAs, Aep1, Sov1, and Atp22, strongly impact the splicing of aI5γ, possibly reflecting that a higher order of organization among these proteins is involved in aI5γ splicing.

Some of the membrane-bound translational activators may be inserted into the inner membrane with the assistance of the insertase, Oxa1, whose deletion results in strong splicing defects in aI5γ and bI1.

One interpretation of these data suggests the presence of a system at the mt inner membrane that monitors the status of the mitoribosome, possibly through the general RNA chaperone, Mss116, and is linked to the splicing apparatus. This putative splicing system may lend support to the previously proposed "translational integrator complex" thought to link transcription to translation (Bryan et al. 2002; Krause et al. 2004; Shadel 2004) and is further supported by recent work in which the mitoribosomes are found to be interacting with proteins involved with mRNA metabolism and maturation (Kehrein et al. 2015).

The data presented here also point to distinctively different auxiliary protein requirements for the splicing of group I introns, group II introns encoding their own maturases, and group II introns aI5γ and bI1 that do not encode their own maturases.

Further study is required to establish the identity of the putative second-site suppressor mutations discussed in Chapter 4. These studies may be complemented by microscopy to confirm the absence of mitoribosomes in the petite strains.

More components of the putative splicing complex may be identified by repeating the Mss116 TAP tag pull-down experiments in Chapter 7 using low salt concentration final washes and testing the effect of RNases.

Appendices

APPENDIX A:

Following are the original Northern hybridizations used in the screen of the ρ^+ strains in Chapter 3. All the hybridizations were performed by the author with the exception of those performed by technician Kathryn Turner, and are labeled KT. The descriptions or functions of the tested proteins, if known, were taken from the Saccharomyces Genome Database unless otherwise noted.

Blot 1

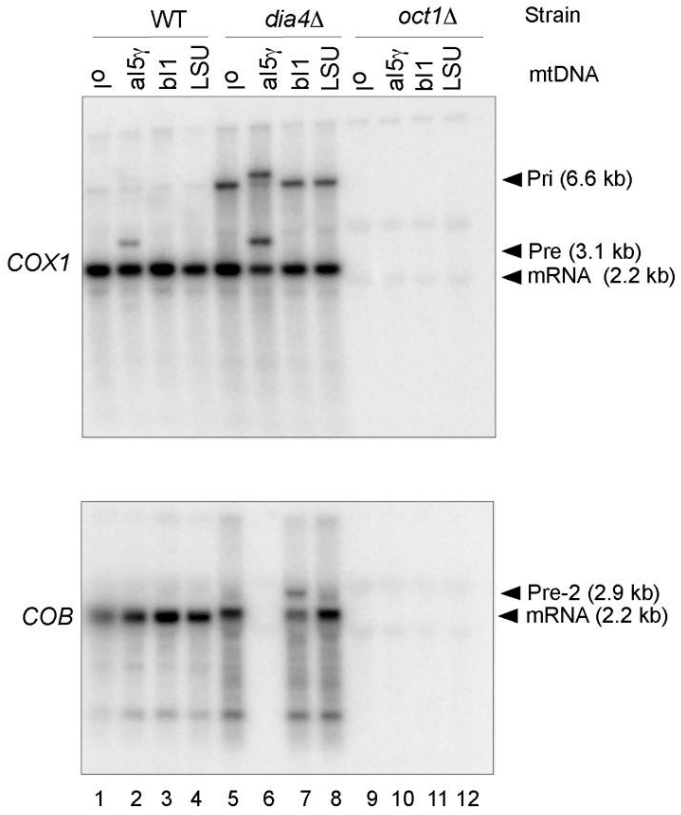

Dia4 = Probable mitochondrial seryl-tRNA synthetase, mutant displays increased invasive and pseudohyphal growth

Oct1 = Mitochondrial intermediate peptidase, cleaves N-terminal residues of a subset of proteins upon import, after their cleavage by mitochondrial processing peptidase

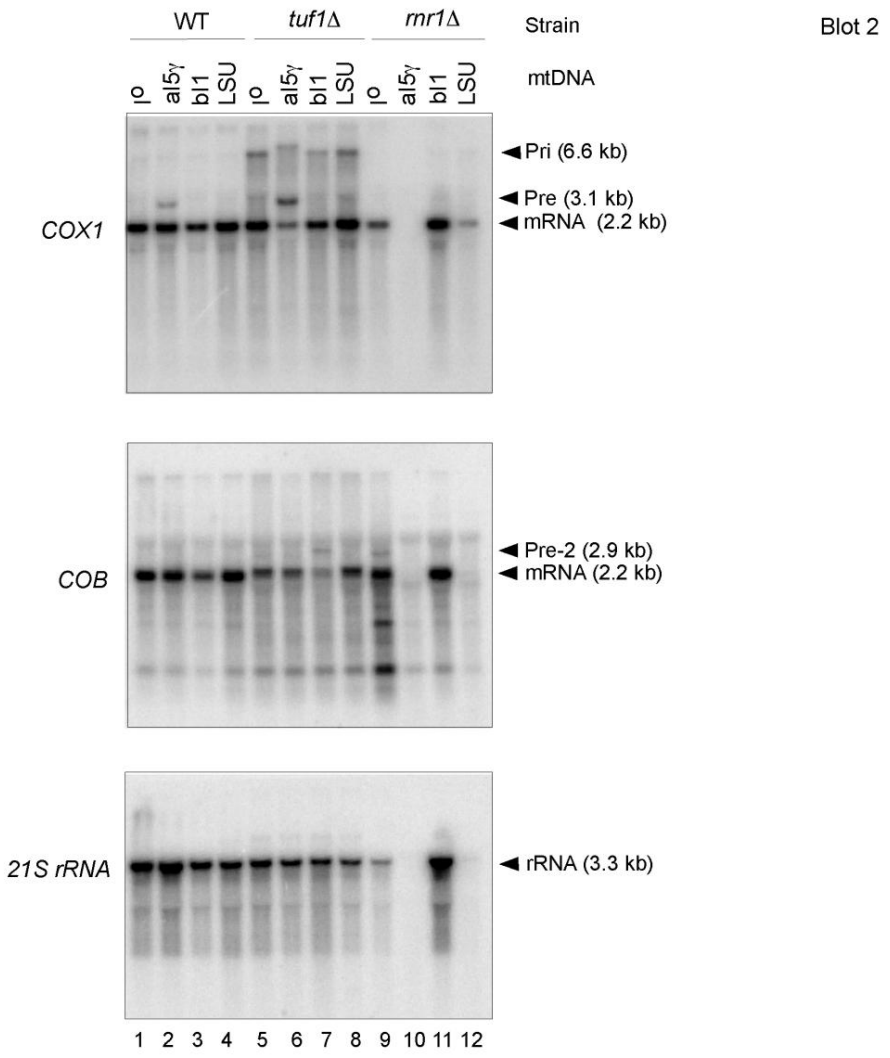

Tuf1= Mitochondrial translation elongation factor Tu; comprises both GTPase and guanine nucleotide exchange factor activities, while these activities are found in separate proteins in *S. pombe* and humans

Rnr1=Major isoform of the large subunit of ribonucleotide-diphosphate reductase; the RNR complex catalyzes rate-limiting step in dNTP synthesis, regulated by DNA replication and DNA damage check-point pathways via localization of small subunits

Blot 3

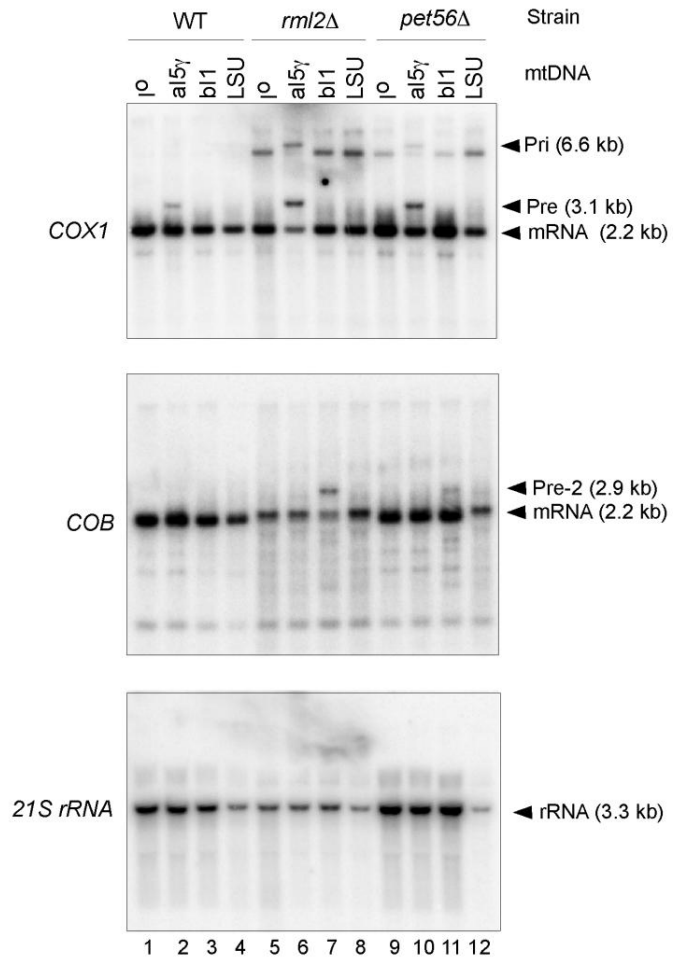

Rml2 = Mitochondrial ribosomal protein of the large subunit, has similarity to *E. coli* L2 ribosomal protein; fat21 mutant allele causes inability to utilize oleate and may interfere with activity of the Adr1 transcription factor

Pet56 = Ribose methyltransferase that modifies a functionally critical, conserved nucleotide in mitochondrial 21S rRNA

Blot 4

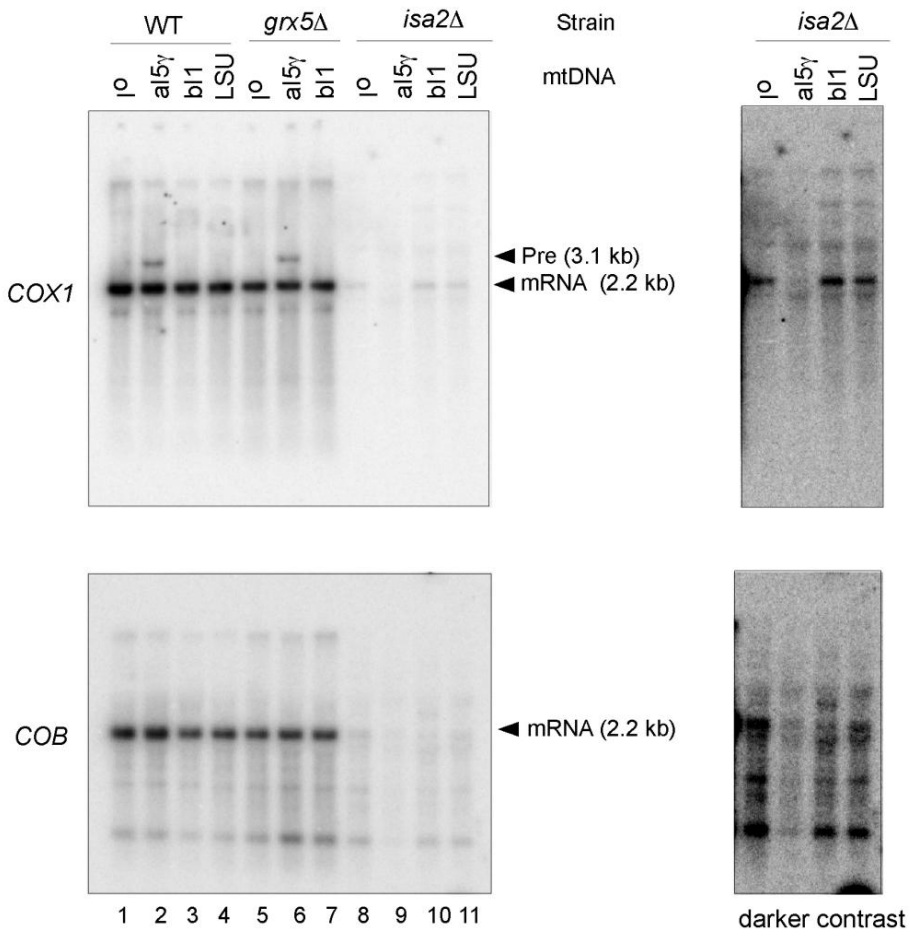

Grx5 = Hydroperoxide and superoxide-radical responsive glutathione-dependent oxidoreductase; mitochondrial matrix protein involved in the synthesis/assembly of iron-sulfur centers; monothiol glutaredoxin subfamily member along with Grx3 and Grx4

Isa2 = Protein required for maturation of mitochondrial and cytosolic Fe/S proteins, localizes to the mitochondrial intermembrane space, overexpression of ISA2 suppresses grx5 mutations

Blot 5

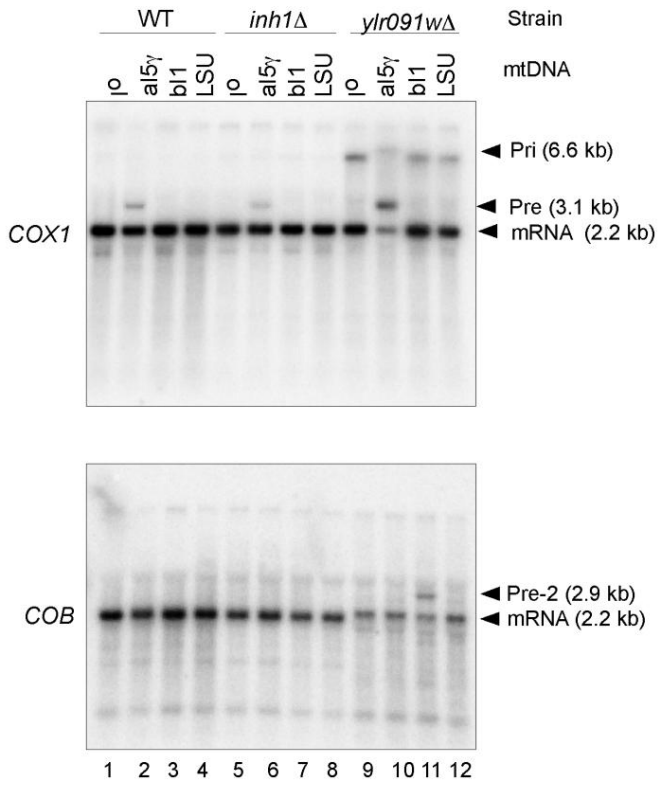

Inh1= Protein that inhibits ATP hydrolysis by the F1F0-ATP synthase; inhibitory function is enhanced by stabilizing proteins Stf1and Stf2; has similarity to Stf1; has a calmodulin-binding motif and binds calmodulin in vitro

Ylr091W = Gep5 = Rrg5 = Protein of unknown function, required for mitochondrial genome maintenance; detected in highly purified mitochondria in high-throughput studies; null mutant has decreased levels of cardiolipin and phosphatidylethanolamine

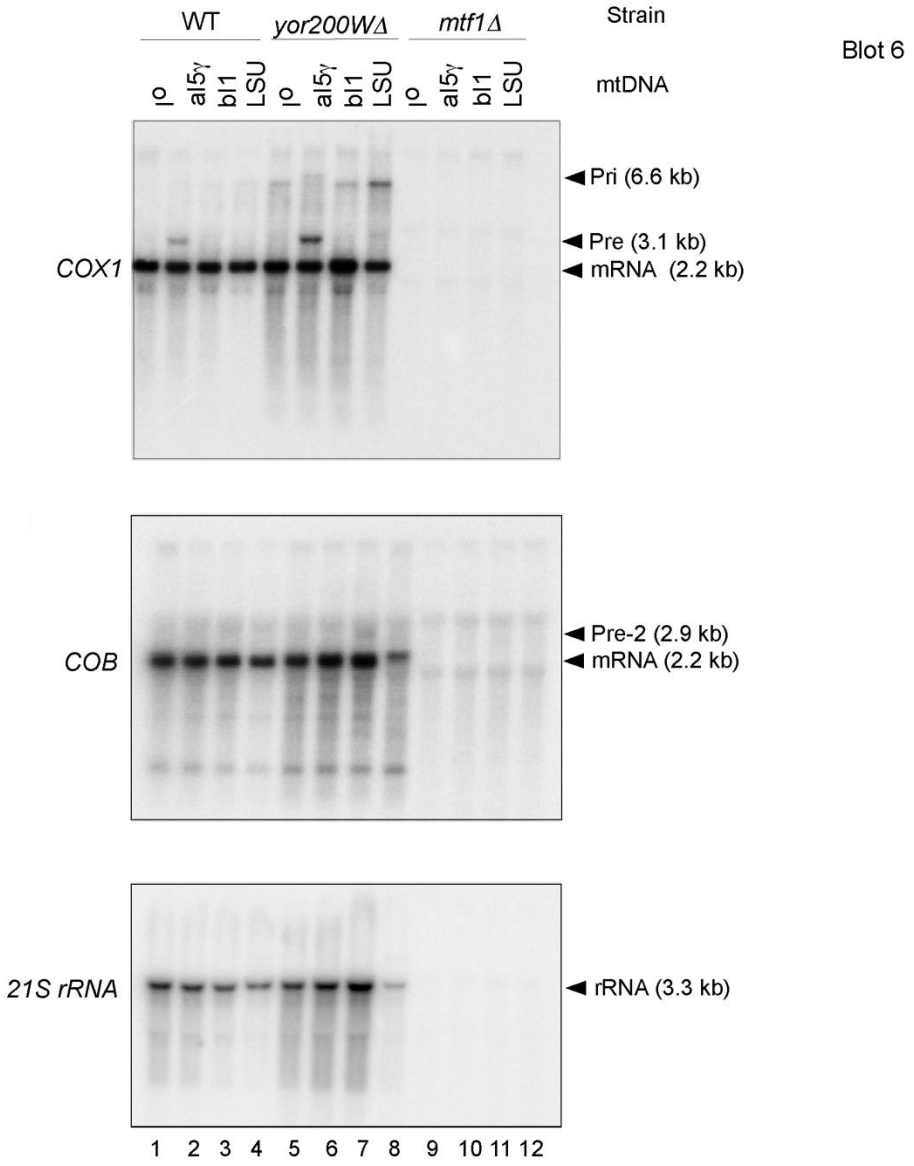

Yor200W = Dubious open reading frame unlikely to encode a protein, based on available experimental and comparative sequence data; partially overlaps the verified ORF MRM1/YOR201C (Mrm1=Ribose methyltransferase that modifies a functionally critical, conserved nucleotide in mitochondrial 21S rRNA)

Mtf1 = Mitochondrial RNA polymerase specificity factor with structural similarity to S-adenosylmethionine-dependent methyltransferases and functional similarity to bacterial sigma-factors, interacts with mitochondrial core polymerase Rpo41

Blot 7

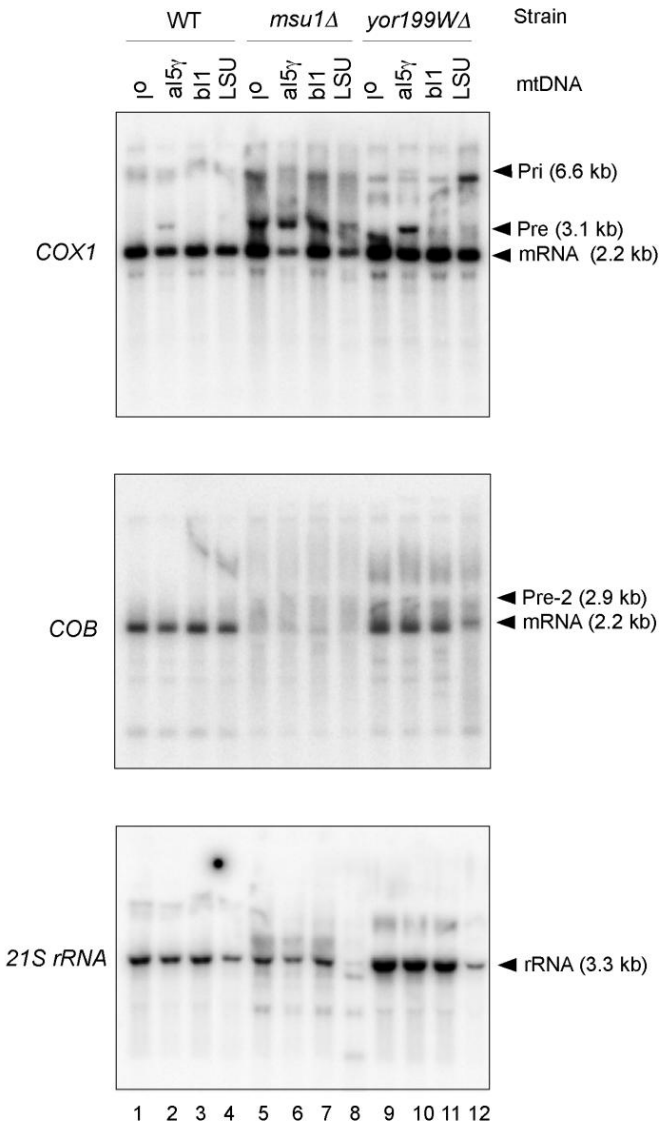

Msu1=3'-5' exoribonuclease, component of the mitochondrial degradosome along with the ATP-dependent RNA helicase Suv3; the degradosome associates with the ribosome and mediates turnover of aberrant or unprocessed RNAs

YOR199W = dubious ORF, partly overlaps *PET56* (Mrm1) = Ribose methyltransferase that modifies a functionally critical, conserved nucleotide in mitochondrial 21S rRNA

Blot 8

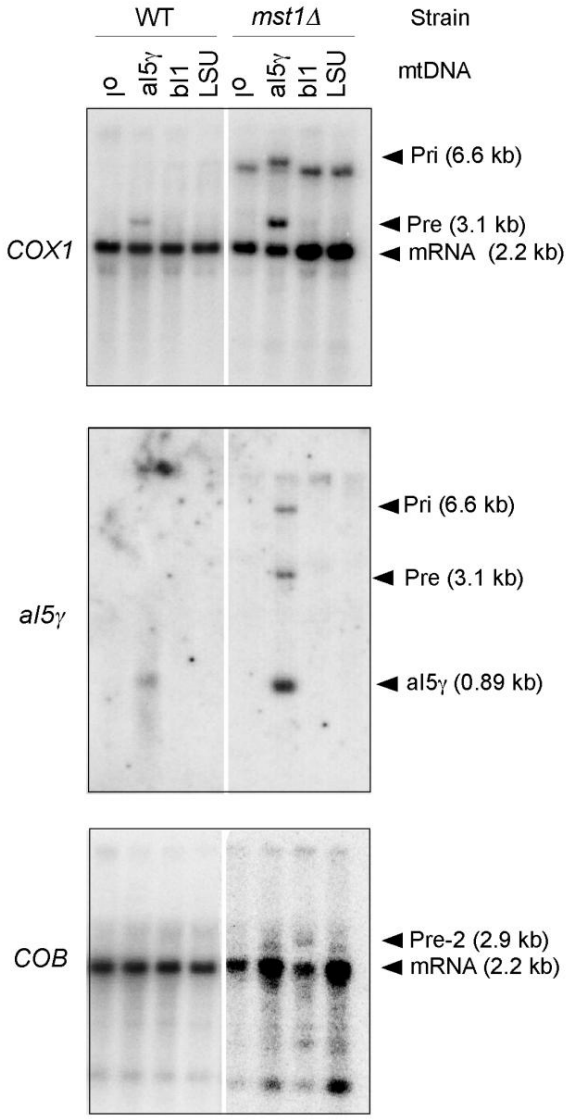

Mst1 =Mitochondrial aminoacyl-tRNA Synthetase, Threonine

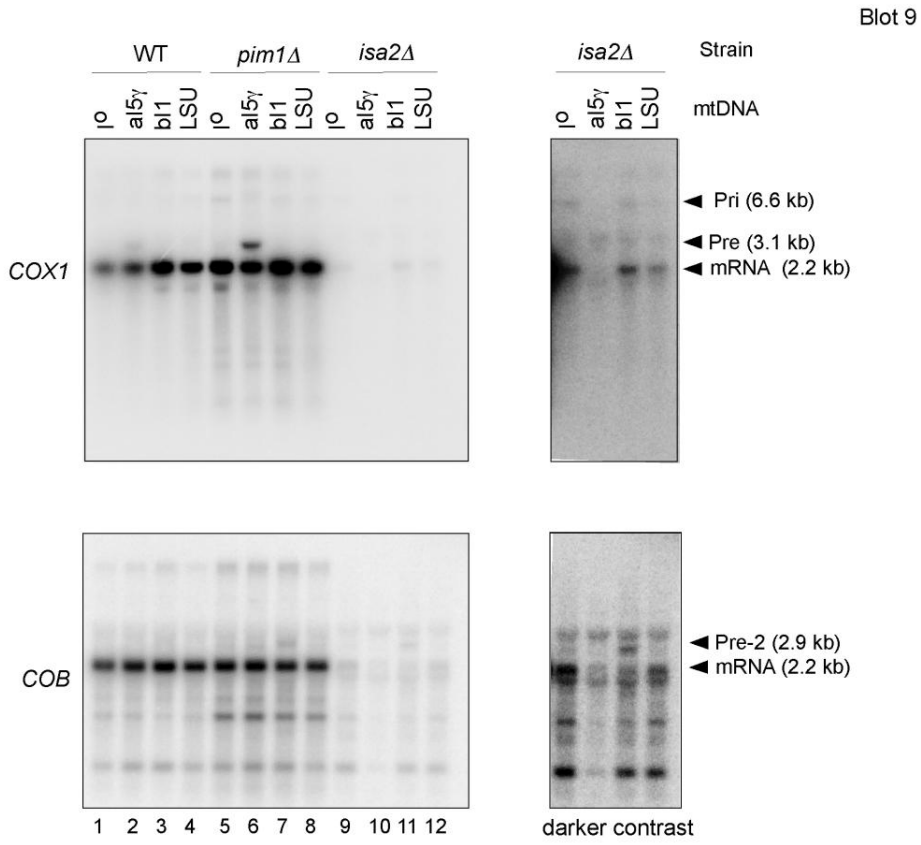

Pim1=ATP-dependent Lon protease, involved in degradation of misfolded proteins in mitochondria; required for biogenesis and maintenance of mitochondria

Isa2 = Protein required for maturation of mitochondrial and cytosolic Fe/S proteins, localizes to the mitochondrial intermembrane space, overexpression of ISA2 suppresses grx5 mutations

Blot 10

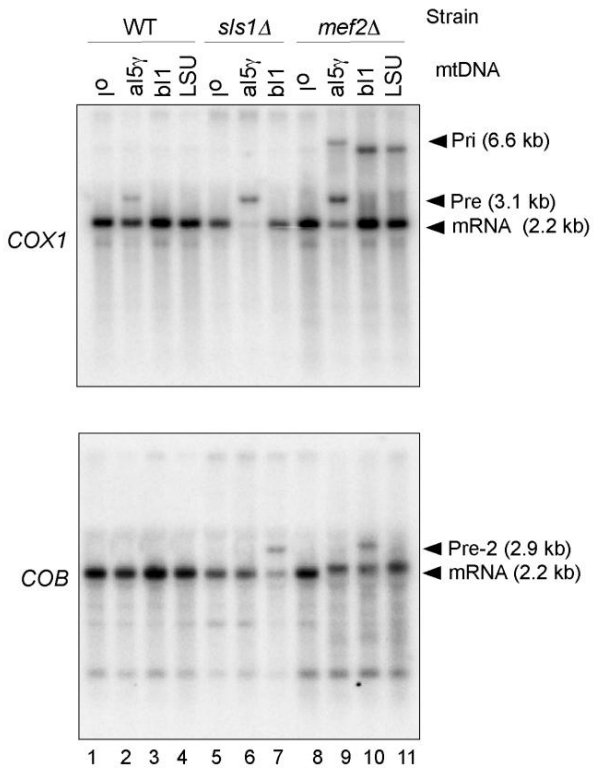

Sls1 = Mitochondrial membrane protein that coordinates expression of mitochondrially-encoded genes; may facilitate delivery of mRNA to membrane-bound translation machinery

Mef2 = Mitochondrial elongation factor involved in translational elongation

Blot 11

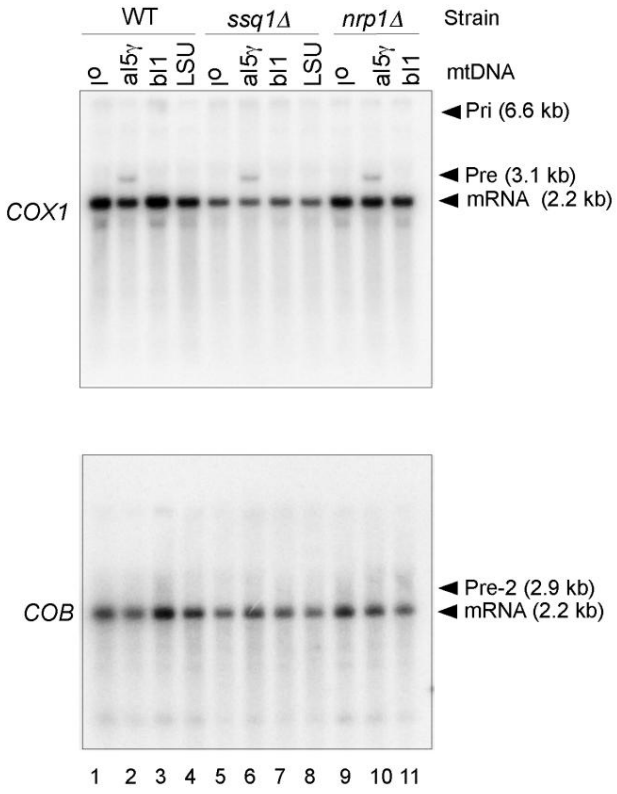

Ssq1= Mitochondrial hsp70-type molecular chaperone, required for assembly of iron/sulfur clusters into proteins at a step after cluster synthesis, and for maturation of Yfh1p, which is a homolog of human frataxin

Nrp1= Putative RNA binding protein of unknown function; localizes to stress granules induced by glucose deprivation; predicted to be involved in ribosome biogenesis

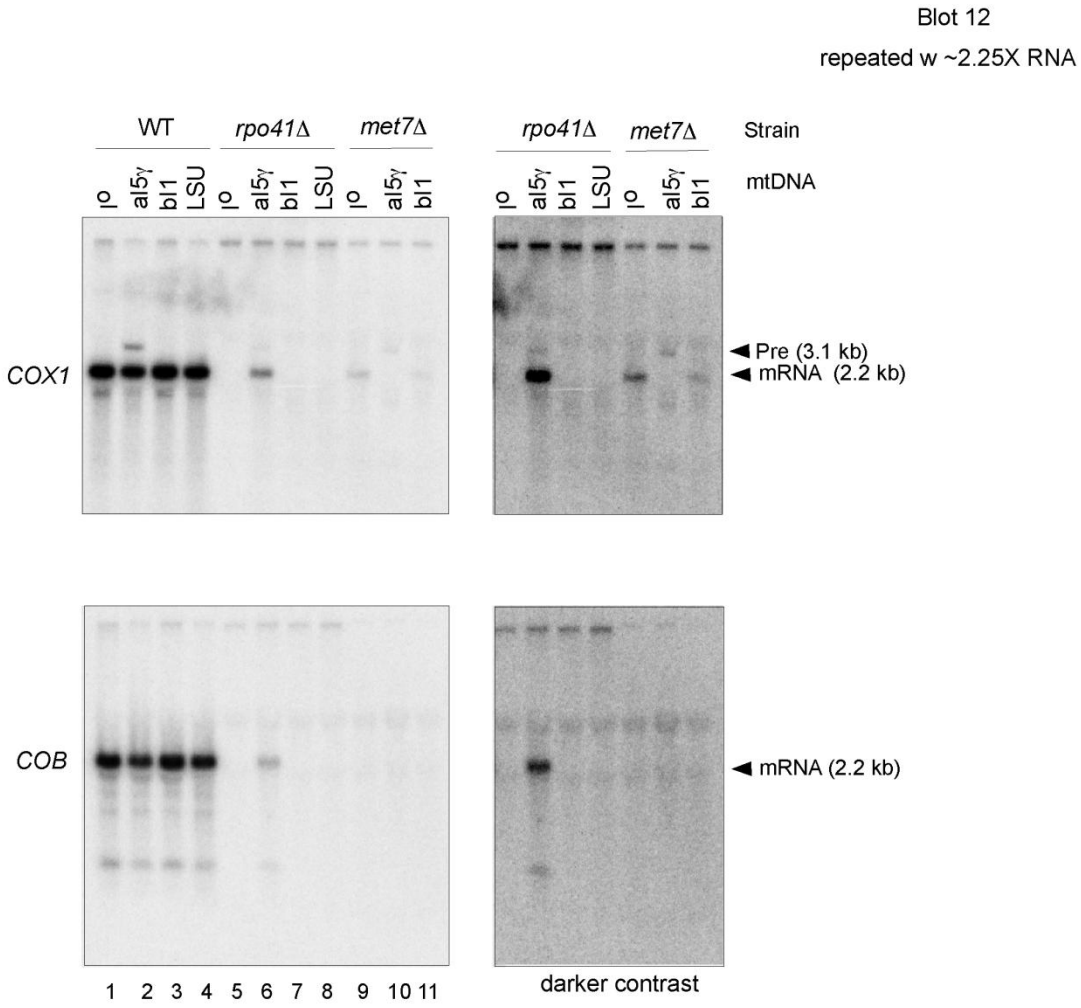

Rpo41: Mitochondrial RNA polymerase; single subunit enzyme similar to those of T3 and T7 bacteriophages; requires a specificity subunit encoded by MTF1 for promoter recognition; Mtf1p interacts with and stabilizes the Rpo41p-promoter complex, enhancing DNA bending and melting to facilitate pre-initiation open complex formation

Met7: Folylpolyglutamate synthetase; catalyzes extension of the glutamate chains of the folate coenzymes, required for methionine synthesis and for maintenance of mitochondrial DNA; protein abundance increases in response to DNA replication stress

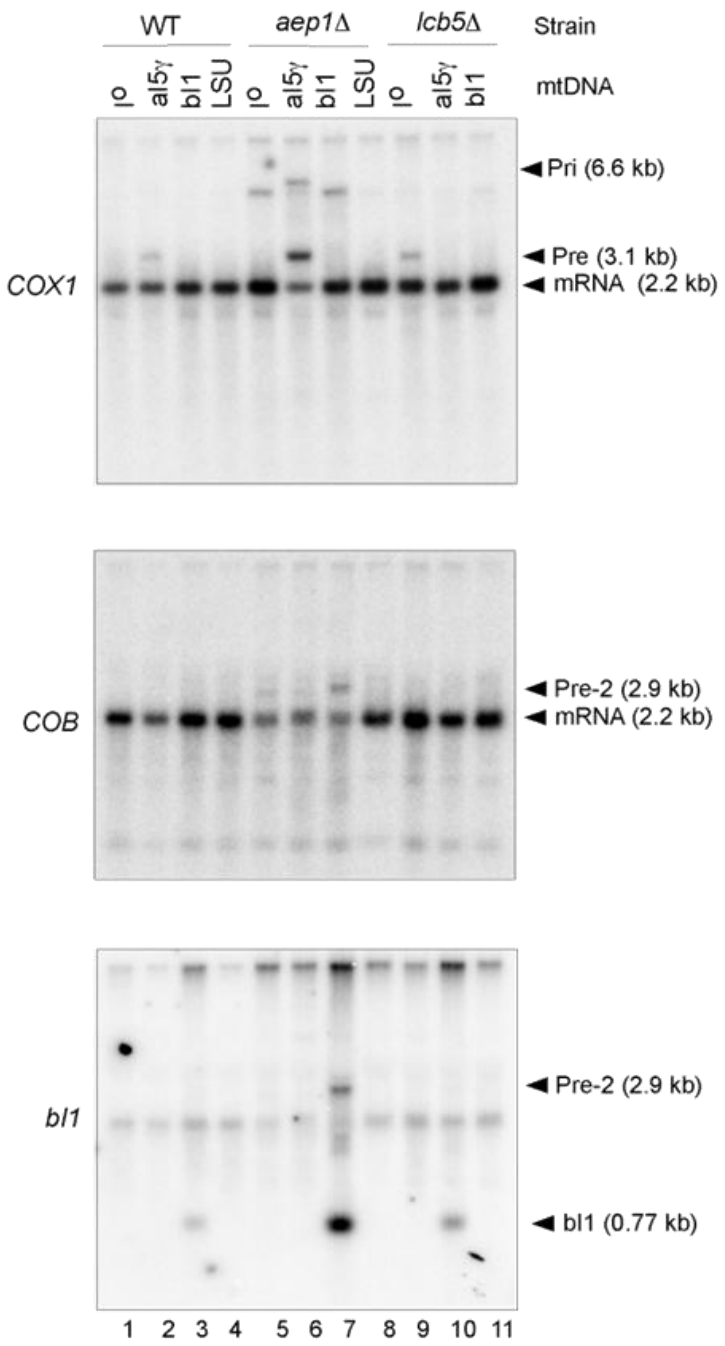

Aep1 : Protein required for expression of the mitochondrial OLI1 gene encoding subunit 9 of F1-F0 ATP synthase

Lcb5: Minor sphingoid long-chain base kinase, paralog of Lcb4p responsible for few percent of the total activity, possibly involved in synthesis of long-chain base phosphates, which function as signaling molecules

Blot 14

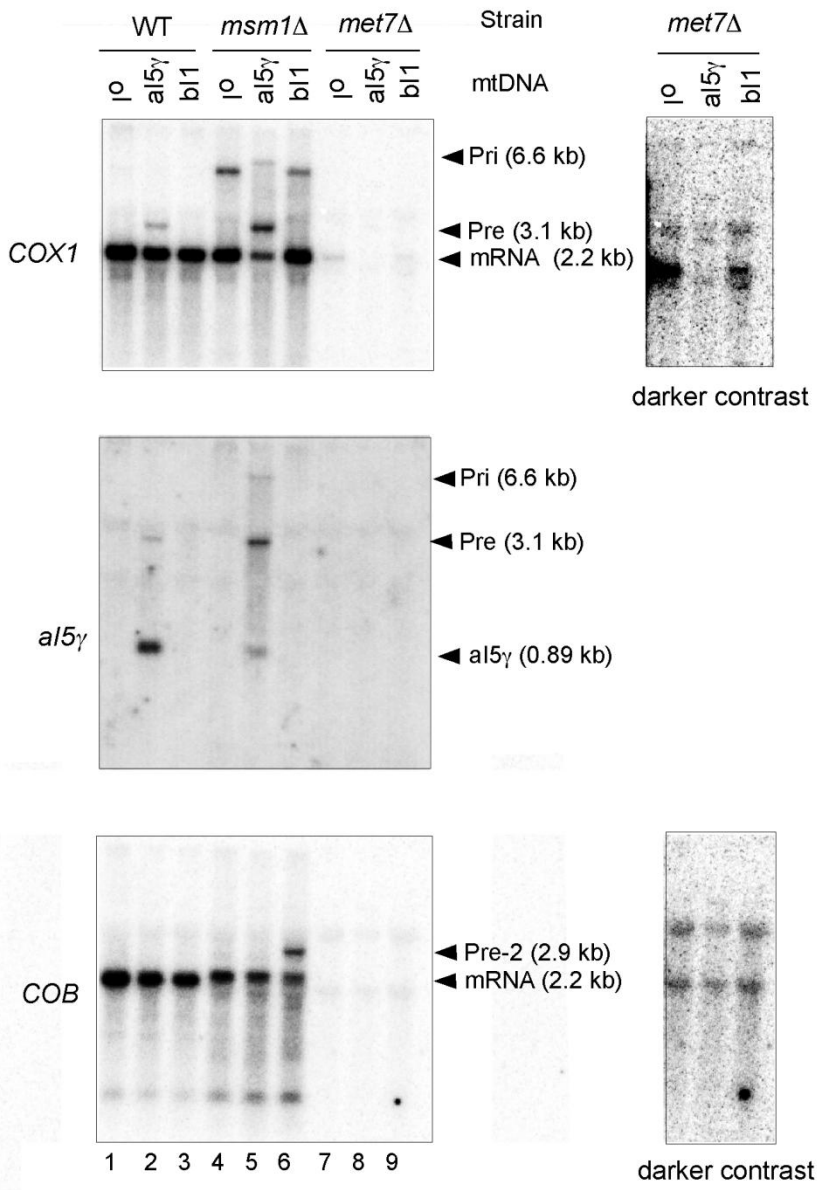

Msm1=Mitochondrial methionyl-tRNA synthetase (MetRS), functions as a monomer in mitochondrial protein synthesis; functions similarly to cytoplasmic MetRS although the cytoplasmic form contains a zinc-binding domain not found in Msm1

Met7=Folylpolyglutamate synthetase, catalyzes extension of the glutamate chains of the folate coenzymes, required for methionine synthesis and for maintenance of mitochondrial DNA

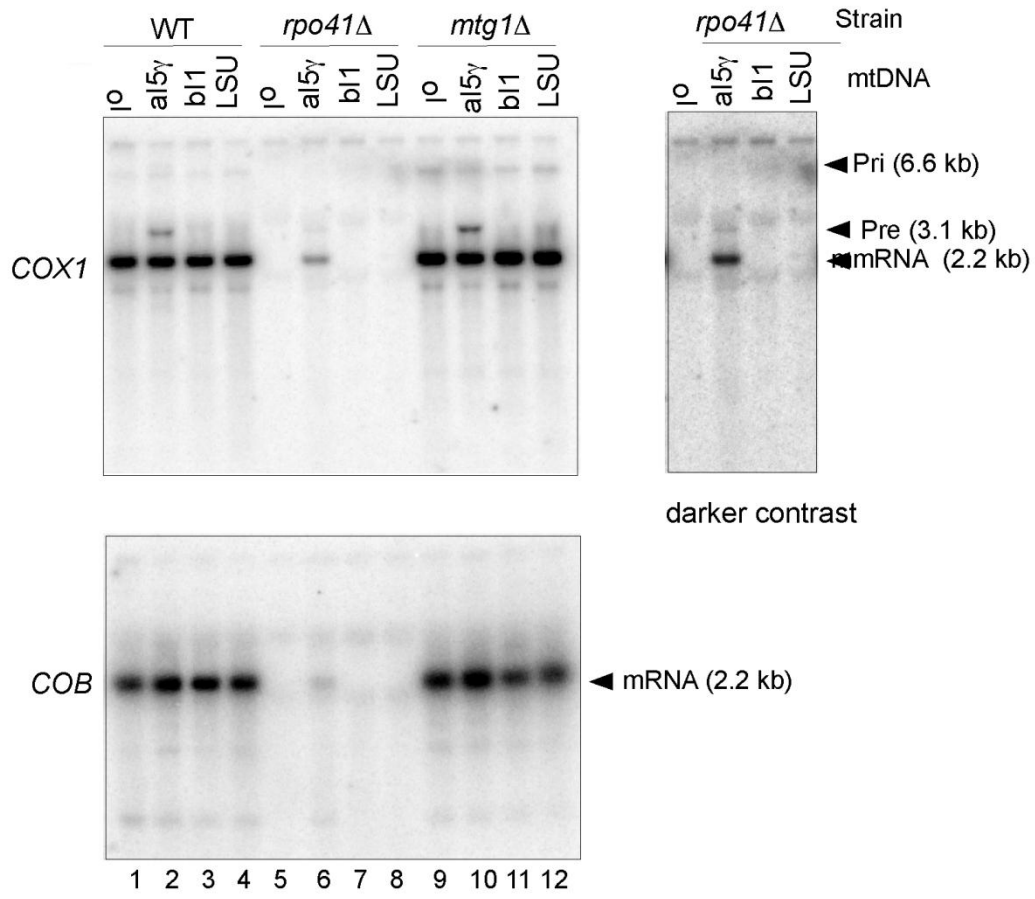

Rpo41= Mitochondrial RNA polymerase; single subunit enzyme similar to those of T3 and T7 bacteriophages; requires a specificity subunit encoded by MTF1 for promoter recognition; Mtf1p interacts with and stabilizes the Rpo41p-promoter complex, enhancing DNA bending and melting to facilitate pre-initiation open complex formation

Mtg1= Putative GTPase peripheral to the mitochondrial inner membrane; essential for respiratory competence,likely functions in assembly of the large ribosomal subunit, has homologs in plants and animals

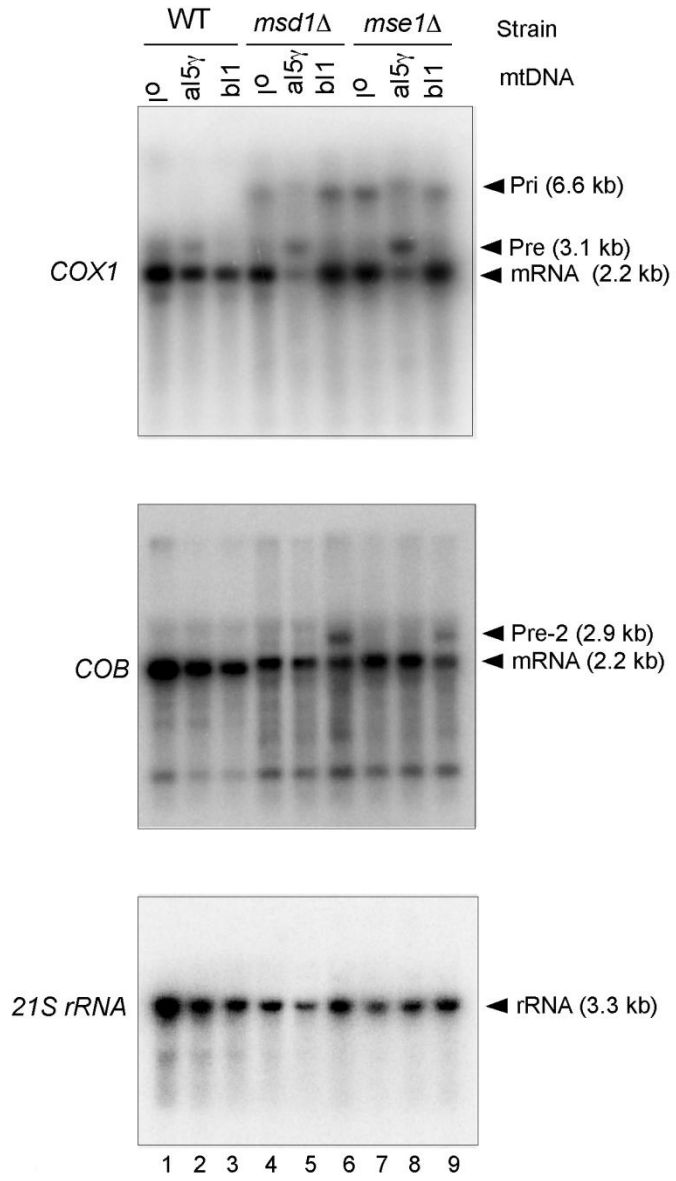

Msd1: Mitochondrial aspartyl-tRNA synthetase; required for acylation of aspartyl-tRNA; yeast and bacterial aspartyl-, asparaginyl-, and lysyl-tRNA synthetases contain regions with high sequence similarity, suggesting a common ancestral gene

Mse1: Mitochondrial aminoacyl-tRNA Synthetase, Glutamate (E)

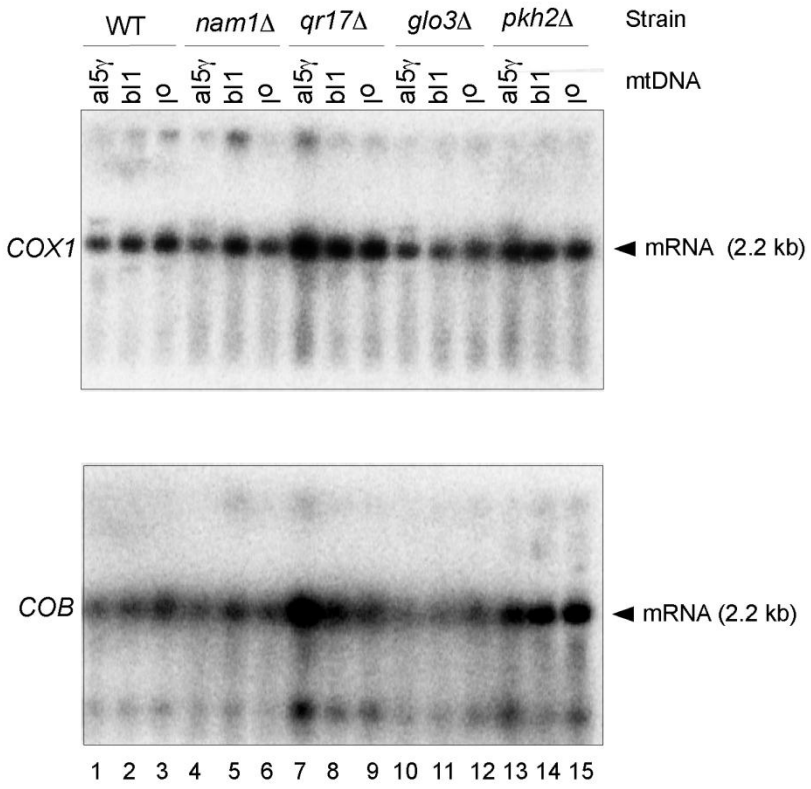

Nam1: Mitochondrial protein that interacts with mitochondrial RNA polymerase; interacts with an N-terminal region of mitochondrial RNA polymerase (Rpo41p) and couples RNA processing and translation to transcription

Qr17: Highly conserved mitochondrial protein; essential for t6A modification of mitochondrial tRNAs that decode ANN codons; similar to Kae1p and *E. coli* YgjD, both of which are also required for tRNA t6A modification

Glo3:ADP-ribosylation factor GTPase activating protein (ARF GAP); involved in ER-Golgi transport; shares functional similarity with Gcs1p

Pkh2: Serine/threonine protein kinase; involved in sphingolipid-mediated signaling pathway that controls endocytosis; activates Ypk1p and Ykr2p, components of signaling cascade required for maintenance of cell wall integrity; redundant with Pkh1p; PKH2 has a paralog, PKH1, that arose from the whole genome duplication

Blot 18

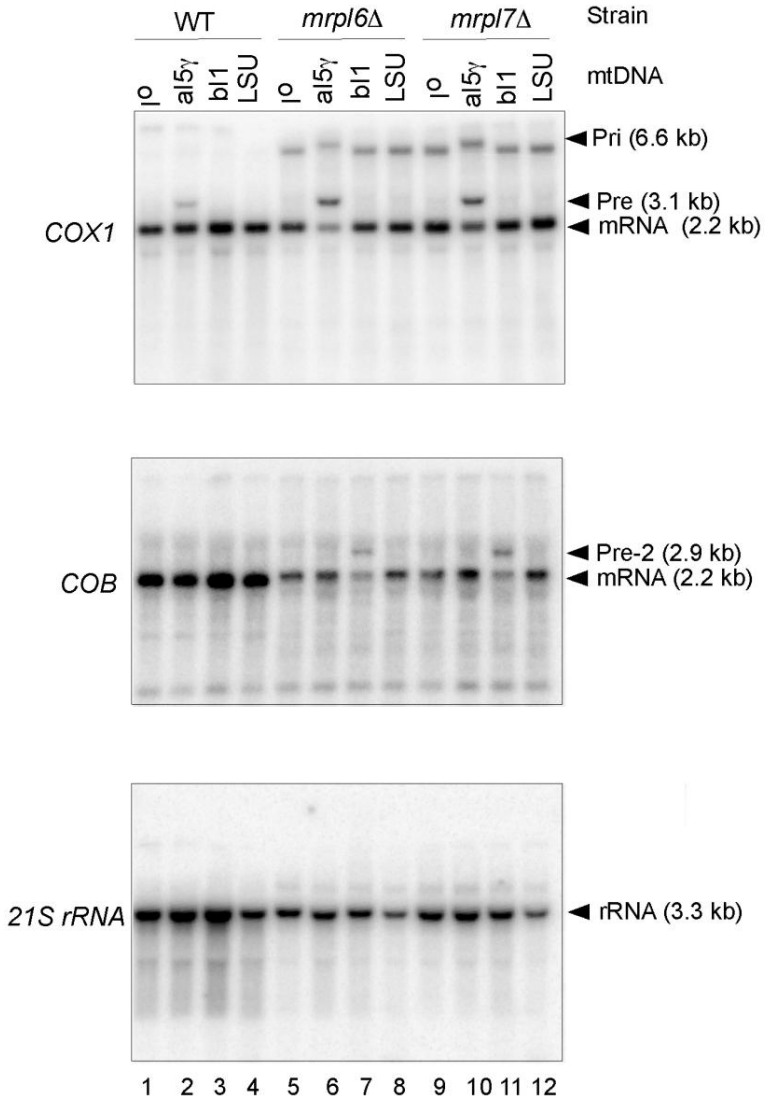

Mrpl6 and Mrpl7: Mitochondrial ribosomal proteins of the large subunit

Blot 19

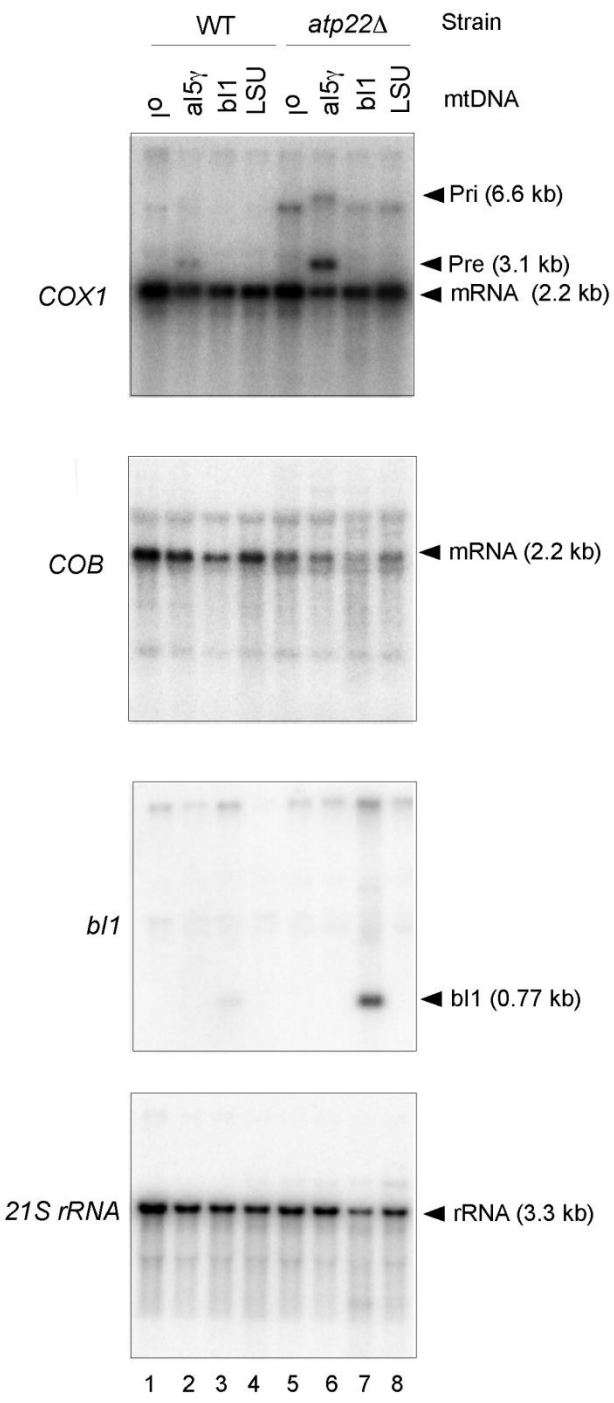

Atp22: Specific translational activator for the mitochondrial ATP6 mRNA; Atp6 encodes a subunit of F1F0 ATP synthase; localized to the mitochondrial inner membrane

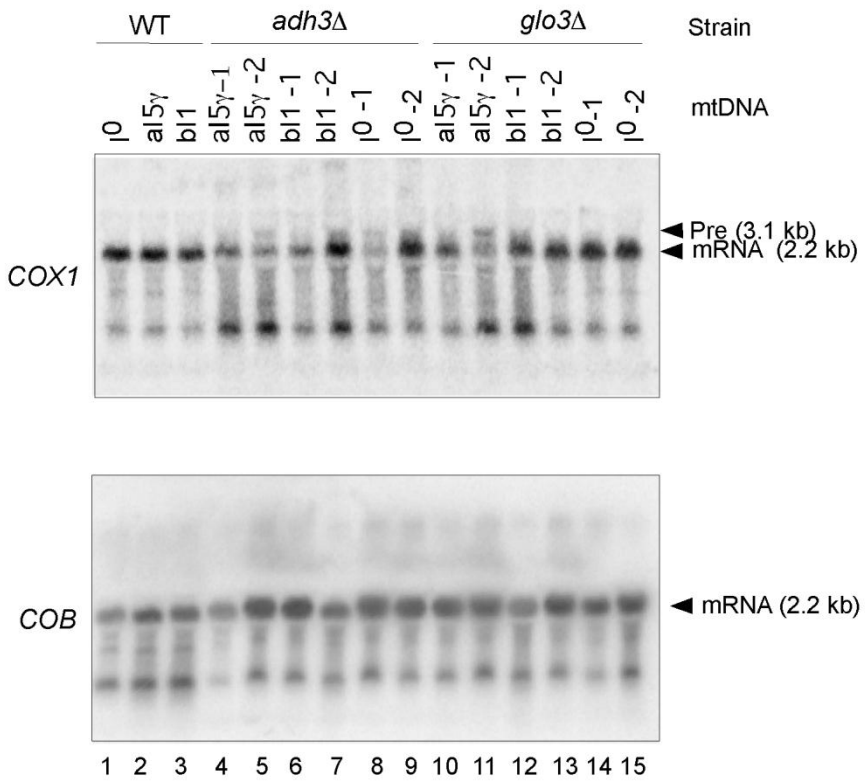

Adh3: Mitochondrial alcohol dehydrogenase isozyme III; involved in the shuttling of mitochondrial NADH to the cytosol under anaerobic conditions and ethanol production

Glo3: ADP-ribosylation factor GTPase activating protein (ARF GAP); involved in ER-Golgi transport; shares functional similarity with Gcs1

Blot 21

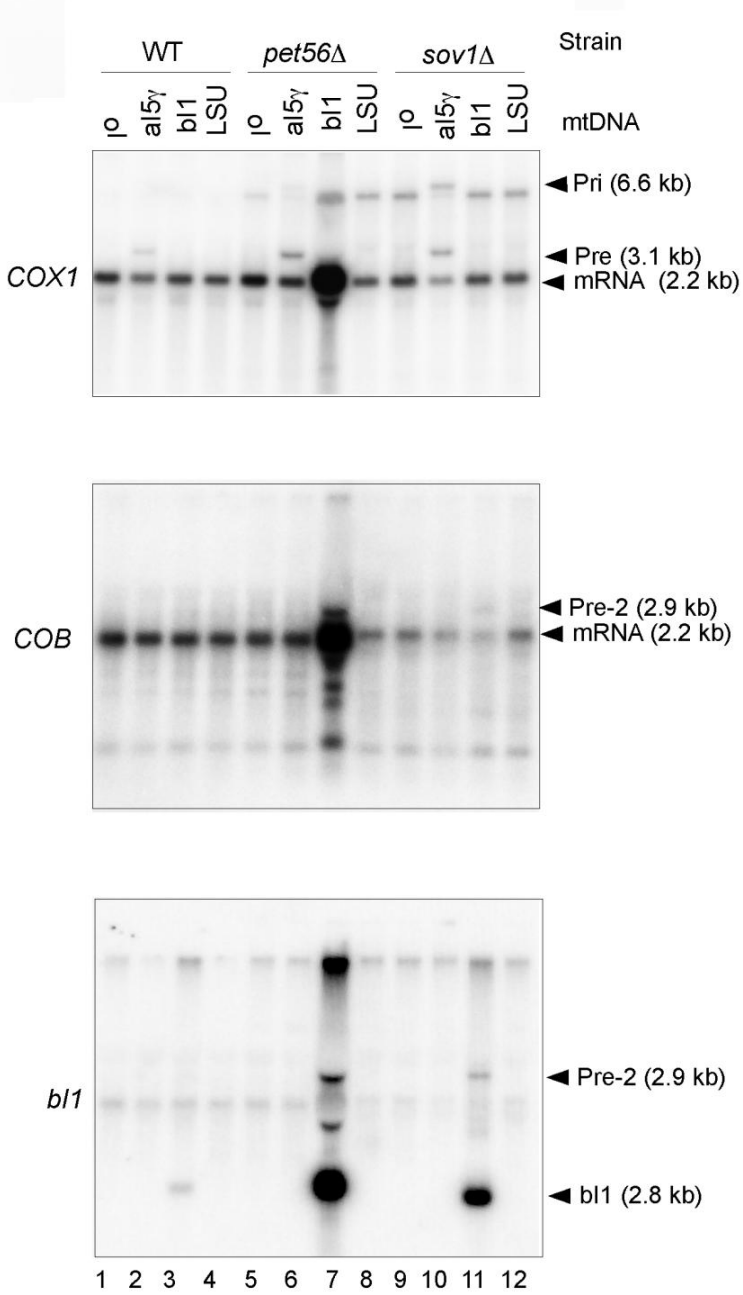

Pet 56: Ribose methyltransferase; modifies a functionally critical, conserved nucleotide in mitochondrial 21S rRNA

Sov1: Translational activator for Var1 (Herrmann, et al.2013)

Blot 22

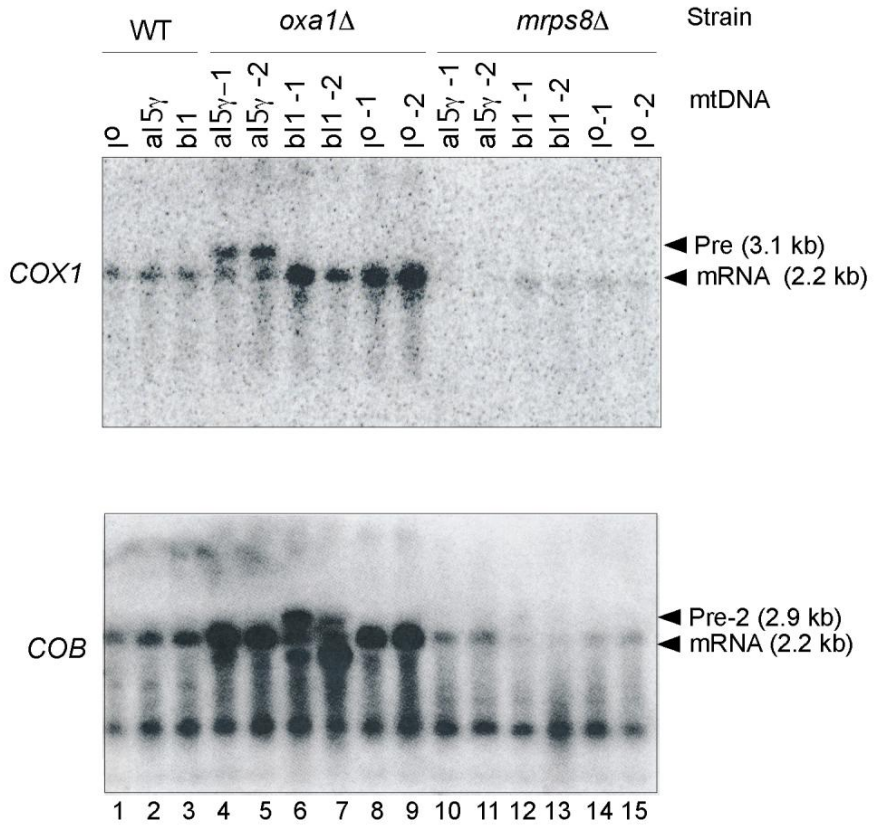

Oxa1: Mitochondrial inner membrane insertase; mediates the insertion of both mitochondrial- and nuclear-encoded proteins from the matrix into the inner membrane; also has a role in insertion of carrier proteins into the inner membrane; interacts with mitochondrial ribosomes; conserved from bacteria to animals

Mrps8: Mitochondrial ribosomal protein of the small subunit

Blot 23

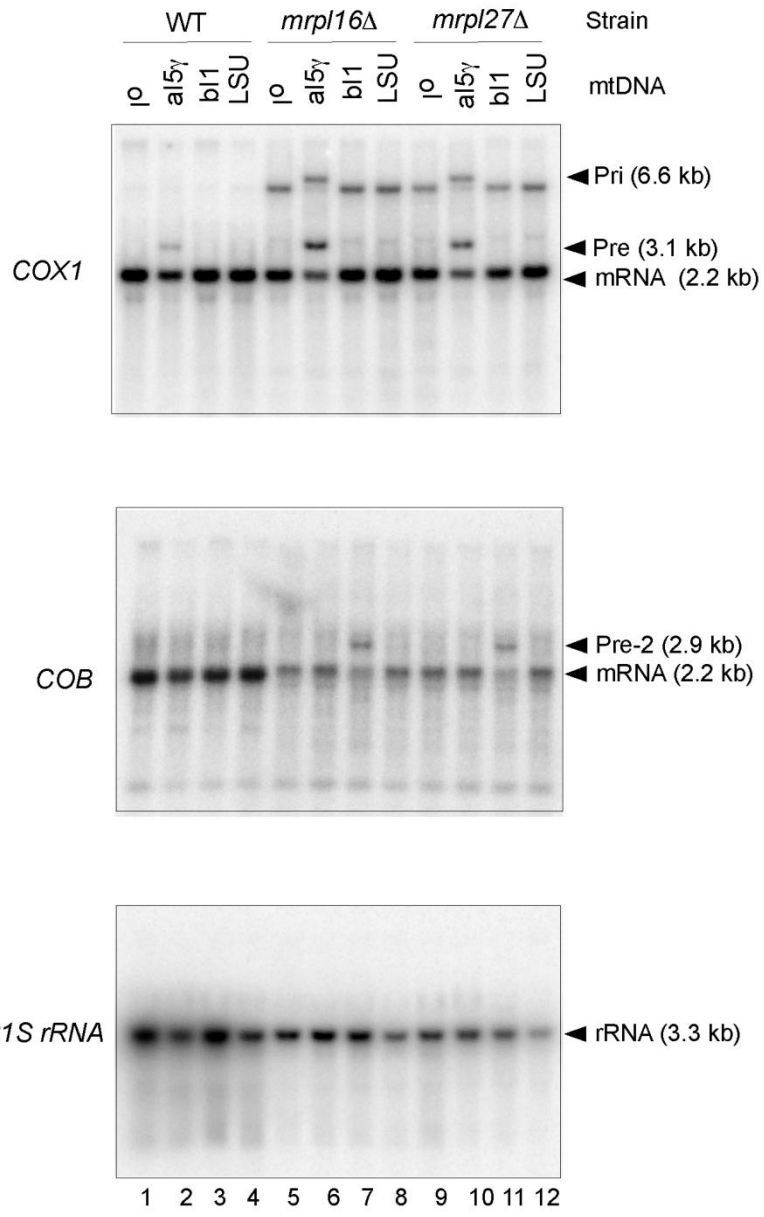

Mrpl16: Mitochondrial ribosomal protein of the large subunit; homologous to bacterial L16 ribosomal protein

Mrpl27: Mitochondrial ribosomal protein of the large subunit; homolog of human Bcl-2 interacting protein BMRP

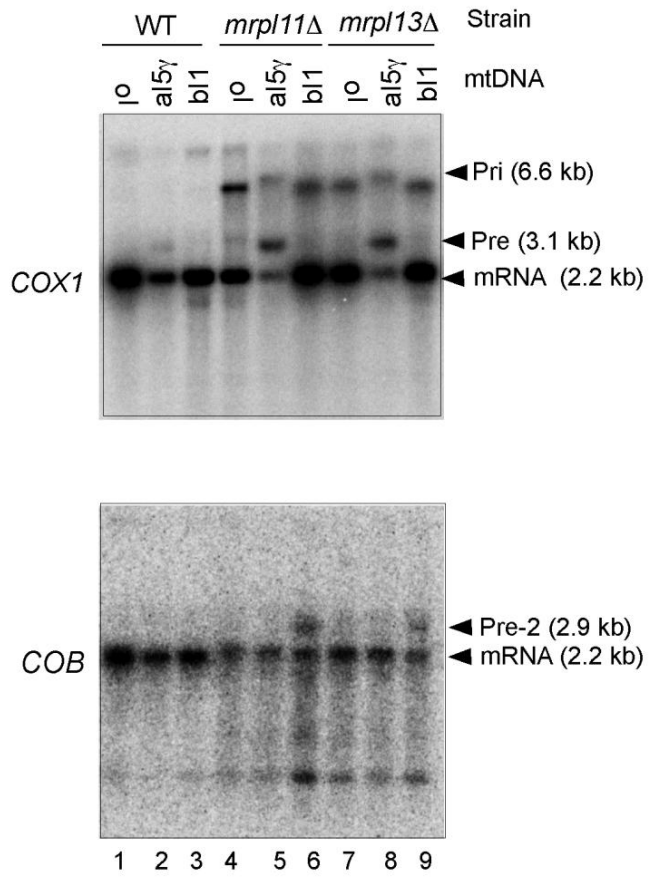

Mrpl11: Mitochondrial ribosomal protein of the large subunit

Mrpl13: Mitochondrial ribosomal protein of the large subunit; not essential for mitochondrial translation

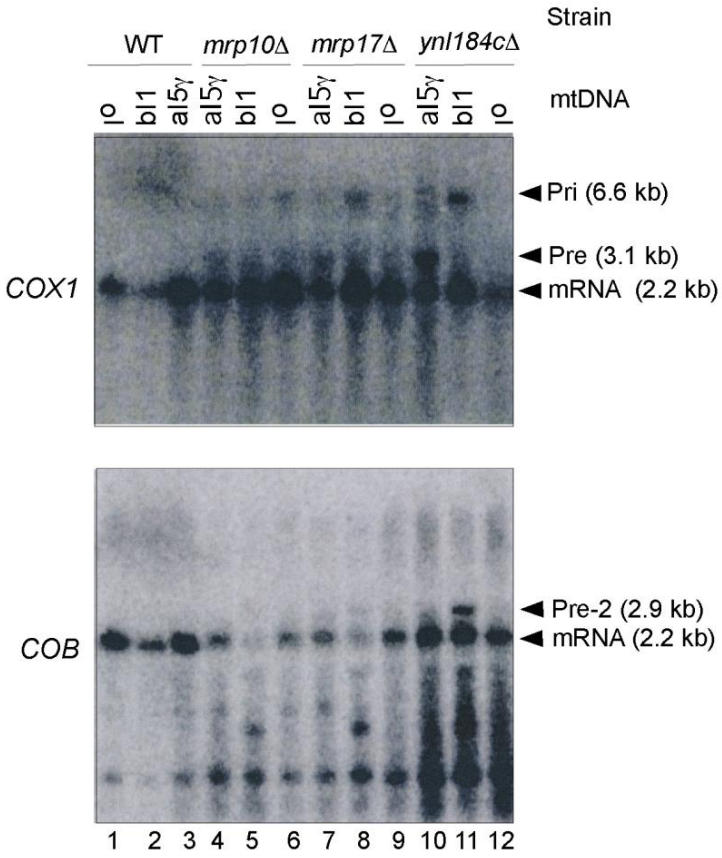

Mrp10: Mitochondrial ribosomal protein of the small subunit; contains twin cysteine-x9-cysteine motifs

Mrp17: Mitochondrial ribosomal protein of the small subunit; MRP17 exhibits genetic interactions with Pet122, encoding a COX3-specific translational activator

Ynl184c: Protein of unknown function; expressed at both mRNA and protein levels

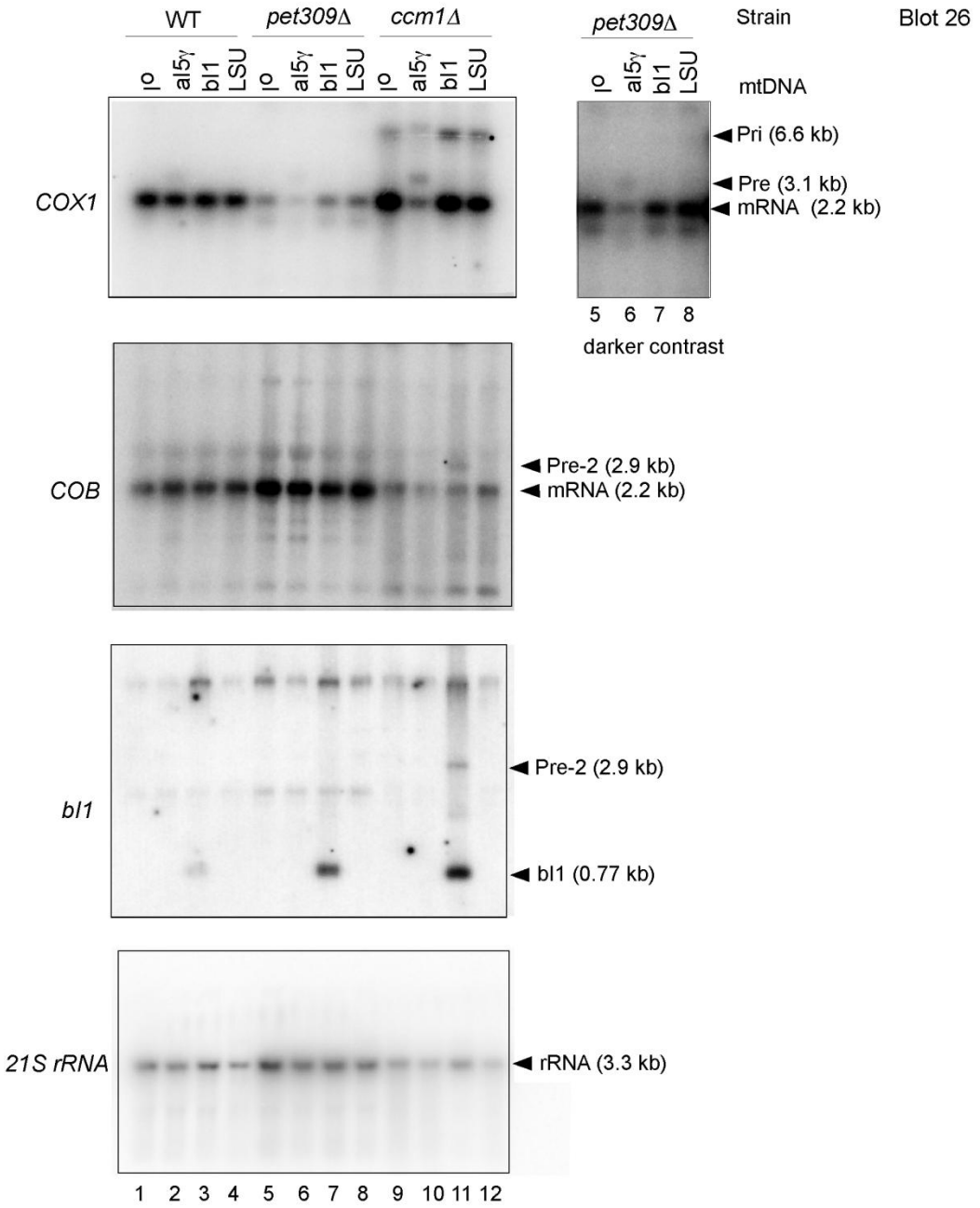

Pet309 : Specific translational activator for the *COX1* mRNA; also influences stability of intron-containing *COX1* primary transcripts; localizes to the mitochondrial inner membrane; contains seven pentatricopeptide repeats (PPRs)

Ccm1= Dmr1= Rrg2: Mitochondrial 15S rRNA-binding protein; required for intron removal of *COB* and *COX1* pre-mRNAs; has separable roles in stabilizing mitochondrial 15S rRNA and in maturation of the *COB* and *COX1* mRNAs; contains pentatricopeptide repeat (PPR) motifs; mutant is respiratory deficient and has defective plasma membrane electron transport

Blot 27

PET309 with 3X RNA

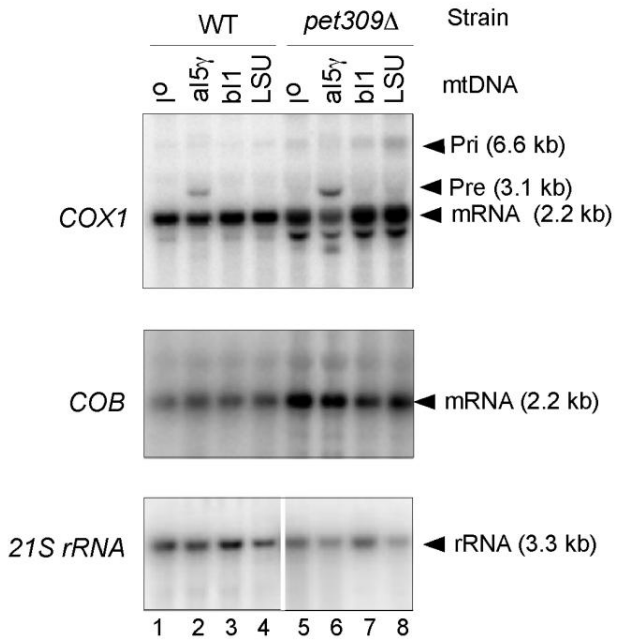

Pet309 : Specific translational activator for the *COX1* mRNA; also influences stability of intron-containing *COX1* primary transcripts; localizes to the mitochondrial inner membrane; contains seven pentatricopeptide repeats (PPRs)

Blot 28-KT

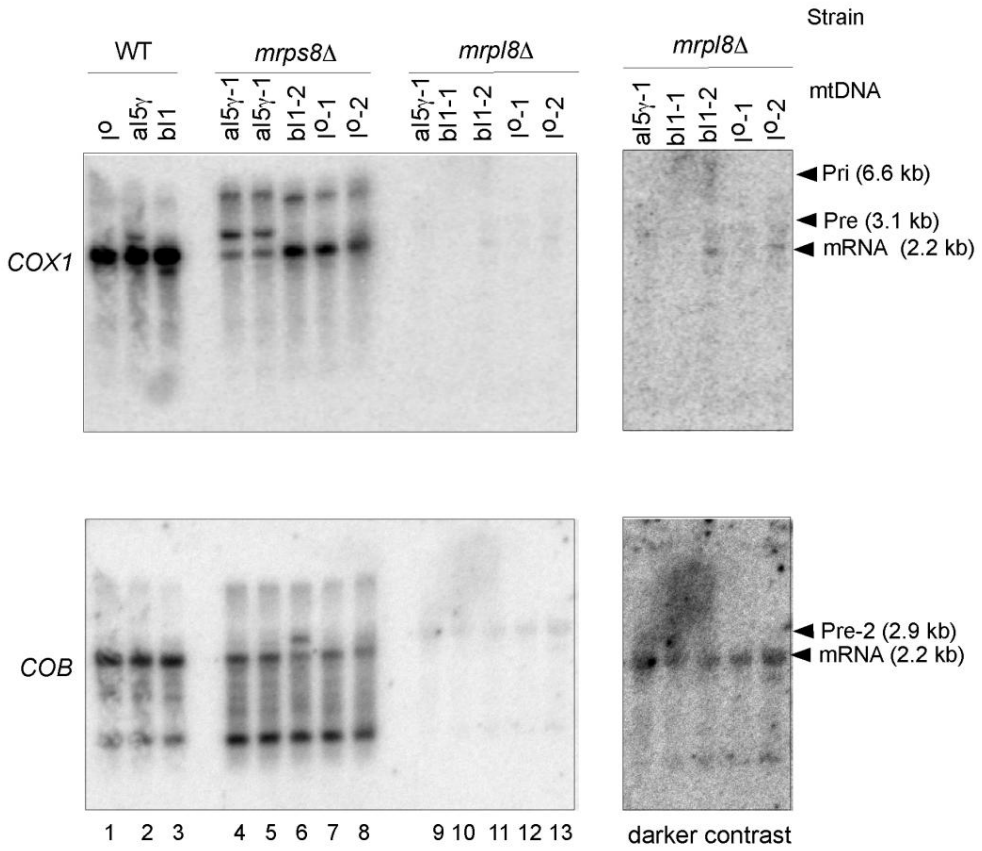

Mrps8: Mitochondrial ribosomal protein of the small subunit

Mrpl8: Mitochondrial ribosomal protein of the large subunit

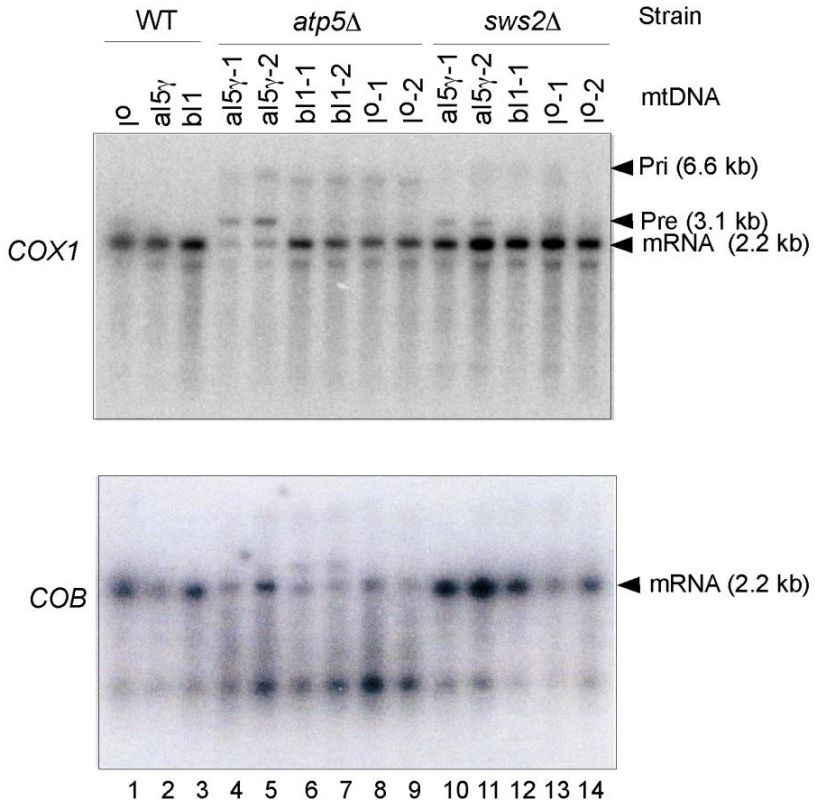

Atp5: Subunit 5 of the stator stalk of mitochondrial F1F0 ATP synthase; F1F0 ATP synthase is a large, evolutionarily conserved enzyme complex required for ATP synthesis; homologous to bovine subunit OSCP (oligomycin sensitivity-conferring protein); phosphorylated

Sws2: Putative mitochondrial ribosomal protein of the small subunit; has similarity to *E. coli* S13 ribosomal protein; participates in controlling sporulation efficiency

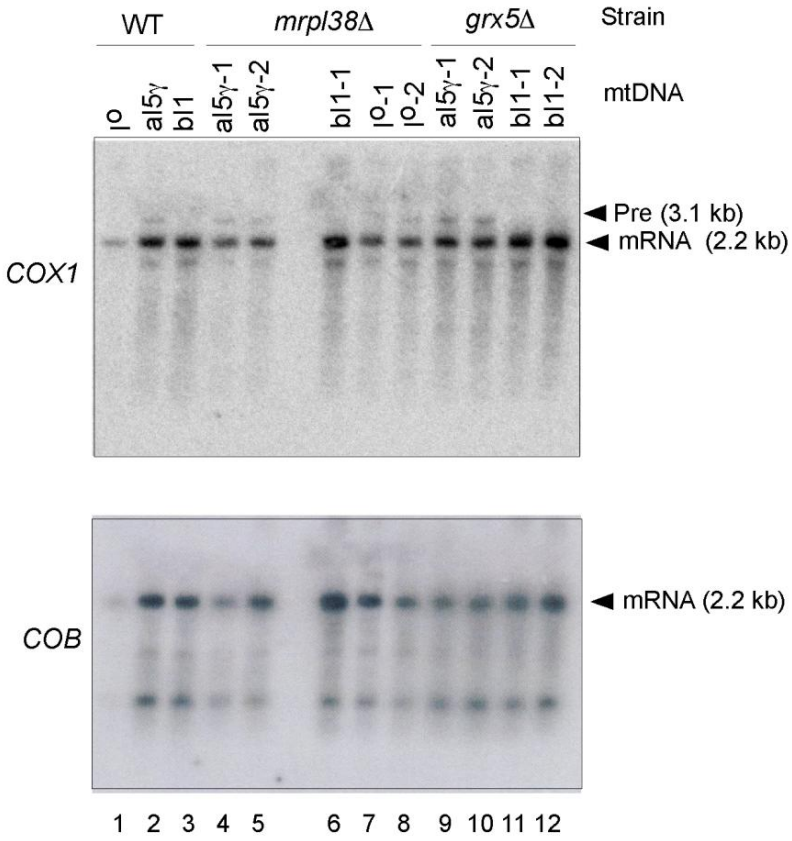

Mrpl38: Mitochondrial ribosomal protein of the large subunit; appears as two protein spots (YmL34 and YmL38) on two-dimensional SDS gels; protein abundance increases in response to DNA replication stress. Also known as: Mrpl34

Grx5:Glutathione-dependent oxidoreductase; hydroperoxide and superoxide-radical responsive; mitochondrial matrix protein involved in the synthesis/assembly of iron-sulfur centers; monothiol glutaredoxin subfamily member along with Grx3 and Grx4

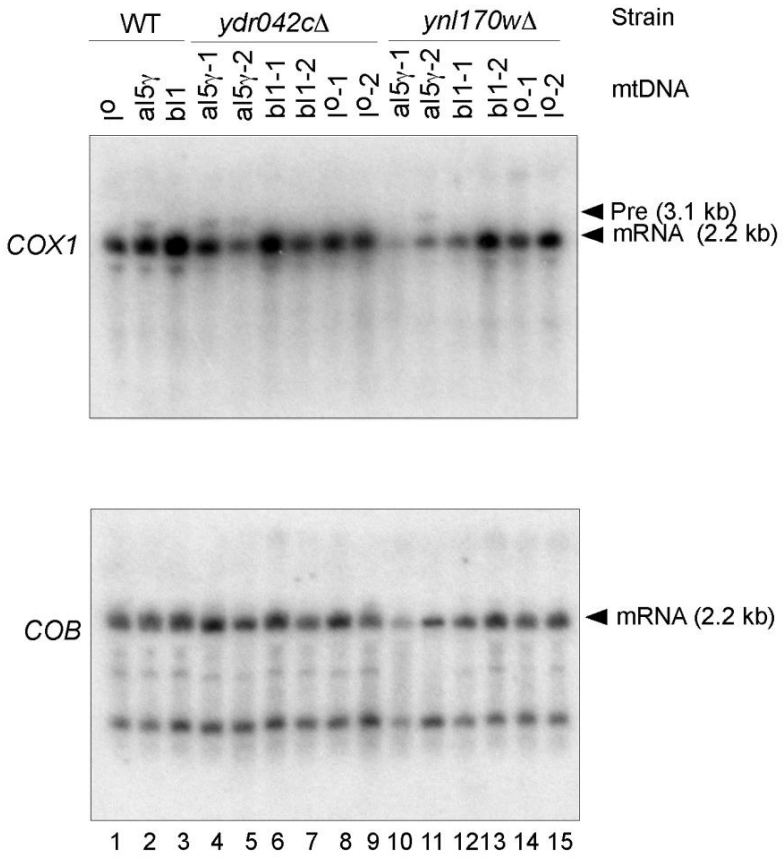

Ydr042C: Putative protein of unknown function; expression is increased in ssu72-ts69 mutant

Ynl170W: Dubious open reading frame; unlikely to encode a functional protein, based on available experimental and comparative sequence data

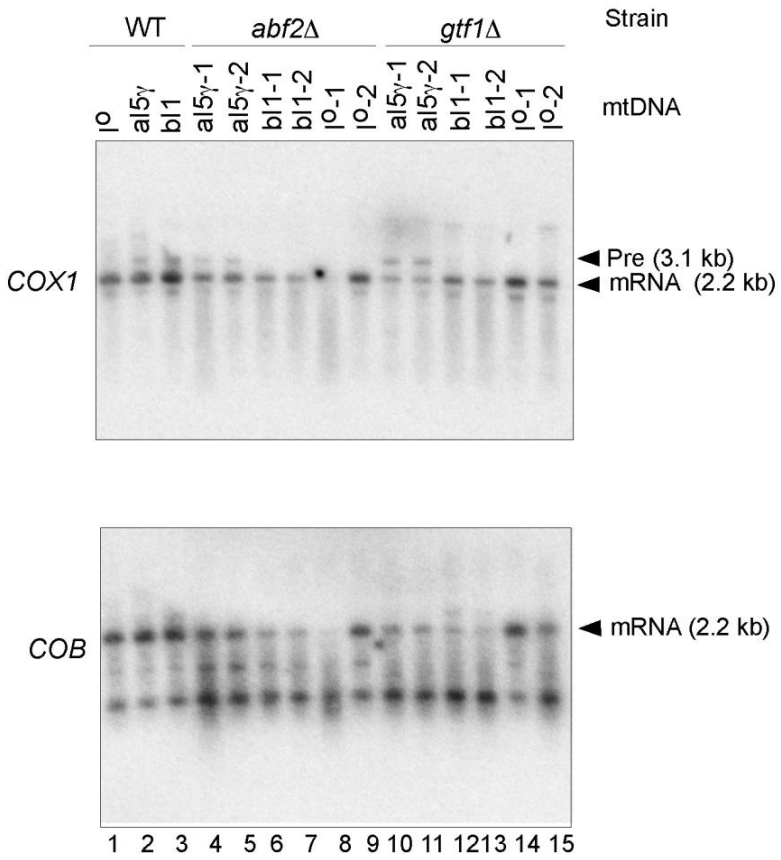

Abf2=Mitochondrial DNA-binding protein; involved in mitochondrial DNA replication and recombination, member of HMG1 DNA-binding protein family; activity may be regulated by protein kinase A phosphorylation; ABF2 has a paralog, IXR1, that arose from the whole genome duplication

Gtf1= Subunit of the trimeric GatFAB AmidoTransferase(AdT) complex; involved in the formation of Q-tRNAQ; transposon insertion mutant is salt sensitive and null mutant has growth defects; non-tagged protein is detected in purified mitochondria

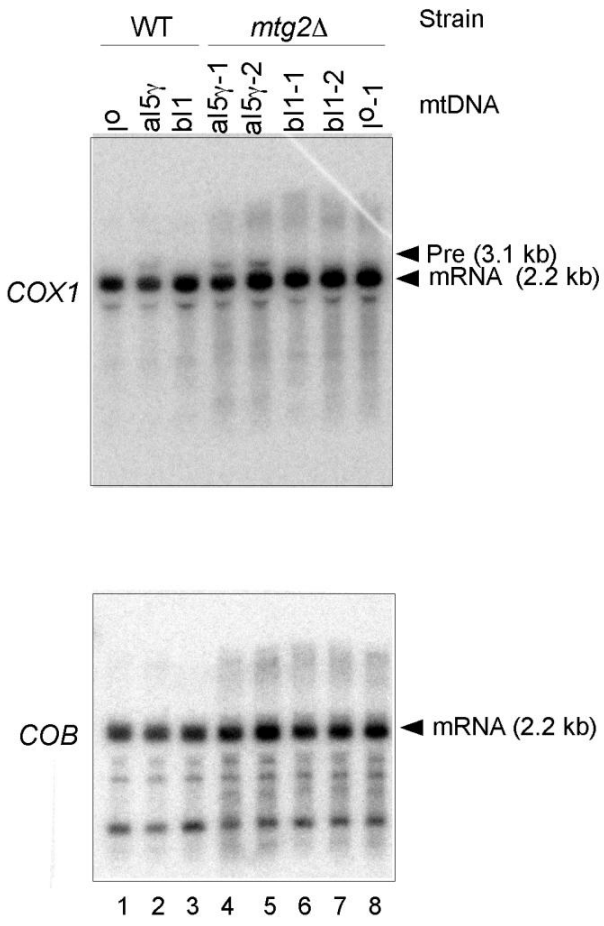

Mtg2= Putative GTPase; member of the Obg family; associates with the large mitoribosomal subunit; required for mt translation, possibly via a role in mitoribosome assembly.

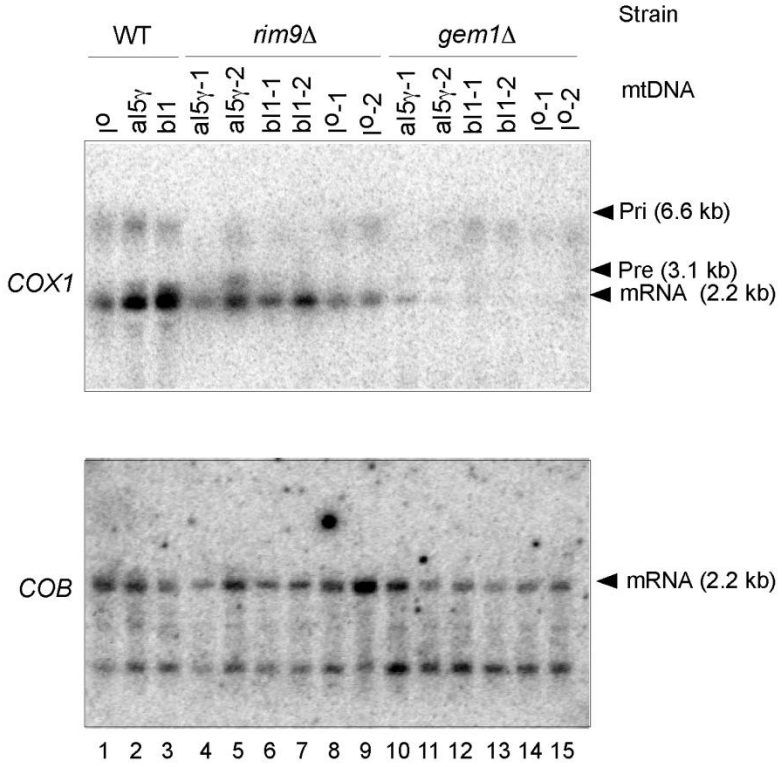

Rim9 =Plasma membrane protein of unknown function; involved in the proteolytic activation of Rim101 in response to alkaline pH; interacts with Rim21 and Dfg16 to form a pH-sensing complex in the Rim101 pathway and is required to maintain Rim21 levels; has similarity to *A. nidulans* PalI.

Gem1= Outer mitochondrial membrane GTPase, subunit of the ERMES complex; potential regulatory subunit of the ERMES complex that links the ER to mitochondria and may promote inter-organellar calcium and phospholipid exchange as well as coordinating mitochondrial DNA replication and growth; cells lacking Gem1 contain collapsed, globular, or grape-like mitochondria; ortholog of metazoan Miro GTPases.

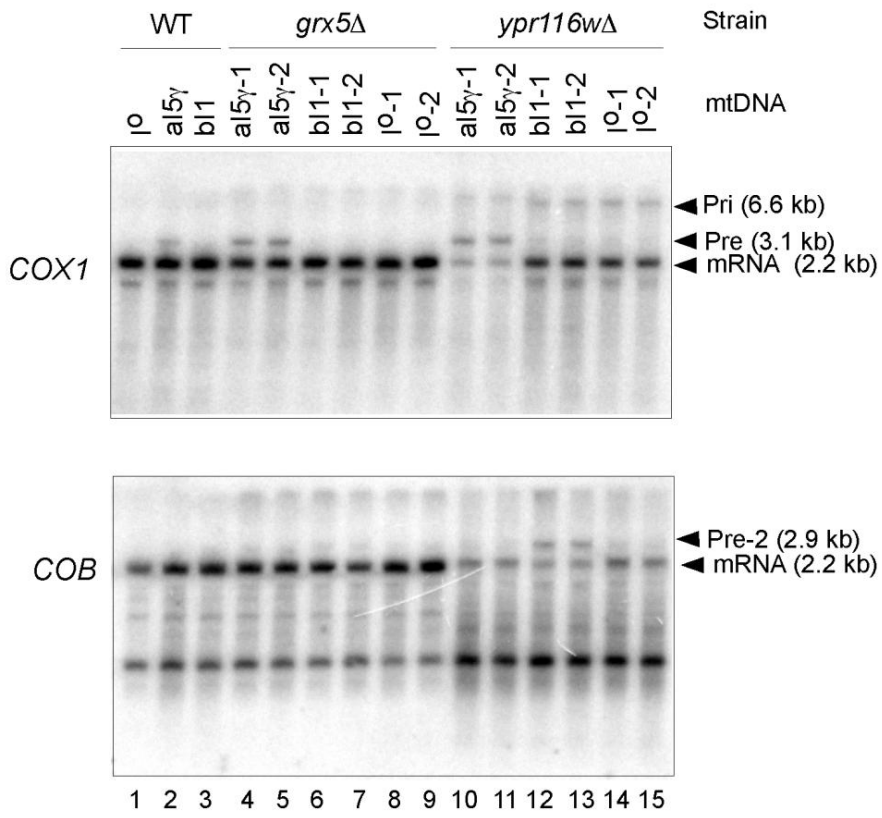

Grx5= Glutathione-dependent oxidoreductase; hydroperoxide and superoxide-radical responsive; mitochondrial matrix protein involved in the synthesis/assembly of iron-sulfur centers; monothiol glutaredoxin subfamily member along with Grx3 and Grx4

Ypr116W/Rrg8= Putative protein of unknown function; required for mitochondrial genome maintenance; null mutation results in a decrease in plasma membrane electron transport

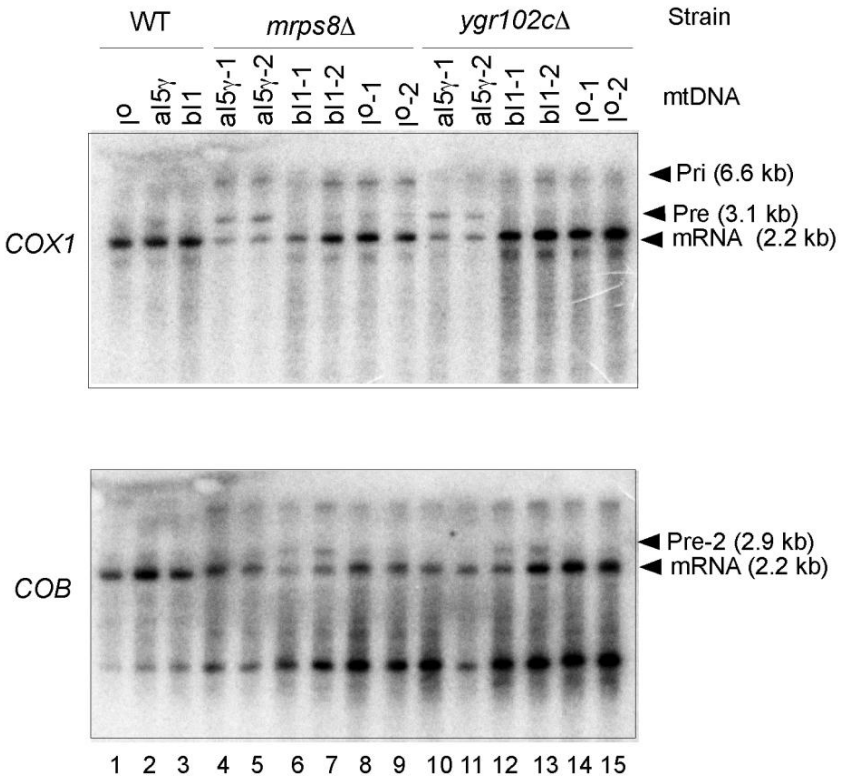

Mrps8: Mitochondrial ribosomal protein of the small subunit

Gtf1 =Ygr102C: Subunit of the trimeric GatFAB AmidoTransferase(AdT) complex; involved in the formation of Q-tRNAQ; transposon insertion mutant is salt sensitive and null mutant has growth defects; non-tagged protein is detected in purified mitochondria

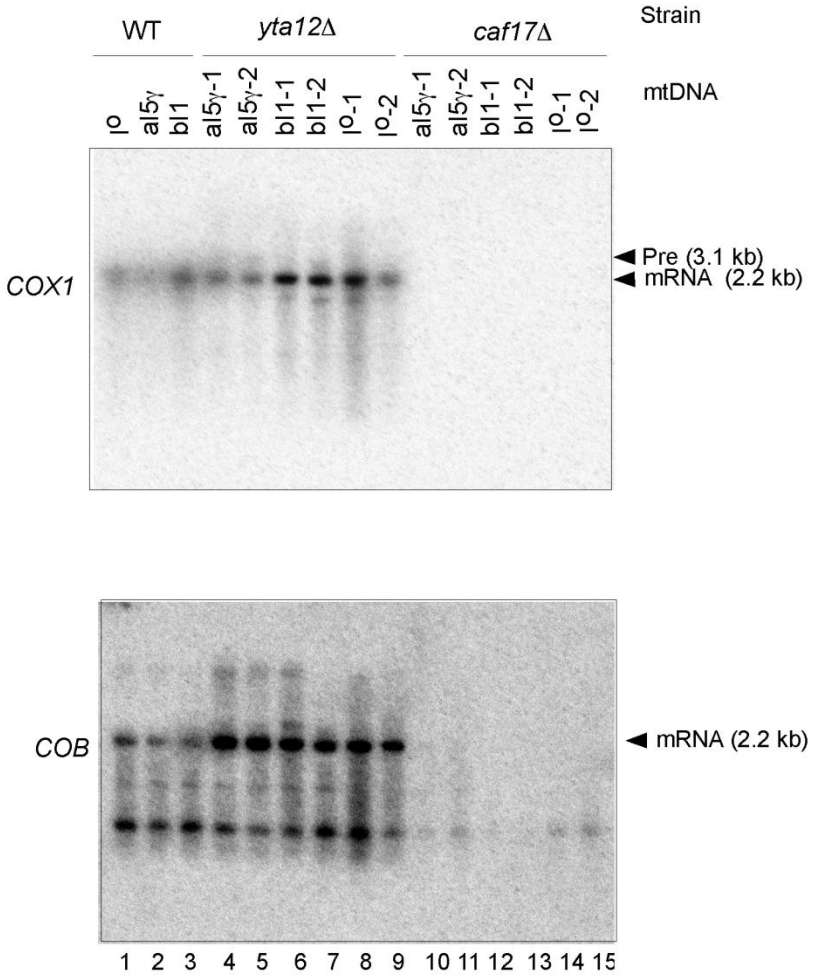

Yta12: Component, with Afg3, of mitochondrial inner membrane m-AAA protease; mediates degradation of misfolded or unassembled proteins; also required for correct assembly of mitochondrial enzyme complexes

Caf17: Protein involved in incorporating iron-sulfur clusters into proteins; mitochondrial matrix protein; involved in the incorporation of iron-sulfur clusters into mitochondrial aconitase-type proteins; activates the radical-SAM family members Bio2 and Lip5; interacts with Ccr4 in the two-hybrid system

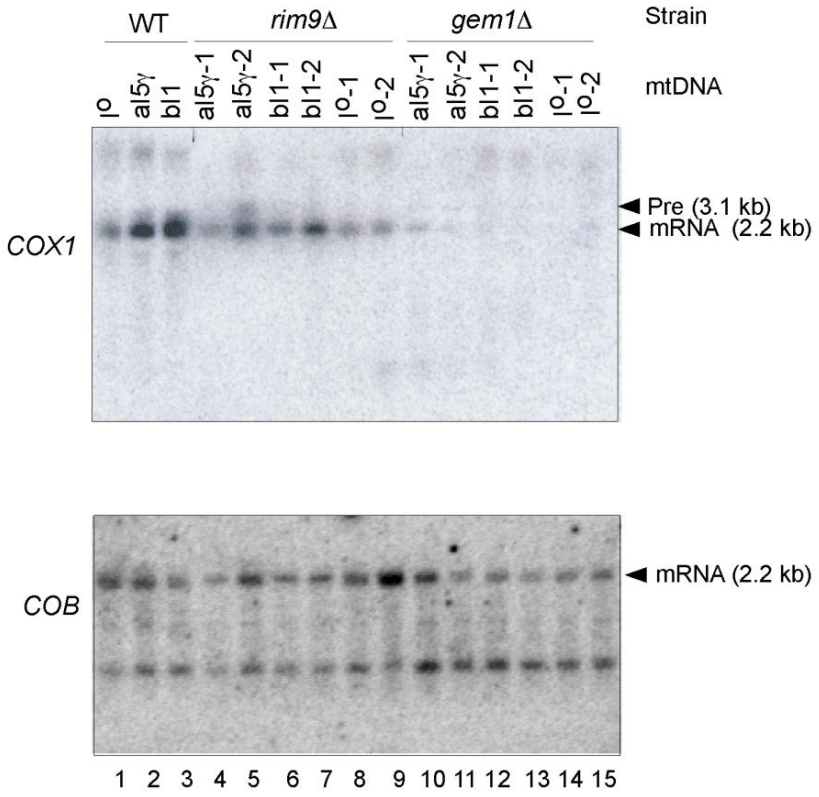

Rim9: Plasma membrane protein of unknown function; involved in the proteolytic activation of Rim101p in response to alkaline pH; interacts with Rim21p and Dfg16p to form a pH-sensing complex in the Rim101 pathway and is required to maintain Rim21 levels; has similarity to *A. nidulans* PalI

Gem1: Outer mitochondrial membrane GTPase, subunit of the ERMES complex; potential regulatory subunit of the ERMES complex that links the ER to mitochondria and may promote inter-organellar calcium and phospholipid exchange as well as coordinating mitochondrial DNA replication and growth; cells lacking Gem1 contain collapsed, globular, or grape-like mitochondria; ortholog of metazoan Miro GTPases

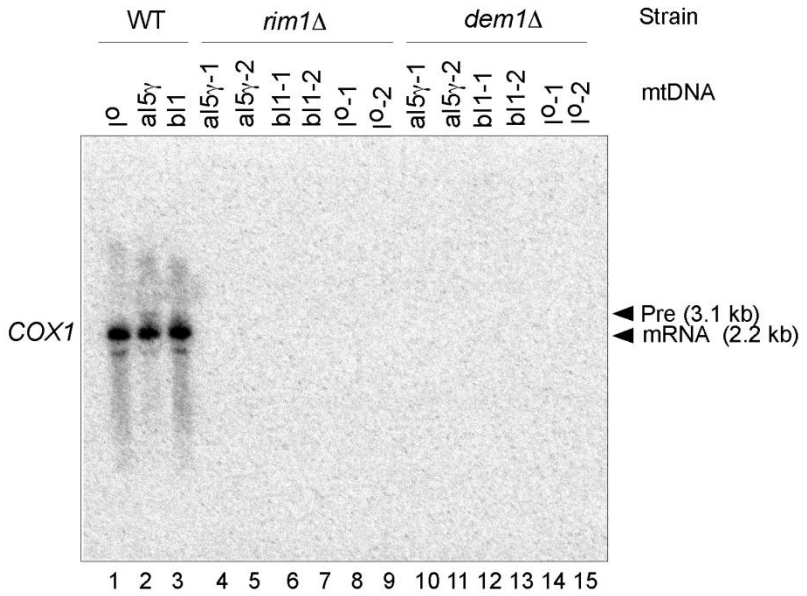

COB Northern not available

Rim1= ssDNA-binding protein essential for mitochondrial genome maintenance; involved in mitochondrial DNA replication

Dem1= Mitochondrial 5'-3' exonuclease and sliding exonuclease; required for mitochondrial genome maintenance; distantly related to the RecB nuclease domain of bacterial RecBCD recombinases; may be regulated by the transcription factor Ace2

APPENDIX B:

Listed below are the oligonucleotides (named ORF 5a and ORF 3a, forward and reverse primers, respectively) used to amplify the kanamycin cassette from the commercial strain BY4741 (Open Biosystems) for knocking out the genes in the 161-U7 strains used in Chapter 3. To confirm the gene replacement, a second set of oligonucleotides were used (named ORF 5b and ORF 3b, forward and reverse primers, respectively) situated outside of the original cassette.

IMG1 5a	AGAAGAAGAAGAAGAATCGAGTCTT
IMG2 5a	CTATAAGCAGTATAGCTCCAGCAAG
MRP1 5a	GTGAATCTCAAGGAGTAATCTTGC
MRP10 5a	TATATGATGACAGGTTCGTTCTCC
MRP17 5a	AGGATGATTTCTGATTAGGAGGAG
MRP20 5a	GTACATACATTTCTTGTGGAGAACG
MRPL11 5a	AGGGCTTAGTAGAGATTCATACAG
MRPL13 5a	TTATTCTTCGTTCTTTATCGCTGC
IMG1 3a	GATGTCTAGCACTTGAGTATACCT
IMG2 3a	GTAAGCAACTTCTTTTCGATGGC
MRP1 3a	CAATGAAGATGAGGAAGACGTTTA
MRP10 3a	GAATTAAGTACGGTTTAACGGAGG
MRP17 3a	TAATGGTGTCTATGTTAAGTGAGG
MRP20 3a	GTTTAGAGATTATGTAGTTTGCTCC
MRPL11 3a	TTATCCTATGGGAACTGCTGAATC
MRPL13 3a	ATTATTCCCTTACTGCTTCTTGAG
IMG1 5b	TATATCTGTATGTGAGTGGTCAATG
IMG2 5b	AAGACAAGTAACATACATGCACATA
MRP1 5b	GTAATCTTTCCCATATTCAGGCTC
MRP10 5b	ATTGATCCGTGTTTATTTCCCTTC
MRP17 5b	TTCTTTCCAAATACCCACTCAAAC
MRP20 5b	TAGAGAATAAATCGACGAAGTGAG
MRPL11 5b	CATCTCAAGCCATCTTCAATACAC
MRPL13 5b	CTATTAGTTTATCGTTGGTGTTTGC
IMG1 3b	CTGTTGGAATTCGAAGTGAATTGTT
IMG2 3b	AACGATAAAGCCTACACACCTTTAA
MRP1 3b	GGAGAGATGATACAGATGATTCTGA
MRP10 3b	TGAGAAAGGACTCCAATAATCCAG
MRP17 3b	CCCTTCGTTATTTGATGGATCTAC
MRP20 3b	CAACATAAGAAGGCAATTTGGTCC
MRPL11 3b	TCTTTACATGCTTCAACTCCTTAC
MRPL13 3b	TTTCGTTTCTTCACATGGATCTTG
MRPL16 5a	CTAGGCTTTGTATCCAGTTGAATC
MRPL27 5a	TCAAGAGCTTCCTTACCATATAAC

YDR114C 5a	CCCTTGATTTCCATCTTCTTTGAC
MRPL16 3a	TTTCACGTCGTCATGTGTTTCTTC
MRPL27 3a	GTTATCGGTGAATCTTTGGGTTTG
YDR114C 3a	TAAGCAACCTACGCTAACAAATAC
MRPL16 5b	TACCCAAGTCCAAATCTGTTTCAC
MRPL27 5b	GGAAATGCAACAATGGATAAGATG
YDR114C 5b	AGGTACGGTGAGTGATGATATAAG
MRPL 37 5b	CGCAAACTTTAATAGCAACACAAC
MRPL16 3b	GTACTTCTTTCTTTGATAGCCACC
MRPL27 3b	TGGTATTTGGTTTGCTGATAAGTG
YDR114C 3b	TCTTTATCTTCGTTAGCTGGCATC
MRPL6 5a	ATTATTGGTTGTGATTATGCCTGG
MRPL7 5a	AGTAATAGACAGGACCGGAAATAG
RML2 5a	ATTGAAAGAGAAAGGGAACGTATG
MRPL6 3a	GGTTTCTAGTCTAAATGGTGTTCC
MRPL7 3a	GAGTTGAGTTGTGAGTTGTGTAAG
RML2 3a	TACAACCTCAAATCATATCGGTCC
MRPL6 5b	TTGACTGCATCTTGTATAGTTTCC
MRPL7 5b	CCTTAATGACTTACCCATACTCTTC
RML2 5b	AGAGCCTAATTCTTTGATAGTTCC
MRPL6 3b	AGTTCGAGAAATTGGAAGGTACAG
MRPL7 3b	TGCTAAGAAGACCAATAAACTTGC
RML2 3b	TGAAGTGATTAAAGTGACGAACAG
YNL184C 5a	CACTTGGTTGAAGATGGATTATCG
YNL184C 3a	CCTTCCATCTCCAATAAACTATGC
YNL184C 5b	TAATGTTAATATCGGGCCACAAAG
YNL184C 3b	TCAGTAGAAAGAAGAAGGAAGGTC
DIA4 5a	TCGTCAACTACAACCATTTATTGC
MSD1 5a	TCATGGTTGGAGTATTGCTATTTG
MSE1 5a	GGTGAAACTTCTAACTACTCATTCG
MSM1 5a	CACACTTACTTCCTTGTATAGTGC
MST1 5a	TATCACGCTTGGAGACCATTTATC
MSU1 5a	ATATCAATGCAAACCCGAATAAGC
DIA4 3a	AAACTGAAAGGTGTTACGGAAATC
MSD1 3a	GTAAACGTAGACTTTGGGAGATTG
MSE1 3a	AGTATAGTTTCGGTTTCGTTCGAG
MSM1 3a	ACAGGAAATGTAACATGGGAATATC
MST1 3a	GAGGAACCTCAAGACAAAGTAAAG
MSU1 3a	TTATAGTGGAGAAGAGAACCATCG
DIA4 5b	AAGCATCAATAGCCACCAAATAAG
MSD1 5b	GATTAGCAGATATTTGTAGCGGAG
MSE1 5b	GAAAGACTTGGAGACCATTAAAGC
MSM1 5b	ATATCTATGGTGTCGCTTTGTTTG
MST1 5b	ACTAACTACTTTGGACGTGACCTC

MSU1 5b	ACATTAACCAAAGCACTATCAGAG
DIA4 3b	TCTGATGCTTTATCTTTCTTCGTG
MSD1 3b	TGACAAGTAACGGCTGTGATAATG
MSE1 3b	GCCTTCCACTCTTCTAATTTCATC
MSM1 3b	AACAACTTCATGTTTGATTCCGAC
MST1 3b	CTGATGACAAGACAACTACTGAAG
MSU1 3b	TAGCCTTTCTCATAACTTCCCTTTC
NAM2 5a	GAATCAAAGAAACCGAAGAAAGTC
PET56 5a	TCATCTTTGCCTTCGTTTATCTTG
SUV3 5a	AAACCAGAATAACAGTAAGAGCAC
MRH4 5a	AGTATCTCTTTATTCTCTGGCCTG
YOR199W 5a	TGTAACTTCTTACGTTCTTGTTGG
YOR200W 5a	ATGAAACTGAACGAAGAAATGACC
RPO41 5a	TGATTATCAACAATACGCTGCTTC
NAM1 5a	TTATATTACTGCTCAACTTCCATGC
SLS1 5a	TAGCTCTTCTTCCACTTCTGTTTC
AEP3 5a	AATGATAACACTAACACAGGCTTC
MTF1 5a	TTTGAATGGTAACACTGTCTCTTG
NAM2 3a	AGAGTCTCTCAAAGTATAGCGTTC
PET56 3a	GAACGAAGAAATGACCAGAATGAG
SUV3 3a	AGGATAGAGAACCCTGGAATGAAC
MRH4 3a	GATTACACTATGTCCTTGTTGCTG
YOR199W 3a	ACGATTTGAACGGATTATGTAACG
YOR200W 3a	ATAGTCGATGAACTGAAGGTTACG
RPO41 3a	TGCAAACGATAAACGCTAAGTATG
NAM1 3a	TGAATTTGAAATCTGCCGAACAAG
SLS1 3a	CGAAAGACAAAGAAGGTTAAATGC
AEP3 3a	AGTCGAAGAAGAGGAAGTTGAATG
MTF1 3a	ATTTAGCTTTGACGGTTCGTAGAG
NAM2 5b	AGTCAGTGAAAGTAGCTCATCATC
PET56 5b	CCTATACCTGTGTGGACGTTAATC
SUV3 5b	GAAGTGCAATCATCGTTAAAGGAG
MRH4 5b	GGGTGGACCAATGAGTATAAATTC
YOR199W 5b	CTCATTGATTCTTTGCTTGGCTTC
YOR200W 5b	TGCTTAATAGAGTCGTGAATGTTG
RPO41 5b	GCTTCCAAAGAAAGAAGATTACAAC
NAM1 5b	TTAAACAAGCCGAACAAGAACAAG
SLS1 5b	ATGTACTTTGGAAGGATGGAACTC
AEP3 5b	CTGCTTTACTTTCATTGTTTGGTG
MTF1 5b	TTCTAGGGCATATACTTCTTCCTC
NAM2 3b	CAATACCCGTCAACAAACAAATTC
PET56 3b	TGCTTAATAGAGTCGTGAATGTTG
SUV3 3b	TGTAGTATGGTGCGTTAGTCATAG
MRH4 3b	AACATCAAAGTGGCAGAACTAAAG
YOR199W 3b	ATAGTCGATGAACTGAAGGTTACG
YOR200W 3b	GTGTTATGACTTCCCTGACTAATG

RPO41 3b	CAAACAATAGACAGGTTTCACTGC
NAM1 3b	GTATAAGGAAAGGCAATATCGCTC
SLS1 3b	TTAACAGCAGTAGGACTAAAGAGC
AEP3 3b	CAATTAGGAACATTGAAGCCTCTG
MTF1 3b	CAAAGCAGCAGAATTATTCAAAGC
AEP1 5a	CAGATAGTCTGATTGCTCCAGAAG
MEF2 5a	CAGAGATCCGAACAAATGATAGTC
MTG1 5a	GTCCGTGGAACAAACAATCAATAG
PET309 5a	ACCTTATACTCCCTCGTAAACTTC
SOV1 5a	GAGATTCTATATCATGGGCACAGG
TUF1 5a	TCTATTATACTGACAACCCTGTTACC
OCT1 5a	AAAGCGAAATGGATCAGAGAATAC
OXA1 5a	ATGACGTGTTCCGTTCTTATGTTC
AEP1 3a	GTATATCAATCTTCCTTGCAGCAG
MEF2 3a	GCCACGAGGAACAAGAATATAAAG
MTG1 3a	GAGTTAATGGGTGGTGTATCAATC
PET309 3a	GTTTGCTAACTTACGGTGAAACTG
SOV1 3a	ACGTTAAACCAATCTCATCCTTTC
TUF1 3a	AATACGCCGGAAAGTAAACAAATC
OCT1 3a	GGGAAAGTGTTCTTTATATCGTAGG
OXA1 3a	TCATGCTATGGTGAACGACTTTAC
AEP1 5b	CTCACCTGAGATGTTATTGTTCAC
MEF2 5b	ACATCATGTATTACCAGCCTCTTC
MTG1 5b	AGATCACTCTACGAGACAATAGAC
PET309 5b	ATCTCCTTCTTCTCGTCTAGTTTC
SOV1 5b	AAATACTACTGGTTACTGTGCTCC
TUF1 5b	CGTCCACGAATGAAGATTCTAAAG
OCT1 5b	ATTGGTAAATCCAAACCTGACATC
OXA1 5b	GACCATTCGTTCTTTATCACTAGG
AEP1 3b	TTTCCACTATAAGTTGTCCACCAC
MEF2 3b	ATTTGCTTTCTACGTGTGATAGAC
MTG1 3b	AGGCATTGGAAGTTGACTATATTG
PET309 3b	GATGATGCTGTGATTGATGTGAAC
SOV1 3b	GACAAAGAGACTTAGAGAGCAATC
TUF1 3b	ATTCAAACTCTTCGTCATCCATAC
OCT1 3b	AATTAAGGGATTTGGATCTTGTGC
OXA1 3b	GACGTTTGTGAAAGAGAGAATACC
PIM1 5a	TAATGTATGGGTGCTTTGTAAAGG
YDL104C 5a	ACAAGTTTGGGTGCTTAGAAGTAG
SSQ1 5a	GATAATGATAAGTTGTGGGAGAGC
MET7 5a	ATTGGAACTGATAGAAGGTTGTTG
MGM1 5a	ATGGATCTAGTGTACTCTTTGAGG
MGM101 5a	AGCAGCAAACGCTAATAAGGTAAC
PIM1 3a	TTTACTTTCTGGTTTCGTTTCTCG
YDL104C 3a	AACATCACTTCACCATTCTTAGAC

SSQ1 3a	GGGTTTCCCTCTGAATAATGTTTAC
MET7 3a	CAGCAATGCCTAACAAATCAAATC
MGM1 3a	CAGATGTGTCTCTGCATACTGTAG
MGM101 3a	AAAGGGTAAGGGTATCAAGTTGTC
PIM1 5b	AGCAGGACTAAGCTAGATAGTAAC
YDL104C 5b	TTGGATCAGTGGTGTGAGAATATG
SSQ1 5b	GATTACGCGATATGTTTCCATACG
MET7 5b	GTAATTTACCTGATGGCGTCGAAC
MGM1 5b	AATCCGATCATACATACCCATCTC
MGM101 5b	ACCCAATCTCATCAAACTTAAAGG
PIM1 3b	GGCAACATTTCTCAATAGCCTATC
YDL104C 3b	CTCAACGAAGAAGGAATAATGACC
SSQ1 3b	TTGGTATTATCAGTCTCTCCACTC
MET7 3b	TGACAGTAATAAGCAAACAGAAGC
MGM1 3b	AAGGTACTGCATTGTCAAGATTAG
MGM101 3b	GGTAAGGTCAAGAAGGTTCAATTAG
MMM1 5a	AAGAACCGTCAACATCCAATAAAG
ADH3 5a	ACATTTGAGGAATCGTATCGAAAC
ATP22 5a	TGTAACGAACGTATGAATGAAAGC
INH1 5a	CTTTCTTTGAATTTGTTCGTGGTTG
ISA2 5a	CGACTGTACTGTTTGTTCAAATTCC
MMM1 3a	GAAGGACCAATTCTGTCAAGAAAG
ADH3 3a	GAGAGTAATATCGAAGTGTGCAAG
ATP22 3a	ATCATTAAATCTAGGCTTGCCATC
INH1 3a	CACACTGTTCCTATCTTTCTATGC
ISA2 3a	TATATGAGATGGAAGGAAGTTCTCG
MMM1 5b	TCGTATTCATCACTTGTCTTGTTC
ADH3 5b	CGTCAGTGCAGGATATAAATGTAG
ATP22 5b	AAATATCTCTGTGCTCGATGTACC
INH1 5b	GGATGACCAAATCAAGGAAGTTAC
ISA2 5b	AATTTGCATCCCGTTCATAGATGG
MMM1 3b	TATTCTCAGTGTTGGGCTGTATTG
ADH3 3b	GATTCCATACACTACGTGCTAGTC
ATP22 3b	TATCAACAATGGAATCCCAACAAG
INH1 3b	TGAAATACTAAACAGCGCAGAAAG
ISA2 3b	AATAATTGAATGTGGTGGTGATGG
YLR091W 5a	TAAATACTGAAGATGACAGCAACC
CAF17 5a	TAAGTTGTAAGTTTGCCTCAACAG
FMP38 5a	CCCATCTCCACTTATTCTATTGTTG
YLR091W 3a	TAACCTTCCCTGGACATATCTTAG
CAF17 3a	ATTATGGGTATATGGGTGTTGTTG
FMP38 3a	TTTATTGACTCGCCTTATACTCTAC
YLR091W 5b	TGTCAAAGAAGGAAATCATCACAG
CAF17 5b	TTCTTATCTCAACCATTTGCTGTC
FMP38 5b	GTTTCTTTCAGCATCTTCACCTTC

YLR091W 3b	TAGGAGTAAGCACCAATAAACGAG
CAF17 3b	GGTAGAAAGAAACAAGGCTTTACG
FMP38 3b	CTGTGTTGTTTGTTTCTCTCTAGC
YGR150C 5a	CCTTGTCGCACATTATCTTACTTC
GLO3 5a	AGTACCTAGATGTTACGAATGCTG
LCB5 5a	TTCAACTGTACTTCTTTGCACAAC
YGR150C 3a	GCTACCTACTATATCGACCACTAC
GLO3 3a	TGCAAGTGTTTCTAACGAATATGG
LCB5 3a	TTGATATTTCTACAGCAGAGGAGC
YGR150C 5b	GTCATCCCTCCTTTAATACGAAAC
GLO3 5b	TGCTCTAACTCTATCAATCATTTGC
LCB5 5b	CTTTATGAGAGGAGTAAGCACGAC
YGR150C 3b	CCCTTTATTATTTGGTTTGGCAATC
GLO3 3b	AATACATAAACAGCCACCTACTTTC
LCB5 3b	ATTACAGTTATGGGATACAGCAGG
PKH2 5a	TATATTCACATTTCTGAGGCAGAG
RNR1 5a	CTTATTGGGTGTTGAATAGAGGAC
GON1 5a	TAACGGCAACTCCAAATAAAGAAC
NRP1 5a	GAAGACGATGAAGACAGTGAGTAG
PKH2 3a	CTCAAGGTTTCACTGTCGAAATAG
RNR1 3a	TTGAAATAAAGGATGGAAGGAGTG
GON1 3a	TTGTTCTGCTGTAGTTAGACGTAG
NRP1 3a	GTCGAAGAATTTATCACTCACAGG
PKH2 5b	AGACTATTGCTTCTGATCCTTCTG
RNR1 5b	TTTCTATGGCCTTTGTTTACTATCG
GON1 5b	AACCAAAGAACTGGAAACTCAGAC
NRP1 5b	TAAAGATGGAAGCAAGACGGTATG
PKH2 3b	GAATTGTATTTGGAAAGGTTGCAG
RNR1 3b	GTCTCTATACATTTCCCAGTTTGC
GON1 3b	TCAGGAGAATGTCTTTGAAACCAG
NRP1 3b	TTTACTGGGTTGTGGTGTTACTAC

References

Agatep, R., R. D. Kirkpatrick, D. L. Parchaliuk, R. A. Woods and R. D. Gietz. (1998). "Transformation of Saccharomyces cerevisiae by the lithium acetate/single-stranded carrier DNA/polyethylene glycol (LiAc/ss-DNA/PEG) protocol." Technical Tips Online, from http://tto.trends.com.

Akins, R. A. and A. M. Lambowitz (1987). "A protein required for splicing group I introns in Neurospora mitochondria is mitochondrial tyrosyl-tRNA synthetase or a derivative thereof." Cell **50**(3): 331-345.

Alper, H., C. Fischer, E. Nevoigt and G. Stephanopoulos (2005). "Tuning genetic control through promoter engineering." Proceedings of the National Academy of Sciences of the United States of America **102**(36): 12678-12683.

Altamura, N., N. Capitanio, N. Bonnefoy, S. Papa and G. Dujardin (1996). "The Saccharomyces cerevisiae OXA1 gene is required for the correct assembly of cytochrome c oxidase and oligomycin-sensitive ATP synthase." FEBS Lett **382**(1-2): 111-115.

Amberg, D. C., D. J. Burke and J. N. Strathern (2005). Methods in Yeast Genetics: A Cold Spring Harbor Laboratory Course Manual, Cold Spring Harbor Laboratory Press.

Amunts, A., A. Brown, X. Bai, J. L. Llácer, T. Hussain, P. Emsley, F. Long, G. Murshudov, S. H. W. Scheres and V. Ramakrishnan (2014). "Structure of the Yeast Mitochondrial Large Ribosomal Subunit." Science **343**(6178): 1485-1489.

Ashburner, M., C. A. Ball, J. A. Blake, D. Botstein, H. Butler, J. M. Cherry, A. P. Davis, K. Dolinski, S. S. Dwight, J. T. Eppig, M. A. Harris, D. P. Hill, L. Issel-Tarver, A. Kasarskis, S. Lewis, J. C. Matese, J. E. Richardson, M. Ringwald, G. M. Rubin and G. Sherlock (2000). "Gene ontology: tool for the unification of biology. The Gene Ontology Consortium." Nat Genet **25**(1): 25-29.

Azuma, M., Y. Kabe, C. Kuramori, M. Kondo, Y. Yamaguchi and H. Handa (2008). "Adenine nucleotide translocator transports haem precursors into mitochondria." PLoS One **3**(8): e3070.

Banroques, J., A. Delahodde and C. Jacq (1986). "A mitochondrial RNA maturase gene transferred to the yeast nucleus can control mitochondrial mRNA splicing." Cell **46**(6): 837-844.

Banroques, J., M. Doère, M. Dreyfus, P. Linder and N. K. Tanner (2010). "Motif III in Superfamily 2 “Helicases” Helps Convert the Binding Energy of ATP into a High-Affinity RNA Binding Site in the Yeast DEAD-Box Protein Ded1." Journal of Molecular Biology **396**(4): 949-966.

Barros, M. H., A. M. Myers, S. Van Driesche and A. Tzagoloff (2006). "COX24 Codes for a Mitochondrial Protein Required for Processing of the COX1 Transcript." Journal of Biological Chemistry **281**(6): 3743-3751.

Barros, M. H., M. Rak, J. A. Paulela and A. Tzagoloff (2011). "Characterization of Gtf1p, the connector subunit of yeast mitochondrial tRNA-dependent amidotransferase." J Biol Chem **286**(38): 32937-32947.

Bifano, A. L., E. M. Turk and M. G. Caprara (2010). "Structure-Guided Mutational Analysis of a Yeast DEAD-Box Protein Involved in Mitochondrial RNA Splicing." Journal of Molecular Biology **398**(3): 429.

Bohnert, M., P. Rehling, B. Guiard, J. M. Herrmann, N. Pfanner and M. van der Laan (2010). "Cooperation of stop-transfer and conservative sorting mechanisms in mitochondrial protein transport." Curr Biol **20**(13): 1227-1232.

Bordonne, R., G. Dirheimer and R. P. Martin (1988). "Expression of the oxi1 and maturase-related RF1 genes in yeast mitochondria." Curr Genet **13**(3): 227-233.

Borst, P. and L. A. Grivell (1978). "The mitochondrial genome of yeast." Cell **15**(3): 705-723.

Bousquet, I., G. Dujardin, R. O. Poyton and P. P. Slonimski (1990). "Two group I mitochondrial introns in the cob-box and coxI genes require the same MRS1/PET157 nuclear gene product for splicing." Curr Genet **18**(2): 117-124.

Bousquet, I., G. Dujardin, R. O. Poyton and P. P. Slonimski (1990). "Two group I mitochondrial introns in the cob-box and coxI genes require the same MRS1/PET157 nuclear gene product for splicing." Curr Genet **18**(2): 117-124.

Bryan, A. C., M. S. Rodeheffer, C. M. Wearn and G. S. Shadel (2002). "Sls1p Is a Membrane-Bound Regulator of Transcription-Coupled Processes Involved in Saccharomyces cerevisiae Mitochondrial Gene Expression." Genetics **160**(1): 75-82.

Callegari, S., R. A. McKinnon, S. Andrews and M. A. de Barros Lopes (2011). "The MEF2 gene is essential for yeast longevity, with a dual role in cell respiration and maintenance of mitochondrial membrane potential." FEBS Lett **585**(8): 1140-1146.

Cao, W., M. M. Coman, S. Ding and A. Henn, Middleton ER, Bradley MJ, Rhoades E, Hackney DD, Pyle AM, de la Cruz EM (2011). "Mechanism of Mss116 ATPase reveals functional diversity of DEAD-Box proteins." J Mol Biol **409**(3): 399-414.

Cate, J. H., A. R. Gooding and E. Podell, Zhou K, Golden BL, Kundrot CE, Cech TR, Doudna JA (1996). "Crystal Structure of a Group I Ribozyme Domain: Principles of RNA Packing." Science **273**(5282): 1678-1685.

Cavalier-Smith, T. (1991). "Intron phylogeny: a new hypothesis." Trends in Genetics **7**(5): 145-148.

Cech, T. R. (1986). "The generality of self-splicing RNA: Relationship to nuclear mRNA splicing." Cell **44**(2): 207-210.

Cech, T. R. (1990). "Self-Splicing of Group I Introns." Annual Review of Biochemistry **59**: 543-568.

Cech, T. R. (1993). The RNA World. The RNA world: the nature of modern RNA suggests a prebiotic RNA world. J. F. Atkins and R. F. Gesteland. Cold Spring Harbor, NY, Cold Spring Harbor Laboratory Press**:** 239-270.

Chen, W. and C. L. Dieckmann (1994). "Cbp1p is required for message stability following 5'-processing of COB mRNA." Journal of Biological Chemistry **269**(24): 16574-16578.

Chen, X. J., M. X. Guan and G. D. Clark-Walker (1993). "MGM101, a nuclear gene involved in maintenance of the mitochondrial genome in Saccharomyces cerevisiae." Nucleic Acids Res **21**(15): 3473-3477.

Chiron, S., A. Suleau and N. Bonnefoy (2005). "Mitochondrial Translation: Elongation Factor Tu Is Essential in Fission Yeast and Depends on an Exchange Factor Conserved in Humans but Not in Budding Yeast." Genetics **169**(4): 1891-1901.

Coppee, J. Y., K. J. Rieger, A. Kaniak, J. P. di Rago, O. Groudinsky and P. P. Slonimski (1996). "PetCR46, a gene which is essential for respiration and integrity of the mitochondrial genome." Yeast **12**(6): 577-582.

Cordin, O., D. Hahn and J. D. Beggs (2012). "Structure, function and regulation of spliceosomal RNA helicases." Curr Opin Cell Biol **24**(3): 431-438.

Costanzo, M. C., E. C. Seaver and T. D. Fox (1989). "The PET54 gene of Saccharomyces cerevisiae: characterization of a nuclear gene encoding a mitochondrial translational activator and subcellular localization of its product." Genetics **122**(2): 297-305.

Crabtree, H. G. (1928). "The carbohydrate metabolism of certain pathological overgrowths." Biochem J **22**(5): 1289-1298.

Cruz-Torres, V., M. Vazquez-Acevedo, R. Garcia-Villegas, X. Perez-Martinez, G. Mendoza-Hernandez and D. Gonzalez-Halphen (2012). "The cytosol-synthesized subunit II (Cox2) precursor with the point mutation W56R is correctly processed in yeast mitochondria to rescue cytochrome oxidase." Biochim Biophys Acta **1817**(12): 2128-2139.

Cukras, A. R., D. R. Southworth, J. L. Brunelle, G. M. Culver and R. Green (2003). "Ribosomal Proteins S12 and S13 Function as Control Elements for Translocation of the mRNA:tRNA Complex." Molecular Cell **12**(2): 321-328.

Da Cruz, S., I. Xenarios, J. Langridge, F. Vilbois, P. A. Parone and J.-C. Martinou (2003). "Proteomic Analysis of the Mouse Liver Mitochondrial Inner Membrane." Journal of Biological Chemistry **278**(42): 41566-41571.

Dardalhon, M., W. Lin, A. Nicolas and D. Averbeck (2007). "Specific transcriptional responses induced by 8-methoxypsoralen and UVA in yeast." FEMS Yeast Res **7**(6): 866-878.

Davies, C., S. W. White and V. Ramakrishnan (1996). "The crystal structure of ribosomal protein L14 reveals an important organizational component of the translational apparatus." Structure **4**(1): 55-66.

de la Cruz, J., D. Kressler and P. Linder (1999). "Unwinding RNA in Saccharomyces cerevisiae: DEAD-box proteins and related families." Trends in Biochemical Sciences **24**(5): 192-198.

de Longevialle, A. F., L. Hendrickson, N. L. Taylor, E. Delannoy, C. Lurin, M. Badger, A. H. Millar and I. Small (2008). "The pentatricopeptide repeat gene OTP51 with two LAGLIDADG motifs is required for the cis-splicing of plastid ycf3 intron 2 in Arabidopsis thaliana." Plant J **56**(1): 157-168.

De Silva, D., F. Fontanesi and A. Barrientos (2013). "The DEAD-Box Protein Mrh4 Functions in the Assembly of the Mitochondrial Large Ribosomal Subunit." Cell metabolism **18**(5): 10.1016/j.cmet.2013.1010.1007.

Del Campo, M. and A. M. Lambowitz (2009). "Structure of the Yeast DEAD Box Protein Mss116p Reveals Two Wedges that Crimp RNA." Molecular Cell **35**(5): 598.

Del Campo, M., S. Mohr, Y. Jiang, H. Jia, E. Jankowsky and A. M. Lambowitz (2009). "Unwinding by local strand separation is critical for the function of DEAD-box proteins as RNA chaperones." J Mol Biol **389**(4): 674-693.

Devenish, R. J., M. Prescott, X. Roucou and P. Nagley (2000). "Insights into ATP synthase assembly and function through the molecular genetic manipulation of subunits of the yeast mitochondrial enzyme complex." Biochimica et Biophysica Acta (BBA) - Bioenergetics **1458**(2–3): 428-442.

Dimmer, K. S. and D. Rapaport (2012). "Unresolved mysteries in the biogenesis of mitochondrial membrane proteins." Biochimica et Biophysica Acta (BBA) - Biomembranes **1818**(4): 1085-1090.

Dorsman, J. C. and L. A. Grivell (1990). "Expression of the gene encoding subunit II of yeast QH2: cytochrome c oxidoreductase is regulated by multiple factors." Curr Genet **17**(6): 459-464.

Dunn, C. D., M. S. Lee, F. A. Spencer and R. E. Jensen (2006). "A genomewide screen for petite-negative yeast strains yields a new subunit of the i-AAA protease complex." Mol Biol Cell **17**(1): 213-226.

Eckdahl, T. (2014). from http://gcat.davidson.edu/mediawiki-1.15.0/index.php/Davidson_Missouri_W/colony_PCR.

Elstner, M., C. Andreoli, T. Klopstock, T. Meitinger and H. Prokisch (2009). "The mitochondrial proteome database: MitoP2." Methods Enzymol **457**: 3-20.

Fairman-Williams, M. E., U. P. Guenther and E. Jankowsky (2010). "SF1 and SF2 helicases: family matters." Current Opinion in Structural Biology **20**(3): 313-324.

Foury, F., T. Roganti, N. Lecrenier and B. Purnelle (1998). "The complete sequence of the mitochondrial genome of Saccharomyces cerevisiae." FEBS Lett **440**(3): 325-331.

Funes, S., A. Hasona, H. Bauerschmitt, C. Grubbauer, F. Kauff, R. Collins, P. J. Crowley, S. R. Palmer, L. J. Brady and J. M. Herrmann (2009). "Independent gene duplications of the YidC/Oxa/Alb3 family enabled a specialized cotranslational function." Proceedings of the National Academy of Sciences **106**(16): 6656-6661.

Funes, S., F. Kauff, E. O. van der Sluis, M. Ott and J. M. Herrmann (2011). "Evolution of YidC/Oxa1/Alb3 insertases: three independent gene duplications followed by functional specialization in bacteria, mitochondria and chloroplasts." Biol Chem **392**(1-2): 13-19.

Gampel, A. and T. R. Cech (1991). "Binding of the CBP2 protein to a yeast mitochondrial group I intron requires the catalytic core of the RNA." Genes Dev **5**(10): 1870-1880.

Gampel, A., M. Nishikimi and A. Tzagoloff (1989). "CBP2 protein promotes in vitro excision of a yeast mitochondrial group I intron." Mol Cell Biol **9**(12): 5424-5433.

Gan, X., M. Kitakawa, K. Yoshino, N. Oshiro, K. Yonezawa and K. Isono (2002). "Tag-mediated isolation of yeast mitochondrial ribosome and mass spectrometric identification of its new components." Eur J Biochem **269**(21): 5203-5214.

Ghaemmaghami, S., W. K. Huh, K. Bower, R. W. Howson, A. Belle, N. Dephoure, E. K. O'Shea and J. S. Weissman (2003). "Global analysis of protein expression in yeast." Nature **425**(6959): 737-741.

Gietz, R. D. and R. H. Schiestl (2007). "Quick and easy yeast transformation using the LiAc/SS carrier DNA/PEG method." Nat Protoc **2**(1): 35-37.

Gilbert, W. (1986). "Origin of life: The RNA world." Nature **319**(6055): 618-618.

Goguel, V., J. Perea and C. Jacq (1989). "Synthesis and function of the mitochondrial intron--encoded bI4 RNA maturase from Saccharomyces cerevisiae. Effects of upstream frame-shift mutations." Curr Genet **16**(4): 241-246.

Gray, M. W., G. Burger and B. F. Lang (1999). "Mitochondrial evolution." Science **283**(5407): 1476-1481.

Green-Willms, N. S., C. A. Butler, H. M. Dunstan and T. D. Fox (2001). "Pet111p, an inner membrane-bound translational activator that limits expression of the Saccharomyces cerevisiae mitochondrial gene COX2." J Biol Chem **276**(9): 6392-6397.

Grohmann, L., M. Kitakawa, K. Isono, S. Goldschmidt-Reisin and H. R. Graack (1994). "The yeast nuclear gene MRP-L13 codes for a protein of the large subunit of the mitochondrial ribosome." Curr Genet **26**(1): 8-14.

Gruschke, S., K. Gröne, M. Heublein, S. Hölz, L. Israel, A. Imhof, J. M. Herrmann and M. Ott (2010). "Proteins at the Polypeptide Tunnel Exit of the Yeast Mitochondrial Ribosome." Journal of Biological Chemistry **285**(25): 19022-19028.

Gruschke, S. and M. Ott (2010). "The polypeptide tunnel exit of the mitochondrial ribosome is tailored to meet the specific requirements of the organelle." BioEssays **32**(12): 1050.

Haffter, P. and T. D. Fox (1992). "Suppression of carboxy-terminal truncations of the yeast mitochondrial mRNA-specific translational activator PET122 by mutations in two new genes, MRP17 and PET127." Mol Gen Genet **235**(1): 64-73.

Haffter, P., T. W. McMullin and T. D. Fox (1991). "Functional interactions among two yeast mitochondrial ribosomal proteins and an mRNA-specific translational activator." Genetics **127**(2): 319-326.

Halls, C., S. Mohr, M. Del Campo, Q. Yang, E. Jankowsky and A. M. Lambowitz (2007). "Involvement of DEAD-box proteins in group I and group II intron splicing. Biochemical characterization of Mss116p, ATP hydrolysis-dependent and -independent mechanisms, and general RNA chaperone activity." J Mol Biol. **365**(3): 835-855.

Hamel, P., C. Lemaire, N. Bonnefoy, P. Brivet-Chevillotte and G. Dujardin (1998). "Mutations in the membrane anchor of yeast cytochrome c1 compensate for the absence of Oxa1p and generate carbonate-extractable forms of cytochrome c1." Genetics **150**(2): 601-611.

Hanson, P. I. and S. W. Whiteheart (2005). "AAA+ proteins: have engine, will work." Nat Rev Mol Cell Biol **6**(7): 519-529.

He, S. and T. D. Fox (1997). "Membrane translocation of mitochondrially coded Cox2p: distinct requirements for export of N and C termini and dependence on the conserved protein Oxa1p." Mol Biol Cell **8**(8): 1449-1460.

Hell, K., J. Herrmann, E. Pratje, W. Neupert and R. A. Stuart (1997). "Oxa1p mediates the export of the N- and C-termini of pCoxII from the mitochondrial matrix to the intermembrane space." FEBS Lett **418**(3): 367-370.

Herbert, C. J., M. Labouesse, G. Dujardin and P. P. Slonimski (1988). "The NAM2 proteins from S. cerevisiae and S. douglasii are mitochondrial leucyl-tRNA synthetases, and are involved in mRNA splicing." EMBO J **7**(2): 473-483.

Herrmann, J. M., M. W. Woellhaf and N. Bonnefoy (2013). "Control of protein synthesis in yeast mitochondria: the concept of translational activators." Biochim Biophys Acta **1833**(2): 286-294.

Hetzer, M., G. Wurzer, R. J. Schweyen and M. W. Mueller (1997). "Trans-activation of group II intron splicing by nuclear U5 snRNA." Nature **386**(6623): 417-420.

Hildenbeutel, M., M. Theis, M. Geier, I. Haferkamp, H. E. Neuhaus, J. M. Herrmann and M. Ott (2012). "The Membrane Insertase Oxa1 Is Required for Efficient Import of Carrier Proteins into Mitochondria." Journal of Molecular Biology **423**(4): 590-599.

Hillenmeyer, M. E., E. Fung, J. Wildenhain, S. E. Pierce, S. Hoon, W. Lee, M. Proctor, R. P. St Onge, M. Tyers, D. Koller, R. B. Altman, R. W. Davis, C. Nislow and G. Giaever (2008). "The chemical genomic portrait of yeast: uncovering a phenotype for all genes." Science **320**(5874): 362-365.

Hu, Y., A. Rolfs, B. Bhullar, T. V. Murthy, C. Zhu, M. F. Berger, A. A. Camargo, F. Kelley, S. McCarron, D. Jepson, A. Richardson, J. Raphael, D. Moreira, E. Taycher, D. Zuo, S. Mohr, M. F. Kane, J. Williamson, A. Simpson, M. L. Bulyk, E. Harlow, G. Marsischky, R. D. Kolodner and J. LaBaer (2007). "Approaching a complete repository of sequence-verified protein-encoding clones for Saccharomyces cerevisiae." Genome Res. **17**(4): 536-543.

Huang, H.-R. (2004). Functional Studies of Intron- and Nuclear-encoded Splicing Factors in the Mitochondria of *Saccharomyces cerevisiae.* Ph.D. dissertation, University of Texas Southwestern Medical Center, Dallas.

Huang, H.-R., C. E. Rowe, S. Mohr, Y. Jiang, A. M. Lambowitz and P. S. Perlman (2005). "The splicing of yeast mitochondrial group I and group II introns requires a DEAD-box protein with RNA chaperone function." Proceedings of the National Academy of Sciences of the United States of America **102**(1): 163-168.

Huh, W.-K., J. V. Falvo, L. C. Gerke, A. S. Carroll, R. W. Howson, J. S. Weissman and E. K. O'Shea (2003). "Global analysis of protein localization in budding yeast." Nature **425**(6959): 686-691.

Iost, I., M. Dreyfus and P. Linder (1999). "Ded1p, a DEAD-box protein required for translation initiation in Saccharomyces cerevisiae, is an RNA helicase." J Biol Chem **274**(25): 17677-17683.

Jarmoskaite, I. and R. Russell (2011). "DEAD-box proteins as RNA helicases and chaperones." Wiley Interdisciplinary Reviews: RNA **2**(1): 135.

Jarmoskaite, I. and R. Russell (2014). "RNA helicase proteins as chaperones and remodelers." Annu Rev Biochem **83**: 697-725.

Jarrell, K. A., C. L. Peebles, R. C. Dietrich, S. L. Romiti and P. S. Perlman (1988). "Group II intron self-splicing. Alternative reaction conditions yield novel products." J Biol Chem **263**(7): 3432-3439.

Jia, L., M. Dienhart, M. Schramp, M. McCauley, K. Hell and R. A. Stuart (2003). "Yeast Oxa1 interacts with mitochondrial ribosomes: the importance of the C-terminal region of Oxa1." EMBO J **22**(24): 6438-6447.

Jia, L., J. Kaur and R. A. Stuart (2009). "Mapping of the Saccharomyces cerevisiae Oxa1-mitochondrial ribosome interface and identification of MrpL40, a ribosomal protein in close proximity to Oxa1 and critical for oxidative phosphorylation complex assembly." Eukaryot Cell **8**(11): 1792-1802.

Jiang, F., M. Chen, L. Yi, J.-W. de Gier, A. Kuhn and R. E. Dalbey (2003). "Defining the Regions of Escherichia coli YidC That Contribute to Activity." Journal of Biological Chemistry **278**(49): 48965-48972.

Jin, C., A. M. Myers and A. Tzagoloff (1997). "Cloning and characterization of MRP10, a yeast gene coding for a mitochondrial ribosomal protein." Curr Genet **31**(3): 228-234.

Jones, E. W. and G. R. Fink (1982). Regulation of amino acid and nucleotide biosynthesis in yeast. . The Molecular Biology of the Yeast Saccharomyces: Metabolism and Gene Expression. J. Strathern, Jones, EW, and Broach, JR. Cold Spring Harbor, NY, Cold Spring Harbor Laboratory Press**:** 181-299.

Karunatilaka, K. S., A. Solem, A. M. Pyle and D. Rueda (2010). "Single-molecule analysis of Mss116-mediated group II intron folding." Nature **467**(7318): 935-939.

Kaspar, B. J., A. L. Bifano and M. G. Caprara (2008). "A shared RNA-binding site in the Pet54 protein is required for translational activation and group I intron splicing in yeast mitochondria." Nucleic Acids Res. **36**(9): 2958-2968.

Kehrein, K., R. Schilling, Braulio V. Möller-Hergt, Christian A. Wurm, S. Jakobs, T. Lamkemeyer, T. Langer and M. Ott (2015). "Organization of Mitochondrial Gene Expression in Two Distinct Ribosome-Containing Assemblies." Cell Reports **10**(6): 843-853.

Keil, M., B. Bareth, M. W. Woellhaf, V. Peleh, M. Prestele, P. Rehling and J. M. Herrmann (2012). "Oxa1-Ribosome Complexes Coordinate the Assembly of Cytochrome c Oxidase in Mitochondria." Journal of Biological Chemistry **287**(41): 34484-34493.

Kennell, J. C., J. V. Moran, P. S. Perlman, R. A. Butow and A. M. Lambowitz (1993). "Reverse transcriptase activity associated with maturase-encoding group II introns in yeast mitochondria." Cell **73**(1): 133-146.

Kispal, G., P. Csere, C. Prohl and R. Lill (1999). "The mitochondrial proteins Atm1p and Nfs1p are essential for biogenesis of cytosolic Fe/S proteins." EMBO J **18**(14): 3981-3989.

Kispal, G., P. Csere, C. Prohl and R. Lill (1999). The mitochondrial proteins Atm1p and Nfs1p are essential for biogenesis of cytosolic Fe/S proteins.

Kohler, R., D. Boehringer, B. Greber, R. Bingel-Erlenmeyer, I. Collinson, C. Schaffitzel and N. Ban (2009). "YidC and Oxa1 Form Dimeric Insertion Pores on the Translating Ribosome." Molecular Cell **34**(3): 344-353.

Koonin, E. V. (2006). "The origin of introns and their role in eukaryogenesis: a compromise solution to the introns-early versus introns-late debate?" Biol Direct **1**: 22.

Krause, K., R. Lopes de Souza, D. G. Roberts and C. L. Dieckmann (2004). "The mitochondrial message-specific mRNA protectors Cbp1 and Pet309 are associated in a high-molecular weight complex." Mol Biol Cell **15**(6): 2674-2683.

Krüger, V., M. Deckers, M. Hildenbeutel, M. van der Laan, M. Hellmers, C. Dreker, M. Preuss, J. M. Herrmann, P. Rehling, R. Wagner and M. Meinecke (2012). "The Mitochondrial Oxidase Assembly Protein1 (Oxa1) Insertase Forms a Membrane Pore in Lipid Bilayers." Journal of Biological Chemistry **287**(40): 33314-33326.

Kuzmenko, A., G. C. Atkinson, S. Levitskii, N. Zenkin, T. Tenson, V. Hauryliuk and P. Kamenski (2014). "Mitochondrial translation initiation machinery: Conservation and diversification." Biochimie **100**(0): 132-140.

Labouesse, M. (1990). "The yeast mitochondrial leucyl-tRNA synthetase is a splicing factor for the excision of several group I introns." Mol Gen Genet **224**(2): 209-221.

Lambowitz, A. and M. Caprara (1999). Group I and group II ribozymes as RNPs: clues to the past and guides to the future. The RNA World. R. Gesteland, T. Cech and J. Atkins, Cold Spring Harbor Laboratory Press**:** 451-485.

Lambowitz, A. M. and M. Belfort (2015). "Mobile Bacterial Group II Introns at the Crux of Eukaryotic Evolution." Microbiology Spectrum **3**(1).

Lambowitz, A. M., M. G. Caprara, S. Zimmerly and P. S. Perlman (1999). The RNA World. Plainview, NY, Cold Spring Harbor Lab. Press.

Lambowitz, A. M. and S. Zimmerly (2004). "Mobile Group II Introns." Annual Review of Genetics **38**: 1-35.

Lambowitz, A. M. and S. Zimmerly (2011). "Group II Introns: Mobile Ribozymes that Invade DNA." Cold Spring Harbor Perspectives in Biology **3**(8).

Lee, C., A. S. Tibbetts, G. Kramer and D. R. Appling (2009). "Yeast AEP3p Is an Accessory Factor in Initiation of Mitochondrial Translation." Journal of Biological Chemistry **284**(49): 34116-34125.

Lehmann, K. and U. Schmidt (2003). "Group II Introns: Structure and Catalytic Versatility of Large Natural Ribozymes." Critical Reviews in Biochemistry and Molecular Biology **38**(3): 249-303.

Lemaire, C., F. Guibet-Grandmougin, D. Angles, G. Dujardin and N. Bonnefoy (2004). "A Yeast Mitochondrial Membrane Methyltransferase-like Protein Can Compensate for oxa1 Mutations." Journal of Biological Chemistry **279**(46): 47464-47472.

Lemaire, C., P. Hamel, J. Velours and G. Dujardin (2000). "Absence of the mitochondrial AAA protease Yme1p restores F0-ATPase subunit accumulation in an oxa1 deletion mutant of Saccharomyces cerevisiae." J Biol Chem **275**(31): 23471-23475.

Linder, P. (2003). "Yeast RNA helicases of the DEAD-box family involved in translation initiation." Biology of the Cell **95**(3-4): 157.

Lipinski, K. A., A. Kaniak-Golik and P. Golik (2010). "Maintenance and expression of the S. cerevisiae mitochondrial genome—From genetics to evolution and systems biology." Biochimica et Biophysica Acta (BBA) - Bioenergetics **1797**(6–7): 1086-1098.

Lipinski, K. A., O. Puchta, V. Surandranath, M. Kudla and P. Golik (2011). "Revisiting the Yeast PPR Proteins – Application of an Iterative Hidden Markov Model Algorithm Reveals New Members of the Rapidly Evolving Family." Molecular Biology and Evolution.

Lu, P., C. Vogel, R. Wang, X. Yao and E. M. Marcotte (2007). "Absolute protein expression profiling estimates the relative contributions of transcriptional and translational regulation." Nat Biotechnol **25**(1): 117-124.

Luttik, M. A., K. M. Overkamp, P. Kotter, S. de Vries, J. P. van Dijken and J. T. Pronk (1998). "The Saccharomyces cerevisiae NDE1 and NDE2 genes encode separate mitochondrial NADH dehydrogenases catalyzing the oxidation of cytosolic NADH." J Biol Chem **273**(38): 24529-24534.

Macierzanka, M., M. Plotka, D. Pryputniewicz-Drobinska, A. Lewandowska, R. Lightowlers and J. Marszalek (2008). "Maintenance and stabilization of mtDNA can be facilitated by the DNA-binding activity of Ilv5p." Biochim Biophys Acta **1783**(1): 107-117.

Mallam, A. L., M. Del Campo, B. Gilman, D. J. Sidote and A. M. Lambowitz (2012). "Structural basis for RNA-duplex recognition and unwinding by the DEAD-box helicase Mss116p." Nature **490**(7418): 121-125.

Mallam, A. L., I. Jarmoskaite, P. Tijerina, M. Del Campo, S. Seifert, L. Guo, R. Russell and A. M. Lambowitz (2011). "Solution structures of DEAD-box RNA chaperones reveal conformational changes and nucleic acid tethering by a basic tail." Proceedings of the National Academy of Sciences **108**(30): 12254-12259.

Manthey, G. M. and J. E. McEwen (1995). "The product of the nuclear gene PET309 is required for translation of mature mRNA and stability or production of intron-containing RNAs derived from the mitochondrial COX1 locus of Saccharomyces cerevisiae." EMBO J **14**(16): 4031-4043.

Manthey, G. M., B. D. Przybyla-Zawislak and J. E. McEwen (1998). "The Saccharomyces cerevisiae Pet309 protein is embedded in the mitochondrial inner membrane." European Journal of Biochemistry **255**(1): 156-161.

Marcia, M., S. Somarowthu and A. Pyle (2013). "Now on display: a gallery of group II intron structures at different stages of catalysis." Mobile DNA **4**(1): 14.

Martin, W. and E. V. Koonin (2006). "Introns and the origin of nucleus–cytosol compartmentalization." Nature **440**(7080): 41-45.

Martin, W. and M. Muller (1998). "The hydrogen hypothesis for the first eukaryote." Nature **392**(6671): 37-41.

Martinez-Abarca, F. and N. Toro (2000). "Group II introns in the bacterial world." Mol Microbiol **38**(5): 917-926.

Martinis, S. A., P. Plateau, J. Cavarelli and C. Florentz (1999). "Aminoacyl-tRNA synthetases: a family of expanding functions. Mittelwihr, France, October 10-15, 1999." EMBO J **18**(17): 4591-4596.

Matera, A. G. and Z. Wang (2014). "A day in the life of the spliceosome." Nat Rev Mol Cell Biol **15**(2): 108-121.

Matsuura, M., J. W. Noah and A. M. Lambowitz (2001). "Mechanism of maturase-promoted group II intron splicing." The EMBO Journal **20**(24): 7259-7270.

McGraw, P. and A. Tzagoloff (1983). "Assembly of the mitochondrial membrane system. Characterization of a yeast nuclear gene involved in the processing of the cytochrome b pre-mRNA." The Journal of biological chemistry **258**(15): 9459 - 9468

McMullin, T. W. and T. D. Fox (1993). "COX3 mRNA-specific translational activator proteins are associated with the inner mitochondrial membrane in Saccharomyces cerevisiae." J Biol Chem **268**(16): 11737-11741.

Merten, S., R. M. Synenki, J. Locker, T. Christianson and M. Rabinowitz (1980). "Processing of precursors of 21S ribosomal RNA from yeast mitochondria." Proc Natl Acad Sci U S A **77**(3): 1417-1421.

Merz, S. and B. Westermann (2009). "Genome-wide deletion mutant analysis reveals genes required for respiratory growth, mitochondrial genome maintenance and mitochondrial protein synthesis in Saccharomyces cerevisiae." Genome Biology **10**(9): 2009-2010.

Merz, S. and B. Westermann (2009). "Genome-wide deletion mutant analysis reveals genes required for respiratory growth, mitochondrial genome maintenance and mitochondrial protein synthesis in Saccharomyces cerevisiae." Genome Biology **10**(9): R95.

Miran, S. G., J. E. Lawson and L. J. Reed (1993). "Characterization of PDH beta 1, the structural gene for the pyruvate dehydrogenase beta subunit from Saccharomyces cerevisiae." Proc Natl Acad Sci U S A **90**(4): 1252-1256.

Mittelmeier, T. M., Dieckmann, C.L. (1993). "In vivo analysis of sequences necessary for CBP1-dependent accumulation of cytochrome b transcripts in yeast mitochondria." Mol. Cell. Biol. **13**(7): 4203-4213

Mohr, G., M. Del Campo, S. Mohr, Q. Yang, H. Jia, E. Jankowsky and A. M. Lambowitz (2008). "Function of the C-terminal Domain of the DEAD-box Protein Mss116p Analyzed in Vivo and in Vitro." Journal of Molecular Biology **375**(5): 1344.

Mohr, G., M. Del Campo, K. G. Turner, B. Gilman, R. Z. Wolf and A. M. Lambowitz (2011). "High-Throughput Genetic Identification of Functionally Important Regions of the Yeast DEAD-Box Protein Mss116p." Journal of Molecular Biology **413**(5): 952-972.

Mohr, S., M. Matsuura, P. S. Perlman and A. M. Lambowitz (2006). "A DEAD-box protein alone promotes group II intron splicing and reverse splicing by acting as an RNA chaperone." Proc Natl Acad Sci **10310**: 3569-3574.

Moreno, J. I., K. S. Buie, R. E. Price and M. A. Piva (2009). "Ccm1p/Ygr150cp, a pentatricopeptide repeat protein, is essential to remove the fourth intron of both COB and COX1 pre-mRNAs in Saccharomyces cerevisiae." Curr Genet **55**(4): 475-484.

Myers, A. M., L. K. Pape and A. Tzagoloff (1985). "Mitochondrial protein synthesis is required for maintenance of intact mitochondrial genomes in Saccharomyces cerevisiae." EMBO J **4**(8): 2087-2092.

Naithani, S., S. A. Saracco, C. A. Butler and T. D. Fox (2003). "Interactions among COX1, COX2, and COX3 mRNA-specific Translational Activator Proteins on the Inner Surface of the Mitochondrial Inner Membrane of Saccharomyces cerevisiae." Mol. Biol. Cell **14**(1): 324-333.

Nyberg, T. (2006). In vivo Studies of Yeast Mitochondrial Intron Splicing: Ectopic Branching and a Screen for Nuclear Encoded Splicing Factors. Ph.D. Dissertation, The University of Texas Southwestern Medical Center at Dallas.

Osinga, K. A., E. DeVries, G. Van der Horst and H. F. Tabak (1984). "Processing of yeast mitochondrial messenger RNAs at a conserved dodecamer sequence." EMBO J. **3**(4): 829-834.

Pan, C. and R. Russell (2010). "Roles of DEAD-box proteins in RNA and RNP Folding." RNA Biology **7**(6): 667-676.

Paukstelis, P. J. and A. M. Lambowitz (2008). "Identification and evolution of fungal mitochondrial tyrosyl-tRNA synthetases with group I intron splicing activity." Proc Natl Acad Sci U S A **105**(16): 6010-6015.

Paul, M. F., G. M. Alushin, M. H. Barros, M. Rak and A. Tzagoloff (2012). "The putative GTPase encoded by MTG3 functions in a novel pathway for regulating assembly of the small subunit of yeast mitochondrial ribosomes." J Biol Chem **287**(29): 24346-24355.

Payne, M. J., P. M. Finnegan, P. M. Smooker and H. B. Lukins (1993). "Characterization of a second nuclear gene, AEP1, required for expression of the mitochondrial OLI1 gene in Saccharomyces cerevisiae." Curr Genet **24**(1-2): 126-135.

Peebles, C. L., P. S. Perlman, K. L. Mecklenburg, M. L. Petrillo, J. H. Tabor, K. A. Jarrell and H. L. Cheng (1986). "A self-splicing RNA excises an intron lariat." Cell **44**(2): 213-223.

Pel, H. J. and L. A. Grivell (1993). "The biology of yeast mitochondrial introns." Molecular Biology Reports **18**(1): 1-13.

Perocchi, F., L. J. Jensen, J. Gagneur, U. Ahting and C. von Mering (2006). "Assessing Systems Properties of Yeast Mitochondria through an Interaction Map of the Organelle." PLoS Genetics **2**(10).

Petrossian, T. C. and S. G. Clarke (2009). "Multiple Motif Scanning to identify methyltransferases from the yeast proteome." Mol Cell Proteomics **8**(7): 1516-1526.

Potratz, J. P., M. Del Campo, R. Z. Wolf, A. M. Lambowitz and R. Russell (2011). "ATP-dependent roles of the DEAD-box protein Mss116p in group II intron splicing in vitro and in vivo." J Mol Biol **411**(3): 661-679.

Puchta, O., M. Lubas, K. A. Lipinski, J. Piatkowski, M. Malecki and P. Golik (2010). "DMR1 (CCM1/YGR150C) of Saccharomyces cerevisiae Encodes an RNA-Binding Protein from the Pentatricopeptide Repeat Family Required for the Maintenance of the Mitochondrial 15S Ribosomal RNA." Genetics **184**(4): 959-973.

Puig, O., F. Caspary, G. Rigaut, B. Rutz, E. Bouveret, E. Bragado-Nilsson, M. Wilm and B. Séraphin (2001). "The Tandem Affinity Purification (TAP) Method: A General Procedure of Protein Complex Purification." Methods **24**(3): 218.

Pyle, A. M. and A. M. Lambowitz (2006). 17 Group II Introns: Ribozymes That Splice RNA and Invade DNA.

Reif, S., O. Randelj, G. Domańska, E. A. Dian, T. Krimmer, C. Motz and J. Rassow (2005). "Conserved Mechanism of Oxa1 Insertion into the Mitochondrial Inner Membrane." Journal of Molecular Biology **354**(3): 520-528.

Reinders, J., K. Wagner, R. P. Zahedi, D. Stojanovski, B. Eyrich, M. van der Laan, P. Rehling, A. Sickmann, N. Pfanner and C. Meisinger (2007). "Profiling phosphoproteins of yeast mitochondria reveals a role of phosphorylation in assembly of the ATP synthase." Mol Cell Proteomics **6**(11): 1896-1906.

Reinders, J., R. P. Zahedi, N. Pfanner, C. Meisinger and A. Sickmann (2006). "Toward the complete yeast mitochondrial proteome: multidimensional separation techniques for mitochondrial proteomics." J Proteome Res **5**(7): 1543-1554.

Rho, S. B. and S. A. Martinis (2000). "The bI4 group I intron binds directly to both its protein splicing partners, a tRNA synthetase and maturase, to facilitate RNA splicing activity." RNA **6**(12): 1882-1894.

Rigaut, G., A. Shevchenko, B. Rutz, M. Wilm, M. Mann and B. Seraphin (1999). "A generic protein purification method for protein complex characterization and proteome exploration." Nat Biotechnol **17**(10): 1030-1032.

Rodeheffer, M. S. and G. S. Shadel (2003). "Multiple Interactions Involving the Amino-terminal Domain of Yeast mtRNA Polymerase Determine the Efficiency of Mitochondrial Protein Synthesis." Journal of Biological Chemistry **278**(20): 18695-18701.

Rogers, J. H. (1989). "How were introns inserted into nuclear genes?" Trends in Genetics **5**(0): 213-216.

Rogozin, I. B., L. Carmel, M. Csuros and E. V. Koonin (2012). "Origin and evolution of spliceosomal introns." Biol Direct **7**: 11.

Rout, M. P., G. Blobel and J. D. Aitchison (1997). "A distinct nuclear import pathway used by ribosomal proteins." Cell **89**(5): 715-725.

Rudolph, M. G., R. Heissmann, J. G. Wittmann and D. Klostermeier (2006). "Crystal structure and nucleotide binding of the Thermus thermophilus RNA helicase Hera N-terminal domain." J Mol Biol **361**(4): 731-743.

Russell, R., I. Jarmoskaite and A. M. Lambowitz (2013). "Toward a molecular understanding of RNA remodeling by DEAD-box proteins." RNA Biology **10**(1): 44-55.

Sagan, L. (1967). "On the origin of mitosing cells." J Theor Biol **14**(3): 255-274.

Saldanha, R., G. Mohr, M. Belfort and A. M. Lambowitz (1993). "Group I and group II introns." FASEB J **7**(1): 15-24.

Sanchirico, M. (1998). Understanding Mitochondrial Biogenesis Through Gene Relocation. Ph.D. thesis, University of Massachussetts, Amherst, MA,.

Sarastea, M., P. R. Sibbalda and A. Wittinghoferb (1990). "The P-loop — a common motif in ATP- and GTP-binding proteins" Trends in Biochemical Sciences **15**(11): 430-434.

Sarkar, J., K. Poruri, M. T. Boniecki, K. K. McTavish and S. A. Martinis (2012). "Yeast mitochondrial leucyl-tRNA synthetase CP1 domain has functionally diverged to accommodate RNA splicing at expense of hydrolytic editing." J Biol Chem **287**(18): 14772-14781.

Sashital, D. G., G. Cornilescu, C. J. McManus, D. A. Brow and S. E. Butcher (2004). "U2-U6 RNA folding reveals a group II intron-like domain and a four-helix junction." Nat Struct Mol Biol **11**(12): 1237-1242.

Schmelzer, C. and R. J. Schweyen (1986). "Self-splicing of group II introns in vitro: mapping of the branch point and mutational inhibition of lariat formation." Cell **46**(4): 557-565.

Schneider, J. C. and L. Guarente (1991). "Regulation of the yeast CYT1 gene encoding cytochrome c1 by HAP1 and HAP2/3/4." Mol Cell Biol **11**(10): 4934-4942.

Seetharaman, M., N. V. Eldho, R. A. Padgett and K. T. Dayie (2006). "Structure of a self-splicing group II intron catalytic effector domain 5: Parallels with spliceosomal U6 RNA." RNA **12**(2): 235-247.

Senissar, M., A. Le Saux, N. Belgareh-Touze, C. Adam, J. Banroques and N. K. Tanner (2014). "The DEAD-box helicase Ded1 from yeast is an mRNP cap-associated protein that shuttles between the cytoplasm and nucleus." Nucleic Acids Res **42**(15): 10005-10022.

Sentandreu, M., M. V. Elorza and R. Sentandreu (1997). "Isolation of a putative prolyl-tRNA synthetase (CaPRS) gene from Candida albicans." Yeast **13**(14): 1375-1381.

Seraphin, B., M. Simon, A. Boulet and G. Faye (1989). "Mitochondrial splicing requires a protein from a novel helicase family." Nature **337**(6202): 84.

Seraphin, B., M. Simon and G. Faye (1988). "MSS18, a yeast nuclear gene involved in the splicing of intron aI5 beta of the mitochondrial cox1 transcript." EMBO J **7**(5): 1455-1464.

Shadel, G. S. (2004). "Coupling the mitochondrial transcription machinery to human disease." Trends in Genetics **20**(10): 513-519.

Sharp, P. A. (1985). "On the origin of RNA splicing and introns." Cell **42**(2): 397-400.

Sharp, P. A. (1991). ""Five Easy Pieces"." Science **254**(5032): 663.

Sherman, F. (1965). The Genetic Control of the Cytochrome System in Yeast. Mécanismes de régulation des activités cellulaires chez les microorganismes. Marseille, Centre national de la recherche scientifique**:** 465-479.

Shingu-Vazquez, M., Y. Camacho-Villasana, L. Sandoval-Romero, C. A. Butler, T. D. Fox and X. Perez-Martinez (2010). "The carboxyl-terminal end of Cox1 is required for feedback-assembly regulation of Cox1 synthesis in Saccharomyces cerevisiae mitochondria." Journal of Biological Chemistry.

Sickmann, A., J. Reinders, Y. Wagner, C. Joppich, R. Zahedi, H. E. Meyer, B. Schonfisch, I. Perschil, A. Chacinska, B. Guiard, P. Rehling, N. Pfanner and C. Meisinger (2003). "The proteome of Saccharomyces cerevisiae mitochondria." Proc Natl Acad Sci U S A **100**(23): 13207-13212.

Simon, D. M., N. A. Clarke, B. A. McNeil, I. Johnson, D. Pantuso, L. Dai, D. Chai and S. Zimmerly (2008). "Group II introns in eubacteria and archaea: ORF-less introns and new varieties." RNA **14**(9): 1704-1713.

Simon, M. and G. Faye (1984). "Steps in processing of the mitochondrial cytochrome oxidase subunit I pre-mRNA affected by a nuclear mutation in yeast." Proceedings of the National Academy of Sciences **81**(1): 8-12.

Sirum-Connolly, K. and T. L. Mason (1993). "Functional requirement of a site-specific ribose methylation in ribosomal RNA." Science **262**(5141): 1886-1889.

Smits, P., J. A. Smeitink, L. P. van den Heuvel, M. A. Huynen and T. J. Ettema (2007). "Reconstructing the evolution of the mitochondrial ribosomal proteome." Nucleic Acids Res **35**(14): 4686-4703.

Smits, P., J. A. M. Smeitink, L. P. van den Heuvel, M. A. Huynen and T. J. G. Ettema (2007). "Reconstructing the evolution of the mitochondrial ribosomal proteome." Nucleic Acids Res. **35**(14): 4686-4703.

Solem, A., N. Zingler and Anna M. Pyle (2006). "A DEAD Protein that Activates Intron Self-Splicing without Unwinding RNA." Molecular Cell **24**(4): 611.

Stoldt, S., D. Wenzel, M. Hildenbeutel, C. A. Wurm, J. M. Herrmann and S. Jakobs (2012). "The inner-mitochondrial distribution of Oxa1 depends on the growth conditions and on the availability of substrates." Molecular Biology of the Cell **23**(12): 2292-2301.

Story, R. M., H. Li and J. N. Abelson (2001). "Crystal structure of a DEAD box protein from the hyperthermophile Methanococcus jannaschii." Proc Natl Acad Sci U S A **98**(4): 1465-1470.

Szyrach, G., M. Ott, N. Bonnefoy, W. Neupert and J. M. Herrmann (2003). "Ribosome binding to the Oxa1 complex facilitates co-translational protein insertion in mitochondria." EMBO J. **22**(24): 6448-6457.

Tavares-Carreón, F., Y. Camacho-Villasana, A. Zamudio-Ochoa, M. Shingú-Vázquez, A. Torres-Larios and X. Pérez-Martínez (2008). "The Pentatricopeptide Repeats Present in Pet309 Are Necessary for Translation but Not for Stability of the Mitochondrial COX1 mRNA in Yeast." Journal of Biological Chemistry **283**(3): 1472-1479.

Thomson, J. M., E. A. Gaucher, M. F. Burgan, D. W. De Kee, T. Li, J. P. Aris and S. A. Benner (2005). "Resurrecting ancestral alcohol dehydrogenases from yeast." Nat Genet **37**(6): 630-635.

Thorsness, P. E. and T. D. Fox (1993). "Nuclear mutations in Saccharomyces cerevisiae that affect the escape of DNA from mitochondria to the nucleus." Genetics **134**(1): 21-28.

Tkach, J. M., A. Yimit, A. Y. Lee, M. Riffle, M. Costanzo, D. Jaschob, J. A. Hendry, J. Ou, J. Moffat, C. Boone, T. N. Davis, C. Nislow and G. W. Brown (2012). "Dissecting DNA damage response pathways by analysing protein localization and abundance changes during DNA replication stress." Nat Cell Biol **14**(9): 966-976.

Tocchini-Valentini, G. D., P. Fruscoloni and G. P. Tocchini-Valentini (2011). "Evolution of introns in the archaeal world." Proceedings of the National Academy of Sciences **108**(12): 4782-4787.

Turk, E. M. and M. G. Caprara (2010). "Splicing of yeast aI5beta group I intron requires SUV3 to recycle MRS1 via mitochondrial degradosome-promoted decay of excised intron ribonucleoprotein (RNP)." J Biol Chem **285**(12): 8585-8594.

Turk, E. M., V. Das, R. D. Seibert and E. D. Andrulis (2013). "The mitochondrial RNA landscape of Saccharomyces cerevisiae." PLoS One **8**(10): e78105.

Valencik, M. L., B. Kloeckener-Gruissem, R. O. Poyton and J. E. McEwen (1989). "Disruption of the yeast nuclear PET54 gene blocks excision of mitochondrial intron aI5 beta from pre-mRNA for cytochrome c oxidase subunit I." The EMBO Journal **8**(12): 3899-3904.

Walker, J. E., M. Saraste, M. J. Runswick and N. J. Gay (1982). "Distantly related sequences in the alpha- and beta-subunits of ATP synthase, myosin, kinases and other ATP-requiring enzymes and a common nucleotide binding fold." EMBO Journal **1**(8): 945-951.

Wallin, I. (1927). Symbioticisim and the Origin of Species. Baltimore, The Williams and Wilkins Co.

Watts, T., O. Khalimonchuk, R. Z. Wolf, E. M. Turk, G. Mohr and D. R. Winge (2011). "Mne1 Is a Novel Component of the Mitochondrial Splicing Apparatus Responsible for Processing of a COX1 Group I Intron in Yeast." Journal of Biological Chemistry **286**(12): 10137-10146.

Weber, E. R. and C. L. Dieckmann (1990). "Identification of the CBP1 polypeptide in mitochondrial extracts from Saccharomyces cerevisiae." Journal of Biological Chemistry **265**(3): 1594-1600.

Welcsh, P. L., D. R. Johnson and C. A. Breitenberger (1994). "The yeast nuclear Mef2 gene encodes a second mitochondrial EF-G-like protein. ." EMBL/GenBank/DDBJ databases

Williamson, D. (2002). "The curious history of yeast mitochondrial DNA." Nat Rev Genet **3**(6): 475-481.

Williamson, D. H. (1976). Packaging and recombination of mitochondrial DNA in vegetatively growing yeast cells.Berlin.

Woodson, S. A. (2005). "Structure and assembly of group I introns." Curr Opin Struct Biol **15**(3): 324-330.

Yaffe, M. P. and G. Schatz (1984). "Two nuclear mutations that block mitochondrial protein import in yeast." Proc Natl Acad Sci **81**(15): 4819-4823.

Zamudio-Ochoa, A., Y. Camacho-Villasana, A. E. Garcia-Guerrero and X. Perez-Martinez (2014). "The Pet309 pentatricopeptide repeat motifs mediate efficient binding to the mitochondrial COX1 transcript in yeast." RNA Biol **11**(7): 953-967.

Vita

Rachel Zepeda Wolf received a Bachelor of Arts degree from Trinity University in San Antonio, Texas in 1976. Later that year, she began her teaching career as a science teacher in the public school systems of San Antonio. In 1984, she earned a Master of Science degree in Marine Biology from the University of Texas at San Antonio through a joint program with the University of Texas Marine Science Institute in Port Aransas, Texas. Following her retirement from a 30-year teaching career, Ms. Zepeda Wolf completed a Master of Science degree in Microbiology from the University of Texas Health Science Center at San Antonio. In 2007, she entered the Cell and Molecular Biology Graduate Program at the University of Texas at Austin.

Permanent email address: rzwolf@yahoo.com

This dissertation was typed by the author